ACTIVE POWER CONTROL RESPONSE FROM LARGE OFFSHORE WIND FARMS

A thesis submitted in partial fulfilment for the degree of Engineering Doctorate

This research programme was carried out in collaboration with GE Energy's Power Conversion business

by
Dominic Banham-Hall

Supervised by Dr Gareth Taylor

Brunel Institute of Power Systems, Department of Electronic and Computer Engineering, Brunel University, UK
March 2012

Abstract

The GB power system will see huge growth in transmission connected wind farms over the next decade, driven by European clean energy targets. The majority of the UK's wind development is likely to be offshore and many of these wind farms will be interfaced to the grid through power converters. This will lead to a loss of intrinsic inertia and an increasing challenge for the system operator to keep grid frequency stable. Given this challenge, there is increasing interest in understanding the capabilities of converter control systems to provide a synthesised response to grid transients. It is interesting to consider whether this response should be demanded of wind turbines, with a consequential reduction in their output, or if advanced energy storage can provide a viable solution.

In order to investigate how large offshore wind farms could contribute to securing the power system, wind turbine and wind farm models have been developed. These have been used to design a patented method of protecting permanent magnet generator's converters under grid faults. Furthermore, these models have enabled investigation of methods by which a wind turbine can provide inertial and frequency response. Conventionally inertial response relies on the derivative of a filtered measurement of system frequency; this introduces either noise, delay or both. This research proposes alternative methods, without these shortcomings, which are shown to have fast response. Overall, wind farms are shown to be technically capable of providing both high and low frequency response; however, holding reserves for low frequency response inevitably requires spilling wind.

Wind's intermittency and full output operation are in tension with the need of the power system for reliable frequency response reserves. This means that whilst wind farms can meet the technical requirements to hold reserves, they bid uncompetitive prices in the market. This research shows that frequency response market prices are likely to rise in future suggesting that the Vanadium Redox Flow Battery is one technology which could enter this market and also complement wind power. Novel control incorporating fuzzy logic to manage the battery is developed to allow a hybrid wind and storage system to aggregate the benefits of frequency response and daily price arbitrage. However, the research finds that the costs of smoothing wind power output are a burden on the store's revenue, leading to a method of optimising the combined response from an energy store and generator that is the subject of a patent application. Furthermore, whilst positive present value may be derived from this application, the long payback periods do not represent attractive investments without a small storage subsidy.

Acknowledgements

I would like to start by thanking my industrial supervisor, Dr Chris Smith, for guiding this project into interesting areas and providing me with opportunities to present this work at many levels within the company. Dr Gary Taylor, my principle academic supervisor has been a source of interesting ideas, new contacts and experience to ensure this project stays relevant and that I stay abreast of wider developments in power engineering, I am in your debt. I would also like to thank Professor Malcolm Irving, who as second supervisor has had disproportionate involvement in the less interesting task of paper reviews, but has always provided useful insight.

I acknowledge here the contribution of the Brunel University Environmental Technology Engineering Doctorate centre. In particular I would like to recognise the contribution of the research office at Brunel University. This office has always been prompt in dealing with admin and practical matters, for which I particularly thank Janet Wheeler.

I would also like to thank the directors and staff of GE Energy for their support of this research, particularly the Modelling team, the Drives development team, Derek Grieve, the External Communications team, the Energy business and those who were once in the Renewables department. The input to my project from across the company has undoubtedly shaped it and made it a far more enjoyable experience.

I would particularly like to thank National Grid's Jonathan Horne, Helge Urdal and Neil Rowley for fielding endless Grid Code questions and then, when they had dried up, starting all over again to field endless Electricity Markets questions. Jonathan and Helge's input to progress meetings has contributed significantly to the shape of the research.

The project has been financially supported by The Engineering and Physical Sciences Research Council (EPSRC) and GE Energy, this support is gratefully acknowledged here.

Personally I would like to thank my wife, Katharine, for supporting me not only at the start of this research but throughout. Finally, I would like to thank my daughter, Emma, for providing me with an expensive reason to hurry up and finish!

Contents

List of Figures

List of Tables

List of Abbreviations

AC	Alternating Current
AVR	Automatic Voltage Regulator
AFE	Active Front End
CAES	Compressed Air Energy Storage
CCGT	Combined Cycle Gas Turbine
CCL	Capped Committed Level
CIGRE	International Council on Large Electric Systems
Cp	Coefficient of Performance
d-axis	Direct axis
DBERR	Department of Business, Enterprise and Regulatory Reform
DBR	Dynamic Brake Resistor
DC	Direct Current
DCF	Discounted Cash Flow
DECC	Department of Energy and Climate Change
DFIG	Doubly Fed Induction Generator
DTI	Department for Trade and Industry
EMF	Electro-motive Force
EngD	Engineering Doctorate
ENTSO-E	European Network of Transmission System Operators for Electricity
EPRI	Electric Power Research Institute
ESA	Electricity Storage Association
FFIG	Fully Fed Induction Generator
FFPMG	Fully Fed Permanent Magnet Generator
FFSG	Fully Fed Synchronous Generator
FPN	Final Physical Notification
FSIG	Fixed Speed Induction Generator
FSM	Frequency Sensitive Mode
GFR	Grid Fault Ride-through
GWEC	Global Wind Energy Council
HVAC	Heating, Ventilation and Air Conditioning
HV	High Voltage
HVDC	High Voltage Direct Current
IGBT	Insulated Gate Bipolar Transistor
KE	Kinetic Energy
LFSM	Limited Frequency Sensitive Mode
LV	Low Voltage
MEL	Maximum Export Limit
MV	Medium Voltage
NPV	Net Present Value
OFTO	Offshore Transmission Owner
3p	Three times the blade rotational frequency
PI	Proportional-Integral
PLL	Phase Locked Loop
PMG	Permanent Magnet Generator
pu	Per Unit
PWM	Pulse Width Modulation
q-axis	Quadrature axis
ROC	Renewable Obligation Certificate
ROCOF	Rate Of Change Of Frequency

RPM	Revolutions Per Minute
SMES	Superconducting Magnetic Energy Storage
SBP	System Buy Price
SoC	State of Charge
SSP	System Sell Price
STOR	Short Term Operational Reserve
SVC	Static VAR Compensator
TSO	Transmission System Operator
TSR	Tip Speed Ratio
UPS	Uninterruptible Power Supply
VRFB	Vanadium Redox Flow Battery
VRIG	Variable Resistance Induction Generator

Mathematical Notation

General Notation Conventions

X	Scalar Quantity, X
$\underline{X}$	Vector, X
$\hat{X}$	Peak value of X
$\tilde{X}$	Root mean square (RMS) value of X
$\angle \underline{X}\ \underline{Y}$	Angle between vectors $\underline{X}$ and $\underline{Y}$
$\lvert\underline{X}\rvert$	Magnitude of the vector $\underline{X}$
$\overline{X}$	Per unit value of X
X_d	d-axis component of $\underline{X}$
X_q	q-axis component of $\underline{X}$
X_m, X_{mag}	Magnetising branch value of X
X_r	Rotor side value of X
X_s	Stator side value of X
X_t	Total air-gap value of X
X_w	Wind side value of X
X_{grid}	Grid side value of X
X_{gen}	Generator side value of X
X_{DC}	DC link side value of X
X_{ref}	Set-point value of the controlled variable, X
$X \cdot Y$	Multiplication of X and Y
$\underline{X} \bullet \underline{Y}$	Dot product of X and Y
$\underline{X} \times \underline{Y}$	Cross product of X and Y

Specific Notation Used

β	Blade Pitch Angle (º)
δ	Generator Load Angle (º)
Φ	cos Φ is the power factor
η	Efficiency in %
ρ	Air density in kg/m^3
λ	Tip speed ratio of the wind turbine blades
θ	Angle (rad)
Ψ	Magnetic flux linkage (Vs)
π, Π	Revenue is £
ω	Rotational frequency in rad/s
A	Swept area of the blades in m^2
B	Magnetic Field in Wb
C_{dc}	DC link capacitance in F
C_p	Coefficient of performance
D	Mechanical damping component in Nms/Rad
E	Electromotive force in V
E^{Θ}	Electrochemical Potential in V
f	Frequency in Hz
H	Per unitised moment of inertia in s
I,i	General Current in A
I_{chop}	Chopper current in A
J	Moment of inertia in kgm^2
KE	Kinetic Energy in J
K_{shaft}	Shaft Stiffness in Nm/rad

K_p	Proportional Gain
K_i	Integral Gain
L	Inductance in H
m	Mass of Air in kg
n_{gear}	Gearbox ratio
n_{cycles}	Life time of energy store in cycles
N	Number of turns
p	Pole pairs
P	Power in W
R	Resistance in Ω
R_b	Blade radius in m
R_{dbr}	Dynamic Brake Resistor in Ω
S	Apparent Power in VA
s	Induction Generator slip
t	Time in s
T, T_q	Torque in Nm
U	Terminal Voltage in V
v_{mean}	Average effective wind speed in m/s
v_w	Instantaneous effective wind speed in m/s
V	General Voltage in V
X	General Reactance in Ω

Executive Summary

Introduction

Widespread offshore wind power development is fundamental to meeting the UK's share of the European target of generating 20% of all energy renewably by 2020. Large offshore wind farms will be connected to the transmission system and will displace conventional generation at times of high output. Concurrent with this development will be the replacement of the UK's nuclear fleet, potentially with fewer, larger individual generators. Historically sudden loss of a major generator, such as a nuclear station trip, has been covered by frequency response reserve, held as a contingency, on large, mainly fossil fuelled, power stations. However, the displacement of traditional generation by wind power challenges this model.

Challenges for Wind Power and the Power System

Conventional synchronous generators provide an inherent reactive power in-feed to system voltage disturbances such as grid fault events, helping to trigger protection devices and secure system voltages. Modern wind turbines connect to the grid through voltage source power electronic converters. Power electronic converters permit the use of new machine topologies such as the direct-drive permanent magnet generator, which in turn simplifies the wind turbine design for the offshore environment. The control of these converters has extended to providing a reactive current in-feed to low grid voltages from full converter wind turbines, with this in-feed limited to the current rating of the power converter. These voltage events, characterised by real power output reduction within a mains cycle, can however, cause significant electrical and mechanical transients. These transients present a particular challenge to direct-drive permanent magnet generator wind turbines owing to a relatively high shaft mechanical resonant frequency and the fact that the rotor field can not be weakened if the generator exceeds its nominal speed, leading to a tendancy for over-voltage.

One of the main benefits of a power converter is that it controls the turbine to operate at variable speed, maximising energy yield. But this inherently also decouples the rotating inertia of the blades and generator from the grid. Conventional generators' rotational inertia acts as an energy buffer to the grid, ensuring that supply and demand imbalances do not lead to large frequency changes on the power system. Removing inertia from the system at a time when larger single nuclear generators are proposed therefore threatens to lead to decreased frequency stability.

The power converter also adds flexibility and controllability to the wind turbines, which allows them to meet increasingly advanced Grid Codes. Given the potential impact of rising levels of wind power on the GB system, it is of increasing interest to establish whether the control of the wind turbine and power converter can be modified to support the system frequency.

Energy Storage to Complement Wind Power

The challenges presented by wind power's intermittency and optimal output tracking may well find their natural solution in advanced energy storage technologies. Energy storage offers the prospect of allowing wind to be dispatchable as well as being capable of holding reserves for securing the power system's frequency. However, whilst the intuitive link between energy storage and wind power is obvious, the technical integration is more complex. Control of the energy store has to consider intermittent charging in the context of finite energy capacity and provision of frequency response may still have to account for the variable power capacity of the energy store required for wind smoothing. Furthermore, adding equipment and complexity to the wind farm would increase cost, so a return is necessary.

The challenge with energy storage is to identify the right technology to operate in tandem with a wind farm and establish whether it can be integrated into the power system in a manner that is economically viable. Frequency response offers a high value application for technology with a fast dynamic response, whilst energy time-shifting offers further benefit to technologies with high energy capacities at low cost, but can the two be integrated?

Aims and Objectives

The current trend in GB Grid Code development is to mandate technical capabilities, in line with the inherent behaviour of conventional synchronous plant, regardless of technology, and ensure compliance through type-testing and commissioning. This places a burden of technical requirements on all new technologies connecting to the grid, including wind power. Research into grid connection of renewable generators generally focuses exclusively on the development of control algorithms and techniques to provide a particular service to the power system. This research aims to distinguish itself in the following ways:

- Addressing the implications of Grid Code requirements on direct-drive permanent magnet generator based power trains and highlighting how the Grid Code requirements influence the design of the physical system.

- Extending the techniques used in wind turbines to emulate a synchronous machine's fast frequency response by considering the controllability of the power converter.
- Investigating the technical and economic status of different emerging and traditional energy storage technologies in order to assess the best technology to complement wind power.
- Developing control techniques for aggregating benefits of energy storage and wind power, whilst ensuring that the combined system can meet the Grid Code frequency response requirement in the place of the wind farm alone.
- Assessing the economic viability of providing frequency response services and determining whether an integrated energy storage system would offer a genuine benefit over a stand alone wind farm.

Contributions to Knowledge

The research has developed four main key findings supported by a number of subsidiary results.

Grid Fault Ride-through of Permanent Magnet Generator based Wind Turbines

Direct-drive Permanent Magnet Generators (PMGs) are typically characterised by:

- Stiff shaft systems with higher resonant frequencies than conventional wind turbines.
- Intrinsically linked speed and open-circuit voltage owing to the fixed rotor flux provided by the magnets.
- High stator reactance to protect the magnets under short circuit conditions.

These three factors contribute to the conclusion that it is essential for direct-drive PMG's power converters to be equipped with choppers and brake resistors in order to ride-through low voltage grid events. Under grid faults these absorb the stator magnetic energy as well as prevent excitation of the shaft and acceleration of the generator. However, as a patented alternative to using a fully rated chopper to ride-through the complete grid fault, this work presents a novel technique of controlling the power converter to minimise chopper use. The energy capacity of this chopper and brake resistor can be significantly reduced by controlling the generator's maximum torque ramp rates to match the resonant period of the shaft system. This minimises mechanical excitation and avoids converter DC link over-voltage.

Fast Frequency Response from Wind Turbines

Research on synthetic inertial response from wind turbines has focussed mainly on methods that rely on a measurement of the derivative of system frequency. System frequency is a noisy signal and taking the derivative either increases noise, thereby reducing controller robustness, or else requires filtering, thereby increasing controller delay. Integration of synthetic inertia with the power converter control capability has allowed two alternative methods of inertial provision to be identified. Either the magnitude of the frequency deviation can be used to modify the speed set point of the turbine through a speed control loop, which offers tuneable inertial response. Or alternatively, the integral of the frequency error can be used to derive an angle analogous to a synchronous machine's load angle change. This offers fast, noise insensitive response in line with a conventional generator. However, the work also confirms that fast inertial and primary response from wind turbines in low wind conditions inevitably leads to mechanical speed changes, which in turn lead to periods of reduced power output as the turbine recovers. This recovery period threatens to limit the true usefulness of wind farms' inertial and frequency response capability.

Energy Storage for Wind Power

An appraisal of the status of energy storage technologies shows that, for the specific requirements of frequency response provision with intermittent wind power, the Vanadium Redox Flow Battery is an attractive option. This conclusion is helped by the flow battery's long cycle life, fast response and cheap energy capacity. Such an energy storage system could be readily integrated with power converter based reactive power compensation equipment for AC connected wind farms. A novel incremental improvement is made to the control of a flow battery connected to the grid through a boost converter and IGBT SVC. This adaptation allows the battery to support the power converter's DC link voltage through extreme low voltage events so that a continuous reactive current output can be maintained.

Application of energy storage with wind power for frequency response under current GB regulations requires that the store first smoothes the wind output. This means that the control of the energy store must manage the battery's state of charge as well as provide frequency response capability and energy time shifting. An innovative fuzzy logic controller has been developed to manage the state of charge of the battery, whilst the reference state of charge level can be scheduled to manage energy time-shifting thereby presenting aggregation of multiple benefits alongside frequency response.

Economics of Frequency Response

The GB Grid Code mandates core technical requirements on plant, but it is the prices set in the separate frequency response market that ultimately determines whether that capability is used. The increasing requirement for primary and secondary frequency response is likely to lead to increased prices for frequency response services by 2020.

Integration of energy storage with a wind farm for frequency response is disadvantaged by the Grid Code requirement to regulate relative to a fixed output. Revenues from increased output firmness do not compensate for the reduced capacity available for frequency response. Nevertheless, sharing high frequency response capacity with the wind farm, whilst the store is charging, permits the energy store to offer greater frequency response capacity and thereby increases revenues. The frequency response revenues are the dominant source of income as round trip energy losses in the flow battery offset arbitrage gains. If the energy store offers frequency response services, with the wind farm only offering high frequency balance control, the revenues can be maximised by a method that is the subject of a patent application.

Discounted Cash Flow analysis shows that present prices are insufficient to lead to a positive present value from an energy store; however, likely price trends suggest this will change before 2020. Even with positive present value, the payback periods are unlikely to be short enough to represent an attractive investment. Nevertheless, only a small subsidy would be needed to change this and the Electricity Market Reform may deliver this through a potential capacity mechanism.

Publications

Conference Papers

1. D. D. Banham-Hall, C. A. Smith, G. A. Taylor, M. R. Irving. "Grid Connection Oriented Modelling of Wind Turbines with Full Converters." *In Proc. 44th Universities Power Eng. Conf. (UPEC),* Glasgow, UK, 1-4 Sept. 2009.

   The associated presentation won the 'Best Presentation' award at the conference.

2. D. D. Banham-Hall, C. A. Smith, G. A. Taylor, M. R. Irving. "Grid Connection Oriented Modelling for Simulation of Frequency Response and Inertial Behaviour of Full Converter Wind Turbines." *In Proc. 8th Int. Workshop on Large Scale Integration of Wind Power into Power Syst.,* Bremen, Germany, Oct. 2009.

3. D. D. Banham-Hall, C. A. Smith, G. A. Taylor, M. R. Irving. "Grid Connection Oriented Modelling of Wind Farms to Support Power Grid Stability." *In Proc. the 21st Int. Conf. on Syst. Eng. (ICSE),* Coventry, UK, Sept. 2009.

4. D. D. Banham-Hall, C. A. Smith, G. A. Taylor, M. R. Irving. "Towards Large-scale Direct Drive Wind Turbines with Permanent Magnet Generators and Full Converters." *In. Proc. IEEE Power and Energy Soc. General Meeting,* Minneapolis, USA, July 2010, doi: 10.1109/PES.2010.5589780.

5. D. D. Banham-Hall, C. A. Smith, G. A. Taylor, M. R. Irving. "Investigating the Limits to Inertial Emulation with a Large-scale Wind Turbines with Direct-Drive Permanent Magnet Generators." *In Proc. UKACC Control 2010 Conference, Coventry, UK*, Sept. 2010.

6. D. D. Banham-Hall, C. A. Smith, G. A. Taylor, M. R. Irving. "Investigating the Potential Contribution of Future Offshore Wind Turbines to Frequency Stability During Major System Disturbances." *In Proc. IET ACDC 2010 Conf.,* London, UK, 19-22 Oct. 2010, doi: 10.1049/cp.2010.1004.

7. D. D. Banham-Hall, C. A. Smith, G. A. Taylor, M. R. Irving. "Frequency Control Using Vanadium Redox Flow Batteries on Wind Farms." *In Proc. IEEE Power and Energy Soc. General Meeting,* Detroit, USA, 24-29 July 2011, doi: 10.1109/PES.2011.6039520.

Patent Applications

1. D. D. Banham-Hall, C. A. Smith, G. A. Taylor. Generator torque control methods. European Patent Application no. EP10006961.1 filed 06/07/2010.

2. D. D. Banham-Hall, C. A. Smith, G. A. Taylor. Frequency reserves from an Energy store and a generator. European Patent Application no. EP10007692.4 filed 26/09/2011.

Journal Articles

1. D. D. Banham-Hall, C. A. Smith, G. A. Taylor, M. R. Irving. "Meeting Modern Grid Codes With Large Direct-Drive Permanent Magnet Generator Based Wind Turbines – Low Voltage Ride-through." *Accepted for publication in Wind Energy*.

2. D. D. Banham-Hall, C. A. Smith, G. A. Taylor, M. R. Irving. "Meeting Modern Grid Codes With Large Direct-Drive Permanent Magnet Generator Based Wind

Turbines – Frequency and Inertial Response." *Submitted and under revision for publication in Wind Energy*.

3. D. D. Banham-Hall, C. A. Smith, G. A. Taylor, M. R. Irving. "Flow Batteries for Enhancing Wind Power Integration." *Accepted for publication in IEEE Transactions on Power Systems*.

1 Introduction

1.1 Overview

This section is intended to act as an introduction and a reader's guide to the thesis. The widespread deployment of wind power on the GB transmission system together with the technological advance of energy storage are highlighted as the motivation behind investigating future active power control from large offshore wind farms. The key research objectives and findings are introduced.

1.2 Wind Power development in the UK

The UK government [1] has enacted a legally binding commitment to reduce Carbon Dioxide and associated greenhouse gas emissions by 80% by 2050, relative to 1990 levels. To achieve this, it is likely that emissions will have to be cut by 34% by 2020. In order to achieve these goals the electricity sector, which accounts for a third of emissions and is the largest single source, must see rapid and extensive decarbonisation. Indeed the Department of Energy and Climate Change's (DECC) [2] own roadmap foresees a central scenario where over 30GW of wind power is added to the GB power system by 2020. Furthermore, offshore wind power alone is projected to exceed 40GW from 2030. This trajectory is reinforced by National Grid's [3] projections for the transmission level connected generating capacity on the power system in 2020, given the right incentives, as shown in Figure 1.1.

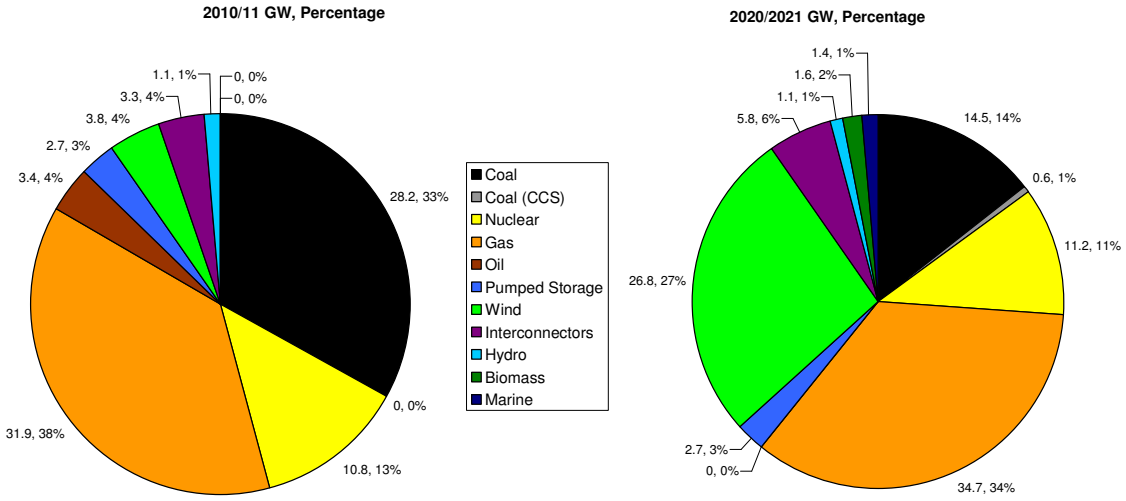

Figure 1.1: National Grid's 'Gone Green' capacity projections for 2020/2021 (right) compared to 2010/11 (left)

The large scale development of wind, which is inherently an intermittent resource, will have a significant impact on the operation of the power system. Balancing supply and demand in real time will become increasingly challenging due to wind's intermittency.

Furthermore, power electronic interfaced wind turbines with low inherent inertia will replace conventional high inertia rotating generators, thereby removing a stabiliser from the grid system. Additionally, large offshore wind farms and nuclear power stations will present a larger potential single loss of generation than the current largest in-feed loss on the system (Sizewell B, 1200MW approx.). These factors combined lead to an increased requirement for reserves and response on the power system, with National Grid's [3] estimates shown in Figure 1.2.

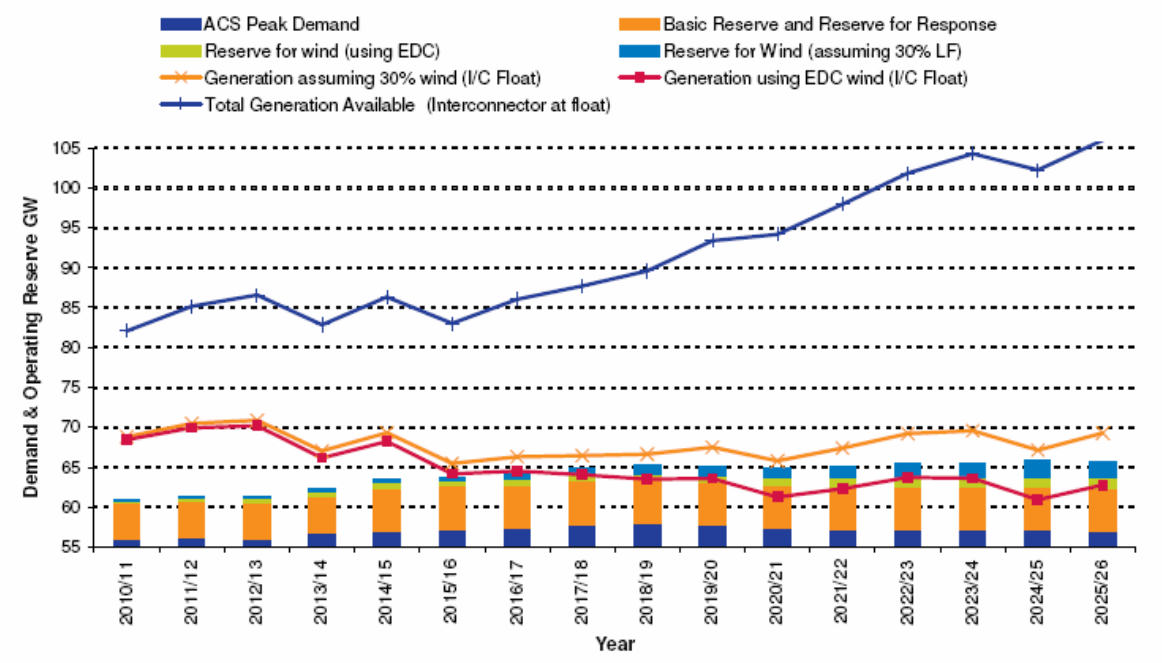

Figure 1.2: National Grid's [3] Projections for Reserve Requirements

Figure 1.2 clearly illustrates that the requirements for many types of response and reserve are likely to grow significantly over the current decade. Large offshore wind farms are likely to be the dominant source of new transmission connected wind generation. Active power control from large offshore wind farms will therefore be increasingly important, but can wind contribute to securing the power system as well as supply clean energy.

1.3 An opportunity for energy storage?

The challenges of integrating high levels of wind energy into the GB power system may represent a significant opportunity for energy storage. Storage's flexibility to operate as dynamic generation or demand could help to alleviate the power swings associated with intermittent wind power. Furthermore, advanced battery technologies can offer fast response to the power system to meet the requirements for increased response. The Energy Research Partnership [4] has shown how the diverse range of developing energy storage technologies can meet many of the challenges posed by a grid served by renewable power in 2020, this is shown in Figure 1.3.

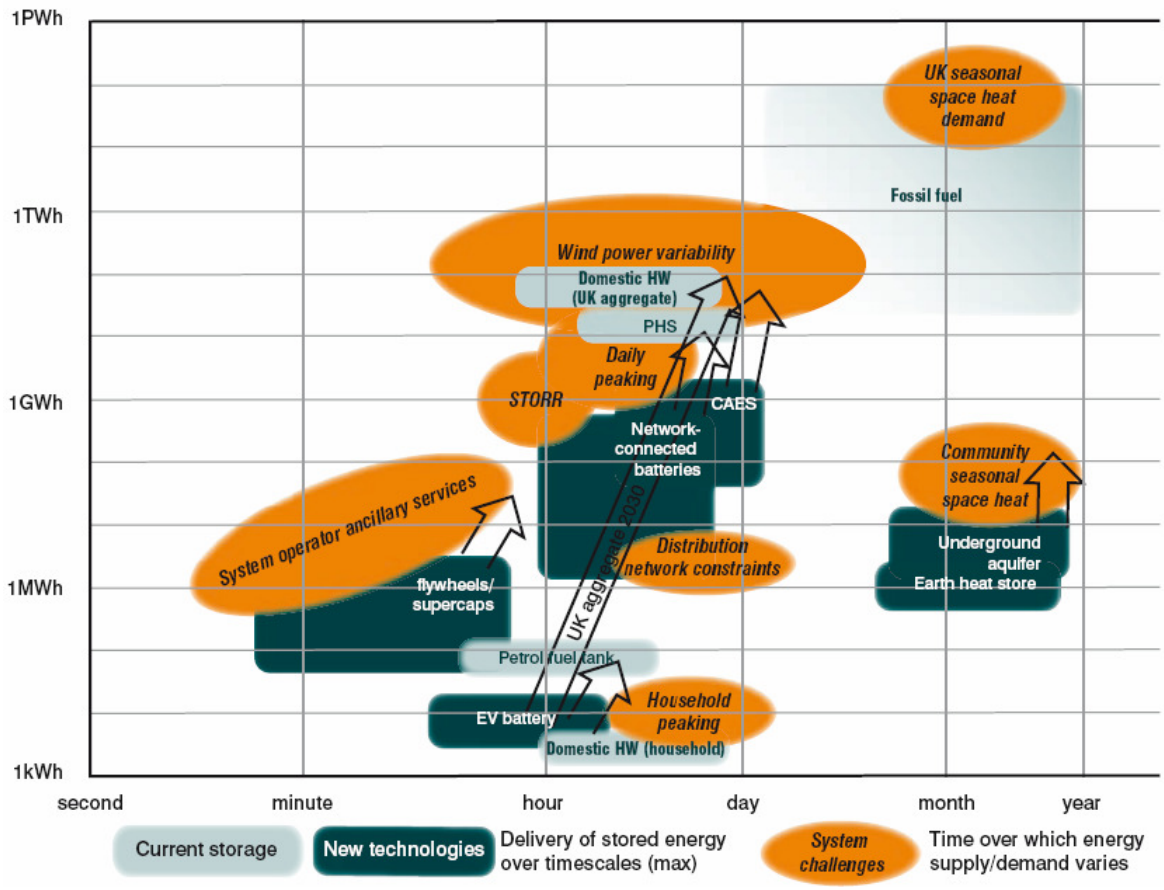

Figure 1.3: Energy Research Partnership's [4] assessment of the scale of challenges facing the power system and the solutions that energy storage systems offer

Conventional energy storage, in the form of pumped hydroelectric power, has supported the power system for decades. Today, the scale of the challenges facing the power system, combined with the advance of energy storage technologies, suggests it may be time for new technologies to emerge to assist with active power control from large offshore wind farms.

1.4 Research objectives

Planning for the security of the GB power system in 2020 must incorporate a considered assessment of the behaviour of widespread, intermittent wind power. To address this, the general research area considers the differences between conventional generators and modern wind turbines, particularly in view of the turbines' power electronic interface to the grid and then develops control methods for wind plant to emulate the behaviour of the conventional plant. This research specifically addresses modern wind turbines equipped with full rating converters and either induction or permanent magnet generators. It aims to assess their capability to control active power in response to transient changes on the power grid, investigating both low voltage events and frequency changes. This contributes to the technical capability of modern wind farms to provide for the increasing reserve

services required by the grid. Can wind power provide reserves and response to help secure the power system in 2020?

Historically, different generation technologies have always offered different dynamic performance capabilities and varying capacity factors. However, today's approach to provision of dynamic response is based on requiring mandatory basic performance through compliance with Grid Code technical requirements. Whilst it is important to understand the technical capabilities of wind plant to meet these requirements and offer ancillary services, it is worth considering whether this capability may become redundant in the face of energy storage technologies that are advancing both economically and technically. The research therefore also aims to investigate the integration of energy storage with wind power to offer reserve services to the power system in terms of both their potential control schemes and their financial viability. Does energy storage provide a better means of offering frequency response services than relying on spilling wind and limiting a free, but intermittent resource?

1.5 Contributions to knowledge

The trend in wind turbine design, particularly for offshore, is leading to ever larger machines and designs which simplify the drive train through use of multi-pole permanent magnet generators. Such machines offer lower maintenance and potentially higher efficiency; however, the permanent magnets mean that the rotor flux is fixed. The lack of control over rotor flux leads to potential over-voltage in the event of turbine over speed or loss of load under a grid fault. In chapter 4 and Banham-Hall *et al.* [80] a modification to the control technique of the power converter is proposed to address low voltage ride-through with permanent magnet generator based wind turbines. This control forces a ramped reduction of generator torque at a rate determined by the fundamental frequency of the mechanical shaft system. The energy from the generator is diverted to a brake resistor on the power converter's DC link; however, this resistor need not be rated for the full turbine energy for the duration of the fault. Furthermore, the appropriate torque ramp rate ensures that mechanical oscillations of the wind turbine shaft are avoided, thereby minimising the transient over-voltages from the permanent magnet generator that could result from grid faults.

The trend to ever larger turbines with permanent magnet generators is also part of a move towards power electronic converter interfaced wind farms, whether they are turbine level converters or DC connected wind farms. This implicitly implies a decoupling of the physical rotating inertia from the power output of the wind farm. Conventional approaches

to imposing inertial response from converter interfaced wind plant rely on taking a measurement of the derivative of power system frequency. This inherently introduces noise or delay to the response as the initial frequency measurements are noisy and therefore either the increased noise of the derivative must be tolerated or a low pass filter must be applied, thereby slowing down the response. Chapter 4 and Banham-Hall *et al.* [87] propose methods that allow a wind turbine to offer inertial response without relying on taking the frequency's derivative; these offer a means to fast response more akin to a conventional generator.

Whilst the thesis demonstrates key methods of providing frequency response from a stand alone wind farm, it moves on to develop novel methods of providing this service from a wind farm equipped with a Vanadium Redox Flow Battery. Chapter 6 begins by developing a simplified model of a Vanadium Redox Flow Battery and power converter for interface to the grid. Chapter 6 and Banham-Hall *et al.* [138] then explore the control methods that can be used to regulate the battery's state of charge, whilst also offering reserve for frequency response and smoothing of the wind farm's output power. These control methods depend on a novel fuzzy logic controller, which manages the energy store and wind farm's power output and also allows the energy store to offer some daily price arbitrage. The flow battery is shown to be technically capable of being integrated with a wind farm to offer combined frequency response services.

Ultimately, the provision of frequency response reserves on the GB power system depends on selection in the market. Whilst stand alone wind farms and those potentially equipped with energy storage could offer these services to the grid, either solution would have to compete with conventional plant. Chapter 7 therefore analyses the economics surrounding the deployment of energy storage on the power system for frequency response. It highlights the importance of using wind's capability to provide high frequency response in conjunction with energy storage's capability to provide low frequency response and daily arbitrage. Whilst it ultimately finds that the economic case alone is not sufficient to justify Vanadium Redox Flow Batteries, it concludes by illustrating that storage would offer environmental benefits and argues in favour of a subsidy, which could see this application become an economically viable application for energy storage.

1.6 EngD Scheme

Brunel and Surrey Universities have offered an "Environmental Technology" Engineering Doctorate since near the inception of the scheme in 1993. The Engineering Doctorate (EngD) scheme itself is a four year research degree where the researcher is based in

industry in order to tackle industrially relevant research problems. The EngD is supported by a series of professional development modules covering a range of environmental and technology matters.

It is expected that an EngD should be of at least the same quality as the traditional PhD and commensurate with 4 years of study. Nevertheless, the EngD differs from a PhD both in its industrial location and its focus on innovation as opposed to scientific discovery. As such an EngD may be developed as a portfolio, where it is the synthesis of the portfolio itself that presents the key contribution to knowledge. In this vein, whilst this thesis presents specific new control methods for both wind turbines and energy storage systems; these alone do not define the contribution of the EngD. Over-arching these specific contributions this thesis aims to question whether securing the power system, particularly system frequency, with ever more onerous requirements on wind turbines, is necessarily desirable.

This EngD has been sponsored by GE Energy's Power Conversion business and located within the Modelling and Simulation team of the Central Engineering department. In addition to the sponsorship from GE Energy's Power Conversion business, National Grid has provided regular input to the project by attending and hosting some project progress meetings.

It should be noted that GE Energy bought Converteam, the original sponsors of this work, in 2011 and Converteam became GE Energy's Power Conversion business. Converteam were a supplier of power conversion equipment to a wide range of wind turbine manufacturers including Siemens Wind Power. However, GE Wind historically internally supplied their own power converters. When this thesis refers to GE Energy's technology, it is referring to the technology derived from Converteam and associated with multiple wind turbine manufacturers and not that of GE Wind.

1.7 Thesis overview

Chapter 1: Introduction

This section begins by providing the foundational knowledge regarding active power control on the GB transmission system and from offshore wind farms. The section aims to provide a readers guide to the thesis, highlighting the research approach, the key contributions to knowledge and the over-arching structure of the thesis as a whole. It also sets the project within the field of Environment Technology.

Chapter 2: Wind Power and the GB Grid

Chapter 2 forms a technical introduction to the changes in power generation characteristics on the GB transmission system. After reviewing the exponential growth in the wind industry globally, it shows that the UK is likely to lead globally in the development of offshore wind resources. Alongside the industry's growth has come technology development that will mean that the GB system faces a rapidly increasing share of generation that is connected via a power converter. This power converter interface is highlighted as providing both flexibility and a significant change from conventional synchronous plant.

Chapter 3: Modelling of Full Converter Wind Turbines

The principle research method applied within this thesis is modelling and simulation. This chapter reviews the existing literature covering modelling of wind turbines and develops individual modules to represent the key aerodynamic, mechanical, electrical and control systems. The chapter includes a comprehensive comparison of the two alternative power converter control strategies for use with a full converter wind turbine as well as an introduction to simplified representation of the wind turbine and wind farm controllers for use in power system simulations. The two software packages used for dynamic simulation throughout this research project are introduced. Finally, key sub-system models are validated, as independent modules, against real world data and test bench data, which in turn permitted the development of a suite of different full converter wind turbine models.

Chapter 4: Grid Connection of Full Converter Wind Turbines

Grid Codes place an increasing technical burden on wind turbines; this section reviews three areas of present and future compliance: Grid fault ride-through, frequency response and inertial response. It reviews the existing and developing codes, defines control schemes to meet their requirements and presents validation results for a full wind turbine model against a grid fault. The particular challenges of riding-through grid faults with a permanent magnet generator and full converter are introduced leading to the development of a novel control scheme that meets this requirement whilst only using a minimally rated chopper to avoid fundamental drive-train oscillations. The existing requirement to provide frequency response is reviewed and further control is developed for application with a control strategy from a wind turbine manufacturer proposing an alternative turbine control methodology. Finally, against a background of regulatory uncertainty, innovative control methods are presented for providing fast acting inertial response, whilst minimising

sensitivity to frequency noise. Whilst the chapter shows the technical capabilities of wind, it is against a backdrop of uncertain reserves from a fickle resource.

Chapter 5: Energy Storage Development

This chapter acts as a bridge between the work on wind turbines and that on energy storage. It shows that at a time when regulations are mandating wind farms have the capability to provide frequency response, increasing numbers of energy storage manufacturers are taking an interest in the economic viability of meeting this requirement from storage technology. Furthermore, the chapter highlights the complementary nature of wind and storage for smoothing power output and shifting power generation to times of high demand. As such there appears to be a potential market for storage if only suitable aggregation of energy storage's benefits can be realised. The chapter therefore critically reviews the technical and economic status of electrical energy storage systems for this application and concludes that the Vanadium Redox Flow Battery offers great potential.

Chapter 6: Modelling of Vanadium Redox Flow Batteries

In many ways this chapter parallels chapters 3 and 4, but for an energy store, beginning by building up a model of the Vanadium Redox Flow Battery, validating it and then developing control methodologies for meeting the rigours of Grid Codes. The developed model of the flow battery is innovative for both its simplicity and its accurate representation of output voltage and energy efficiency. This flow battery model is integrated with the grid via a power converter for which a novel adaption allows the grid fault ride-through control to enhance the operation of the power converter at low voltage. Finally, a new integrated controller is developed that manages the battery's state of charge whilst also aggregating several different benefits of the storage technology in conjunction with the capabilities of an offshore wind farm.

Chapter 7: Frequency Response from Wind in 2020

The first half of the thesis advanced control methods for frequency response from wind power, demonstrating the technical capabilities of power converter interfaced plant. However, it also identified the challenge of providing reliable frequency response from an intermittent resource. Therefore, chapters 5 and 6 introduced the advances in energy storage technologies and the potential of the Vanadium Redox Flow Battery, in particular, to complement wind power. Ultimately, the direction the power system takes will be dictated by the economic merit of the different solutions. This chapter investigates the frequency response market, attempting to establish a value for this service, and then

conducts a scenario analysis to investigate the economics of wind power and storage acting in tandem. It is a chapter that applies the models developed in chapters 3, 4 and 6 with real wind data to assess the frequency response market. It also introduces a concept of operation for holding frequency response on a wind farm and an energy store that optimises their combined operation.

Chapter 8: Conclusions and Further Work

This chapter summarises the contribution of the thesis in the context of the transmission system, equipment manufacturers and academia. It restates the key contributions to knowledge and demonstrates how they contribute to the thesis as a whole. As with any research project, this thesis has raised many more areas that are worthy of further research and these are addressed here.

2 Wind Power and the GB Grid

2.1 Introduction

This chapter will demonstrate that the development of large scale wind power is likely to run contrary to the historic development practises of the Great Britain transmission system. Furthermore, the technology behind wind turbines and wind farms is advancing rapidly. This chapter introduces the technological challenges that arise when emulating synchronous machines' fault and frequency response behaviour.

Section 2.4 follows the trends in electrical systems at both the wind farm and wind turbine level. It highlights the increasing use of power converter technology, at both the transmission scale and the wind turbine scale, to meet the challenges of optimising wind farm yield and meeting modern grid codes.

Section 2.5 introduces, mathematically, the behaviour of the conventional synchronous machine under both voltage and frequency disturbances. This section highlights how the inherent fault and inertial behaviour of such generators, which currently provide the mainstay of the UK's power industry today, acts as an automatic stabiliser to the grid.

The grid of 2020 is likely to include many new offshore wind farms and section 2.6 introduces two consequential challenges. First the challenge to the UK's offshore wind farms to provide the same service as synchronous generators whilst presenting a power electronic interface to the grid. Second the challenge to the grid of providing the same security of supply with changing generation characteristics.

2.2 The Growth of the Wind Power Industry

Mankind has been harnessing natural power, to do work, for centuries, with the first conclusive evidence of windmills attributable to Persia in the 10th century. Carlin, Laxson and Muljadi [5] assert that electricity generation from the wind has been developing since at least 1888, when the 'Brush Wind Turbine' in Cleveland, U.S. produced up to 12kW peak power output. However, they also show that the grid connection of wind farms was not an option until the 1970's.

The oil price shock of the 1970's combined with air pollution and other environmental concerns, led to a surge of development of Wind Turbines in the 1980s. By the late 1980s machines such as NASA's MOD-5 had peak power generation ratings of over 1MW. Growing machine ratings led to economies of scale and a gradual decrease in the cost of wind power.

The improving economics of wind power combined with the increasing cost of fossil fuels has driven market growth for nearly two decades. Figure 2.1 and Figure 2.2 have been compiled from the Global Wind Energy Council's (GWEC) [6] annual statistics digests. Figure 2.1 shows that there was exponential growth in annual installations until 2010, when installations fell slightly. Whether 2010 comes to be seen as a blip, as a result of the global financial crisis, or supply chain issues; or else the end of wind power's accelerating growth remains to be seen. However, over this period, the development of wind has seen it become a mainstream energy source.

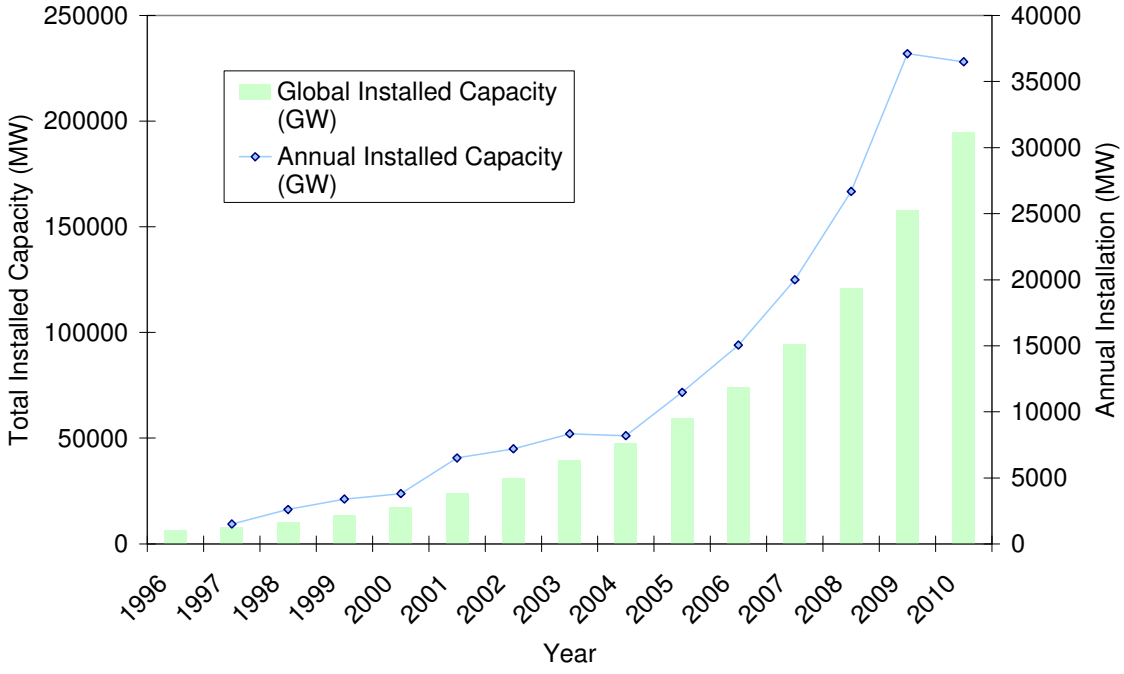

Figure 2.1: Global Installed Wind Power Growth

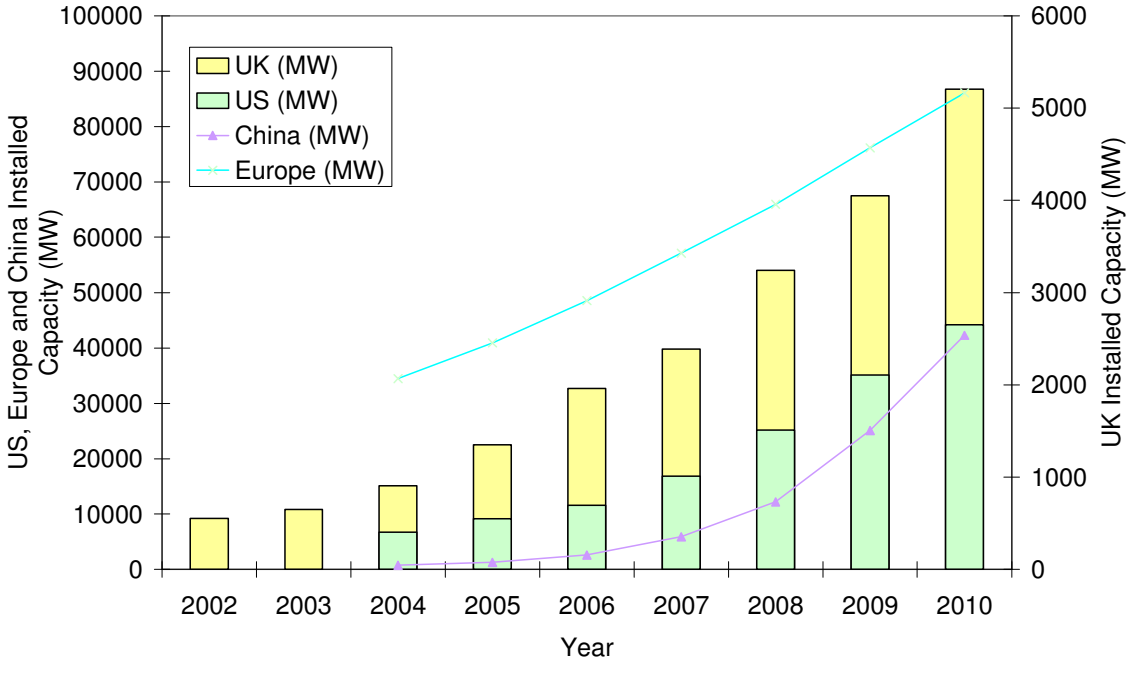

Figure 2.2: Wind Markets by Installed Capacity

Figure 2.2 shows the growth in wind power installations in the UK in comparison to the three key wind power markets: China, Europe and the USA. Europe's historic role in the early development of wind energy can be seen by the high number of installations pre-dating 2004. Whilst Europe continued to see significant growth in the wind industry since 2004, the USA showed an increasing appetite for clean energy sources in the last decade to become a second key market. The third key market resulted from China's fast growth rate, which has led it from relative insignificance in 2004 to being the principal market globally today. In comparison, the UK is a relatively small contributor to the wind market as a whole, but with a relatively small islanded grid system could see very high proportions of energy derived from wind.

2.3 The UK Wind Industry

There are two underlying drivers of the UK's wind industry: concerns surrounding climate change and concerns regarding security of the energy supply. International concern about the impact of rising atmospheric Carbon Dioxide levels has led to European legislation from the Commission of the European Communities [7] targeting a European-wide 20% contribution to energy supply from renewables by 2020. Additionally, the UK has historically depended on North Sea fossil fuel reserves to provide security of supply. However, Department of Energy and Climate Change (DECC) statistics [8] show that the North Sea gas output has been in long term decline owing to resource depletion, as shown in Figure 2.3. This decline has already made the UK a net importer of oil and gas and will lead to decreasing security of supply.

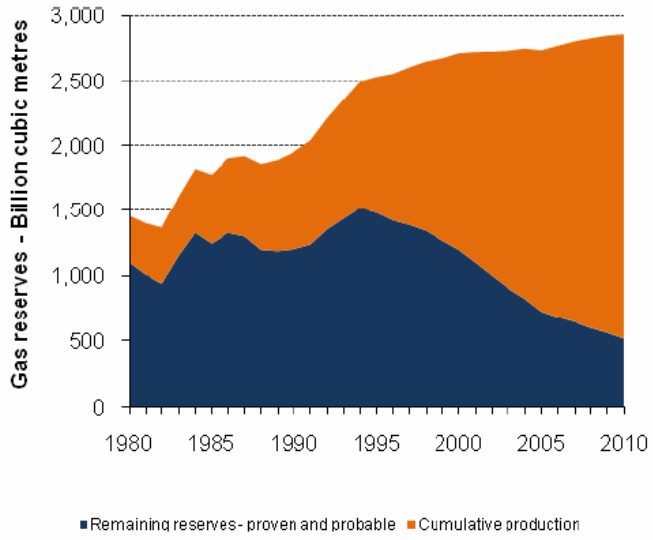

Figure 2.3: North Sea Gas Reserves according to DECC [8] statistics

The UK's relatively shallow continental shelf has traditionally aided the North Sea industries and also provides a significant advantage for offshore wind power deployment.

Shallow waters, close to shore, typically permit simpler foundations and less costly connection to the onshore electricity network. The UK has a relative abundance of such sites, as shown in Figure 2.4 from the Department of Business, Enterprise and Regulatory Reform (DBERR) [9].

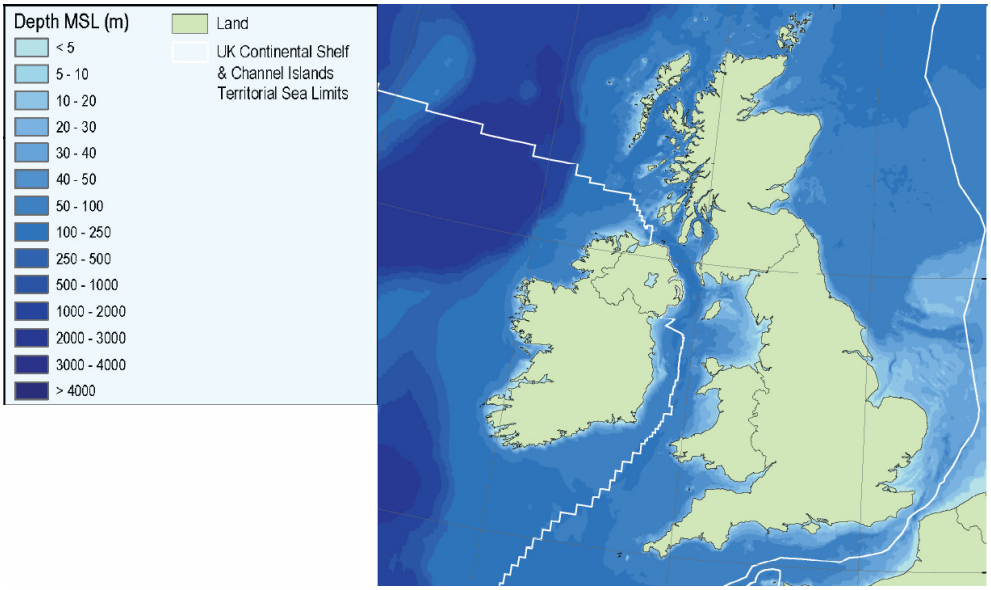

Figure 2.4: UK Continental Shelf Water Depth according to DBERR[9]

Landscape protection interests are cited by Toke [10] as a barrier to widespread onshore wind power development in the UK. However, he finds the UK has significant strengths including a central planning regime for offshore wind developments and the historic development of offshore energy assets. Overall Toke concludes that the UK is very likely to receive 20% of its electrical energy from wind power by 2020, but that distinctively, much of this power will come from offshore wind development.

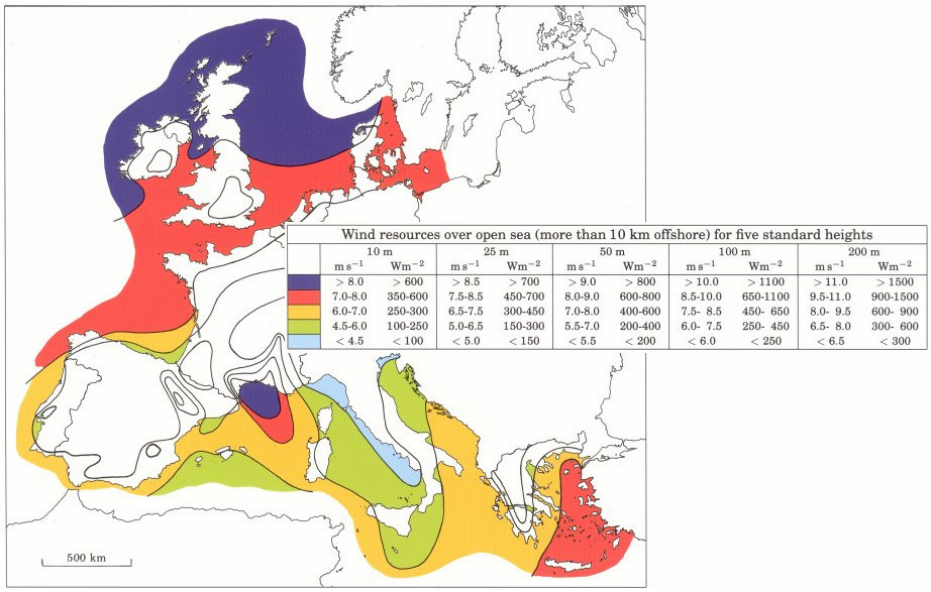

Figure 2.5: European Offshore Wind Resources, Copyright © 1989 by Risø National Laboratory, Roskilde, Denmark, used with permission

Figure 2.5 illustrates that the UK has the best offshore wind resource in Europe, which, coupled to the relatively shallow continental shelf makes it favourable for offshore development. As such, the Crown Estate has operated three rounds of leasing for development of offshore wind farms, using a zone based approach. These leases have a maximum cumulative capacity of 40GW, with single zones of up to 9GW.

The mass development of wind power in the UK is expected to have a significant impact on the operation of other generators. Figure 2.6, compiled by Pőyry Consulting [11] based on real demand and wind output data, shows that wind's intermittency will even require that base load generators be sufficiently flexible to reduce power output in periods of high wind. Meanwhile, in low wind periods, the back-up of gas fired plant would be critical. However, in a grid where wind could instantaneously supply upwards of 75% of demand, it is essential to understand the technology behind wind power plants and how it behaves in grid connected applications.

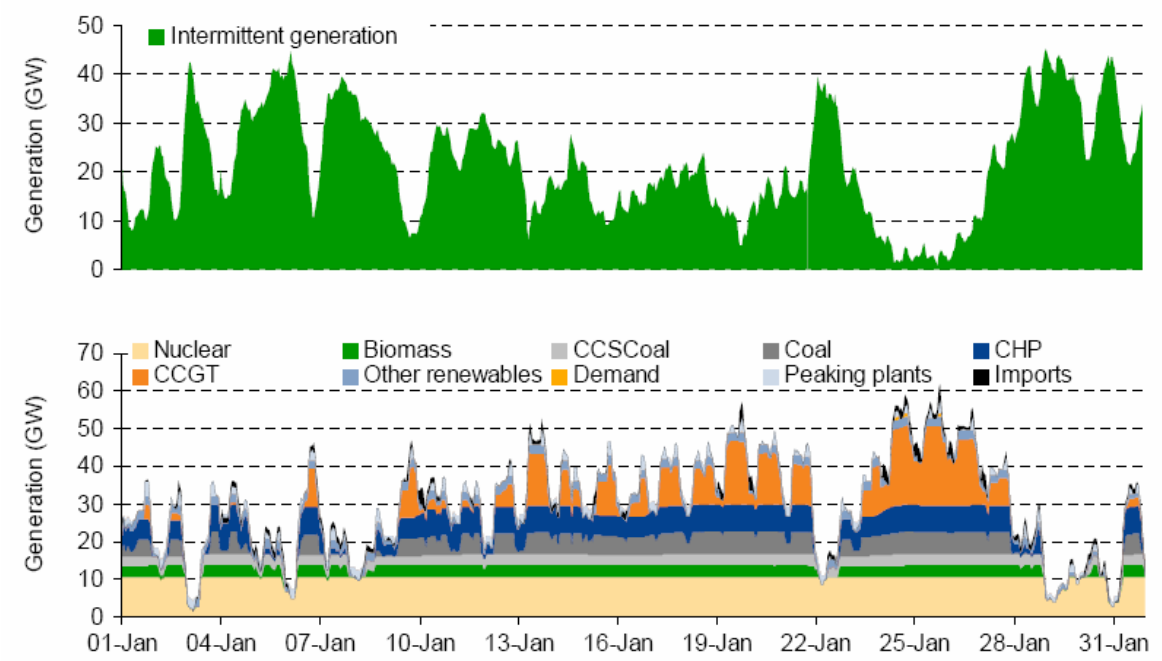

Figure 2.6: Pöyry's [11] Assessment of the Impact of Wind Generation on the UK in 2030

2.4 Wind Farm Development

The offshore wind farms that will provide a significant proportion of the UK's energy supply are likely to consist of hundreds of turbines, each individually connected to the wind farm's collector network. Figure 2.7 shows a typical wind farm arrangement, with individual turbines in series and 'strings' of turbines connected in parallel, however, overall, the power is collected and connected to the onshore grid at a single interface point. Often reactive power compensation is then required at the onshore substation such

as Insulated Gate Bipolar Transistor (IGBT) based Static VAR Compensators (SVCs). From a power system perspective, when the UK is subject to good wind conditions, these wind farms will dominate the power system and will need to provide some of the ancillary services that help to maintain a secure grid today.

The behaviour of the turbines is therefore critical to the operation of the wind farm as a whole. Additionally, the technology used in the wind farm's grid connection will affect the interface that the grid sees with the wind farm. These two aspects are explored in this section.

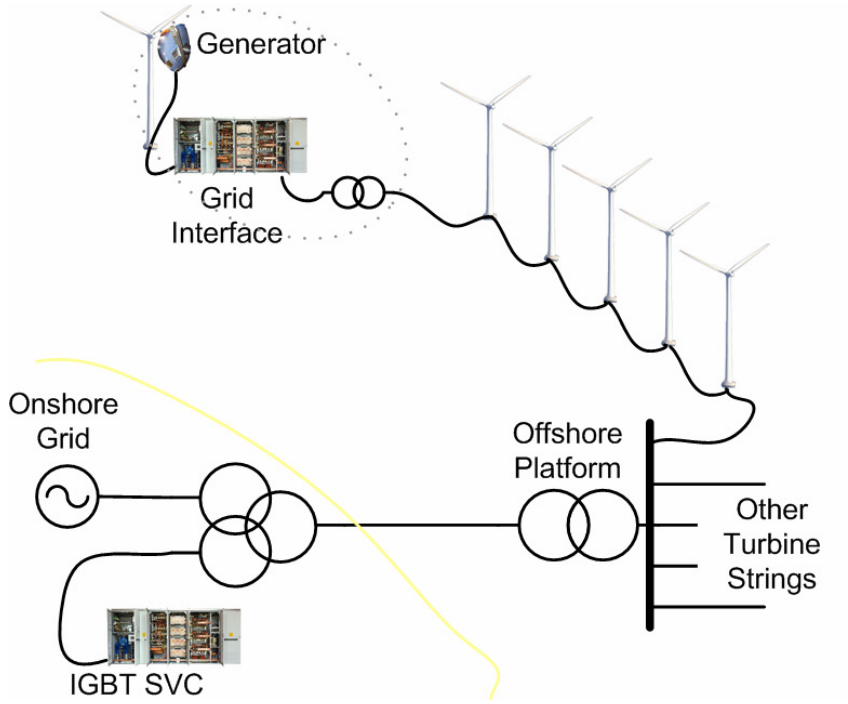

Figure 2.7: Typical Offshore Wind Farm Arrangement (Photos courtesy of GE Energy Power Conversion)

2.4.1 Wind Turbine Development

Hansen and Hansen [12] categorises wind turbines by two independent metrics, power control and speed control type. This work identifies the evolution of four distinct types of wind turbine, 1, 2, 3 & 4, these will be introduced in detail in sections 2.4.1.1 to 2.4.1.4. Figure 2.8, taken from this work, shows the gradual decline in importance of Type 1 and 2 wind turbines and the increasing use of later designs relying on power electronics, pitch control and variable speed generators. This is a trend which has only continued since 2005.

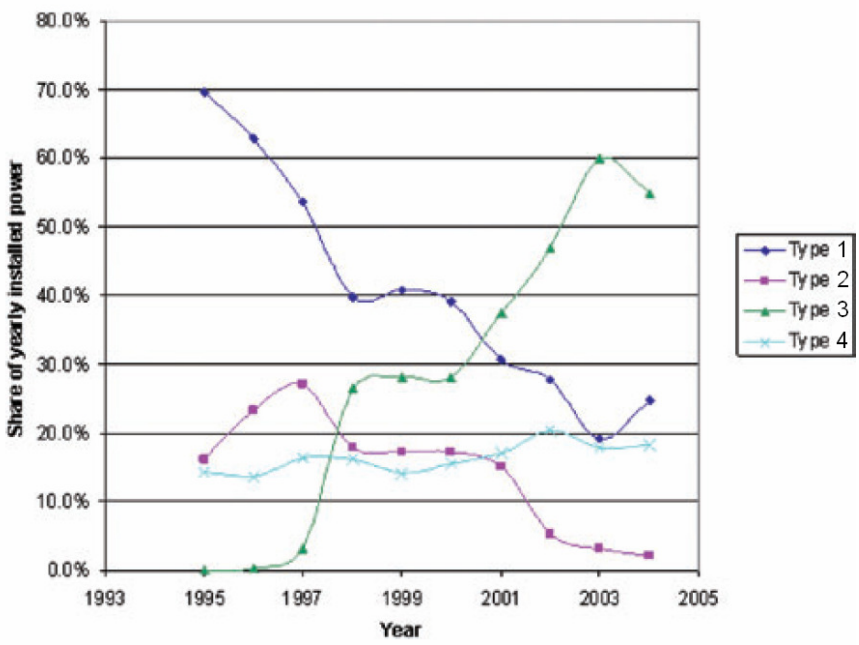

Figure 2.8: Market Share of the Different Wind Turbine Types (from Hansen and Hansen [12], with modified legend)

2.4.1.1 Type 1: Fixed Speed Induction Generator

The synchronous machine is the natural generator choice for conventional power stations; however, its rigidly fixed speed is not ideal for wind applications where rotational speed has a critical influence of energy yield. Soter and Wegener [13] have shown that instead, the induction generator, with a narrow range of speed determined by the slip, provides a slight improvement. This meant that most early turbines consisted of induction generators directly coupled to the grid, however, their limited speed range still led to them becoming known as Fixed Speed Induction Generator (FSIG) type turbines.

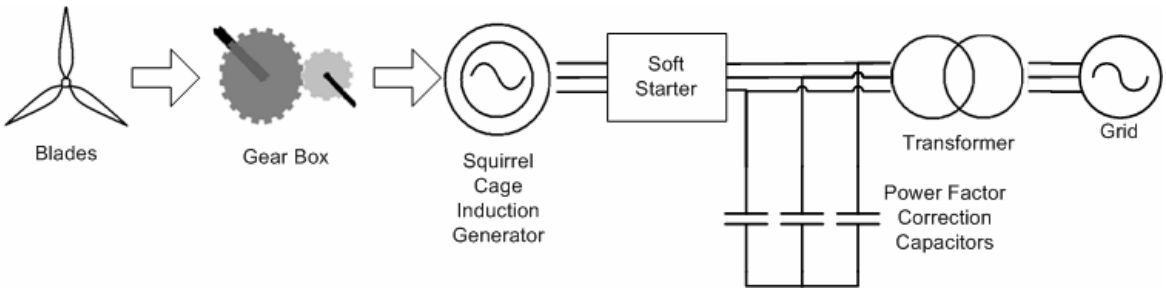

Figure 2.9: Fixed Speed Induction Generator Wind Turbine

Figure 2.9 shows the key components of an FSIG turbine. The grid's 50Hz, combined with a typically 4 pole induction generator mean that the high speed side of the gear box spins at around 1500 revolutions per minute (rpm). A high ratio, multi-stage, gear box would then step this down to around 20rpm blade speed for a large scale wind turbine. The induction machine's reactive power consumption necessitates power factor correction capacitors connected across the machine's terminals, to avoid drawing excess reactive

power from the grid. The blades are designed to aerodynamically stall when the wind speed exceeds the rated speed for the turbine, thus limiting power capture.

The fixed speed induction generator's simple design and low cost made it successful in the early development of the wind industry. However, it suffered from several drawbacks; first the fixed speed limited its capacity to capture all of the available wind power. Second, the machines tended to trip under large voltage disturbances, which whilst acceptable when wind was a small percentage of generation, became unacceptable as the industry advanced. Further, wind gusts led to both mechanical stresses on the turbine and power fluctuations into the grid.

2.4.1.2 Type 2: Variable Resistance Induction Generator

In order to improve on the FSIG's energy yield and reduce mechanical stress, the Variable Resistance Induction Generator (VRIG) was developed. This uses a wound rotor induction generator, with a switchable rotor resistance, allowing the turbine to be operated at variable speed. This design is shown in Figure 2.10. With a power electronic component switching the three phase rotor resistance, reasonable control over the torque-slip characteristic can be achieved. This meant that power quality improved and noise reduced.

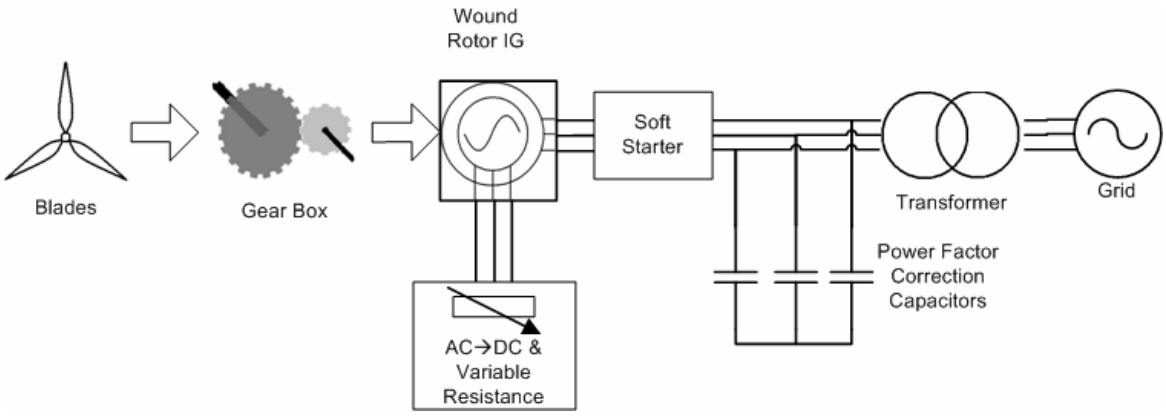

Figure 2.10: Variable Speed Induction Generator Wind Turbine

The VRIG still has drawbacks, however, as the range of speeds that the turbine can operate over is typically still narrow at around 10% of the rated speed according to Muljadi *et al.* [14]. This means that it is not possible to operate the turbine at the optimal aerodynamic point in all conditions. Further, the switchable rotor resistance is inherently high loss and the wound rotor induction generator is more complex and expensive than the equivalent squirrel cage machine would be.

2.4.1.3 Type 3: Doubly Fed Induction Generator

Given the additional expense of the wound rotor induction generator, combined with the falling costs of power electronics, the natural successor to the VRIG was the Doubly Fed Induction Generator (DFIG). In this design, the rotor of the induction generator is fed with a back to back power converter. Hansen and Michalke [15] have suggested this power converter only needs to be sized at 20-30% of the rating of the machine. This power converter rectifies the output of the generator to DC before inverting it back to AC. This means that, within the limits of the power converter, the rotational speed of the turbine blades is completely decoupled from the electrical grid frequency. This typically permits a ±30% speed range relative to synchronous and this decoupling allows optimal aerodynamic performance over the vast majority of the turbine's operating range.

The DFIG has many other advantages, as the power electronics can compensate the reactive power requirement of the generator and allow output operation at a range of power factors. However, the direct grid connection of the stator can cause high rotor currents and voltages during grid disturbances, the rotor could then feed these directly to the power converter, which is not designed for high over currents or over voltages. This sometimes necessitated the use of a crowbar, which short circuits the rotor to protect the power converter during faults. This increases significantly the control complexity of the turbine during grid voltage disturbances.

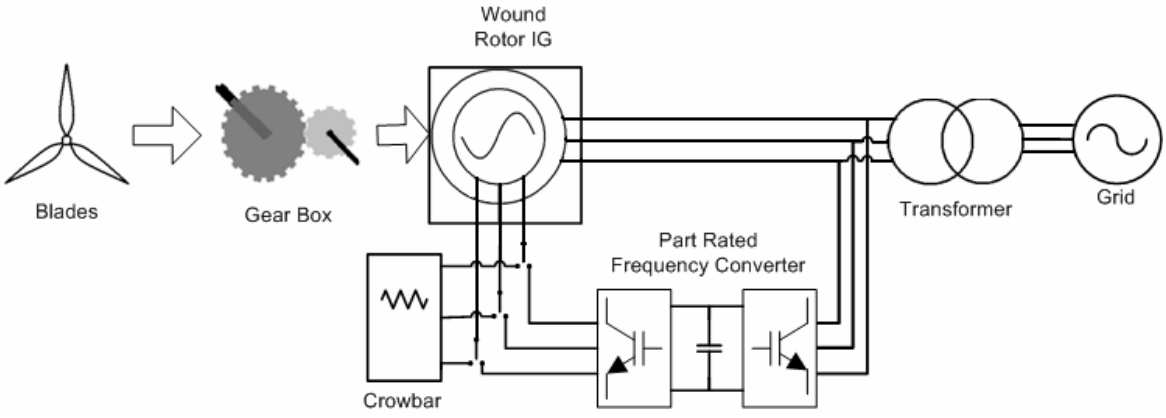

Figure 2.11: Doubly Fed Induction Generator Wind Turbine

2.4.1.4 Type 4: Full Converter

An alternative approach to achieving variable speed operation is to fully decouple the generator from the grid via a power electronic converter. Chen, Guerrero and Blaabjerg [16] conclude that such decoupling gives the advantage that they are less complicated to control and can provide active grid support during faults, without the drawback of DFIG

protection schemes. Three different generator types can be used under this scheme, which are outlined here.

- ***Fully Fed Synchronous Generators (FFSG)***

The early full converter wind turbines were developed around synchronous generators of the so called 'Enercon-concept'. The use of a full converter allows excellent grid side control, whilst the familiar synchronous generator has the benefits of rotor excitation control and fully decoupled speed. However, Jauch [17] has shown that such systems require active damping of the mechanical system as a result of this decoupling. Furthermore, Jauch asserts that grid codes have become more comprehensive requiring wind turbines such as FFSGs to provide more grid services such as power system damping.

Figure 2.12 shows the arrangement of a FFSG, either a single stage gearbox with medium speed generator, or even no gearbox with a low speed generator is possible. The direct-drive version benefitting from gear box elimination and hence reduced maintenance, but at the expense of a very large diameter machine. However, the rotor requires electrical excitation and the power electronics required can be expensive.

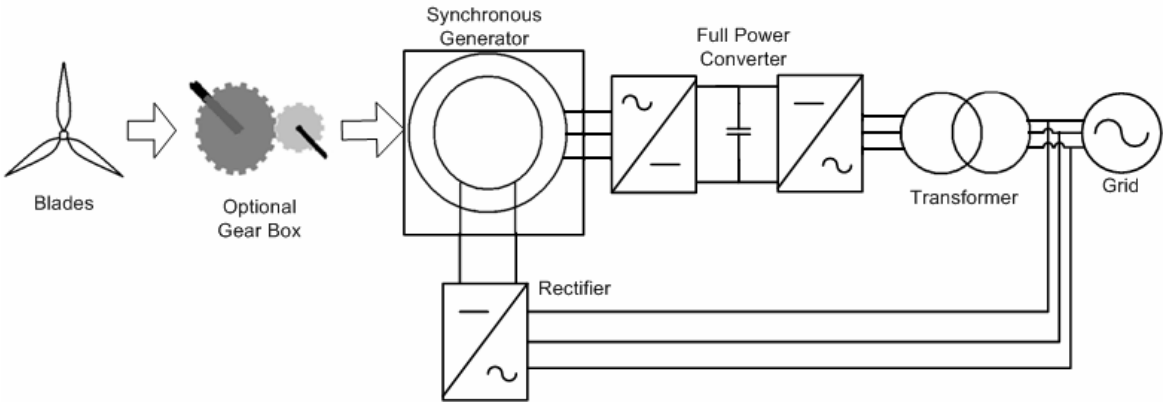

Figure 2.12: Fully Fed Synchronous Generator Wind Turbine

- ***Fully Fed Induction Generators (FFIG)***

An alternative full converter wind turbine concept was proposed by Peña *et al.* [18] comprising an induction generator with back to back converters. The simple, low cost of a squirrel cage induction generator, together with control to operate at optimal speeds therefore promised an improvement in turbine economics.

Molinas *et al.* [19] have shown that this type of turbine could meet the requirements of low voltage ride-through and other challenges of grid codes in the same way that the FFSG could. However, the rotor still requires excitation, increasing the stator currents and losses even in low wind conditions. Furthermore, this design typically requires a

multistage gearbox to increase the generator's rotor speed. Hence, a lighter machine is traded off against a more complex gearbox in comparison to the FFSG.

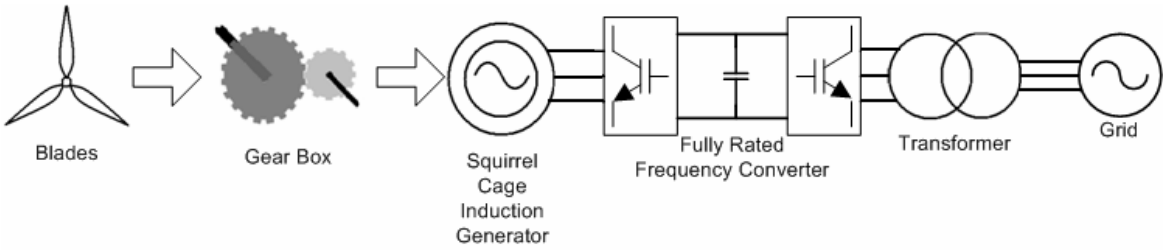

Figure 2.13: Fully Fed Induction Generator Wind Turbine

- ***Fully Fed Permanent Magnet Generators (FFPMG)***

Permanent Magnet Generators (PMGs), despite being considered for wind power applications for years, were only appearing in Megawatt class turbines from 2005 onwards, with GE and Siemens leading the way according to Akhmatov [20]. The magnetic rotor excitation offers the promise of higher efficiency, particularly at low loads. Further, high pole number machines can be designed to eliminate the need for a gearbox, whilst the power converter maintains the decoupling from the grid frequency. Figure 2.14 shows the key components of a PMG wind turbine system and highlights that gear boxes for this scheme are optional.

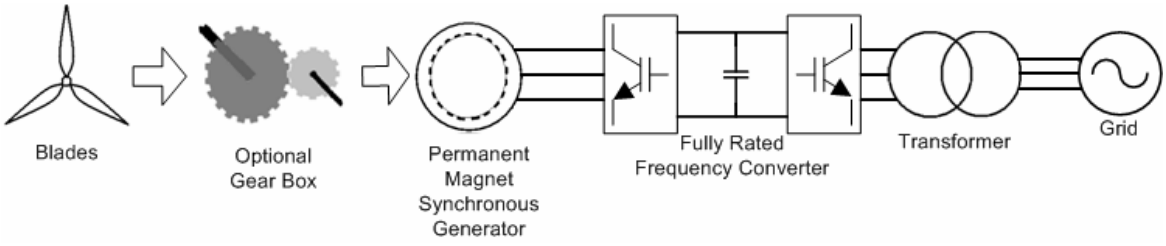

Figure 2.14: Fully Fed Permanent Magnet Generator Wind Turbine

Despite the PMG's many advantages, it still suffers two significant shortcomings; first the rotor excitation is fixed, meaning that the power converter must be designed carefully to match a specific machine. Second, for direct-drive designs, as the wind turbine blade diameters increase, their rotational speed falls; this means that multi-pole machines must have ever higher pole numbers. Hence, large PMG designs are likely to lead to rising generator diameters and masses.

2.4.1.5 Future Advances

In order to address the problem of the increasing mass of direct-drive turbines, high temperature superconducting generators for wind turbines have been proposed by Lewis and Műller [21]. This type of generator is estimated to lower the mass of the generator, compared to a standard PMG, by around 50%, whilst also potentially allowing further

efficiency gains through the use of superconducting wires. However, currently the costs of superconducting wires prohibit the uptake of these designs.

An alternative approach also aimed at reducing mass and volume is to integrate the power electronic converter with the stator of the generator, creating an advanced DC generator. Loddick [22] asserts that such a machine is particularly suited to wind power's torque-speed characteristic for low speed direct drive applications. Further, he proposes the integration of this technology with DC networks as a step forward for wind farms as a whole.

The common feature of proposed advances in wind turbine technology is the increasing integration of sophisticated power conversion technology with the generators. These power converters offer excellent controllability and flexibility but present inherently different characteristics to the grid to a conventional synchronous power plant.

2.4.2 Grid Connection

The changing electrical technology in wind turbines is not the only area that is affecting wind farms' integration with the grid. The UK's moves to offshore wind power will necessitate new transmission connections. Djapic and Strbac [23] identify that of the UK offshore wind farms allocated during the Crown Estate's licensing, some will be AC connected and some DC connected, whilst there are also some opportunities for interconnection of the various wind farm zones.

2.4.2.1 AC Connection

All of the round one offshore wind farms in UK waters were close to shore in shallow waters. This meant that AC connection remained the preferred grid connection option, with a variety of different voltage levels either available or in development for offshore applications. Morton *et al.* [24] looked at the possible configurations for Round Two developments, which are further from shore and generally in deeper water and concluded that all but two of these were likely to still be using a standard 132kV AC connection to shore with little or no redundancy.

Figure 2.15 shows that the AC connection of offshore wind farms is a simple design with a synchronous link either connecting into a distribution network at 132kV or being stepped up and connected into the transmission network at 275 or 400kV. The differences to an onshore wind farm's electrical system are two-fold, first additional power factor correction equipment is necessary at the point of connection to the grid to compensate for the offshore cable. Second, distribution network connected wind farms and small

installations of less than 50MW are not subjected to many of the regulatory requirements of Grid Code. Whilst most onshore wind farms avoid this burden, the majority of new offshore wind farms will not.

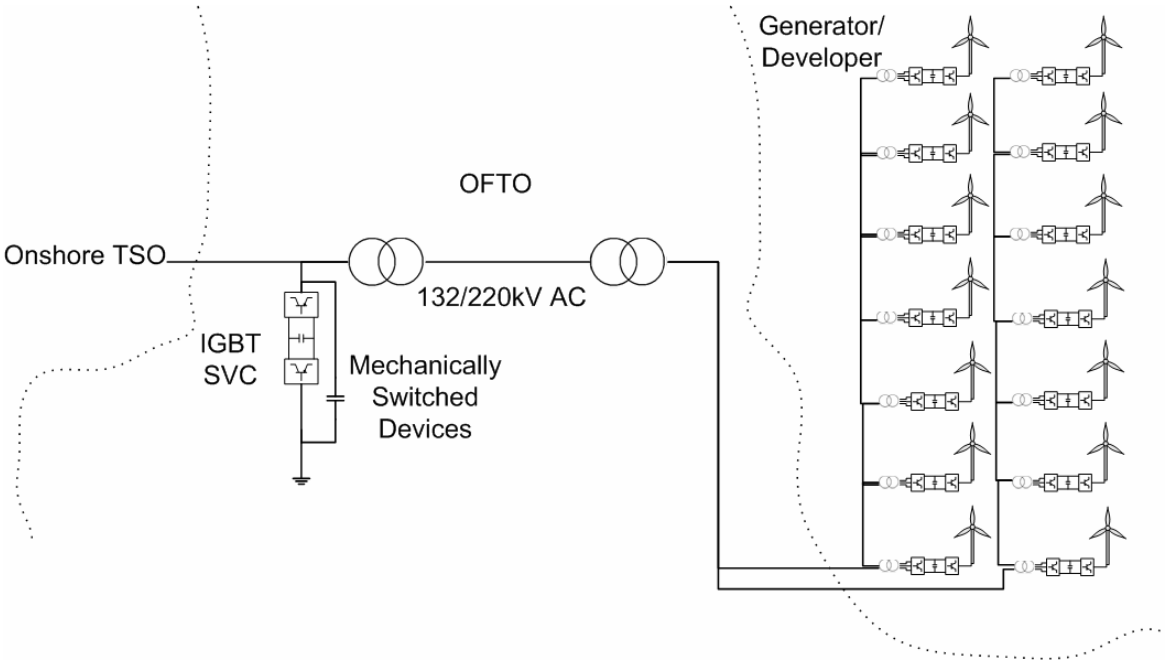

Figure 2.15: Offshore Wind Farm with AC Connection

Under the regime set up to deliver the offshore wind farm grid connections, the Offshore Transmission Owner (OFTO) would be responsible for delivering a connection from the HV side of the onshore step up transformer to the LV side of the offshore transformer on the offshore platform. Under such a scheme, the offshore generator can be considered as an extension to the GB onshore transmission network, albeit a remote one.

2.4.2.2 DC Connection

The use of a DC connection has the benefit of reducing the number of expensive subsea cables required for connection to shore. Further, over long distances AC connections require periodic voltage compensation and additional capacitive charging current, therefore suffering from higher losses. These effects mean that over long distances DC transmission is preferable to AC transmission.

Round three wind farms are again further offshore than the previous two rounds of Crown Estate licenses. This means that there is significant scope for DC grid connection. This removes the need for onshore power factor correction equipment owing to the four quadrant capability of the link's onshore inverter. Typically the offshore AC grid is still maintained as an AC grid at 50Hz owing to the standardised equipment for this

application. However, this offshore grid is decoupled from the onshore grid through high voltage power electronics (either conventional thyristor based or modern IGBT based).

Under this regime, the OFTO's scope of ownership would include the DC connection and associated converter equipment as shown in Figure 2.16. The control of real power remains the responsibility of the wind farm, whilst reactive power becomes the responsibility of the onshore High Voltage Direct Current (HVDC) converter owned by the OFTO. This effectively means that the offshore wind farm operates as an island isolated from the onshore network, with only control schemes linking the two, but the wind farm must still have appropriate real power control.

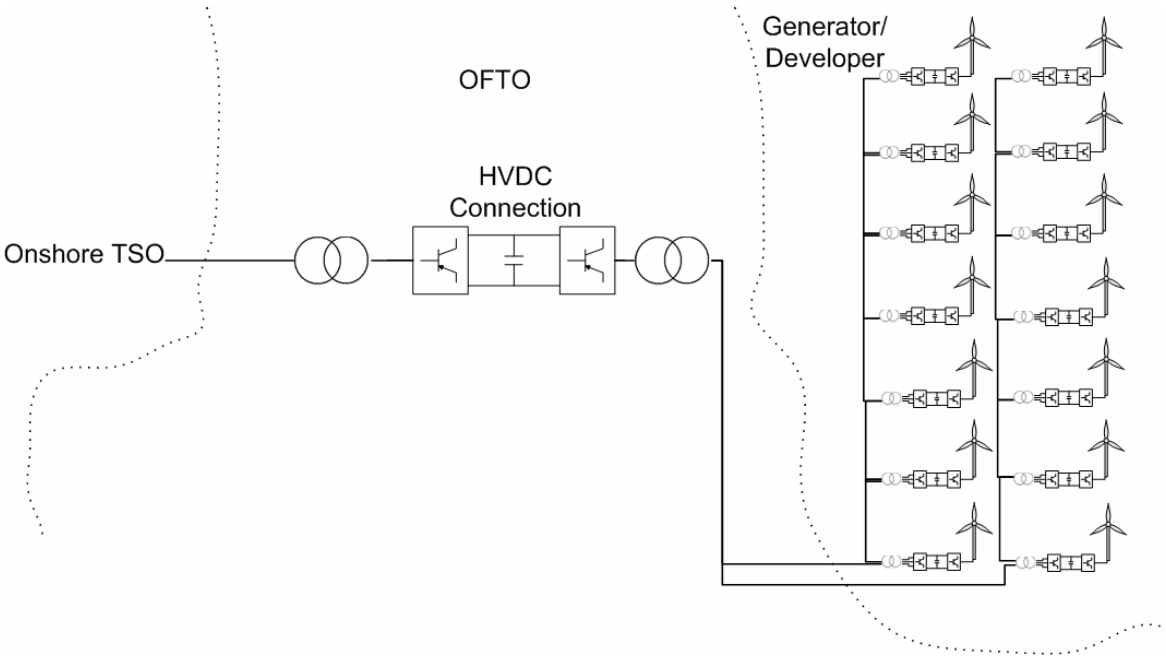

Figure 2.16: Offshore Wind Farm with DC Connection

2.4.2.3 Future Advances

The move towards HVDC transmission of offshore wind farms' power has led some, such as Zhan *et al*. [25] to propose DC collector networks for the offshore wind farm as well. Such a scheme claims higher efficiency, availability and power density than the existing AC collector networks. The offshore wind farm, as in the DC connected case, is largely isolated from the onshore grid and reliant on control schemes to provide the necessary real power control.

2.4.2.4 European Supergrid

The widespread development of wind power has led to the proposal, originally by Airtricity, that a pan-European HVDC grid could lower the costs of integrating renewable energy into the grid. This concept has now been developed into a more detailed design.

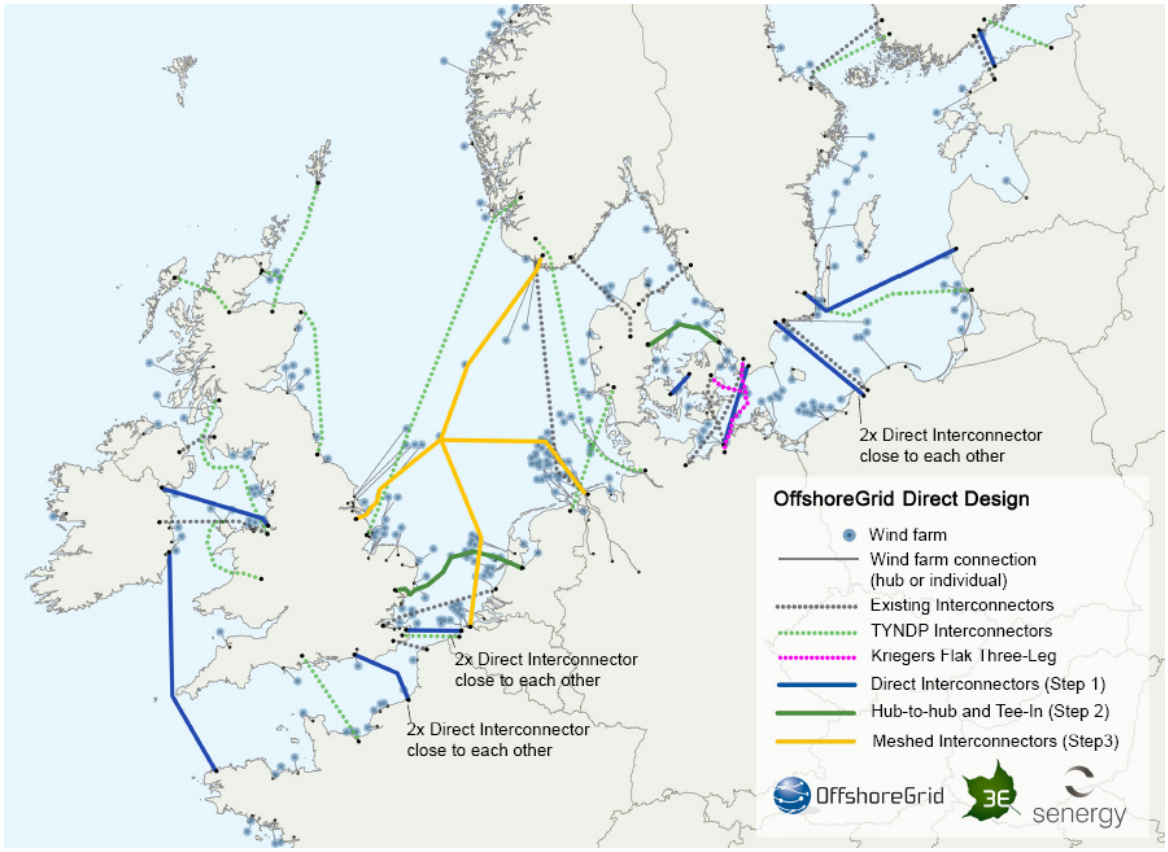

Figure 2.17: A map of the offshore supergrid from Offshore Grid [26]

Figure 2.17 shows this scheme, as proposed by Offshore Grid [26], which would greatly increase the integration of Europe's energy markets as well as allowing greater cross-border power transfers. Technically, however, it could leave offshore wind farms connected to multiple countries with differing real power control obligations to each nation. Offshore generation would no longer be just an extension to the UK's grid, but part of a much wider scheme of interconnection across Europe.

2.5 Changing Generation Characteristics

2.5.1 Conventional Synchronous Plant

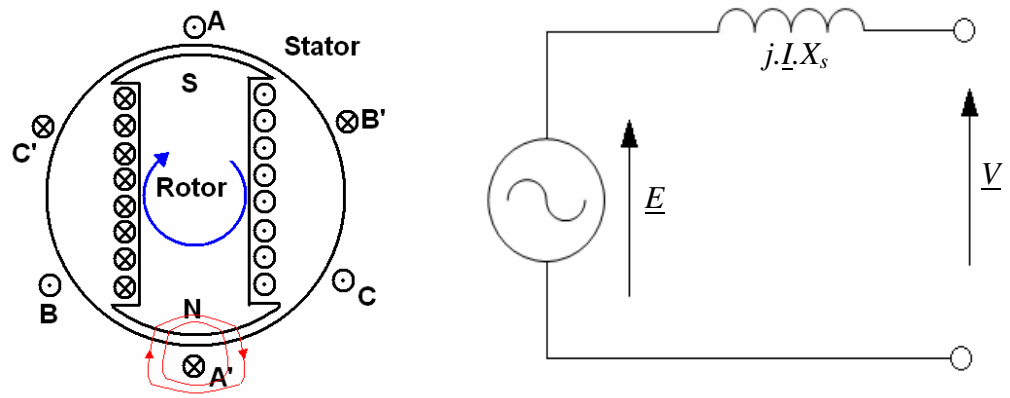

Figure 2.18: Synchronous Generator and Single Phase Equivalent Circuit

The majority of the UK's conventional power plants use steam or gas turbines to drive synchronous generators directly coupled to the electric grid. As the synchronous machine has provided the mainstay generator for the UK's power grid, understanding its basic behaviour is fundamental to understanding the changes that wind farm technology will bring to the grid. Some of the key grid interactions of these plants can be understood by considering an idealised synchronous machine as shown in Figure 2.18 and considering a single phase representation of the machine, which assumes that the system is balanced.

The three-phase grid voltage drives the current in the stator windings to produce a magnetic field in the machine's air gap that rotates at a speed (ω_s) defined by the grid frequency (f_{grid}) and the machine's pole pairs (p). This is shown in Equation 2.1 and Equation 2.2.

Equation 2.1 $$\omega_s = \frac{2 \cdot \pi \cdot f_{grid}}{p}$$

Equation 2.2 $$\underline{B_s} = \hat{B}_s \cdot \cos \omega_s \cdot t$$

The rotor of a synchronous machine is fed with a DC current which sets up a fixed magnetic field, in effect as a dipole magnet. Careful design of the rotor windings ensures that the rotor field is sinusoidally distributed round the air gap. When this rotor is driven to rotate, either motored by the stator field or by the action of a prime mover, then the dipole rotates, setting up a second sinusoidally rotating component of magnetic field in the machine's air gap as in Equation 2.3. The rotor and stator magnetic fields rotate synchronously, ensuring that the total field also rotates with a sinusoidal distribution.

Equation 2.3: $$\underline{B_r} = \hat{B}_r \cdot \cos(\omega_r \cdot t - \theta)$$

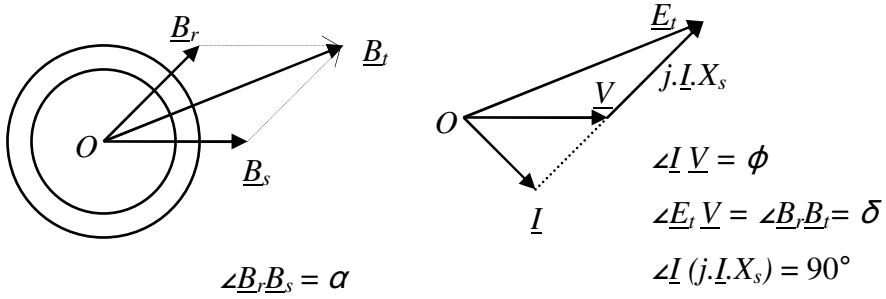

Figure 2.19: Synchronous Machine Vector Diagrams

The total rotating air gap magnetic field, comprised of both the stator and the rotor components, leads by Faraday's law ($E = -N \cdot \frac{d\psi}{dt}$), to a back Electromotive Force (EMF) induced in the stator windings, E, as given in Equation 2.4.

Equation 2.4 $\underline{E} = \hat{E} \cdot \cos(\omega_r \cdot t + \delta)$

Figure 2.19 shows the magnetic field (left) vector diagram for the case of a rotor field lagging the stator field, alongside the phasor diagram for the machine (right).

The magnetic torque acting on the rotor can be defined according to the equation for the magnetic moment acting in a magnetic field, $\underline{T} = \underline{m} \times \underline{B}$. Hence the torque can be seen to be given by Equation 2.5 where *D* is a constant.

Equation 2.5 $T = D \cdot \hat{B}_r \cdot \hat{B}_s \cdot \sin\alpha$

By considering that from the vector diagram $\hat{B}_s \cdot \sin\alpha = \hat{B}_t \cdot \sin\delta$

Equation 2.6 $T = D \cdot \hat{B}_t \cdot \hat{B}_r \cdot \sin\delta$

The implication of this is that the torque produced by the synchronous machine is dependent upon the angle between the rotor magnetic field and the total magnetic field, also known as the load angle. Hence, for steady torque production, this angle must be constant and the rotor and stator must be rotating synchronously. Furthermore, the torque from the synchronous machine varies in a sinusoidal relationship with the load angle.

This can also be deduced by considering the phasor diagram, the back EMF is defined as in Equation 2.7.

Equation 2.7 $\underline{E} = \underline{V} + j \cdot \underline{I} \cdot X_s$

The real power output from the machine can then be defined by Equation 2.8.

Equation 2.8 $P = T \cdot \omega_s = 3 \cdot \tilde{V} \cdot \tilde{I} \cdot \cos\phi$

By considering the phasor diagram trigonometric relationships:

Equation 2.9 $|\underline{E}| \cdot \sin\delta = |\underline{I}| \cdot X_s \cdot \sin(90 - \phi) = |\underline{I}| \cdot X_s \cdot \cos\phi$

So $\frac{|\underline{E}| \sin\delta}{X_s} = |\underline{I}| \cdot \cos\phi$ from Equation 2.9 and hence:

Equation 2.10 $P = T \cdot \omega_s = 3 \cdot |\underline{V}| \cdot \frac{|\underline{E}| \cdot \sin\delta}{X_s}$

So the torque can be expressed as:

Equation 2.11 $T = \frac{3 \cdot V \cdot E}{\omega_s \cdot X_s} \cdot \sin\delta$

Equation 2.11 shows that the generator torque is critically dependent on the angle between the generator's internal EMF and the network voltage.

2.5.2 Grid Faults

The phasor diagram of Figure 2.20 shows the effect of a grid voltage that is transiently suppressed from its nominal rating. The rotor field windings initially continue to be fed with the same DC current, so the rotor magnetic field is unaffected, supporting the internal EMF. However, to compensate for the reduced grid voltage, an increased reactive current is drawn from the machine, dropping voltage across the stator reactance and closing the phasor triangle. An Automatic Voltage Regulator (AVR) could then act to control to voltage or reactive power fed into the grid, but there is still an initial current increase. This current in-feed helps to trip protection devices in the event of a grid fault.

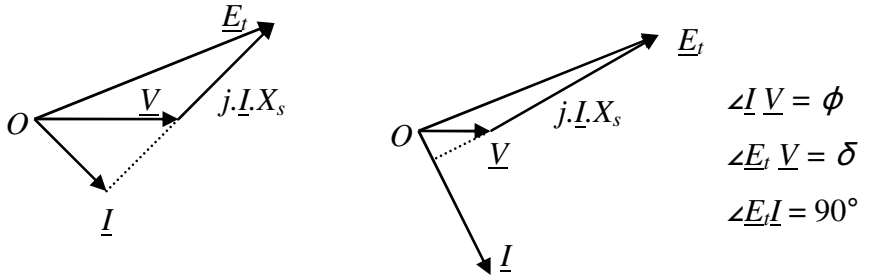

Figure 2.20: Phasor Diagram under Normal (left) and Suppressed (right) Voltage

2.5.3 Grid Inertia

Equation 2.11 considers the torque dependency on the machine's load angle, but this inherently assumes constant frequency behaviour of both the rotor and the stator. A reduction in grid frequency has the effect of gradually changing the angle between the stator and rotor magnetic fields, and therefore increasing the load angle of the machine.

This relationship between the machine's frequency and torque means that falling grid frequency automatically increases the torque, provided it does not exceed the maximum torque at 90°. This torque increase draws kinetic energy ($KE = \frac{1}{2} \cdot J \cdot \omega^2$) from the rotor and accompanying spinning mass. Given that the machine's rotor must ultimately remain synchronous to the grid's frequency, the power output from the machine can be approximately found by differentiating the rotor's stored kinetic energy with respect to time as shown in Equation 2.12. This means that the power output of a synchronous machine has been shown by Morren, Pierik and de Haan [27] to be broadly proportional to the rate of change of frequency, acting as an automatic stabiliser to rapid frequency changes.

Equation 2.12 $$\frac{d(KE)}{dt} = \frac{1}{2} \cdot J \cdot 2\omega \cdot \frac{d\omega}{dt} = J \cdot \omega \cdot \frac{d\omega}{dt}$$

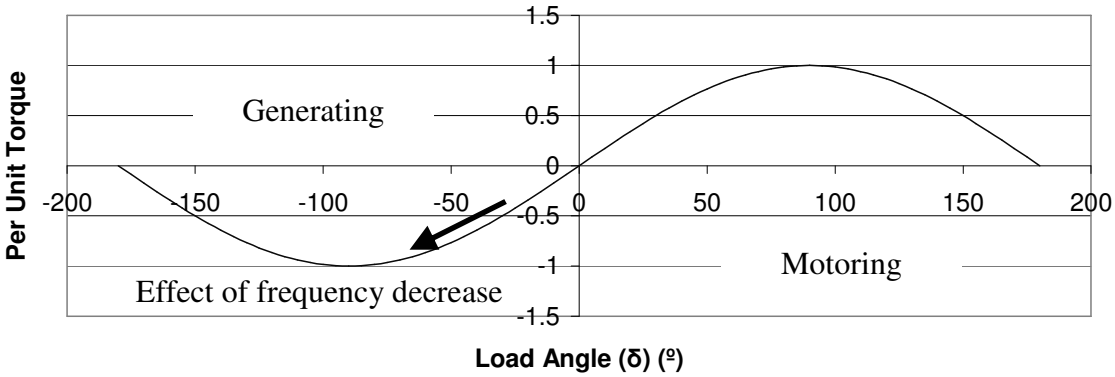

Figure 2.21: Effect of Frequency Decrease on Load Angle and Torque

Specifically, however, the machine's output will be dependent on the change in torque, which is in turn dependent on the change in load angle. The torque will follow the sinusoidal load profile as the load angle increases or decreases as shown in Figure 2.21. A frequency difference between the rotor and stator fields creates the change in load angle. This acts to smooth out the inertial contribution to rapid frequency deviations as the torque does not step from one level to another.

2.5.4 Grid Frequency

Grid frequency changes result from imbalance between generation and demand, and whilst the inertia of synchronous machines helps to arrest rapid deviations, ultimately the imbalance must be eliminated before the frequency can be brought back to target. With a synchronous generator, this is achieved through governor action, whereby a generator will increase or decrease its output in proportion to the magnitude of the frequency excursion, through increased steam raising or boiler action.

2.6 A Challenge for the GB Grid

2.6.1 The UK's Offshore Wind Farms

Section 2.4.1 highlighted the move in wind turbine technology towards increasing use of power electronics. These power converters involve extremely fast control loops that are flexible to react rapidly to desired changes. Fast control is also essential because of power electronic switches' sensitivity to over current and the need to rapidly reduce currents in the event of a fault on the output. The impact of the fast control of a power converter is to limit the in-feed current in the case of a fault to a much lower level than might be the case with a traditional synchronous generator.

The power converters are also deliberately designed to decouple the rotational frequency of the blades from the grid frequency so as to maximise the energy capture from the wind. Yet this removes the inertia to frequency changes that synchronous machines inherently provide to stabilise the grid. A frequency change on the grid side is rectified to DC and not automatically seen by the machine side. Hence, the kinetic energy of the blades does not automatically stabilise the grid.

In response to supply shortfalls causing a frequency change, a wind turbine's output is limited by the available wind power. Whereas a conventional synchronous plant could increase its output by burning more fuel or steam raising, the wind turbine has no equivalent extra resource. This means that for a wind turbine to provide low frequency response, it would have to deliberately operate at a reduced output. This involves spilling wind energy in order to hold a margin and have the potential to increase its output in response to a falling frequency, but does not have associated fuel savings.

These three differences, which are inherent to the design of wind turbines, and provide them with exceptional controllability, mean that power converter interfaced wind turbines behave very differently to grid disturbances to the familiar synchronous generators.

Section 2.4.2 highlighted the trends in grid connection which will further distance offshore wind farms from the grid of today. The increasing use of DC transmission and potentially distribution will lead to isolation of the offshore wind farms from the behaviour of the onshore grid. This provides not only technical challenges, to ensure the continued security of the GB grid, but also regulatory ones.

Today the effects of rising wind power levels are already beginning to be felt, with the National Grid having to act to constrain wind in 2011 to ensure the security of the GB system according to the Renewable Energy Foundation [28]. With ever growing levels of wind power, the challenges of managing the system will continue to grow and challenges other than constraints will emerge. These challenges, combined with the technological differences of wind farms will mean that the grid in 2020 with 33GW of offshore wind is likely to have to look very different to the grid of today. The challenge is to deliver this whilst protecting the security of supply and grid stability experienced today.

2.6.2 The Grid's Frequency Challenge

Major frequency deviations on a power system usually occur as the result of a large generator or load tripping and disconnecting. Such events are currently extremely rare; however, the GB grid was shown to be susceptible to sizeable frequency deviations by the

events of 27th May 2008. On this occasion, the UK's largest nuclear plant, Sizewell B, tripped offline shortly after a coal plant of 345MW. This led to a supply shortfall of around 1582MW having to be picked up by responsive generators. This is just within the 1600MW maximum loss that the GB grid is typically secured against.

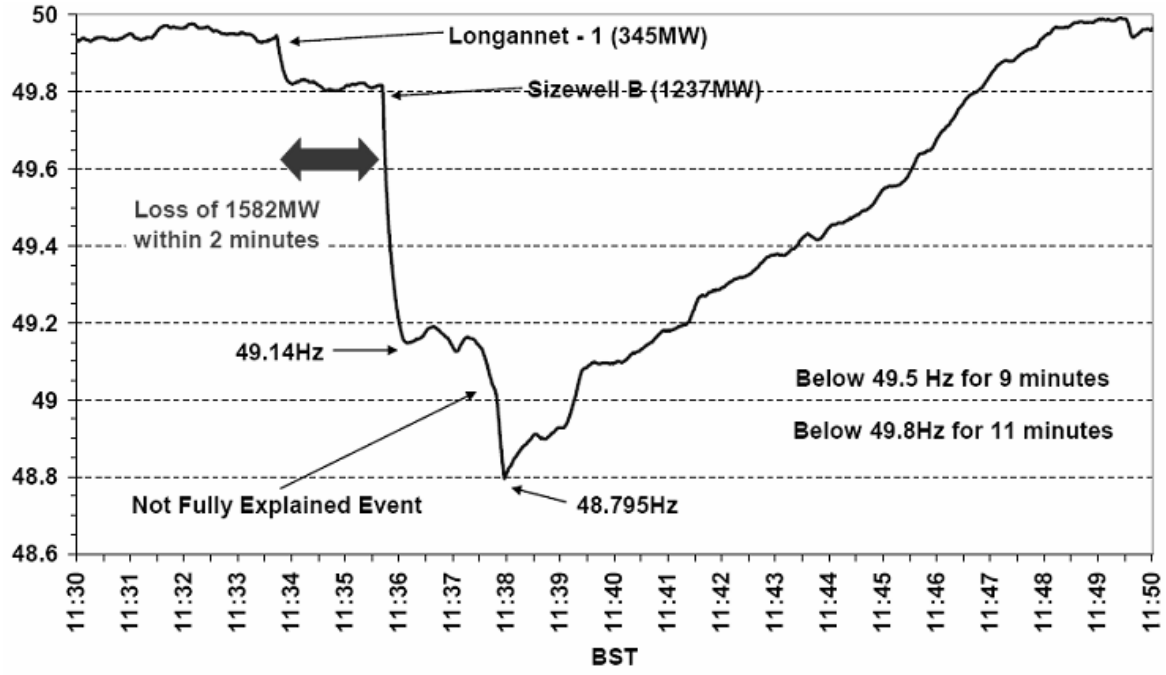

Figure 2.22: GB System Frequency 27th May 2008

After the loss of these two generators, the subsequent frequency fall, whilst initially arrested, then accelerated again and was ultimately only stopped by the activation of automatic demand disconnection at 48.8Hz. This further frequency fall is not totally explained, however, the official report, from National Grid [29], found that "The unexpected loss of a significant amount of small embedded generation resulted in a total loss of some 1993MW in 3.5 minutes". This embedded generation was outside of the scope of the transmission system Grid Code and therefore was subject to G59, which the National Grid [30] review found at the time set recommended frequencies at which generation should trip; this is the reverse philosophy to that applied in Grid Code. It brought forward the activation of automatic demand disconnection.

Immediately after the loss of each generator, the inertia of the large number of synchronous machines on the system helped to slow the Rate of Change of Frequency (ROCOF) such that the maximum ROCOF was 0.073Hz. This provided time for other plant to increase their output powers to compensate for the lost plant and prevented the level of demand disconnection being worse. This event demonstrates the importance of synchronous machines' inherent inertia in securing the grid.

In the run up to 2020 the UK may have single generation connections of 2GW as a result of the offshore wind development plans. Partly as a consequence of this, the power system will be secured against a loss of 1.8GW by National Grid [31] and will also have to deal with connections from wind turbine technologies with very different grid interfaces to conventional generation. In a small islanded system, where frequency can already see significant deviations, this thesis addresses what future offshore wind farms can do to support the grid's frequency stability and whether energy storage is ready to provide a more robust solution.

2.6.3 Power System Oscillation

Ashton *et al.* [32] have shown that the UK transmission system currently experiences a number of power system events due to circuit switching as well as a significant major oscillation between the generators of Scotland and those of England and Wales. Currently limited capacity across the North/South boundary does not help this situation. Figure 2.5 shows that the UK's best wind resources are located in the North, beyond the constraint boundary. Development of these resources will lead to increased stress of the system and is part of the cause of National Grid's installation of a wide area monitoring system based on phasor measurement unit installations at some substations.

The installed monitoring system has been shown by Ashton to have measured the time delay as a large frequency deviation rippled through the system following a loss of a generator. A time delay of 0.65s was observed between the frequency deviation occurring at the closest substations to the lost generator and those furthest away. The monitoring system provides a large amount of real time data which will in future enhance the system operator's visibility of events such as that in Figure 2.22, the challenge will be to use that data to secure the system's stability in the face of these multiple challenges.

2.7 Potential Application of Energy Storage?

Concurrent with the development of large scale offshore wind power, National Grid's "Gone Green" scenario anticipates a renewed development of Nuclear Power in the UK. These two factors contribute to National Grid's [33] projections that the GB system requirements for frequency response reserves will be significantly increased before 2020, as outlined in Figure 2.23. This increase in low frequency response requirement, to cover loss of generation, together with the high price that wind power would require to provide such services, suggests that the value of frequency response will inevitably significantly increase in the coming decade.

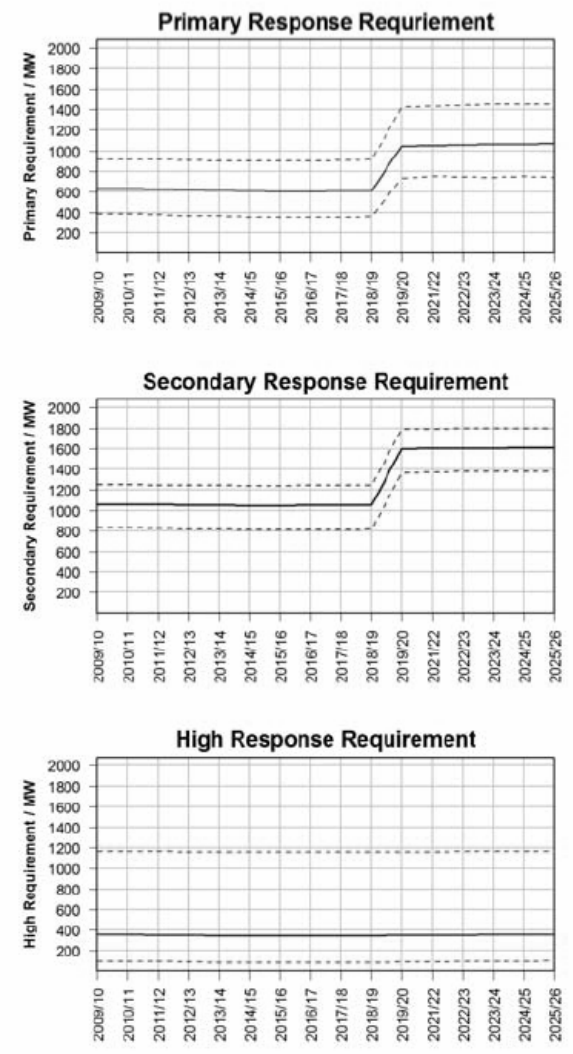

Figure 2.23: National Grid's [33] Projection for Requirement for Frequency Response (The solid line represents the typical requirement, with maximum and minimum requirements shown by the dashed lines)

The increasing importance of providing balancing services to transmission systems is not a phenomenon specific to the GB system. Walawalker, Apt and Mancini [34] investigated the economics of frequency regulation services in New York and concluded that there were "significant opportunities" for the application of flywheels to frequency regulation in New York state. They also noted the developments of Beacon Power towards commercial application of frequency response services with flywheels in both California and New York states. Alongside Beacon Power, other energy storage manufacturers, such as A123 Systems, according to Vartanian and Bentley [35], have been investigating the frequency response market as a potential opportunity for their products.

Oudalov, Chartouni and Ohler [36] of ABB Ltd. have had a detailed look at the potential for energy storage solutions to provide primary frequency control (*i.e.* short time-scale only) on part of the European transmission system. Their comparison of Vanadium Redox Flow, Sodium Sulphur, Lead Acid and Nickel Cadmium batteries concluded that Lead

Acid is viable for this application, in conjunction with dump resistors for accommodating high frequency response when the battery is fully charged. However, their analysis was limited to primary frequency control and therefore considered only relatively short timescales. Nevertheless, this further demonstrates the increasing interest that manufacturers are taking in the frequency response markets.

Despite the growing interest of manufacturers, Beacon Power, who backed by a US government loan guarantee program built their 20MW flywheel based frequency regulation plant in New York State, have recently filed for bankruptcy according to Hals and Hampton [37]. Their brief exploration of this opportunity showed that the commercial environment for application of flywheels to frequency response is not viable yet in the U.S.A.. Their ultimate failure could be put down to technology, timing or both; but they have perhaps pointed to a possible future for power systems; with generators providing bulk energy and energy storage systems providing balancing services.

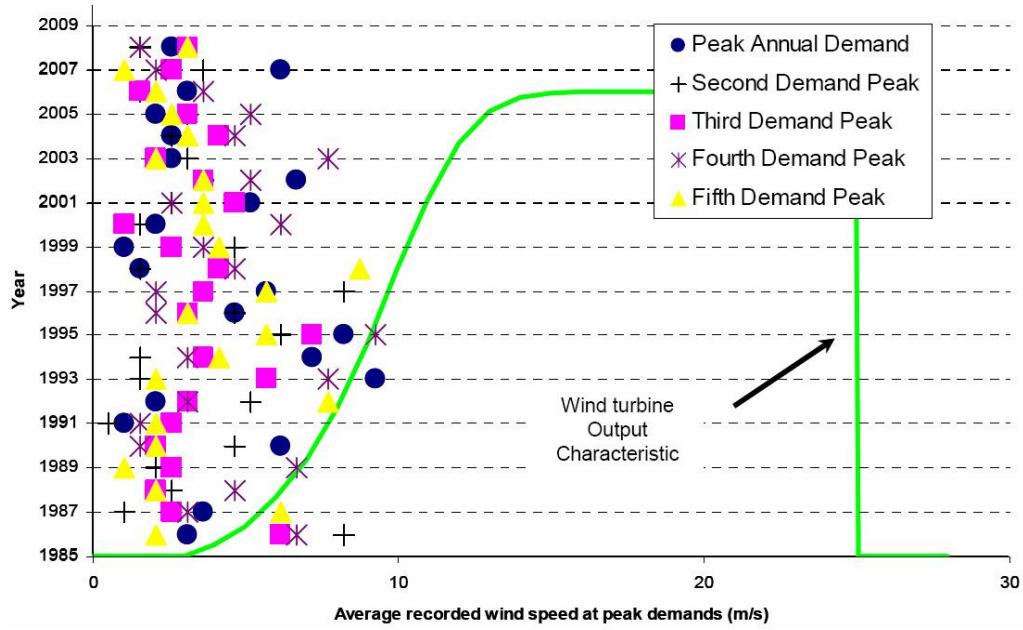

Figure 2.24: Wind Output During Periods of Peak System Demand according to National Grid [38]

In addition to the potential opportunity for energy storage to contribute to system balancing, there are longer timescale opportunities emerging for energy storage. Figure 2.24, from National Grid [38], shows a typical wind turbine output power profile against wind speed, superimposed on the graph are the measured wind speeds during the top five annual power demand periods for the years 1985 to 2008. The y-axis represents both the year and the power output from a typical wind turbine. It highlights that in the 25 year period considered, the average wind speed during the five half-hour periods with highest demand was never above 10m/s. Based on the typical wind turbine's power production curve this illustrates that it would be likely that during peak demand periods wind would

be operating at less than 50% of its capacity. This illustrates the need for firm power capacity.

The broad correlation between low wind speeds and high system demand, during winter anti-cyclones in the UK, illustrates the need that the UK has for firm capacity to provide for the power system's peak demands. This is an area where longer term energy storage may become increasingly technically and economically necessary.

One of the most comprehensive analyses of the application of energy storage in power systems is by Eyer and Corey [39] of Sandia National Laboratories. Their work identifies the need to aggregate different energy storage applications in order to develop "Value Propositions" that are economically viable. One of the eight value propositions they investigate is "Renewables Energy time-shift plus Electric Energy Time-shift plus Electric Supply Reserve Capacity". This value proposition is the only complementary application including supplying reserve power to the power system. It involves using an energy store to provide reserve power at night, whilst charging, and then dispatching that energy into the peak demand periods, such as those of Figure 2.24. By charging at night the store can not only take advantage of typically cheap night time power prices, but can also offer greater capacity for fast reserves as it can revert from charging to discharging.

In the context of this application, the next section will explore the capabilities of different storage technologies to contribute to solving these challenges as wind power deployment grows.

2.8 Summary

The development of the wind industry in the UK is likely to see significant offshore deployment. The technology for both offshore turbines and offshore grid connection is developing towards solutions that decouple the generators from the onshore grid through power electronics incorporating interim DC stages. This means that these offshore wind farms do not provide some of the inherently stabilising actions that a conventional synchronous machine would. This will lead to challenges for the control of offshore wind farms in order to maintain the frequency stability of the onshore grid and to provide fault in-feed currents. These are challenges that the rest of the thesis sets out to address.

3 Modelling of Full Converter Wind Turbines

3.1 Introduction

The growth in wind power on power systems has necessitated development of wind turbine models that are appropriate for the study of grid interactions. Slootweg *et al.* [40] have characterised the key elements that require modelling for power system studies. This chapter therefore covers the development of a suite of full converter wind turbine models appropriate for power system studies. Figure 3.1 illustrates the key elements of such a model, which allows studies from the raw wind input to the grid electrical output.

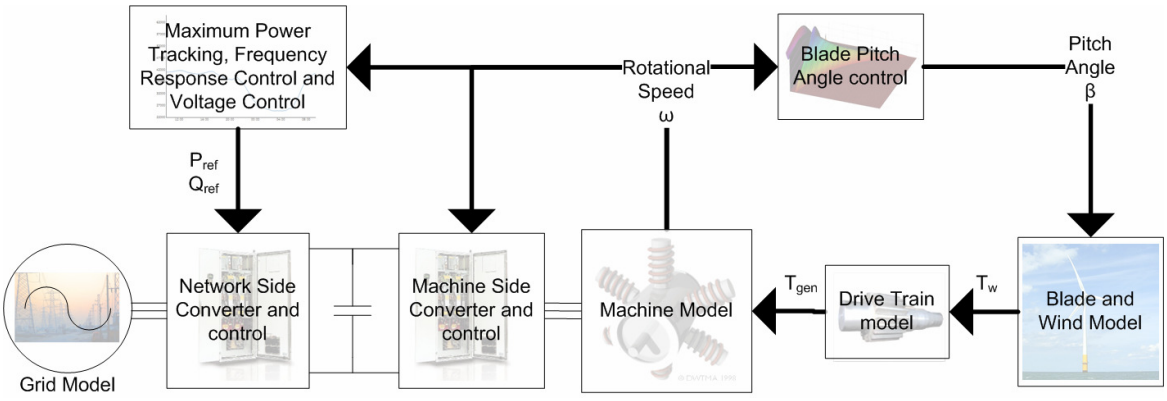

Figure 3.1: Full Converter Wind Turbine Model Elements

Sections 3.2 to 3.4 cover modelling of physical elements of the system, from the blades to the output of the power converter into the grid. Section 3.5 then covers the control of the wind turbine components and system, this section starts at the level of the power converter control and progresses to cover both the wind turbine control and then the control schemes that have been used with large scale wind farms. Section 3.7 then covers the validation of the component parts that make up the wind turbine models.

3.2 Aerodynamics

The available power in the wind can be calculated by considering the kinetic energy of the air passing through the swept area of the blades. Consider that the kinetic energy (KE) of a mass of air is given by:

Equation 3.1 $$KE = \frac{1}{2} \cdot m \cdot v_w^2$$ where m is the mass of the air and v_w, the wind speed.

The power output is given by the differential of the kinetic energy with respect to time.

Equation 3.2 $$P_w = \frac{d\left(\frac{1}{2} \cdot m \cdot v_w^2\right)}{dt}$$

Now the mass flow rate of the air is given by:

Equation 3.3 $$\frac{dm}{dt} = \rho \cdot A \cdot v_w$$ where A is the blades' swept area and ρ is the air density.

Hence, the total power available in the wind, P_w, is proportional to the cube of the wind speed, as shown in Equation 3.4:

Equation 3.4 $$P_w = \frac{1}{2} \cdot \rho \cdot A \cdot v_w^3$$

However, the power captured by the wind turbine, P, will only be a proportion of this, dependent on a performance coefficient C_p. It has been shown by Burton *et al.* [41] that the limit on C_p, known as the Betz Limit, is 59.3%. Equation 3.5 illustrates that there are two key aspects of the aerodynamics which must be modelled in order to accurately reflect a wind turbine's output: The prevailing wind speed and the wind turbine's coefficient of performance.

Equation 3.5 $$P = \frac{1}{2} \cdot C_p \cdot \rho \cdot A \cdot v_w^3$$

3.2.1 Wind Modelling

Sorensen *et al.* [42] have shown that accurate wind power output modelling requires simulations of long slow wind variations that are not typically included in standard turbulence models. Sorensen also shows that individual large offshore wind farms can suffer from greater power fluctuations than would be the case for the onshore fleet. This is caused by the correlation of wind fluctuations at individual turbines being much higher than would be the case for distributed onshore turbines, due to an offshore wind farm's geographical concentration.

This work therefore takes two approaches to modelling the wind: first, when individual wind turbine component design is considered, a single turbine turbulence model is used and fed with extreme wind speed conditions. Second, several months' power output data from the Horns Rev offshore wind farm have been provided by Hugh Sharman at Incoteco. This allows accurate simulation of the output power from an entire wind farm, without the need for this work to investigate detailed farm level wind models.

Sorensen, Hansen and Carvalho-Rosas [43] have presented wind models that are segregated between the wind farm model which provides a hub wind speed reference to a separate wind turbine level turbulence model. Sorenson's model provides a good wind model structure and details of the transfer functions of the output stage filters. IEC 61400 [44] contributes further by recommending the use of independent turbulence in the fundamental, 3p horizontal and 3p vertical elements. The structure of an appropriate wind model is shown in Figure 3.2.

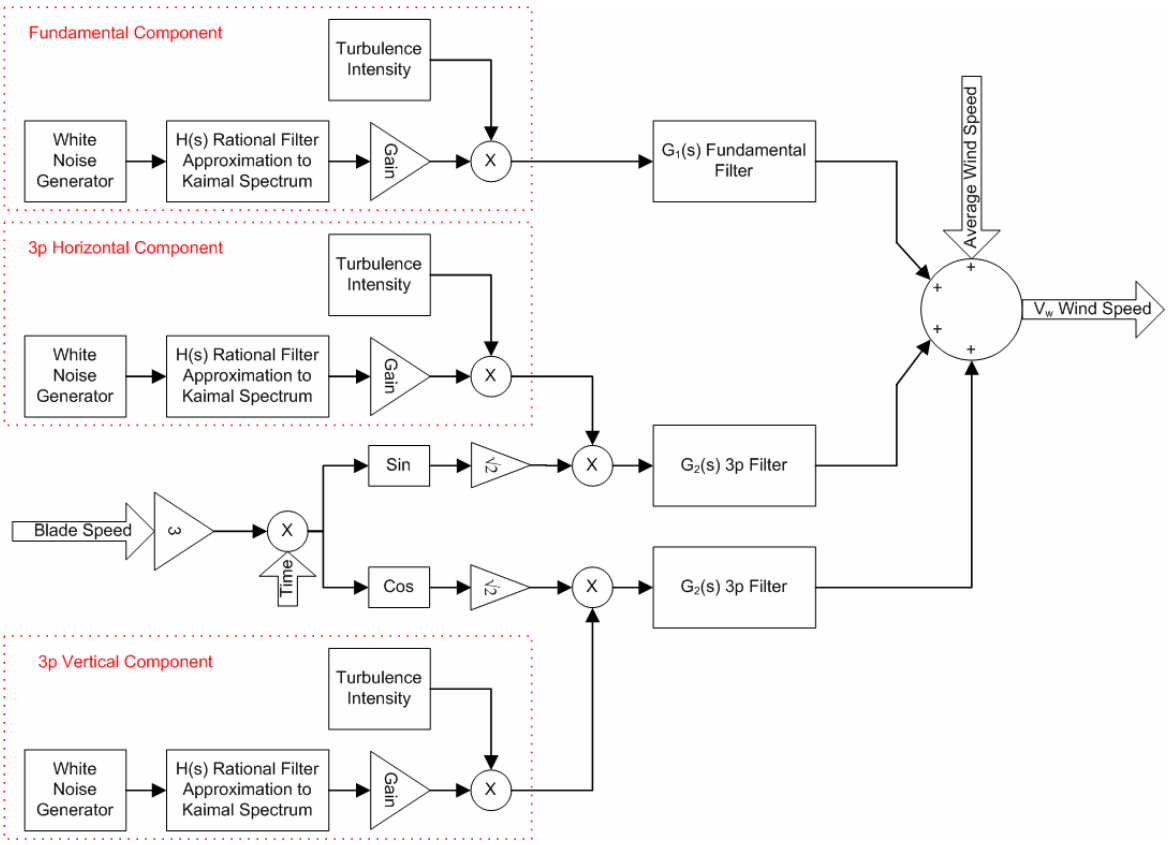

Figure 3.2: Wind Model Structure

In order to implement this wind model with maximum simulation speed, the white noise generators have been implemented according to the Ziggurat algorithm presented by Marsaglia and Tsang [45]. The implementation of this can be found in appendix 9.1.1. The rational filter approximations to the Kaimal spectra are taken from Diop *et al.* [46], whose work demonstrates the application of Von Karman and Kaimal filters to meet the requirements of IEC 61400. The application here considers only the component normal to the blades' swept area. The Kaimal filter, as specified by the IEC standard, therefore reduces to:

Equation 3.6 $$H(s)=\frac{\sqrt{4\cdot T}\cdot(6\cdot m_1\cdot T\cdot s+1)\cdot(6\cdot m_3\cdot T\cdot s+1)\cdot}{(6\cdot T\cdot s+1)\cdot(6\cdot m_2\cdot T\cdot s+1)\cdot(6\cdot m_4\cdot T\cdot s+1)}$$

Where: $\{m_1, m_2, m_3, m_4\} = \{0.745, 0.152, 0.05, 0.0028\}$; $T = 170.1\text{m}/v_{mean}$; v_{mean} is the mean wind speed (m/s).

3.2.2 Blade Modelling

The derivation of the power output from a wind turbine in the introduction to section 3.2 showed that aerodynamically the power available from a wind turbine is critically dependent on the wind speed and the coefficient of performance. Wind turbine performance coefficient relationships are normally manufacturer specific and commercially sensitive. However, differences between curves are usually small and Heier [47] is one of a number of authors presenting a model for a typical coefficient of performance curve as outlined in Equation 3.7 and Equation 3.8.

Equation 3.7 $C_p = c_1\cdot\left(c_2 - c_3\cdot\beta - c_4\cdot\beta^x - c_5\right)\cdot e^{c_6(\lambda,\beta)}$, where β is the pitch angle of the blades of the turbine and λ is the tip speed ratio defined as the ratio of speed of the tip of the blade to the prevailing wind speed $\lambda = \frac{\omega\cdot R_b}{v_w}$.

$c_1 = 0.5$, $c_2 = \frac{116}{\lambda_i}$, $c_3 = 0.4$, $c_4 = 0$, $c_5 = 5$ and $c_6 = \frac{21}{\lambda_i}$ where λ_i is given as:

Equation 3.8 $$\frac{1}{\lambda_i} = \frac{1}{\lambda + 0.08\cdot\beta} - \frac{0.035}{\beta^3 + 1}$$

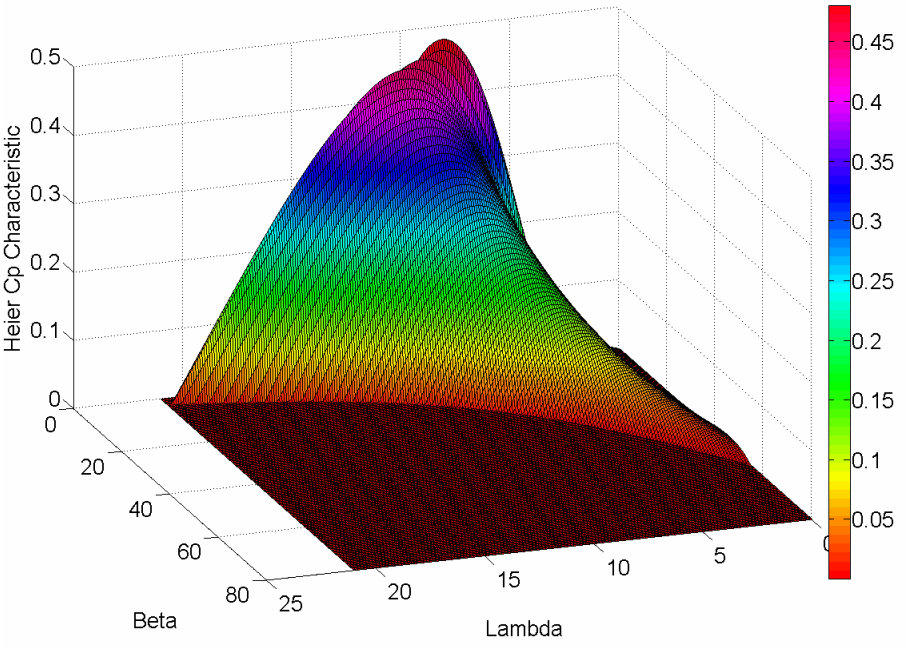

Figure 3.3: Typical Wind Turbine Performance Curve

It should be highlighted that Heier's representation of the blades of a wind turbine is a static approximation to a dynamic system. As such its use represents an approximation of the true case and is a significant simplification in comparison to a dynamic model using dedicated software such as Bladed.

Figure 3.3 shows the impact of the tip speed ratio and pitch angle on the wind turbine's performance curve. It can be clearly seen that the optimal power capture occurs for a single ratio of the blade speed to the wind speed at any given pitch angle. This is the foundation of the benefit of variable speed machines over fixed speed machines, as the wind speed increases the rotational speed of a variable speed machine can also increase to optimise the tip speed ratio and maximise power capture. The plot also illustrates that the coefficient of performance can be reduced by changing the angle of attack of the blades or 'pitching'. Hence, turbines equipped with blades that can be pitched can exercise fine control over power output. This is the subject of section 3.5.2.3.

The controller of a variable speed wind turbine has two primary aims. First, to optimise the rotational speed of the blades so as to maximise the coefficient of performance, second to minimise the effects of loads due to wind turbulence. These aims, at least in part are mutually exclusive as minimising loads in turbulent wind normally requires acceleration or deceleration of the blades away from the optimal operating point so that the torque acting on the drive train is smooth.

3.3 Drive Train

Figure 3.3 shows that the optimal tip speed ratio for a wind turbine is typically around 8. The tip speed ratio is defined as $\lambda = \frac{\omega \cdot R}{v_w}$ and for a typical 2.5MW rating the blade length, *R*, would be approximately 50m. Further, such a turbine would start up in wind speeds of 4m/s and reach rated power output in wind speeds of around 14m/s. Hence, to operate at the optimal coefficient of performance, the optimal blade speed would be:

$\omega_1 = \frac{\lambda \cdot v_w}{R} = \frac{8 \cdot 4}{50} = 0.64 rad/s = 6 rpm$ in low wind conditions up to a maximum of

$\omega_2 = \frac{\lambda \cdot v_w}{R} = \frac{8 \cdot 14}{50} = 2.24 rad/s = 21.4 rpm$ in high wind conditions.

However, typical electrical generator frequencies are around 1500rpm. Hence to deal with such low mechanical frequencies, the drive train either requires gearing or to be connected to a multi-pole generator with high pole number, or possibly a combination of the two approaches.

3.3.1 Geared

The level of detail required to represent the drive train of a traditional geared drive-train has been the subject of much debate. Ramtharan *et al.*[48] compared two and three mass models under transient faults, whilst Muyeen *et al.*[49] investigated 2, 3, transformed 3 and 6 mass models but both ultimately led to an equivalent two-mass model that represents the fundamental resonant mode of the shaft system. Such a two mass system considers a lumped mass broadly representing the inertias of the three blades, hub and low speed part of the gearbox, connected via a spring and damper system to a second inertia representing the generator and high speed side of the gearbox, referred to the low speed shaft. This is illustrated in Figure 3.4.

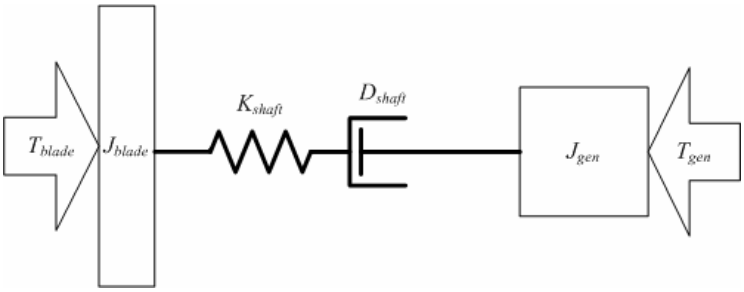

Figure 3.4: Wind Turbine Drive Train System

Ignore the damping and external torques and consider the torque in the spring acting on the inertias alone:

Equation 3.9 $$J_{blade} \cdot \frac{d\omega_{blade}}{dt} = -J_{gen} \cdot \frac{d\omega_{gen}}{dt} = T_{shaft}$$

Now consider the rate of change of the shaft torque:

Equation 3.10 $$\omega_{gen} - \omega_{blade} = \frac{1}{K_{shaft}} \cdot \frac{dT_{shaft}}{dt} \text{ leading to } \omega_{gen} = \omega_{blade} + \frac{1}{K_{shaft}} \cdot \frac{dT_{shaft}}{dt}$$

Hence substituting back into Equation 3.9:

Equation 3.11 $$T_{shaft} = -J_{gen} \cdot \frac{d\left\{\omega_{blade} + \frac{1}{K_{shaft}} \cdot \frac{dT_{shaft}}{dt}\right\}}{dt}$$

Simplifying to $$T_{shaft} = -J_{gen} \cdot \frac{d\omega_{blade}}{dt} - J_{gen} \cdot \frac{1}{K_{shaft}} \cdot \frac{d^2T_{shaft}}{dt^2}$$

And given Equation 3.9 gives $\frac{d\omega_{blade}}{dt} = \frac{T_{shaft}}{J_{blade}}$, substitute into Equation 3.11:

Equation 3.12 $T_{shaft} = \frac{-J_{gen}}{J_{blade}} \cdot T_{shaft} - J_{gen} \cdot \frac{1}{K_{shaft}} \cdot \frac{d^2 T_{shaft}}{dt^2}$ which rearranges to give:

Equation 3.13 $-\frac{K_{shaft}}{J_{eff}} \cdot T_{shaft} = \frac{d^2 T_{shaft}}{dt^2}$ where $\frac{1}{J_{eff}} = \frac{1}{J_{blade}} + \frac{1}{J_{gen}}$

Equation 3.13 solves to give:

Equation 3.14 $T_{shaft} = T_{\max} \cdot e^{-j \cdot \omega t}$ with $\omega = \sqrt{\frac{K_{shaft}}{J_{eff}}}$

Hence there is a natural resonant mode within the shaft system that may be excited by either electrical or mechanical torque steps. Hansen and Michalke [50] have shown that this natural resonant mode is inherently unstable in variable speed wind turbines, owing to the decoupling of the speed of the generator from the grid frequency, which removes the inherent damping in FSIG wind turbines. They highlight the need to implement active damping controllers to remove oscillations in the drive train. This will be covered further in section 3.5.2.3.

3.3.2 Direct-drive

Direct-drive systems allow the generator to be directly coupled to the blades of a wind turbine, with the low mechanical speed stepped up to a higher electrical frequency through the use of a high pole number generator. The removal of the gearbox can increase the physical shaft stiffness significantly, whilst the effective inertia of the system is reduced. These two factors tend to increase the mechanical resonant frequency of the shafts of direct-drive wind turbines. However, opposing this improvement in the stability of the shaft system, Akhmatov [51] has shown that the shaft stiffness is effectively reduced by the pole number of the generator, such that smaller mechanical oscillations are amplified by the electrical system.

Parameter	Geared	Direct-Drive
Blade Inertia (J_{blade}) (kgm^2)	2.5 x 10^7	2.5 x 10^7
Generator Inertia (J_{gen}') (kgm^2)	200	90000
Gearbox ratio (n_{gear})	120	1
Effective Inertia (kgm^2) $\frac{1}{J_{eff}} = \frac{1}{J_{blade}} + \frac{1}{n_{gear}^2 \cdot J'_{gen}}$	2.6 x 10^6	89700
Shaft Stiffness (K_{shaft}) (Nm/rad)	3 x 10^8	1.3 x 10^9
Generator's number of pole pairs	2	60
Mechanical Resonant Frequency $f_{res} = \frac{1}{2 \cdot \pi} \cdot \sqrt{\frac{K_{shaft}}{J_{eff}}}$	1.7	19

Table 3.1: Comparison of Geared and Direct-drive Shaft Parameters (Approximate to protect commercial sensitivity)

Table 3.1 shows a comparison of the mechanical parameters of the shaft systems of a geared and a direct drive generator, both machines are rated identically, with a multi-MW rating. Despite the lower inertia of the low pole number generator, compared to that of the multi-pole generator, the high gearing ratio leads to an effectively higher inertia for the geared shaft than for the direct-drive shaft, as the geared generator's inertia is referred to the low speed side (a ratio of n_{gear}^2). Further, the geared shaft has significantly lower shaft stiffness. It can be seen that this leads the mechanical resonant frequency of the direct drive shaft to be an order of magnitude higher than that of the geared shaft. However, according to Akhmatov's work, it is important still to represent the shaft system with a second order model in direct-drive models, owing to the amplifying effect of the generator's high pole number.

3.4 Electrical System

The mechanical shaft system model includes a representation of the generator's rotor inertia. The output of this mechanical model drives the generator at a set rotational speed whilst the generator exerts an electrical torque on the mechanical shaft model. Section 2.4.1.4 highlighted that three different full converter configurations are possible, consisting of induction generators and both electrically excited and permanent magnet synchronous generators. The trends in wind turbine configuration, alongside GE Energy's Power Conversion business's experience and commercial involvement, have led this work to concentrate on the FFIG and FFPMG.

3.4.1 Park and Clarke's Transforms

Much of the analysis and control of three phase rotating machinery depends on the ability to transform the three phase vectors into an equivalent stationary two axis form (Clarke's transform) or an equivalent synchronously rotating two axis reference frame (Park's transform), this derivation is based on Adkins and Harley [52]. These are introduced here as they underpin much of the subsequent analysis of both induction machines and permanent magnet machines. Clarke's method transforms the ABC three phase system into an αβγ reference frame. The α axis is typically aligned with the A phase, with the β axis lagging by 90°, the γ axis is then analogous to an unbalanced DC offset to this pair, which for simplicity means it is zero for balanced systems. Figure 3.5 shows the relationship of these axes. The transform can then be derived by resolving the components of the ABC system into α and β components. First consider the α component:

Equation 3.15 $$I_\alpha = \hat{I}\cdot\cos(\omega\cdot t-\delta)+\hat{I}\cdot\cos\left(\omega\cdot t-\frac{2\cdot\pi}{3}-\delta\right)+\hat{I}\cdot\cos\left(\omega\cdot t+\frac{2\cdot\pi}{3}-\delta\right)$$

Equation 3.16 $$I_\beta = \hat{I}\cdot\sin(\omega\cdot t-\delta)+\hat{I}\cdot\sin\left(\omega\cdot t-\frac{2\cdot\pi}{3}-\delta\right)+\hat{I}\cdot\sin\left(\omega\cdot t+\frac{2\cdot\pi}{3}-\delta\right)$$

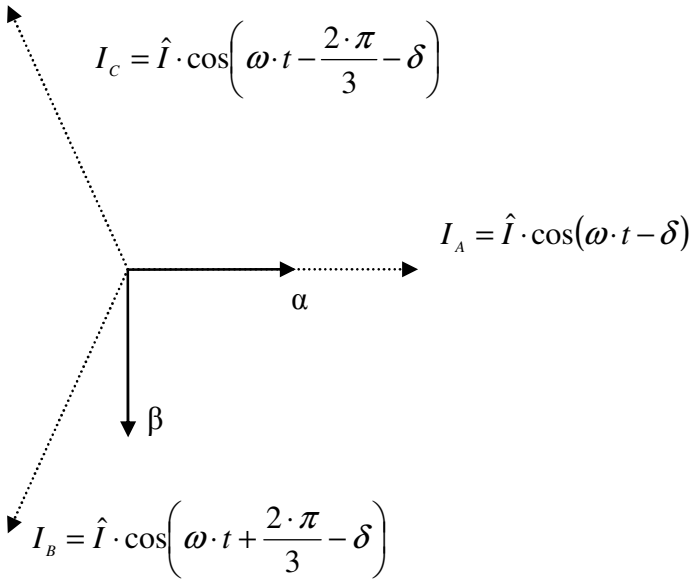

Figure 3.5: Clarke's Transform abc-αβγ

By aligning the α axis with phase A, the angle between the α axis and the A phase becomes zero and the transform reduces in matrix form to (the factor of two thirds is from conservation of power between the axes):

Equation 3.17 $$\begin{bmatrix} I_\alpha \\ I_\beta \end{bmatrix} = \frac{2}{3}\cdot\begin{bmatrix} 1 & -\frac{1}{2} & -\frac{1}{2} \\ 0 & \frac{\sqrt{3}}{2} & -\frac{\sqrt{3}}{2} \end{bmatrix}\begin{bmatrix} I_A \\ I_B \\ I_C \end{bmatrix}$$

The inverse transform can be derived by inverting this and is given as:

Equation 3.18 $$\begin{bmatrix} I_A \\ I_B \\ I_C \end{bmatrix} = \begin{bmatrix} 1 & 0 \\ -\frac{1}{2} & \frac{\sqrt{3}}{2} \\ -\frac{1}{2} & -\frac{\sqrt{3}}{2} \end{bmatrix}\begin{bmatrix} I_\alpha \\ I_\beta \end{bmatrix}$$

Park's transform is in many ways an extension of Clarke's transform which aids with the analysis of rotating machinery as it transforms the three phase equations onto a synchronously rotating reference frame. This in turn allows the AC quantities to be considered as DC components and controlled as such. This is shown in Figure 3.6, where again the three phase system is considered balanced and the d axis is rotating synchronously (speed, ω) at an angle, θ, to the A phase.

Once again the transform can be derived by resolving the components of the three phase currents onto the dq axes.

Equation 3.19 $$I_d = I_A \cdot \cos(\theta) + I_B \cdot \cos\left(\theta - \frac{2\cdot\pi}{3}\right) + I_C \cdot \cos\left(\theta + \frac{2\cdot\pi}{3}\right)$$

Equation 3.20 $$I_q = I_A \cdot \sin(\theta) + I_B \cdot \sin\left(\theta - \frac{2\cdot\pi}{3}\right) + I_C \cdot \sin\left(\theta + \frac{2\cdot\pi}{3}\right)$$

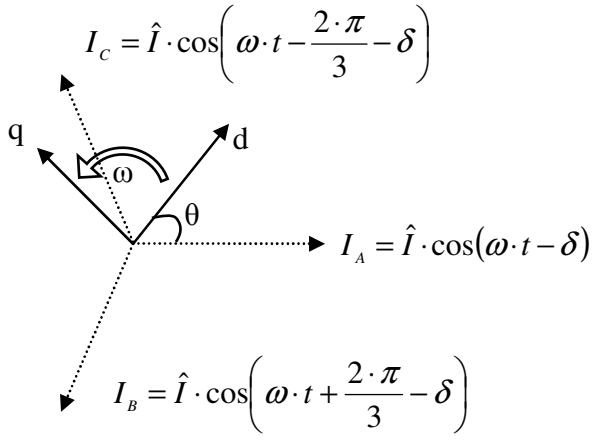

Figure 3.6: Park's Transform αβγ to dq0

These transforms, when power is invariant, in matrix form are then given as:

Equation 3.21 $$\begin{bmatrix} I_d \\ I_q \end{bmatrix} = \sqrt{\frac{2}{3}} \cdot \begin{bmatrix} \cos(\theta) & \cos\left(\theta - \frac{2\pi}{3}\right) & \cos\left(\theta + \frac{2\pi}{3}\right) \\ \sin(\theta) & \sin\left(\theta - \frac{2\pi}{3}\right) & \sin\left(\theta + \frac{2\pi}{3}\right) \end{bmatrix} \begin{bmatrix} I_A \\ I_B \\ I_C \end{bmatrix}$$

The inverse transform can be derived by inverting this and is given as:

Equation 3.22 $$\begin{bmatrix} I_A \\ I_B \\ I_C \end{bmatrix} = \sqrt{\frac{2}{3}} \begin{bmatrix} \cos(\theta) & \sin(\theta) \\ \cos\left(\theta - \frac{2\pi}{3}\right) & \sin\left(\theta - \frac{2\pi}{3}\right) \\ \cos\left(\theta + \frac{2\pi}{3}\right) & \sin\left(\theta + \frac{2\pi}{3}\right) \end{bmatrix} \begin{bmatrix} I_d \\ I_q \end{bmatrix}$$

3.4.2 Induction Generator

Park's transforms greatly help with the analysis of a squirrel cage induction machine. Which can be considered with a reference frame rotating synchronously to machine speed and the d axis aligned with rotor flux as is considered here.

The squirrel cage induction machine was originally the dominant generator technology in fixed speed wind turbines. Hence, the upgrade path to develop a variable speed wind turbine with FFIG is an appealing option. The equivalent circuit of the induction generator is shown in Figure 3.7, with the magnetising branch resistance assumed infinite.

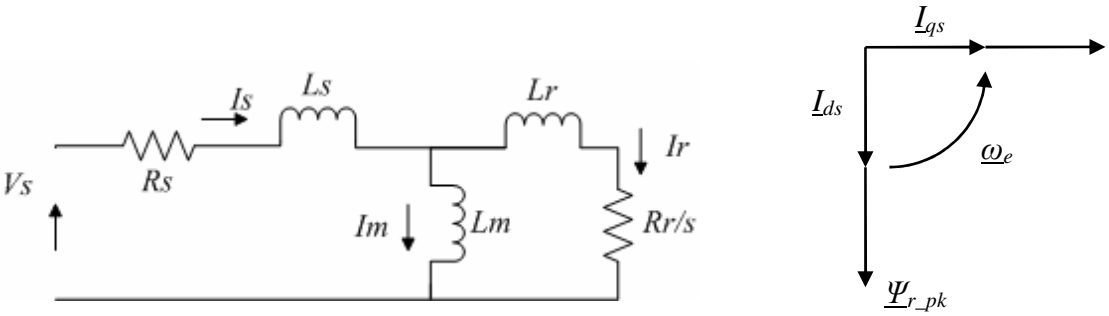

Figure 3.7: Induction Machine Equivalent Circuit (left) and Field Oriented Control (right)

It is desirable to be able to independently control the generator's torque and flux in order to achieve fast transient performance. With this aim Bose [53] provides a synopsis of the current capabilities of vector control for induction machines and highlights the parallel that can be drawn to a DC machine when an induction machine is controlled in a field oriented manner, as in Figure 3.7. The fundamentals of this technique are outlined here.

Consider the current through and voltage across the magnetising and other branches:

Equation 3.23 $$\underline{I}_m = \left|\underline{I}_{md}\right| + j \cdot \left|\underline{I}_{mq}\right| = \frac{\left|\underline{I}_r\right| \cdot \frac{R_r}{s}}{X_m} + j \cdot \frac{\left|\underline{I}_r\right| \cdot X_{Lr}}{X_m}$$

Hence the rotor circuit current can be defined by considering the *d*-axis component:

Equation 3.24 $$I_r = \frac{I_{md} \cdot X_m}{\frac{R_r}{s}} = \frac{s \cdot I_{md} \cdot X_m}{R_r}$$

But by definition, I_r must be in the *q*-axis to be purely torque producing, therefore, the total *q*-axis current is (by Kirchoff's law):

Equation 3.25 $$I_q = I_{mq} + I_r = \frac{s \cdot I_{md} \cdot X_m}{R_r} + \frac{I_r \cdot X_{Lr}}{X_m} = \frac{s \cdot I_{md} \cdot X_m}{R_r} + \frac{\frac{s \cdot I_{md} \cdot X_m}{R_r} \cdot X_{Lr}}{X_m}$$

This can be rearranged to give the q-axis stator current in terms of the magnetising branch current:

Equation 3.26 $$I_q = \frac{s \cdot I_{md} \cdot \left(X_m + X_{Lr}\right)}{R_r} = s \cdot \omega \cdot I_{md} \cdot T_r$$ where the rotor time constant is given by the equation $T_r = \frac{\left(L_m + L_{Lr}\right)}{R_r}$. Furthermore, the *d*-axis stator current must equal the *d*-axis magnetising branch current as I_r has been shown to be in the *q*-axis.

Equation 3.27 $I_d = I_{md}$

The real power and resistive losses in the rotor circuit can be derived by considering the referred rotor resistance as a pure resistance (R_r) in series with the torque producing resistance ($R_r \cdot \frac{1-s}{s}$) and considering the mechanical power to be equal to the three phase electrical power.

Equation 3.28 $$P = T_q \cdot \omega_r = 3 \cdot \left(\frac{s \cdot I_{md} \cdot X_m}{R_r} \right)^2 \left(R_r \cdot \frac{1-s}{s} \right)$$

This simplifies to:

Equation 3.29 $$T_q \cdot \omega_r = 3 \cdot (1-s) \frac{s \cdot {I_{md}}^2 \cdot {X_m}^2}{R_r}$$

And substituting for the rotor frequency ($\omega_r = \frac{2 \cdot \pi \cdot f \cdot (1-s)}{p}$, p is machine pole pairs):

Equation 3.30 $$T_q \cdot \frac{2 \cdot \pi \cdot f \cdot (1-s)}{p} = 3 \cdot (1-s) \frac{s \cdot {I_{md}}^2 \cdot (\omega \cdot L_m)^2}{R_r}$$

Equation 3.31 $$T_q = 3 \cdot p \cdot \frac{s \cdot {I_{md}}^2 \cdot \omega \cdot L_m^2}{R_r}$$

Substituting in I_{md} from Equation 3.26 and recognising Equation 3.27, gives torque in terms of the *q* and *d*-axis stator currents:

Equation 3.32 $$T_q = 3 \cdot p \cdot I_d \cdot I_q \frac{L_m^2}{L_m + L_r}$$

Rearranging to give the *q*-axis current gives:

Equation 3.33 $$I_q = \frac{T_q}{\Psi_r} \cdot \frac{1 + \frac{L_r}{L_m}}{3 \cdot p} \text{ where } \Psi_r = L_m \cdot I_d$$

Equation 3.26 taken together with Equation 3.33 shows how the induction machine can be controlled in the manner of a DC machine, through independent control of *d* and *q*-axis stator currents, where the *d*-axis is aligned with the rotating rotor flux vector. This independent control of the torque and flux allows fast torque response to transients, but also allows fine control over the rotor flux. This has the advantage that the field can be weakened when the rotor speed is high so that the generator's output voltage is lower, so

called “field weakening”. In a wind turbine application, where instantaneous gusts can cause acceleration of the blades and generator, field weakening is a useful feature, as it ensures that the voltage seen by the full converter can be kept within its voltage ratings across a relatively wide speed range.

There are two drawbacks of the induction machine, however, first the machine must be charged with the *d*-axis (magnetising) current even in relatively low winds. This can mean that it is relatively inefficient at the light loads that are common in wind turbine applications. Second, as blade diameters have increased, in order to maintain a constant tip speed ratio, the blade rotational frequency has fallen. This reduction in blade rotational frequency has necessitated increased gearbox ratios; which have come at the expense of increasing gearbox torques.

3.4.3 Permanent Magnet Generator

The twin challenges of FFIG wind turbines’ poor low speed efficiency and gearbox failures are two of the drivers behind many manufacturers developing Permanent Magnet Generator based wind turbines. Troedson [54] finds that all of the top three wind turbine manufacturers are developing new FFPMG based solutions, with part load efficiency, reliability, maintainability and grid compatibility raised as the key advantages over induction generator solutions.

As with the FFIG, it is desirable to independently control the torque on the PMG in a wind turbine application. Figure 3.8 shows the equivalent circuit of the PMG alongside a vector diagram which considers the PMG in the rotor flux oriented reference frame. Here a multi-pole design with equal *d* and *q*-axis stator reactance is considered.

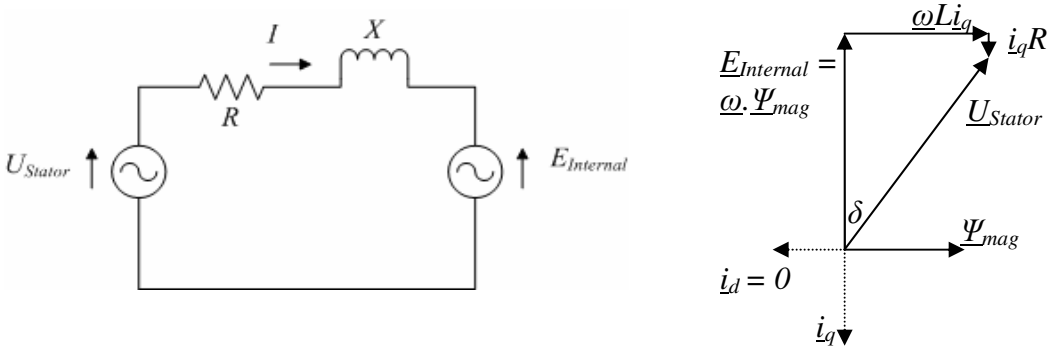

Figure 3.8: Permanent Magnet Generator Equivalent Circuit (left) and Vector Diagram (right)

Considering the rotor flux oriented reference frame of Figure 3.8, the real power can be seen to be given by:

Equation 3.34 $$P = T \cdot \omega = \frac{3}{2} \cdot i_q \cdot U_{Stator} \cdot \cos\delta$$ This is equivalent to:

Equation 3.35 $$T = \frac{3}{2} \cdot i_q \cdot \omega \cdot \Psi_{mag}$$ (Ignoring the stator resistance)

Hence, the torque is directly controlled by the *q*-axis current in this reference frame. Implementation of a non-zero d-axis current varies the *q*-axis stator voltage and allows control over the total voltage seen by the power converter. However, in contrast to the induction machine it cannot change the rotor flux (Ψ_{mag}), as this is fixed by the permanent magnets. This means that as the machine tends to higher speeds, the open circuit voltage of the permanent magnet generator will tend to increase linearly. The equations of the PMG can be written to assess the voltages on the terminals of the PMG and converter. These are shown in Equation 3.36 and Equation 3.37 and highlight the voltage dependency on speed.

Equation 3.36 $$U_d = I_d \cdot R - \omega \cdot I_q \cdot L_s + L_s \cdot \frac{dI_d}{dt}$$

Equation 3.37 $$U_q = I_q \cdot R + \omega \cdot I_d \cdot L_s + \omega \cdot \Psi_{mag} + L_s \cdot \frac{dI_q}{dt}$$

The inability to field weaken is a limitation of the PMG in comparison to a conventional induction or synchronous generator. It has led Michalke, Hansen and Hartkopf [55] to consider what is the most appropriate reference frame for the control of a PMG in order to minimise the risk of transient over-speeds causing excessive voltages which damage the power converter. This problem has also led Li and Chen [56] to suggest optimising the selection of PMGs based on their rated speed for specific wind speed sites.

3.4.4 Converter

The power converter for a modern wind turbine relies on the application of IGBT technology. It has been in large part the technical and economic advancement of IGBT devices that has enabled the widespread deployment of variable speed wind turbines. Today most wind turbine converters are two level designs, incorporating six IGBT devices per bridge, as shown in Figure 3.9. Each bridge can act as a passive three phase rectifier; converting the three phase AC voltage to DC through the anti-parallel diode bridge, or as an Active Front End (AFE) by switching the IGBTs to synthesise a three phase voltage based on Pulse Width Modulation (PWM) of the DC voltage.

The generator AC voltage, which is usually Low Voltage (LV), below 690V according to GE Energy [57], is actively rectified to DC by the machine bridge, which raises the DC

voltage above the peak of the AC waveform. This DC level is then inverted back to AC again to connect into the grid at around 690V, before being stepped up by a transformer to typical levels of 11kV or 33kV.

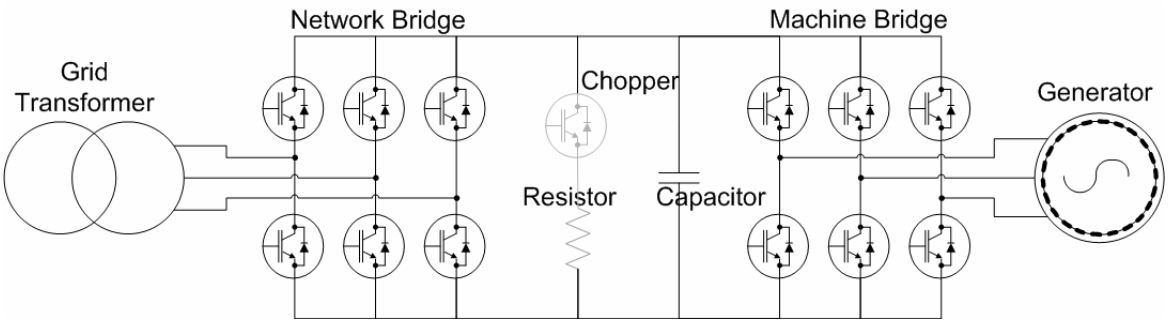

Figure 3.9: Two Level Power Converter

Portillo *et al.* [58] highlighted as early as 2006 that the continued advance in power electronic component cost and performance was making 3 level power converters a potentially better option for high power wind turbine applications. The increased number of levels improves harmonics, raises the operating voltage and increases the efficiency of the power converter. These advantages will continue the increase in power device count in wind turbines.

In both two and three level converters, the switching frequency of the IGBTs is typically over 1 kHz, with low order harmonics generally very low level. The modelling of a power converter including switching cycles and devices is computationally demanding, all the more so with increasing numbers of devices in the power converter.

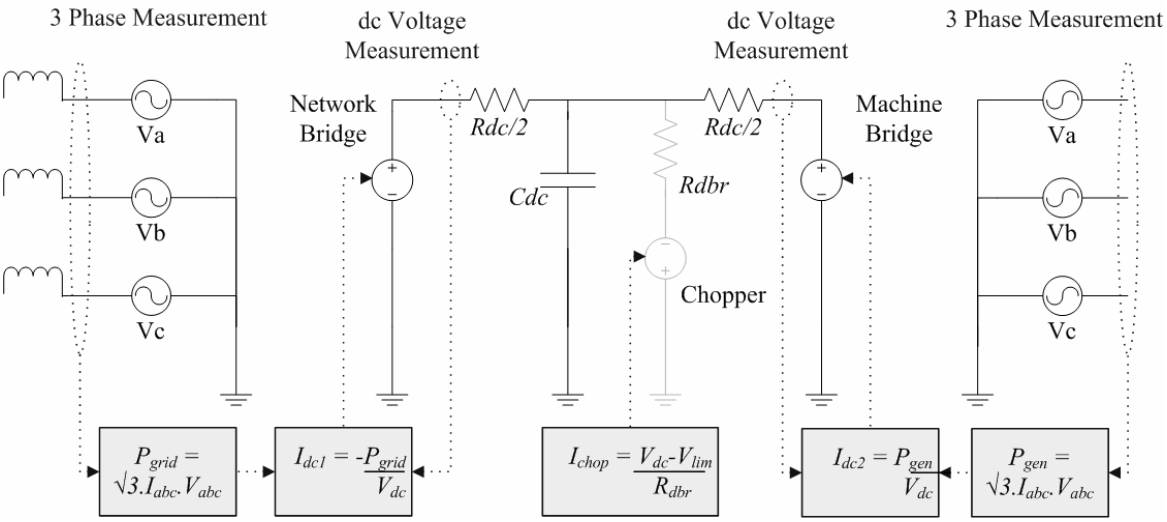

Figure 3.10: Simplified Representation of the Power Converter

Given the high switching frequencies involved and the desire for a model that is effective for power system studies, an idealised model using ideal voltage and current sources has been used to represent the power converter. Figure 3.10 shows how this simplification is

achieved with power balances between ideal three phase AC voltage systems and ideal current sources on the DC link. The use of ideal current sources feeding the DC link allows any major disturbances in DC link voltage to be observed.

In the real converter, the DC link applies a natural limit to the AC side voltages that can be generated by the IGBT bridges as the peak of the AC waveform cannot exceed the DC voltage. However, this natural limit must be replaced by synthetic modulation depth limits in the control layer that take into account the voltage on the DC link and consequently limit the maximum AC voltage. Furthermore, the passive three phase rectifier of the anti-parallel diodes is not represented, meaning that this representation is not appropriate for converter start-up studies, where DC link precharge is necessary.

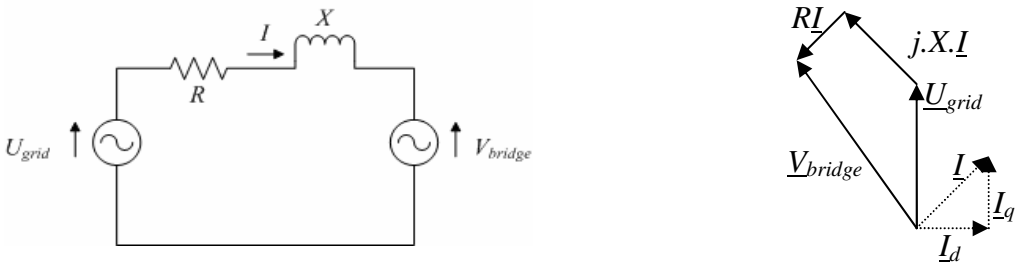

Figure 3.11: Network Bridge Equivalent Output Circuit (left) and Vector Diagram (right)

The network bridge can be controlled in a synchronous reference frame as with the PMG. Figure 3.11 shows how the control of the bridge voltage magnitude and phase controls the *d* and *q*-axis currents, which in turn set the network bridge's real and reactive power outputs.

3.4.4.1 Without Chopper

Under load large steps or severe voltage disturbances, transients on the AC sides of the system can lead to increased DC link voltages. The peak allowable DC voltage is set by the lower of the DC voltage rating of the IGBTs (which may differ between passive rectification and active switching) and the capacitor's voltage rating. The capacitor typically has a time constant of just a few milliseconds and this voltage must not be exceeded, hence high bandwidth control is necessary to ensure that the DC link voltage stays within safe margins. The FFIG does not include or require the use of a DC link chopper, in part because its ability to field weaken ensures generator side speed transients can be protected against in isolation from the DC link.

3.4.4.2 DC Choppers and Brake Resistors

Figure 3.9 shows that it is possible to use an additional IGBT switch connecting a resistor across the DC link. This allows power to be sent to the Dynamic Brake Resistor (DBR) in the event of an over-voltage on the DC link. Typically such events are brief transients, allowing the resistor to be rated at the kW level, whilst thermally absorbing occasional transients in the MW level. Normally chopper control is a simple threshold controller, where the IGBT is switched on as soon as the voltage exceeds a preset level. Figure 3.10 shows that the chopper has been modelled in the simplified model as an anti-parallel current source drawing current from the capacitor in the event of a DC link over voltage.

3.5 Control System

Three layers of control exist within a typical wind farm, with the wind farm controller providing set points to the wind turbine controller, which in turn provides set points to the turbine's power converter. This section covers the implementation of these controllers.

3.5.1 Converter

In 2009, Hansen and Michalke [59] proposed two possible broad methods of controlling the power converter of a wind turbine. What they proposed as a novel method was in fact the method that had already been deployed to meet the rigours of grid codes in GE Energy's power converters. The control scheme that is classified as a 'classical' control scheme is outlined in section 3.5.1.1 whilst section 3.5.1.2 covers the method used in most of GE Energy's Power Conversion business' wind turbine converters.

3.5.1.1 Conventional Control Scheme

Figure 3.12 shows the conventional method of controlling a power converter as implemented in the wind turbine model. The machine side bridge, which acts as a rectifier, receives two set points. One set point controls the torque by controlling the *q*-axis current in accordance with either the PMG or the Induction machine vector control (note an unusual convention is used for *dq* axes in GE Energy's Power Conversion business). A second reference for either the flux or the maximum stator voltage is used as the set point for the *d*-axis current and controls the machine's magnetisation and ultimately the voltage which is seen at the power converter terminals.

Two set points are also provided to the network bridge, one for the AC supply voltage (shown), power factor or reactive power output (both not shown), this set-point is attained by means of a Proportional-Integral (PI) controller setting the *d*-axis current reference. A second reference is the target DC link voltage. The machine bridge pushes power onto the

DC link according to the machine's speed and the torque set point. The network bridge responds through a PI regulator which sees an increase in machine power as an increase DC link voltage and controls the network bridge's *q*-axis current reference so as to increase power output to the grid.

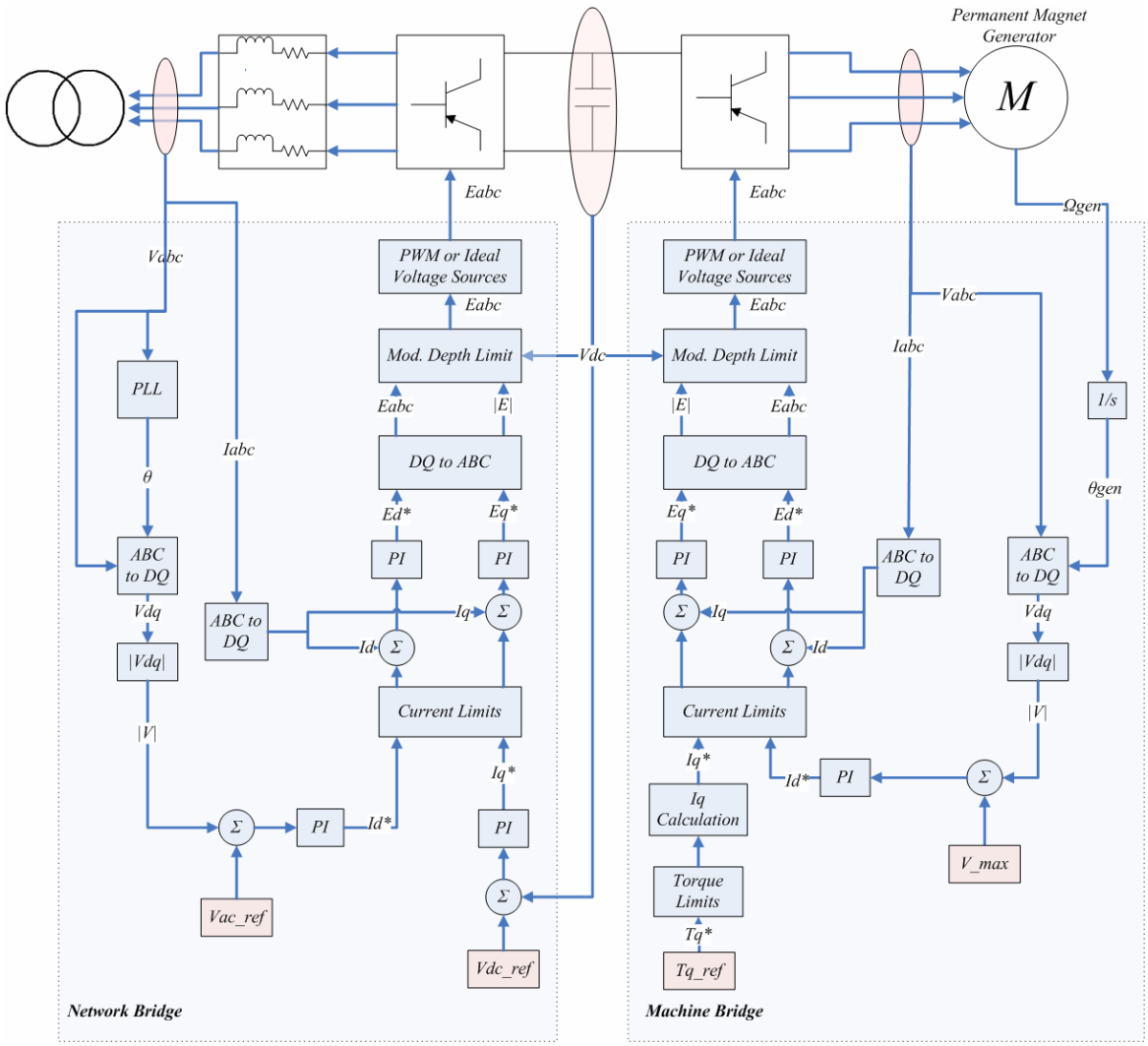

Figure 3.12: Basic Conventional Power Converter Control Strategy

This cascade control scheme uses fast inner current controllers, which control the *d* and *q*-axis voltages to ensure that the *d* and *q*-axis currents follow their set points. Also of note from the control scheme, the grid angle and frequency are tracked by a Phase Locked Loop (PLL), which acts to ensure the network bridge's *dq* reference frame is synchronous to the grid. The modulation depth limits incorporated into the control scheme compensate for the use of ideal voltage sources in place of IGBT switch models.

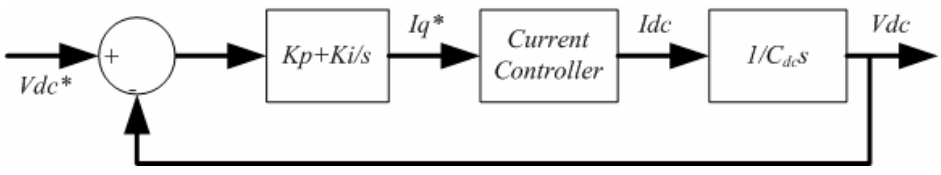

Figure 3.13: Control Block diagram for the DC link

Seok, Lee and Lee [60] have developed tuning techniques for a permanent magnet generator's converter which incorporates a neat method of automatically setting the gain for a PI controller where the plant is an integrator. Their method can be applied to the DC link voltage controller to automatically set the PI controller gains here.

Figure 3.13 shows the block diagram, and if the current controller is assumed to have a very high bandwidth, relative to the DC link voltage controller, its phase delay and gain can be ignored. Hence an approximate open loop transfer function can be seen to be:

Equation 3.38 $$G(s) = \left(K_p + \frac{K_i}{s} \right) \cdot \frac{1}{C_{dc} \cdot s} = \frac{K_p \cdot s + K_i}{C_{dc} \cdot s^2}$$

Now if we desire a DC link controller bandwidth of ω rad/s at the gain cross-over point the phase margin (ϕ) can be considered (Bandwidth and Phase Margin Assignment Method):

Equation 3.39 $$\frac{K_p \cdot \omega}{K_i} = \tan(\phi)$$

Equation 3.40 $$\frac{(K_p \cdot \omega)^2 + K_i^{\,2}}{\omega^4 \cdot C_{dc}^2} = 1$$

Now the proportional gain can be substituted for in Equation 3.40 by rearranging Equation 3.39 to give:

Equation 3.41 $$\frac{\left(\frac{K_i \cdot \tan(\phi)}{\omega} \cdot \omega \right)^2 + K_i^{\,2}}{\omega^4 \cdot C_{dc}^2} = 1 = \frac{K_i^{\,2}(1 + \tan^2(\phi))}{\omega^4 \cdot C_{dc}^2}$$

So rearranging Equation 3.41 allows the integral gain to be assigned by selection of an appropriate phase margin and then the proportional gain can be found from Equation 3.39.

Equation 3.42 $$K_i = \frac{\omega^2 \cdot C_{dc}}{\sqrt{(1 + \tan^2(\phi))}}$$

Automatic tuning of the DC link controller provides benefits when setting up new variants of the wind turbine power converter models as it is the DC link which couples the two IGBT bridges. Therefore, automatic gain setting to ensure that the DC link voltage controller has reasonable stability and hence allows the other controllers to be tuned without interference from the modulation depth limit.

3.5.1.2 Reversed Control Scheme

The classical converter control scheme suffers from two shortcomings, first the network bridge's control over the DC link voltage is not ideal for a generating application. The

tendency is for grid transients to lead to the DC link controller running into current limits. This in turn can cause the DC link voltage to increase as the machine bridge continues to generate into the DC link. The second shortcoming is a commercial block, in that General Electric historically held a US patent by Richardson and Erdman [61] on torque controlling an induction machine with vector control. Hence, Converteam UK Ltd., prior to being taken over by General Electric, developed a control scheme patented by Jones *et al.* [62], that avoided this patent but relied on DC link control on the machine bridge.

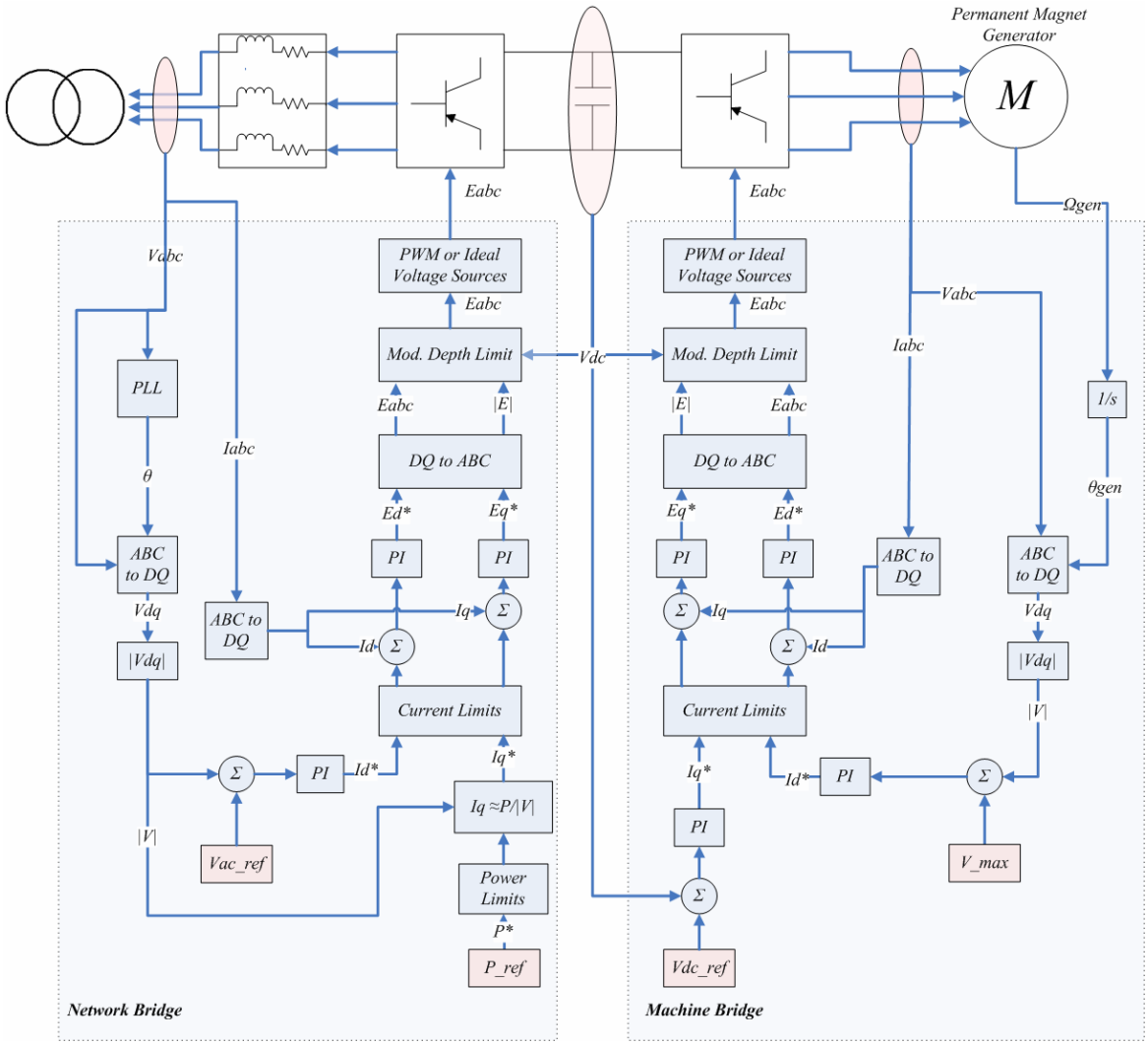

Figure 3.14: Alternative Power Converter Control Strategy

Under this alternative control strategy, the DC link voltage is used to set the machine bridge's *q*-axis current reference, thereby indirectly controlling the generator's torque in order to maintain a constant DC link voltage. The network bridge is provided with a power set point which sets the network bridge's *q*-axis current reference. Hence, power is drawn off the DC link and the DC link controller responds by increasing the generator's torque. This method has the advantage that it makes it simpler to control a converter to

avoid the need for a chopper and DBR. Figure 3.14 shows the overall control strategy of the power converter under this scheme.

The challenge with this control scheme is that it requires a power set point rather than a generator torque set point. This is a slight difference from classical wind turbine controller reference setting, but has the advantage that it ultimately leads to power output optimisation from the machine to the grid, rather than purely of the machine and machine bridge.

Whichever control strategy is selected, it must interface to the wind turbine controller which provides two of the power converter set points. Whereas the DC link voltage and maximum generator side voltage are for the power converter supplier to control, it is desirable for the wind turbine to control the real and reactive power to the grid.

3.5.2 Wind Turbine

The wind turbine controller interfaces with the power converter controller by setting the converter's real power output reference and either a voltage set point, power factor or a reactive power set point. The wind turbine controller may receive a signal from the power converter during a grid fault, to indicate a loss of power output.

The aims of the wind turbine controller are broadly two-fold, first to maximise the energy yield of the turbine and second to ensure the speed of the turbine and the structural loads exerted on the turbine stay within design limits. Section 3.2.2 showed that the optimal coefficient of performance is achieved at a single ratio between the tip speed and the wind speed. Hence, under turbulent wind conditions, the rotational speed of the turbine would have to continuously vary to optimise the power capture and energy yield.

There are two possible approaches to optimising the energy yield which are covered in Camblong *et al*. [63]: "Indirect Speed Control" and "Direct Speed Control". The direct approach is shown to be more flexible to follow the optimal rotational speed as it is not restricted by the inertia of the turbine. Whilst they recommend the direct approach, they also acknowledge the higher torque and electrical power oscillations that result.

3.5.2.1 Indirect Speed Control

Leithead and Connor [64] illustrate that there is no such thing as a single wind speed, for use in the turbine controller, as the wind varies across the swept area of the blades. Hence, it is not possible to optimise the turbine through use of a wind speed input. Further, they highlight four goals for the wind turbine controller, which are summarised here:

- Limit mechanical loads
- Limit and smooth power output
- Damping the shaft system
- Optimising power capture and hence energy yield

They highlight the dynamic stability of a controller that tracks the optimal coefficient of performance by controlling the torque to follow the optimal *Cp* curve. Whilst Leithead and Connor propose complex controllers that are ideal for tracking the maximum power point, for power system applications these can be approximated with a look-up table defining either the generator torque or power dependent on the rotor speed of the turbine. Such a look-up table is graphically illustrated in Figure 3.15. Stability can be intuitively understood as follows; an increase in wind speed causes an increase in aerodynamic torque, which in turn accelerates the blades. The higher rotational speed of the blades leads to an increase in the power reference (from A to B) sent to the power converter. This increase in power reference leads to an increase in the electrical torque to counteract the increased aerodynamic torque and hence stable operation at a new, higher operating speed and output power.

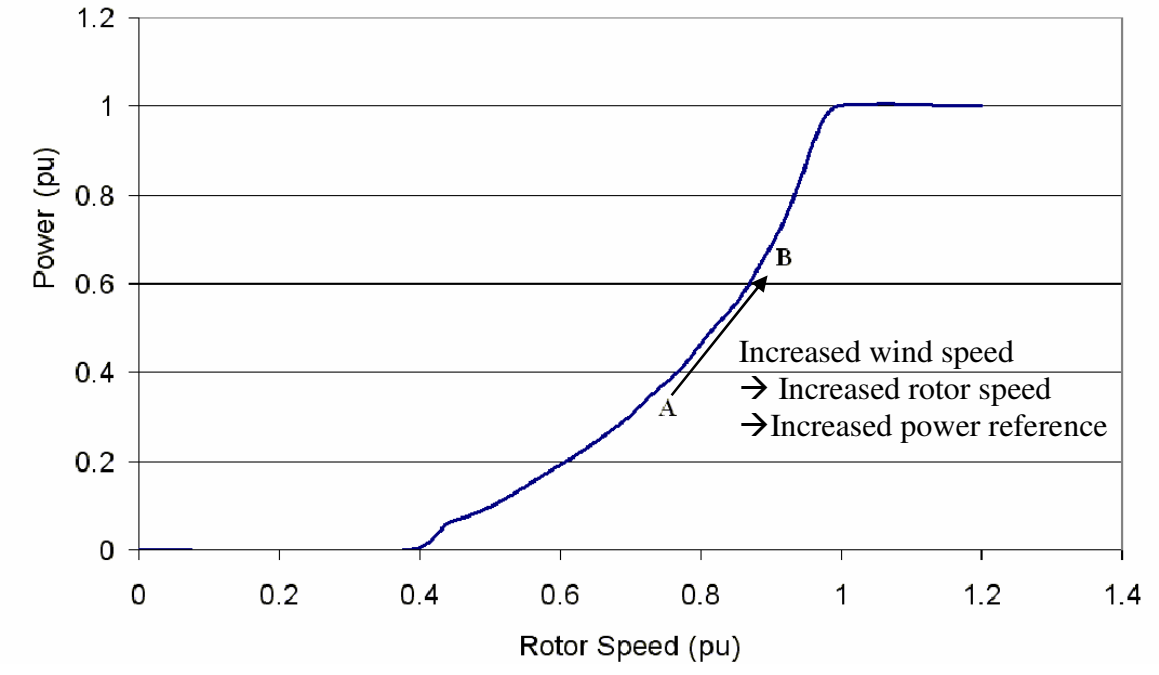

Figure 3.15: Rotor speed to power look-up table

This approach to optimising the energy yield of the turbine implicitly helps to smooth structural loads; sudden generator torque steps are avoided and gusts and lulls in the wind speed are filtered by the blades' inertia, resulting in only small changes in the rotor speed of the blades. However, the inherent use of the blades' inertia means that the optimal *Cp*

curve can only be tracked slowly, resulting in lower than optimal yield particularly in turbulent wind conditions.

This maximum power tracking method achieves a good trade-off between optimising the turbine's energy yield and minimising the structural loads. It is therefore a reasonable approximation to the conventional choice for a full converter wind turbine application.

3.5.2.2 Direct Speed Control

Burton et al. [65] have highlighted that closer tracking of the optimal *Cp* curve than Indirect Speed Control permits could allow an increase in the energy yield of a wind turbine by around 1-3%. This is a sufficient incentive that a new entrant to the wind turbine market proposed using a direct method of controlling the wind turbine's speed in 2009. This method is described here.

Figure 3.16 provides an overview of the salient features of the controller. A key feature is the measurement of output power to the grid and the subsequent setting of a new speed set point based on this, which is a reversal of the indirect method. The pitch controller therefore has to act to limit power output and the turbine controller provides a speed reference to the machine side converter.

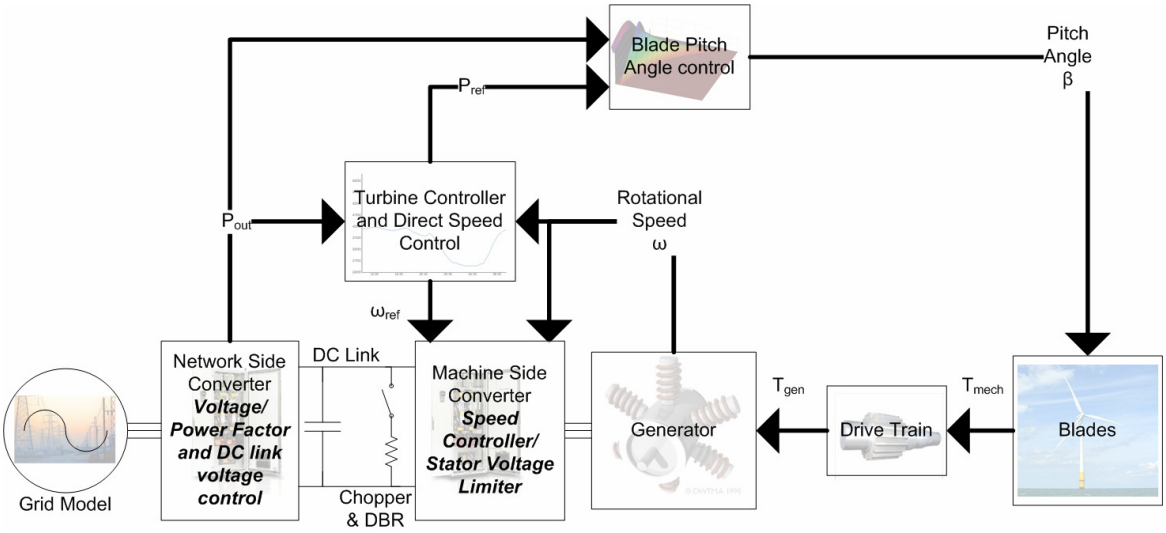

Figure 3.16: Direct Speed Control Overview

The speed set point is set according to an adaptive algorithm that can be seen in Figure 3.17. Essentially, if the power output increases when the speed reference has been increased then the controller sets a new higher speed reference until such a time as the power output decreases. This results in a 'hill-climbing' controller. Conversely, if the power output decreased when the speed reference had been increased then the controller

would set a new lower speed reference. By this means the controller should always look to maintain the optimal speed and therefore the optimal *Cp*.

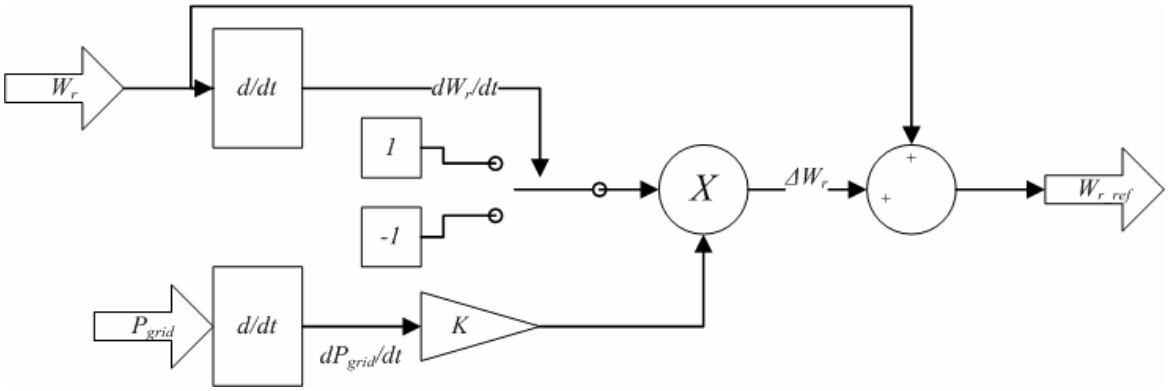

Figure 3.17: Direct Speed Controller (A hill climbing approach)

As the direct speed control method results in a speed reference output, it is necessary to implement a speed controller in order to give a torque reference output to interface with the drive controller. It is the dynamic performance of this speed controller, rather than the rotational inertia, which sets limits on how closely the optimal *Cp* point is tracked in turbulent wind conditions. A simple PI controller is the traditional means of providing speed control and this gives a torque reference which is modified by the maximum and minimum torque limits. The maximum torque is set by the limit on the drive train torque, whilst the minimum torque is likely to be zero or more as it would be unacceptable to motor the blades.

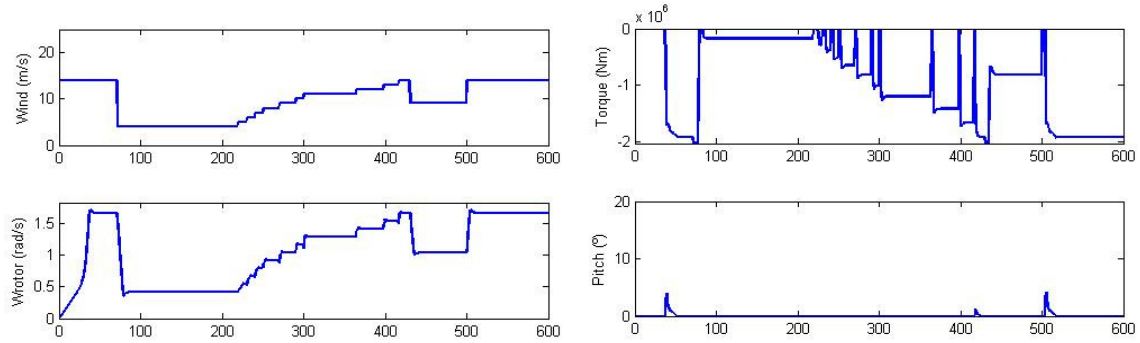

Figure 3.18: Direct Speed Control Torque Swings

Figure 3.18 illustrates the key challenge with direct speed control. Following a sudden increase in the wind speed there could be a significant torque transient, potentially to zero torque, whilst the blades accelerate to the new optimal speed. Given that the blades cannot be motored and the allowable torque is limited, the high inertia of the blades means that the controller can take a significant period of time to reach the new optimal point. The torque swings associated with keeping the wind turbine operating at the optimal *Cp* point

lead to unnecessary wear and tear on the drive train and difficulty achieving the theoretical gains from this strategy.

3.5.2.3 Shaft System Damping

Section 3.3 highlighted that wind turbines can have natural resonant modes between the shaft and the generator that can become unstable in variable speed applications owing to the loss of the grid's stabilising effect. This necessitates active damping of the shaft, which can be achieved in three ways:

- Use of the pitch controller to aerodynamically damp the speed oscillations of the blade. This is limited by the rate at which the pitch actuators can adjust the blades and consequently is the least effective method according to Muyeen *et al*. [66].
- Add a damping term directly to the torque controller of the machine bridge. This is rapid and effective according to Hansen and Michalke [50] but requires the oscillation energy to be stored in the DC link of the converter. This oscillation energy results in higher voltages on the DC link and would necessitate a higher rated and more expensive capacitor.
- The third option is to add a damping term to the converter's power reference; this method has also been shown to be effective but has the side effect of causing a degree of ripple in the power to the grid whenever the mechanical mode is excited.

The third option is the preferred option here as it has the lowest impact on the design requirements for the power converter and wind turbine. It can be implemented by augmenting the power reference derived from the wind turbine's maximum power tracking algorithm and using a damping controller that is similar in structure to that proposed by Hansen and Michalke. This is shown in Figure 3.19, however, it should be noted that the phase delay due to the machine bridge DC link control of the power converter makes the phase lag greater than that seen by Hansen and Michalke's controller, necessitating careful tuning of the phase compensator.

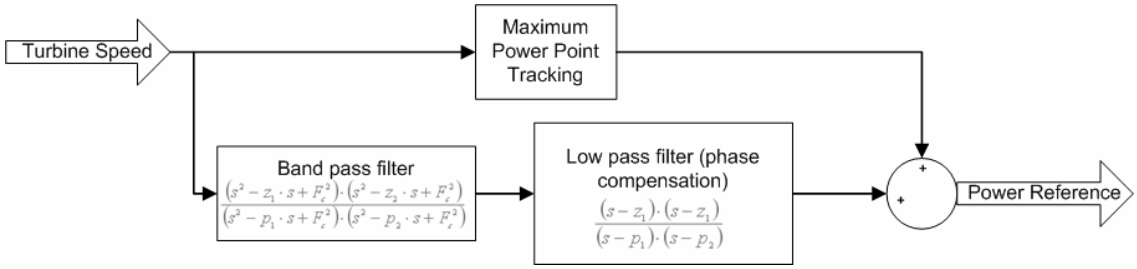

Figure 3.19: Shaft Damping Controller Added to Maximum Power Tracker

3.5.2.4 Pitch Angle Control

Figure 3.1 and Figure 3.16 highlighted the need for pitch angle control of the wind turbine's blades in order to limit the speed and power output of the turbine respectively. The representation of the pitch controller used here ignores the fine tuning of pitch angle that occurs to optimise *Cp* in below rated wind speeds. For the power system models developed here, it is appropriate to concentrate on the primary function of the controller: limiting power or blade speed in above rated wind conditions. As the focus is on large, full converter wind turbines, the pitch strategy considered here is pitch-to-feather owing to the high structural loads that a pitch-to-stall strategy would incur and the more common deployment of pitch-to-feather according to Muljadi and Butterfield [67].

Bossanyi [68] has shown that modern large scale wind turbines have complex pitch controllers fulfilling multiple objectives, including smoothing out tower shadow torque pulsations using individual blade pitch angle control. For the purposes of representing the electrical characteristics of a wind turbine it is not necessary to model the pitch controller in such detail, however, it should be noted that the representation of the pitch controller used in this work is a significant simplification compared to a full controller.

A standard PI controller can be augmented with anti-wind-up control to account for the physical limit on the extent and rate at which the blades can pitch. Muljadi and Butterfield have also shown that slower pitch systems of 4°/s experience significant speed fluctuations and hence wind-up, whilst faster systems (they consider 8°/s) can lead to significantly smoother output. Figure 3.20 shows the key elements of the pitch controller. It can be noted that the modelled pitch controller does not act when the rotor speed is below the rated rotor speed. Thereafter, the pitch angle increases to bring the turbine speed back to target.

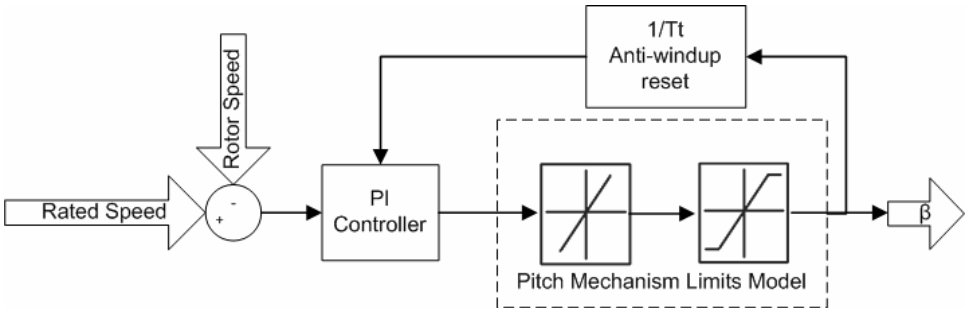

Figure 3.20: Pitch Controller for Indirect Speed Controlled turbine

3.5.3 Wind Farm

The wind turbine's controller is responsible for optimising the power output and behaviour of the wind turbine by controlling the pitch of the turbine's blades and the set points of the power converter. In individual installations or small wind farms this is

sufficient functionality to operate, however, Christiansen [69] has shown the complexity involved in larger scale offshore wind farms which are captured by the requirements of Grid Codes. Under large scale schemes it is necessary to have some control of the individual turbines centrally in order for the wind farm to operate in the manner of a conventional power plant.

Gjengedal [70] has detailed fourteen different means by which centralised wind farm control may be necessary in order to replicate the behaviour of conventional plant. These reasons may be summarised as:

- Reactive power control for voltage stability and variable power factor operation in steady state.
- Reactive power control to feed fault current contributions in transient states.
- Real power control to meet ramping and maximum power limits in steady state.
- Real power control to meet frequency control requirements under transient states.
- Black start and islanding control.

Such control can be implemented by communicating with the individual wind turbine controllers and acting as a system aggregator. Banham-Hall *et al.* [71] have shown a typical scheme where the wind turbines provide the central wind farm controller with a measure of their individual available power. The central controller then dispatches real power and voltage operating points to the individual wind turbines. This ensures that the wind farm operates as a single power plant to meet the requirements of modern Grid Codes, which will be discussed further in chapter 4.

Figure 3.21 considers the case where frequency is centrally controlled, with power set-points sent to each individual turbine. Conversely, the voltage (potentially reactive power or power factor) is controlled locally to the turbines. However, this combination is not unique, alternatively the frequency controller could exist at each turbine, with a central supervisor; or else the control of voltage could be exercised centrally, with a reactive current demand dispatched to each turbine. Overall, however, the central controller has to maintain a supervisory function.

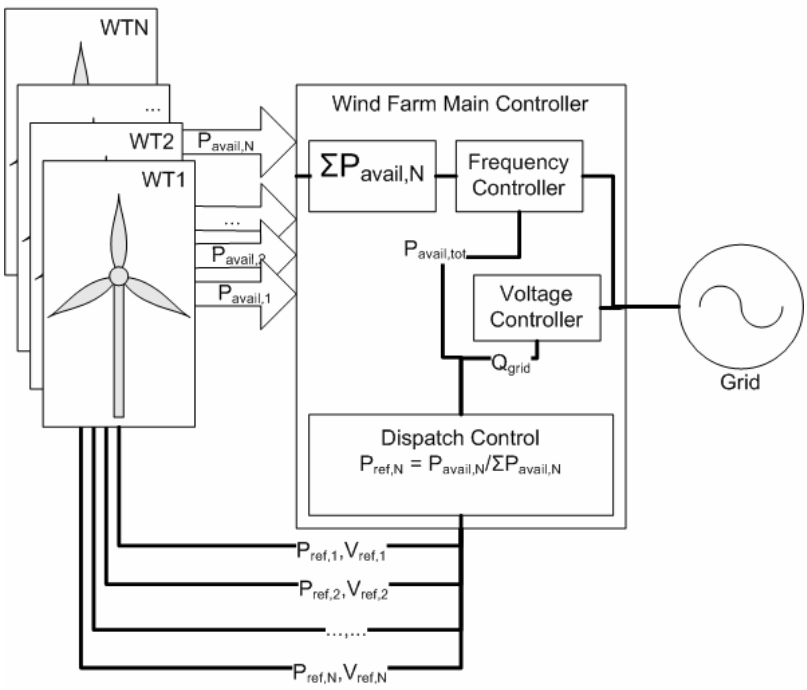

Figure 3.21: Wind Farm Controller, aggregating wind turbine availability and dispatching real and reactive power or voltage set-points to the individual turbines

3.6 Software

3.6.1 Matlab-Simulink

Matlab-Simulink is an ideal environment for development of control systems and single wind turbine models. Iov *et al.* [72] have released a standard library for wind turbine modelling, however, this was developed in the era before the prominence of full converter wind turbines and hence focussed largely on DFIGs and FSIGs. Further, the power converter control systems deployed were not in keeping with the control system used in GE Energy's converter. The library is also restricted to academic and non-commercial use, hence whilst it has provided useful insights, new blocks and models have been developed.

GE Energy use Matlab-Simulink for modelling of the full converter, importing the drive code and wrapping it in s-functions. This modelling includes switching patterns, full internal drive features, such as alarms and protection, and full modelling of the DC link. This model is appropriate for short time scale studies that require absolute detail, such as fault ride-through modelling of single turbines. However, at the outset of this project the simulation times associated with this model were of the order of an hour per fault ride-through study. This demonstrated that it was unfeasibly complex for longer time-scale studies or for multiple turbine studies.

This project has therefore developed a suite of models for use in multiple turbine or longer time-scale studies. These models have in common that they are full converter type wind turbines, but beyond that incorporate different generators, shaft topologies, converter control strategies and maximum power point tracking methods. The range of different models is summarised in Table 3.2.

As can be seen from Table 3.2, the variety of models developed allows comparison between many of the different control techniques and technologies deployed with full converter wind turbines. Often wind turbines with full converters are classified as a single type, this work reveals the variety that can exist within type 4 wind turbines and highlights the risk of assuming generic properties of full converter wind turbines without understanding the underlying technologies.

Model Number	Capacity (MW)	Geared	Generator Type	Converter Voltage (V)	DC Link Chopper and DBR	Converter Control Strategy	Turbine Speed Control
1	2.3	Yes	Induction	690	No	Reversed	Indirect
2	3.6	Yes	Induction	690	No	Reversed	Indirect
3	3.3	Yes	Permanent Magnet	690	Yes	Reversed	Indirect
4	3.0	No	Permanent Magnet	900	Yes	Conventional	Direct
5	3.0	No	Permanent Magnet	900	Yes	Reversed	Indirect
6	Variable	Either	N/A	690	Yes	Reversed	Indirect

Table 3.2: Matlab-Simulink Wind Turbine Models Developed

3.6.2 DIgSILENT PowerFactory

Matlab-Simulink does not lend itself to studies of a wind farm's interaction with the wider power system and grid connection studies. DIgSILENT PowerFactory is fast becoming the standard industry tool for transmission system studies and for analysing the impact of integration of renewable energy into the power grid. National Grid is currently transferring their in-house modelling capability onto DIgSILENT. As such it was appropriate to ensure that the modelling capability in Matlab-Simulink was transferred into PowerFactory for analysis of larger wind farms and integration with the power system.

Hansen *et al.* [73] have released a description of wind turbine models in PowerFactory. However, it suffers from the same restrictions and limitations as the Matlab library. Therefore, a new model of a full converter wind turbine has been developed in

PowerFactory. As the use of the model was geared towards power system application, this model is a generic full converter model in the same style as model 6 from the Matlab-Simulink suite. Further details of this model are given in section 4.2.6. The DigSilent PowerFactory model, whilst introduced and validated here, is only extensively used in chapter 7 where larger systems and longer timescales are considered.

3.7 Validation

Validation of wind turbine models is critical to ensuring the reliability of any studies based on them. Transmission system operators have increasingly required provision of validated wind turbine and wind farm models for use in their power system studies. This has increased the formality of model validation and led Martin, Purellku and Gehlhaar [74] to develop and present software which conducts a formal validation analysis on wind turbine site and model data.

Amongst wind turbine manufacturers, model validation is rigorous but less formalised, typically relying on comparing the outputs from network related fault ride-through events with modelled predictions. Nielsen *et al.* [75] have shown how this typically relies on the use of data from a fault ride-through test facility and involves complete faults with 0% retained volts and partial faults with retained voltage above zero. As the manufacturers' models are for application in wider power system modelling, the relevant parameters are typically:

- Voltage at the turbine terminals.
- Real power exported to the grid.
- Reactive power exported to the grid.
- *d* and *q*-axis current to the grid.
- Speed of the wind turbine.

The models developed as part of this EngD are used for power system studies and hence this level of validation is applicable. However, they are also used internally for addressing the impact of the wind turbine's operation on the generator and power converter system. This additional use is particularly true for the Permanent Magnet Generator wind turbine models where much of the use of the models has been geared towards design impacts for prototype systems. Hence the validation process applied to the models developed as part of this EngD has been two-fold; first, where possible individual subsystem models (for example the drive train) have been validated independently. Second, a complete wind

turbine model of an FFIG has been validated against site data in the manner previously described by Nielsen *et al*. The individual subsystem validation is covered in this section, whilst the second stage grid fault ride-through validation is included in section 4.2.3, following the detailing of grid fault ride-through control and modelling.

3.7.1 Wind Model

The adaption to the wind model presented by Sorenson has been compared to the released model in the Matlab-Simulink library from Aalborg University [72]. The comparison of the power spectral density functions and two time series from the different models can be seen in Figure 3.22 and Figure 3.23.

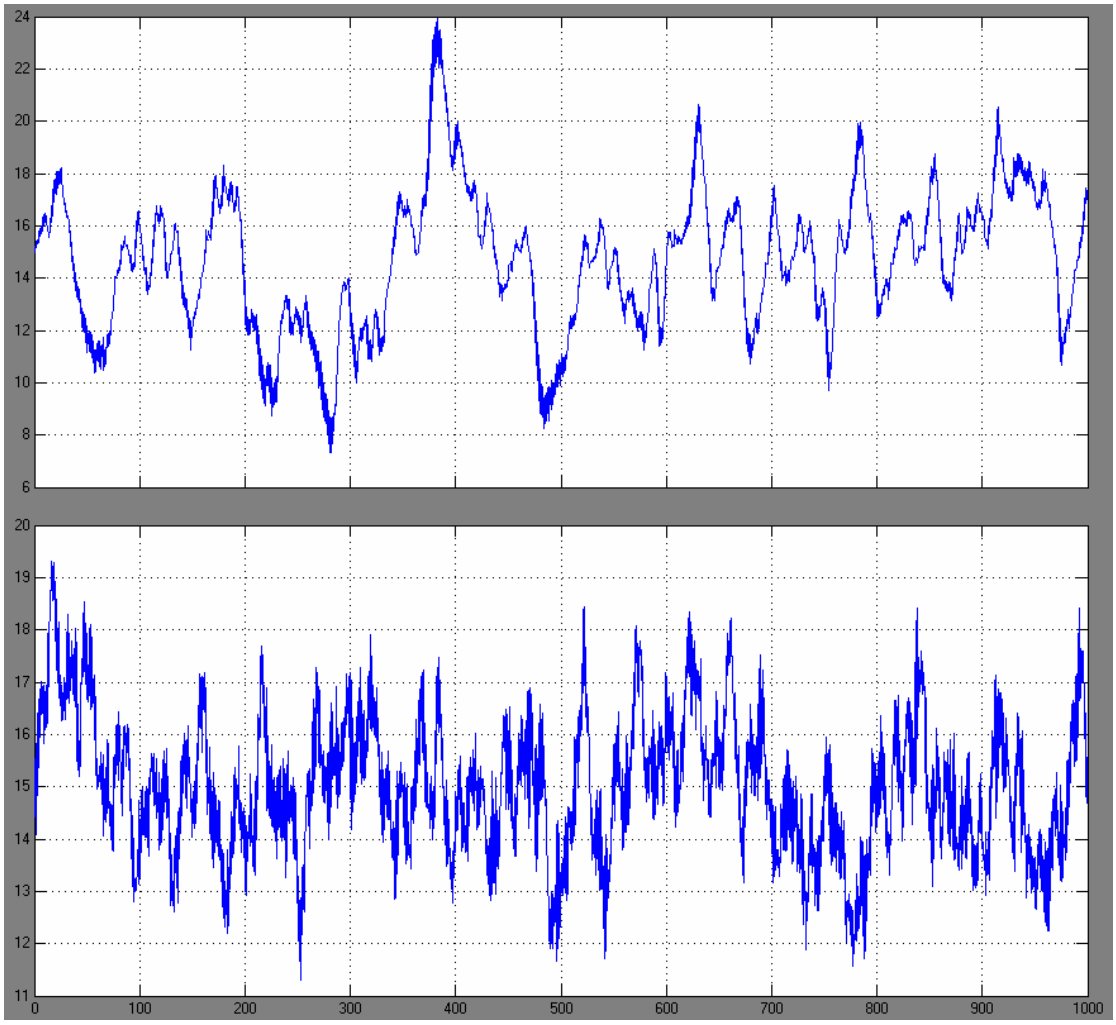

Figure 3.22: Wind Speed Time Series Comparison (Top: Developed model, Bottom: Aalborg Model)

The time series comparison confirms that the fundamental component of turbulence associated with wind peaks and troughs has been exaggerated in the developed model. This brings the developed model into line with the IEC 61400 standard [44] for extreme events and is therefore appropriate for individual extreme loadings, but is less representative of real wind farm conditions. This was desirable for assessing extreme

speeds of PMGs as a result of gusts and turbulence and consequently to assess peak voltages experienced by the machine side rectifier under open circuit conditions.

Comparing the power spectral density functions of Figure 3.23 illustrates that the developed model has a higher power spectral density at low frequency, leading to the higher 0p fluctuations. The 3p component is still clearly in evidence in the developed model, but with a slightly narrower peak.

Overall, the developed wind model is appropriate for investigating individual turbine behaviour under extreme conditions. This is particularly true when considering the variation in wind power available over periods of seconds to minutes as is the case when assessing worst case peak speeds and voltages of PMG based wind turbines. When considering whole wind farms, the Horns Rev actual output data is more applicable.

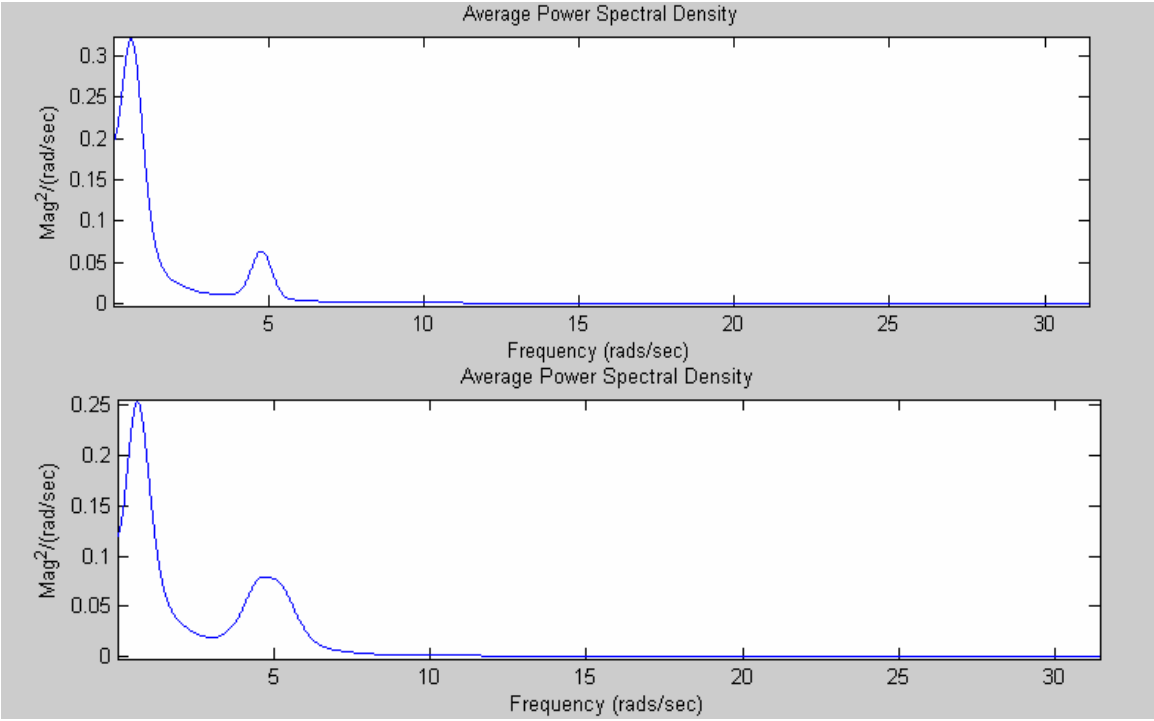

Figure 3.23: Wind Model Power Spectral Density Function Comparison (Top: Developed model, Bottom: Aalborg Model)

3.7.2 Shaft Model

The shaft model has been validated against data provided from a customer's higher order wind turbine direct-drive PMG shaft model. Figure 3.24 shows a comparison between the oscillations predicted by the developed second order shaft model and those of the higher order shaft system. In both cases there is no active damping, so the resonance is a result of free oscillations in the shaft, the only limit on the resonance is provided by the torque limits of the generator. Being a direct-drive system, it also highlights the higher frequency of oscillation that is possible with direct drive shafts.

From a mechanical system perspective, the internal shaft torque is the critical parameter as this determines design loads. However, from a power system modelling perspective, the generator's oscillation is the critical parameter as this directly affects the model's electrical output. Both of these parameters show excellent agreement with the real data. This provides confidence in the shaft model for a wider range of systems.

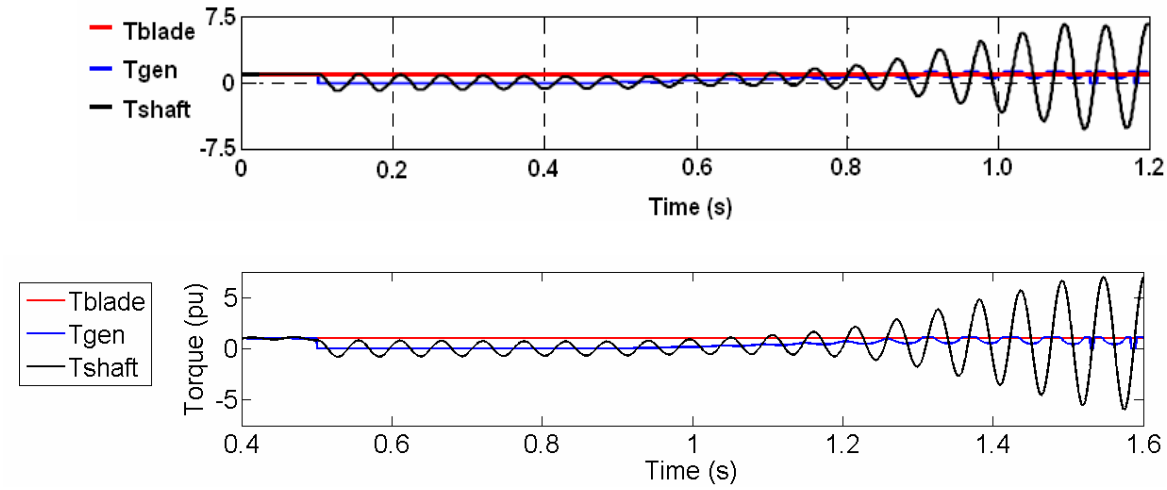

Figure 3.24: Generator, shaft and blade oscillations (Top) and model validation (Bottom)

3.7.3 PMG Model

GE Energy's PMG designers' provide a plot of expected volts against current at a specific power factor, at rated speed for each PMG product. This is a steady state validation as it excludes the effects of changing currents on terminal volts; however, it can provide partial validation of the accuracy of the PMG model. Figure 3.25 shows the projected regulation curve from the machine design for models 4 and 5 on the left, with the model's measured output on the right.

To generate this measured model plot also partially validates the PMG control methodology as it relies on constant power factor control in a stator voltage oriented reference frame. These measurements at all points are within 3% of that projected by the machine designers. This is well within the error band of voltage for variation between different machines. The magnets within PMGs can vary in strength leading to variations in voltage between machines that are greater than the error margin in model accuracy. Furthermore, the representation of the machine assumes that the magnets are operating at their design temperature, as this can have a further significant impact on the internal EMF and output voltage. One point to be aware of, however, is that the model slightly underestimates the peak voltage of the PMG at this power factor (1.5%), illustrating the need to keep a safe headroom margin for converter control.

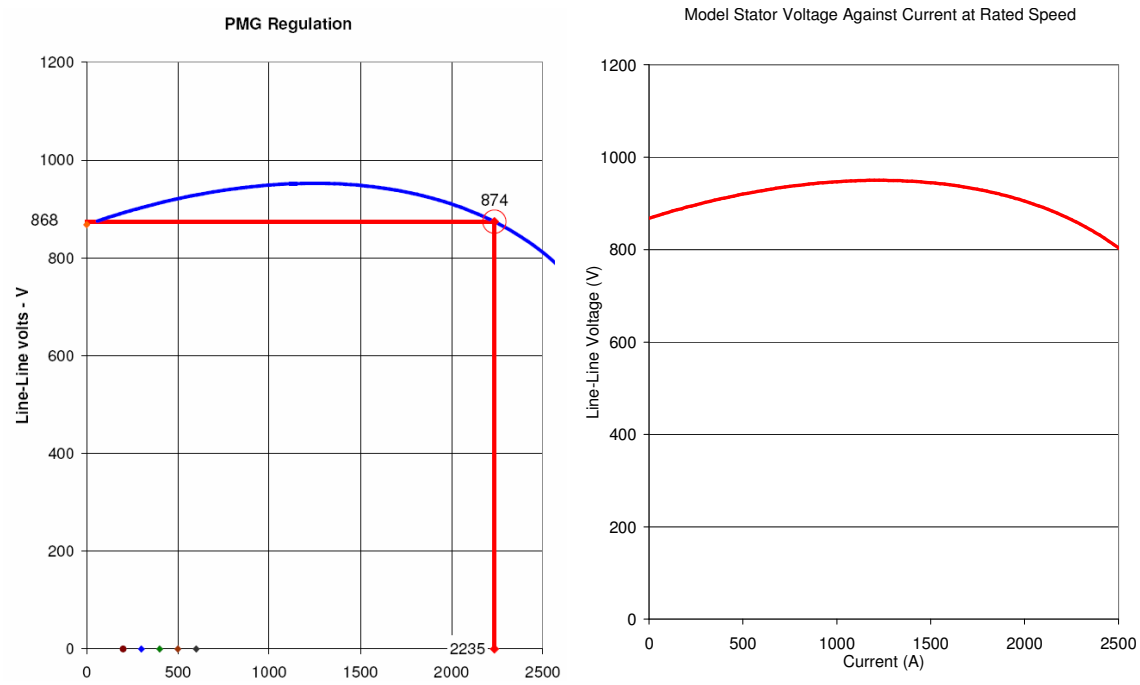

Figure 3.25: PMG Regulation plots from machine designers (left) and PMG model (right)

3.7.4 Converter Control

GE Energy has a 750kW test bench at their converter manufacturing facility with back to back converters. This allows one converter to synthesise grid disturbances whilst the response of the other converter can be measured. This has allowed the dynamic behaviour of the network bridge to be validated against the test bench.

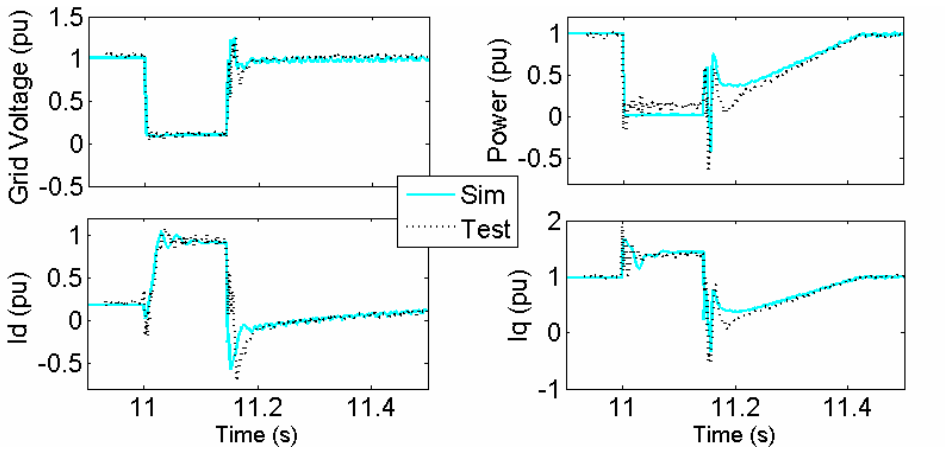

Figure 3.26: Converter Control Validation Plot

Figure 3.26 shows the results from the network bridge model and the test bench under a voltage disturbance. The agreement between the model's output and the test bench data is excellent, demonstrating that the dynamic performance of the model is good. However, this validation process does highlight the limitations of using a fundamental voltage source model, with the magnitude of the fastest transients on the current controllers underestimated. The fundamental voltage source model is limited by the bandwidth of the current controllers to less than 200Hz. However, the switching frequency of the PWM

cycle would typically be around 1.0-2.5kHz. The underestimation in fast transients would be a concern if the model were intended for detailed studies of the power converter, however, for power system study use it is adequate as all transients of 10ms or longer are well represented.

3.8 Summary

The key contribution of this chapter was the development of validated models of full converter wind turbines, permitting wind to grid analysis.

This chapter has covered the development of a suite of full converter wind turbine models in Matlab-Simulink, with a key model also created in DIgSILENT PowerFactory. It has illustrated the diversity in technology and control techniques within this single class of wind turbines. The sub-system models developed have been validated independently to allow confidence in hybrid models using different model combinations.

Whilst the development of these models has depended on the existing literature, it has also extended it. A new wind model, which is appropriate for extreme wind condition scenarios has been developed, this allows assessment of the extreme speeds, leading to extreme voltages that can be seen on generators. This is particularly crucial for PMGs, where it has been shown that their inability to field weaken presents a design challenge with regard to the stator and converter voltage levels. PMGs with direct-drive shafts are also shown to have potentially higher frequency resonant mechanical modes than would be the case with geared solutions.

The full converter induction generator has not been extensively covered by those modelling full converter wind turbines, who typically focus on either conventional synchronous generators or PMGs. These same modellers have historically focussed on only conventional control of the back-to-back IGBT bridge, but here the modelling includes the newer reversed control scheme, which provides benefits in generating applications. The interface of this converter controller to the wind turbine controller is also shown, owing to renewed commercial interest in applying direct speed control to wind turbines in place of the classical indirect control scheme.

The suite of models is built on a fundamental voltage source representation of the converter, which includes power balancing to replace the requirement to physically model the devices and switching patterns. This allows the model to be more appropriate to multiple turbine and longer time-scale studies.

4 Grid Connection of Full Converter Wind Turbines

4.1 Introduction

As the scale and number of large offshore wind farms increases, it is anticipated that increasingly they will be connected directly to the GB transmission system, or possibly even a European Super-grid. As such, it is important that these wind farms interact with the power system in a manner that supports the grid's stability. The approach that the GB Grid Code has taken is one where all generation is required to fulfil a specific set of technical requirements. Urdal and Horne [76] have shown that this approach is technology neutral and encompasses much more than just Grid Fault Ride-through behaviour. They have identified six key areas where Grid Codes impact on wind farm systems: "Fault Ride Through (FRT), Reactive Range, Voltage Control, Frequency Range, Frequency Response and Modelling".

This chapter concentrates mainly on two key areas of Grid Code compliance. First, section 4.2 considers the GFR requirements and their impact on full converter wind turbines. It begins with the FFIG, showing how field weakening can contribute to controlling machine voltage during a fault. It also presents validation results from the derived model and site tests. Section 3.4.3 highlighted that PMG rotor flux is essentially fixed, which places key limits on a FFPMG's ability to replicate this. This leads to new and specific challenges for the FFPMG under GFR which are explored in more detail in section 4.2.4. Section 4.2.5 then contributes new control methods that allow the FFPMG to ride-through grid faults with small choppers and dynamic brake resistors whilst also protecting the wind turbine mechanical system.

Second, section 4.3 considers the frequency response requirements placed on wind farms and the methods that wind farms can use to emulate the behaviour of conventional generators. It specifically explores different methods of providing short term frequency support and compares different control methods for providing response, extending existing knowledge in this area. Section 4.4 then considers in detail the challenge of providing very fast inertial response to rapid grid frequency changes and proposes new control methods that provide a synthetic inertial response without taking the derivative of grid frequency.

4.2 Grid Fault Ride-through

Grid faults may be caused by damage to lines causing single phase, two phase or three phase faults either phase to phase or phase to ground. The most severe case is usually a three-phase to ground fault, which may lead to a complete loss of a wind farm's ability to export power to the grid. It is important that under such faults the transmission system's protection devices operate as intended and that the system subsequently recovers stably. As such Grid Codes have developed specific requirements on generators connected to the transmission system to ensure the secure operation of the system.

The transient nature of grid faults typically leads to a thorough test both of the physical wind turbine system, due to a step change in electrical and mechanical behaviour, and wind turbine models, which try to predict the behaviour of a wind turbine under a specific grid fault.

4.2.1 Grid Code Requirements

GFR requirements are typically specified in terms of an envelope of potential faults for which a wind farm must stay connected to the system and transiently stable. The wind farm usually classifies a voltage of less than 90% of nominal as a fault. Ausin, Gevers and Andresen [77] have provided a worst case envelope from studying several different nation's Grid Codes, which is shown in Figure 4.1. The solid green region is the region for which a wind farm must stay connected. In a worst case, this requires a wind farm to ride-through a zero voltage fault lasting 180ms at the wind farm's connection point. Alternatively, a fault that led to a suppression of the voltage to 50% would require the wind turbine to stay connected and transiently stable for up to 1.8s.

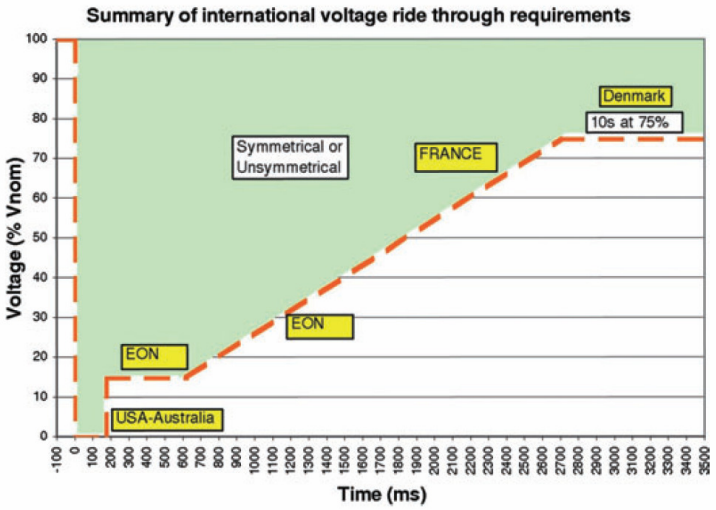

Figure 4.1: International Fault Ride-through Requirements Comparison according to Ausin, Gevers and Andresen [77]

Section 2.5.2 showed that under a transient voltage suppression such as GFR a synchronous machine would inherently provide a high reactive current output. This reactive current output contributes to supporting the voltage at the machine's terminals and triggering any necessary protection devices. Hence, in addition to riding through the fault, it is typical for Grid Codes to mandate that wind turbines output reactive power according to their power converter's current limit for the duration of the fault. This necessitates a priority change for the power converter from outputting real power prior to the fault to outputting reactive power during the fault and back to real power following fault clearance and can contribute to significant mechanical load changes on the turbines.

Following the restoration of voltage to normal, national Grid Codes place different requirements on generators depending on their system characteristics. The relatively small, islanded system of the GB grid prioritises the restoration of real power in order to avoid a subsequent frequency problem. This leads to a requirement on GB connected wind farms to recover their real power output to within 90% of the pre-fault level within 0.5s of system voltage recovering to within 90% of nominal according to National Grid [78]. Such a requirement effectively mandates a fast ramped increase in the wind turbine's output following a fault. Conversely, the large and interconnected Eon Netz system in Germany prioritises the recovery and stabilisation of system voltage following a fault, with reactive power taking priority for the first 500ms following fault clearance. Furthermore, active power is only required to recover at a rate of 20%/s or faster [79] which is much slower than the effective 180%/s rate that National Grid apply.

Typically wind turbines are designed to withstand the combined worst case scenario, such that GFR performance is satisfactory for any market internationally.

4.2.2 Fully Fed Induction Generator

Under a severe grid fault the power output to the grid is instantaneously lost; however, the aerodynamic input power to the blades is initially unchanged. Consequently, initially the machine will tend to continue generating into the power converter's DC link. Without additional control, in the case of the conventional control strategy of section 3.5.1.1, this would lead to the DC link voltage rising beyond its design rating. Conversely, under the reversed strategy, outlined in section 3.5.1.2, the DC link voltage controller would reduce the torque and hence power generated in response to the DC link voltage rise. However, this response to a 100% step in output power may be too slow to stop excessive power in feed to the DC link due to the limited energy storage capacity of the optimally sized capacitors (which have a time constant of around 5ms).

Given the risk of over-voltage on the power converter's DC link, the control strategy has to be modified to protect the DC link capacitors. This is done by first calculating the real current output capacity of the grid (I_{q_lim}) according to Equation 4.1, where the *d*-axis current is set in line with the requirement of the relevant grid code according to Equation 4.2 (k_{Grid_Code} is typically 1 to 1.5 in per unit terms). The current output limit and the instantaneous fault voltage can then be used to estimate the power capacity of the grid (P_{ff}) in per unit, according to Equation 4.3. This power capacity then acts as a feed-forward to the machine bridge, where it limits the power output of the machine and improves the dynamic response of the converter to a grid fault (see Figure 4.2).

Equation 4.1 $I_{q\_\lim} = \sqrt{(I_{rating}^2 - I_d^2)}$ Where I_{rating} is the converter nominal rating.

Equation 4.2 $I_d = k_{Grid\_Code} \cdot (|V_{nom}| - |V|)$ Where $|V_{nom}|$ and $|V|$ are the nominal grid voltage and instantaneous faulted grid voltage magnitudes.

Equation 4.3 $P_{ff} = \frac{3}{2} \cdot |V| \cdot I_{q\_\lim}$

Rapidly reducing the torque on the generator has a two-fold effect, first the machine begins to accelerate as a result of the unrestrained torque from the blades. Second, the torque step would be liable to excite the mechanical shaft resonance discussed in section 3.3. Hence, the GFR strategy leads to activation of the shaft damping controller discussed in section 3.5.2.3 and blade acceleration may lead to activation of the pitch controller discussed in section 3.5.2.4.

The typical pitch controller has a finite response time and a limited pitch rate, meaning that it cannot instantaneously limit the acceleration of the turbine. Hence, the speed of the generator will typically increase due to the slow blade acceleration and the transient oscillations of the shaft. The field weakening strategy of the induction machine therefore has to act to counteract the speed oscillations and to ensure that the consequent voltage oscillations seen at the power converter terminals are within safe operating limits. The vector control of the induction machine allows this to be achieved straightforwardly with a stator voltage limiter modifying the *d*-axis current reference on the machine bridge, which is shown in Figure 4.2.

The final modification to the steady-state control to provide for GFR is to switch from a steady state voltage controller derived I_d reference on the Network Bridge to that defined in Equation 4.2, according to the instantaneous voltage and the relevant Grid Code. This

change in I_d set-point is designed to ensure that the grid voltage support is activated rapidly at the onset of a fault.

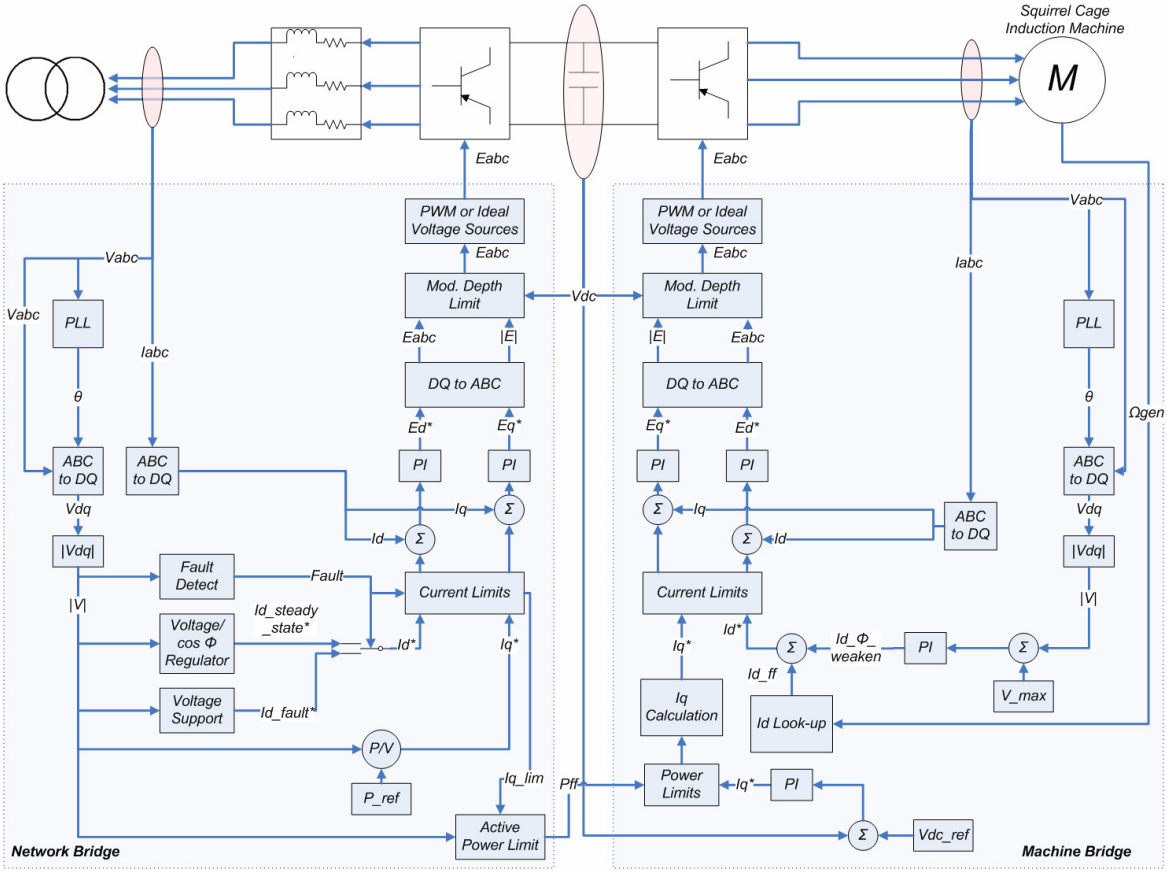

Figure 4.2: FFIG Reversed Converter Control for Fault Ride-through

4.2.3 Model Validation

The severity of GFR, combined with the fact that it activates many of the wind turbine controllers and that there is a requirement for wind turbines to undergo GFR type testing means that it provides ideal data for validation of complete wind turbine models. As such Figure 4.3 and Figure 4.4 show the outputs from a large FFIG wind turbine undergoing type testing against the GFR requirement. Under this specific test the turbine was subjected to a three-phase to ground voltage fault with 50% retained voltage, lasting for 1.8s. This section discusses the degree of agreement between the models and the type tests and identifies the causes for any differences.

Figure 4.3 shows the key parameters of the machine bridge under this GFR scenario. It should be noted at the outset, that the large spike on Wr at the onset of the fault suggests some high frequency noise coupled onto the measured site data, as clearly a speed change such as this is non-physical.

The top sub-plot shows the rapid change in real power on the machine bridge that is achieved as a result of the feed-forward power limit from the network bridge. The initial

spike in power prior to the fault is due to the demagnetisation of the converter's main reactor, whilst the spike at the point of fault recovery is due to the release of the power limit and a transient as the DC link voltage controller recovers control. During the fault, the full current capacity is deployed to fulfil the *d*-axis current requirement and then to maximise real current output, within the limits of the converter. This means that the shaft damping controller is inactive until the post-fault period, whereupon it superposes the decaying sinusoidal damping term on the DC power level. The profile of the power plot and damping show excellent agreement, with the only significant differences due to the model's simplified ideal voltage source behaviour not representing the fastest switching dynamics.

The second to fifth sub-plots show the *dq*-axes' set-point and feedback currents. The *q*-axis plots show good agreement again between the modelled data and the site data, as well as between the set-points and feed-back values. The *q*-axis, aligning with torque and resulting from the DC link controller, closely follows the behaviour of the machine bridge real power.

The *d*-axis currents show reasonable agreement between the site data and modelled data, with the stator voltage limiter acting to sinusoidally modulate the flux in order to maintain a smoother voltage output. This helps to ensure the *q*-axis current is also smoother. However, there are two noteworthy differences in the *d*-axis current. First, the sinusoidal component begins to loose synchronism between the modelled data and the site data following the end of the fault. This is because of differences in the performance of the damping controller between the ideal modelled case and the site case. The second difference in the *d*-axis current can be seen on the peaks of the sinusoids with the model showing a double peak in current for two periods following fault clearance. This is because the *q*-axis current is given priority over the current limits following the fault and the total current runs into the converter's design limit at the peak of the I_d curve; hence the reference is reduced causing the double peak. This double peak is more pronounced than the site data infers, and is largely due to the modelled damping controller superposing a larger sinusoid on the q-axis current reference in the model than the site data, which in turn leads to the faster damping discussed above. Overall, however, the model shows very good agreement with the site current measurements.

The sixth sub-plot shows the DC link voltage. Here, the spike at the onset of the fault is assumed to be noise in the measurement as further investigation has shown it appears and disappears within a couple of switching cycles. With the exception of that spike, the plot

shows the success of the feed-forward power limit in maintaining the DC link voltage within limits. Slight transients can be seen at the beginning and end of the fault, which are larger on the site data than the model data, but the broad shape of the responses at these points are similar.

Finally, the last sub-plot shows the generator speed, where the undamped shaft oscillations can be seen to build up during the fault and then are damped down in the post fault period. The unknown wind conditions of the site test led the turbine to initially be operating slightly above rated speed and this is assumed to be the reason for the slight steady state deceleration in the measured generator speed which is not replicated in the model. However, this discrepancy is small and the mechanical oscillations due to the shaft are seen to be in phase and similar in magnitude throughout the simulation.

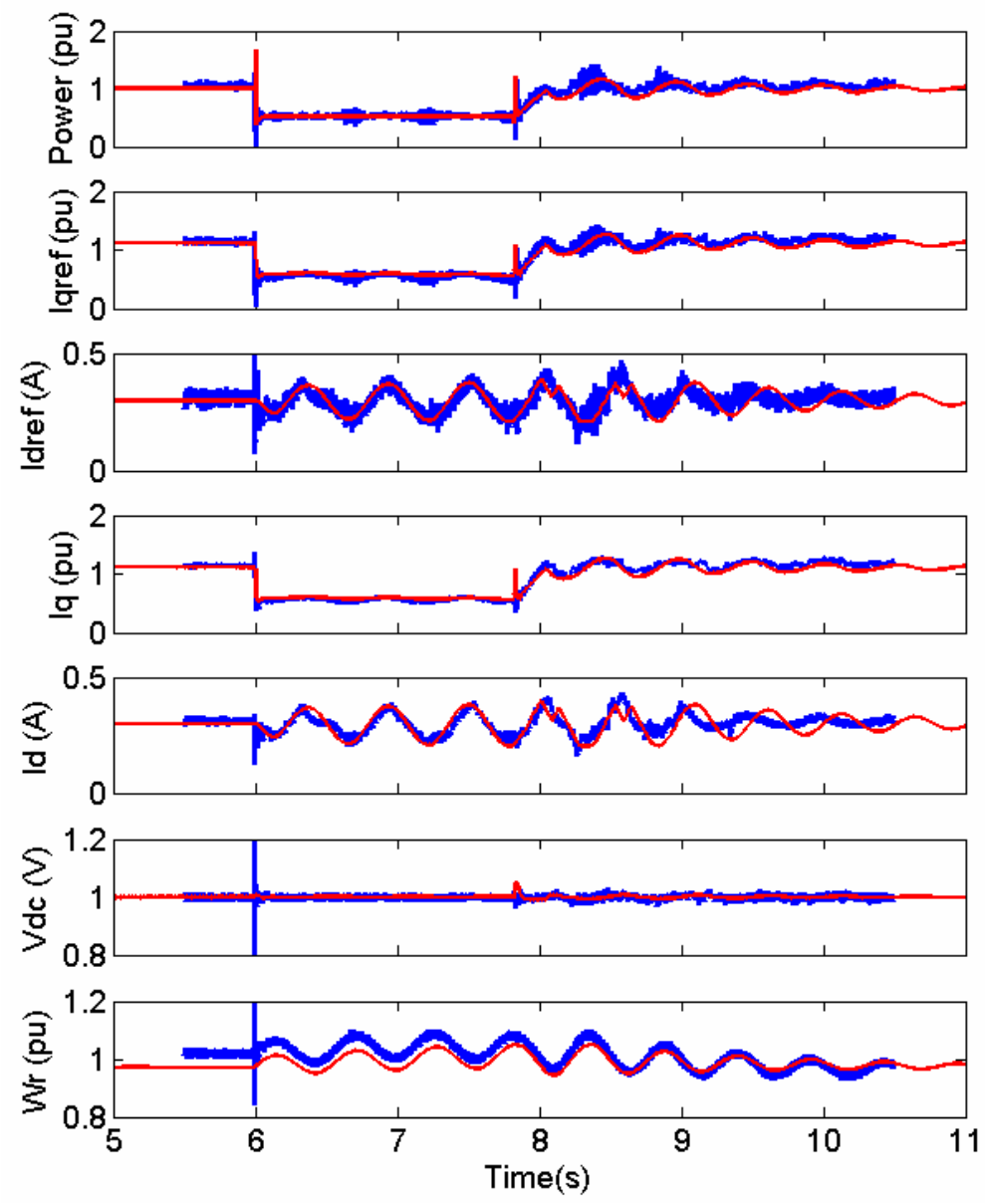

Figure 4.3: FFIG Machine Bridge Fault Ride-through Validation Plot (Site data is shown in blue, modelled predictions in red)

Figure 4.4 shows the key parameters for validating the network bridge model. The top sub-plot shows the voltage profile for the fault, with the sharp fault edges indicating the scale of challenge that GFR sets wind turbines. The fault is applied downstream of the turbine transformer, with the top plot representing the measured voltages on the LV side. Hence, the reactive power output of the converter ensures that the measured voltage is slightly above the 50% retained voltage at the fault site. The simplified grid representation used in the model means that the fast voltage oscillations on fault recovery do not represent those of the network under site tests.

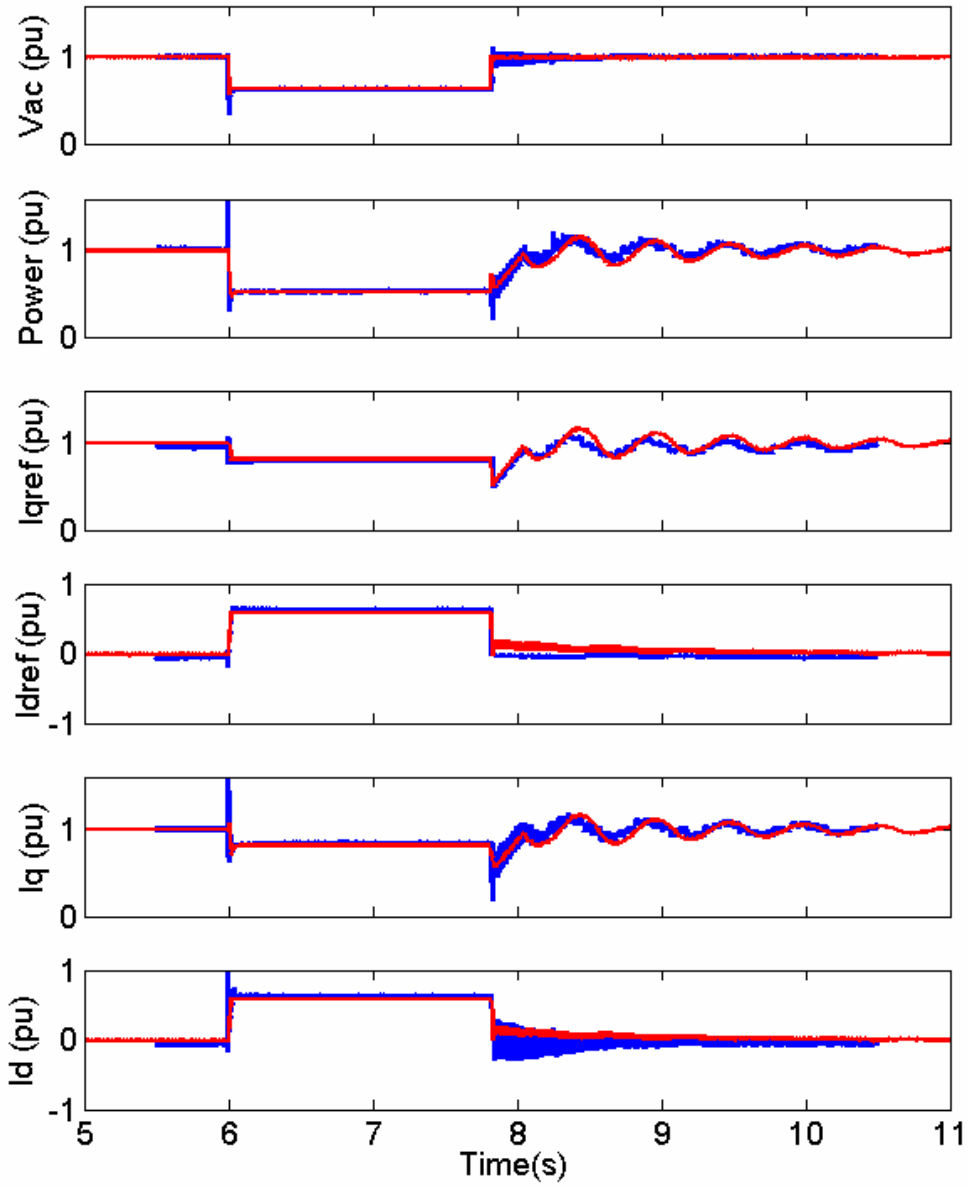

Figure 4.4: FFIG Network Bridge Fault Ride-through Validation Plot (Site data is shown in blue, modelled predictions in red)

The second plot shows the power into the network during the grid fault, with the ramped post-fault recovery of power evident, prior to the damping controller activating. The agreement in power output levels, ramping rates and damping is good. It should be noted,

however, that the damping here reduces the power output below the 90% level 0.5s after the fault is cleared, this test was not for GB grid code. This suggests that under GB grid code, the damping contribution would either have to be reduced, or the interpretation of the Grid Code relaxed slightly.

The third to sixth plots represent the converter current set-points and feedback values. The magnitudes, ramp rates and oscillations are all broadly in agreement between the model and the site data. It is noteworthy from here, however, that the *q*-axis current during the fault is non-zero, being limited only by the *d*-axis current and converter current limits. This means that at the point of voltage recovery, the *q*-axis current is discontinuous, with a step decrease, in order that the output power (second plot) is continuous.

Overall, Figure 4.3 and Figure 4.4 show very good agreement between the site data and the modelled data. This provides further confidence in the models derived in chapter 3. This validation and verification process underpins much of the next section, as at the time of writing, whilst GE Energy have equipped several PMGs which have been operating since 2008, none have yet been type-tested against the GFR requirements. However, the converter control, which represents the fastest dynamics, is only modified between the two cases by changes to the machine bridge vector control. Hence, there is high confidence that the models provide an adequate basis for investigating the FFPMG further.

4.2.4 Fully Fed Permanent Magnet Generator

The following two sections of the thesis have been combined and written up as a peer reviewed journal article in Wind Energy by Banham-Hall et. al. [80]. The new Chopper control method is the subject of a patent application [81].

The validated wind turbine model deployed a FFIG with a reversed control scheme for the power converter, whereby the machine bridge is responsible for the control of the DC link. However, GE Energy's Power Conversion business were approached in 2008 by a company wishing to deploy Direct Speed Control of a PMG wind turbine (see section 3.5.2.2), which necessitated speed control on the machine bridge. This speed controller feeds a torque reference to the vector controller of the machine bridge as seen in Figure 4.5. This necessitated a conventional power converter control strategy with DC link voltage control on the network bridge.

Figure 4.5 shows the control strategy for GFR with a conventional converter control strategy. The key difference to Figure 4.2 is in the formulation of the feed-forward that

acts to limit torque on the machine bridge. In the former case the feed-forward acted only to accelerate the natural response of the DC link controller. However, with conventional control the machine bridge's natural response is to continue to generate according to the torque reference whilst the DC link controller on the network bridge winds up. Without additional control the torque reference would tend to eventually increase as and when the turbine blades accelerate leaving the DC link voltage being pumped up by the generator until the fault clears. To avoid this, the power feed-forward between the bridges is modified. The grid power limit is calculated as Equation 4.1 to Equation 4.3 describe but in addition, the wind up of the DC link controller is also used in the feed-forward so that as it winds up the machine bridge power limit is reduced. This reduction in the machine bridge power limit leads to a reduction in the power fed into the DC link and a subsequent fall in the DC link voltage. As the DC link voltage falls the wind up is reduced and the power limit is correspondingly reduced until a balance is reached between the two bridges. Hence, responsibility for DC link control is shared between the two bridges during the fault.

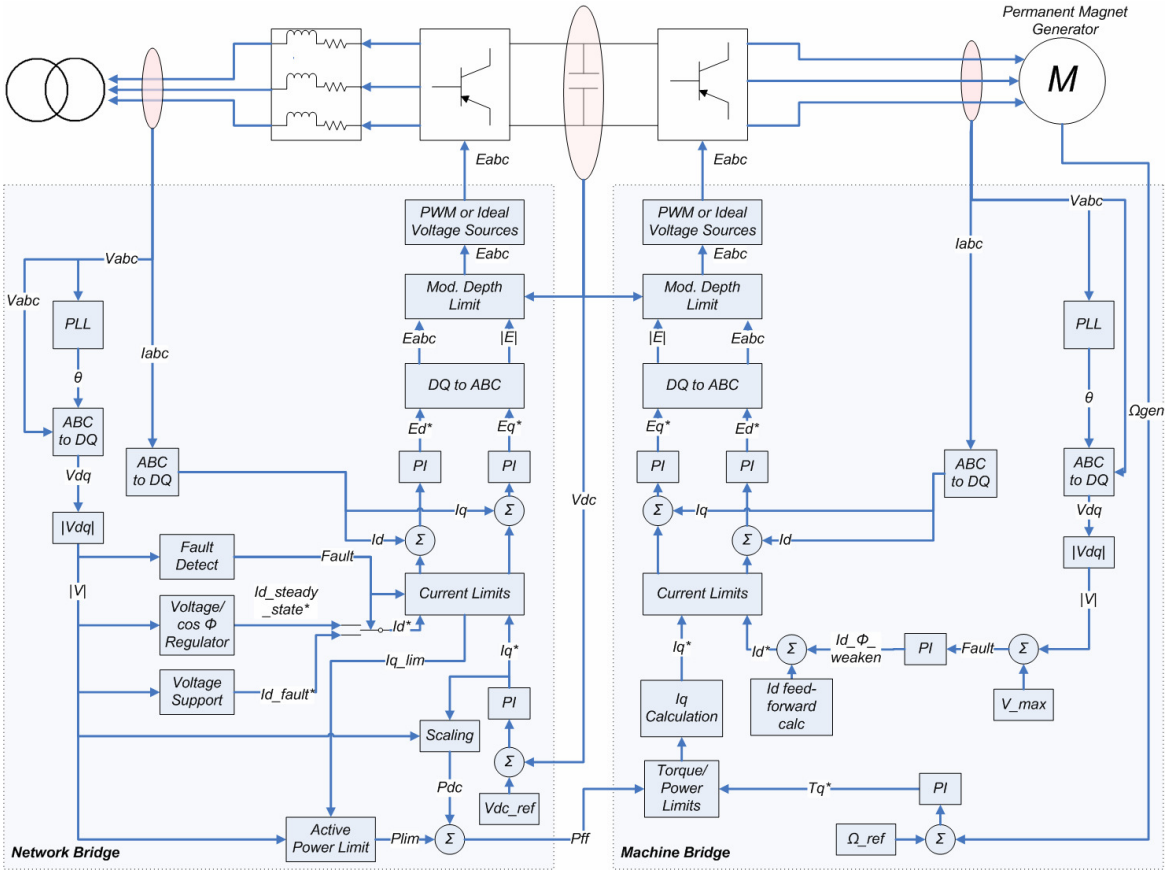

Figure 4.5: PMG Conventional Converter Control for Fault Ride-through

The GFR behaviour of the FFIG showed the benefits of true field weakening control over the generator's magnetic field. However, a PMG effectively has fixed rotor flux leading to

new challenges. Fernandez, Garcia and Jurado [82] have proposed that pseudo-field weakening can still occur with a PMG using reactive power to change the voltage across the stator winding reactance and this is true under normal conditions. The machine bridge's *d*-axis current can still act to reduce the terminal voltage of the PMG under normal conditions. This is shown in Figure 4.6, ignoring the stator resistance. However, the governing equations, repeated below, must be considered.

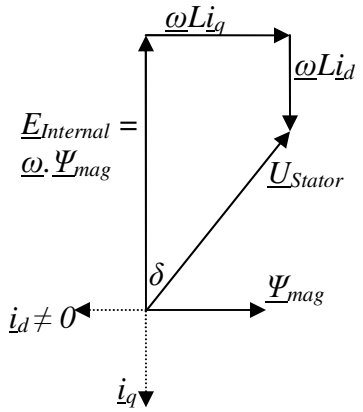

Figure 4.6: PMG Vector Diagram with Pseudo-Field Weakening

Equation 3.36 $$U_d = I_d \cdot R - \omega \cdot I_q \cdot L_s + L_s \cdot \frac{dI_d}{dt}$$

Equation 3.37 $$U_q = I_q \cdot R + \omega \cdot I_d \cdot L_s + \omega \cdot \Psi_{mag} + L_s \cdot \frac{dI_q}{dt}$$

Under normal operating conditions, the power converter maintains control over the PMG current and can act as a four quadrant converter that sources or sinks reactive power to the generator. However, following a converter trip, the IGBT devices inhibit switching and the converter control over the reactive power exchange with the generator is lost. Current flows into the DC link through the converter anti-parallel diodes whenever the peak of the generator voltage exceeds the DC link voltage. Hence, the machine bridge acts as an uncontrolled rectifier. This means that the generator will pump power into the DC link of the converter until the DC voltage is high enough that the diode bridge becomes continuously reverse biased. All currents are then zero, so that Equation 3.36 and Equation 3.37 show the terminal voltage would then become equal to the open circuit voltage of $\omega.\Psi_{mag}$. Hence, any field weakening used to suppress the PMG voltage is lost and voltage ultimately rises to the open circuit EMF.

In the FFIG field weakening was used to suppress the generator voltage when the generator speed exceeded the nominal rating. However, the discussion above shows that this is not sufficient to ensure the correct operation of the PMG, because in a trip situation

the voltage would rise, rather than fall, and could cause an excessive voltage on the converter terminals.

There are two further challenges for the FFPMG system when designing for GFR. First, the higher mechanical resonant frequency of the shaft described in section 3.3.2 could lead to high oscillatory over speeds shortly after the onset of the fault, this in turn would lead to a rise in the open-circuit voltage of the PMG which could cause transients to exceed the converter's voltage rating. Second, the magnetic materials used to manufacture PMGs have to be protected against excessive heat to ensure their magnetic performance. Generator design protects against excessive heating from stator short circuits by using a high stator reactance to limit short circuit currents. This means that the magnetic energy of the stator windings must be considered during a GFR situation. Ultimately, as Equation 4.4 shows, this magnetic energy will be converted into electrostatic energy in the DC link capacitor, hence this increase in DC link voltage must be considered for the GFR case.

Equation 4.4 $$\frac{1}{2}\cdot L_S \cdot I^2 = \frac{1}{2}\cdot C \cdot \left(\left[V_{DC} + \Delta V_{DC}\right]^2 - V_{DC}^2\right)$$

Expanding this gives:

Equation 4.5 $$L_S \cdot I^2 = C \cdot \left(V_{DC}^2 + 2\cdot V_{DC}\cdot \Delta V_{DC} + \Delta V_{DC}^2 - V_{DC}^2\right)$$

Assuming the change in DC voltage is small compared to the absolute link voltage gives:

Equation 4.6 $$L_S \cdot I^2 \approx C \cdot 2 \cdot V_{DC} \cdot \Delta V_{DC}$$

From which the change in link voltage can be found to be approximately:

Equation 4.7 $$\Delta V_{DC} \approx \frac{L_S}{C}\cdot\frac{1}{2}\cdot\frac{I^2}{V_{DC}}$$

Figure 4.7 shows the simulation of a three phase to earth fault with 0% retained voltage on the MV side of the turbine transformer. The fault lasts for 140ms, which is the maximum specified in GB Grid Code, before recovering. The grid power profile (Pgrid) sees a step reduction at the onset of the fault, which is followed by a slower reduction in the generator's power (Pgen). The feed-forward demands a faster power reduction response from the PMG than is achieved. This is due to the magnetic energy of the PMGs stator reactance discussed above.

In order to rapidly reduce the current of the PMG there must be sufficient voltage margin on the power converter to incur a high dI/dt as shown in Equation 3.36 and Equation 3.37. However, the typical power converter design does not have sufficient margin on the modulation depth of the DC link to achieve this, hence, the generator continues generating

into the DC link as the PMG current is reduced at the fastest rate the converter can achieve. This increases the DC link voltage (Vdc) which in turn creates headroom for the PMG voltage to increase (Vpmg). However, both the peak DC link voltage and the peak PMG voltage are well beyond typical design limits here.

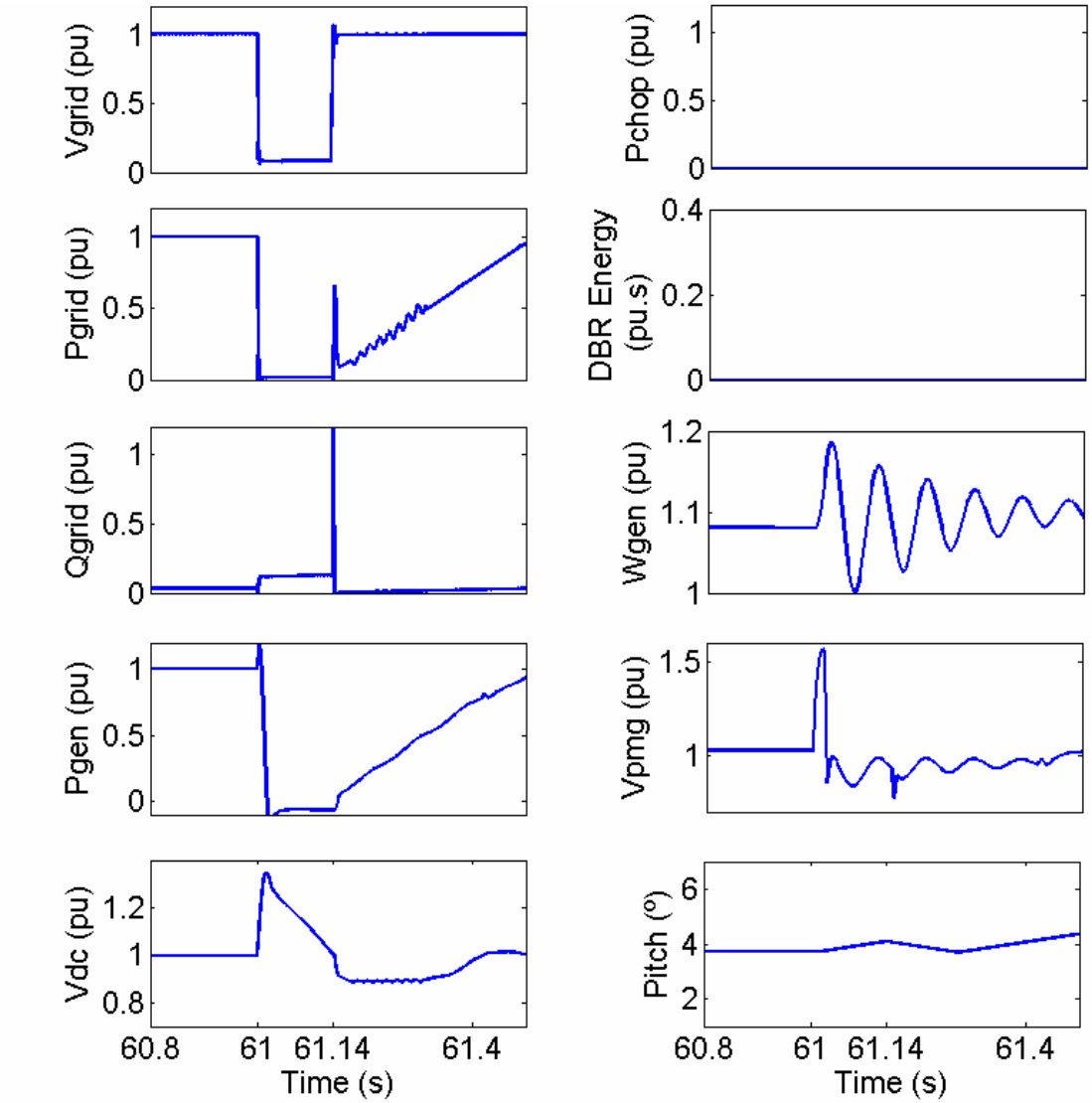

Figure 4.7: PMG Fault Ride-through without a Chopper or Brake Resistor

Despite the slow reduction in torque on the machine bridge, it is still sufficiently fast to appear as a near-step change to the shaft system. This leads to the initiation of high frequency speed oscillations of the generator. These fast oscillations are superposed onto a slower acceleration of the generator as the blades increase speed through the fault. Depending on the specific PMG design, these speeds must be designed to stay inside the rated speed to ensure that the open circuit voltage of the PMG does not exceed the power converter's rating.

Banham-Hall *et al.* [83] have investigated the specific details of GFR with the FFPMG and concluded that normally all direct-drive PMG would require a Chopper and DBR in

order to act both to avoid the mechanical shaft oscillations and to absorb the magnetic energy stored in the PMG's stator windings.

4.2.5 Choppers and Brake Resistors

4.2.5.1 Fully Rated

Conroy and Watson [84] have shown how the use of DBRs and choppers across the DC link of a power converter can suppress otherwise excessive voltages. Their work compares the case of a PMG with and without a fault resistor, but in each case the generator's power is unaffected through the fault, either pumping up the DC link voltage or being diverted to the brake resistor.

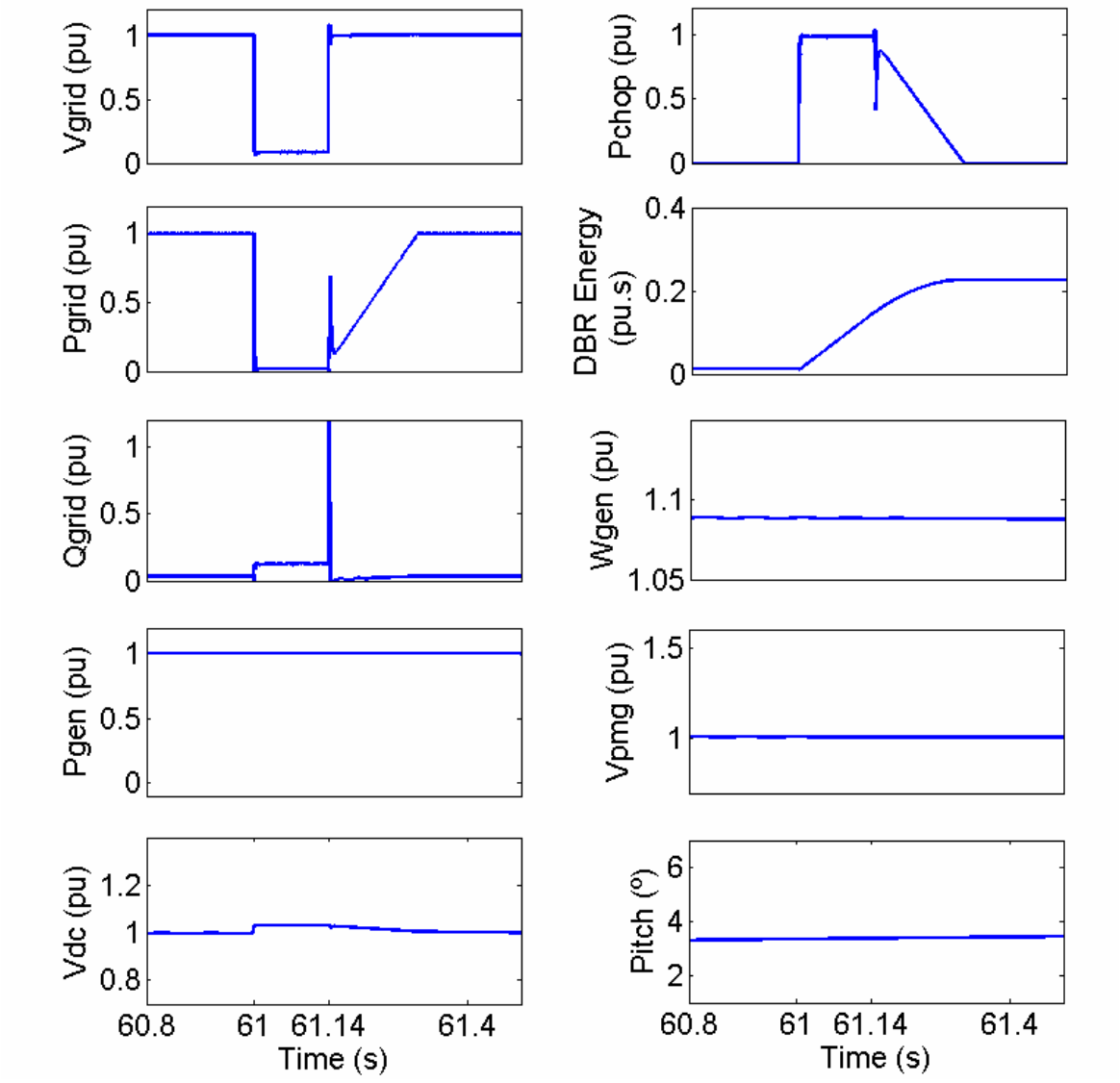

Figure 4.8: Fault Ride-through of a PMG with Fully Rated Chopper

Michalke and Hansen [85] also consider choppers and brake resistors for PMG wind turbines but focus specifically on their benefit in terms of avoiding exciting the shaft resonance. The brake resistor sits across the DC link, switched in or out by an IGBT that

is triggered by a simple threshold controller. The threshold controller works such that the IGBT is on whenever the DC link voltage exceeds a predefined level. The IGBT is then switched off when the voltage falls below a second level, which is set to ensure some hysteresis. This controller is shown to work well to avoid the mechanical shaft oscillations that are present from a grid fault without a brake resistor.

Neither Michalke and Hansen nor Conroy and Watson consider the importance of brake resistors to direct-drive PMG wind turbines in order to avoid generator over-voltages and over-speeds. Furthermore, they model resistors that are rated sufficiently to absorb all the generator energy during a fault. Figure 4.8 shows a simulation of the FFPMG model with a full rating chopper and Dynamic Brake Resistor (DBR). The generator power (Pgen), Speed (Wgen) and Voltage (Vpmg) can be seen to be generally unaffected by the grid fault as the generator power is diverted by the chopper (Pchop) and dissipated as heat by the brake resistor (DBR Energy).

The problem with using a full chopper and brake resistor is the total energy dissipation. The resistor must be sized to absorb 0.25pu.s; which means it must be capable of heating sufficiently to absorb full power output from the generator for ¼s for a zero voltage fault, this in turn can extend to over 1s for a worst case fault of greater retained voltage but also longer fault duration. The resistor does not have to be continuously rated for full power, which would result in an unfeasibly large and expensive solution, but must be sufficiently sized to survive worst case grid faults whilst absorbing energy as heat. This typically leads to designs with a continuous rating of tens of kW. However, informal discussions around Grid Codes have suggested that it may be necessary in future for turbines to ride-through successive faults caused by auto-reclosure of faulted transmission lines. This would mean that the DBR would have to be resized to allow ride-through of multiple faults within a specified period as the under-rated resistors have long thermal time constants leading to long cooling periods before they can be reused. This necessitates an increase in energy rating, size and cost.

4.2.5.2 Partially Rated

The analysis of the PMG without a chopper showed that the voltage rise at the onset of the fault is of key concern to the power electronic system. Additionally fast changes in torque led to mechanical oscillations in the shaft system. However, use of a fully rated chopper and brake resistor necessitates a relatively large resistor, which may in future need to be increased to allow GFR of multiple faults. As an alternative to a fully rated chopper, it is

possible to consider using a partially rated chopper with ramped reduction in machine torque; however, the ramp would ideally be designed to avoid mechanical resonance.

The mechanical response of the generator to a ramped change in torque can be found by considering the blades fixed as in Figure 4.9. This is a reasonable approximation since the blade inertia is typically more than an order of magnitude higher than the generator. As the shaft damping is low, in a typical direct-drive application, this can be considered negligible to simplify the mathematics further. Hence the differential equation governing the angular response of the generator to applied torque is then given in Equation 4.8.

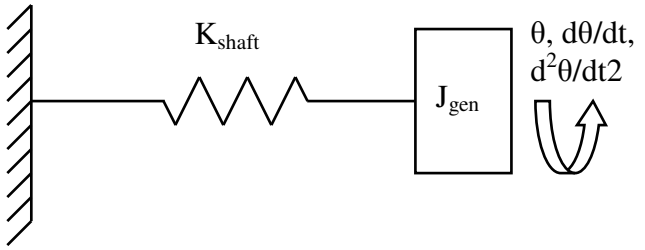

Figure 4.9: Simplified Shaft System

Equation 4.8 $$T(t) = J_{gen} \cdot \ddot{\theta}(t) - K_{shaft} \cdot \theta(t)$$

Now the response of this system to a ramped reduction in torque can be found by setting $T(t) = T_{rated}(t/t_{ramp})$ where t_{ramp} sets the ramp rate.

Equation 4.9 $$T(t) = T_{rated} \cdot \frac{t}{t_{ramp}} = J_{gen} \cdot \ddot{\theta}(t) - K_{shaft} \cdot \theta(t)$$

The homogenous equation for this is then:

Equation 4.10 $$0 = m^2 - \frac{K_{shaft}}{J_{gen}} \text{ so that } m = \pm\sqrt{\frac{K_{shaft}}{J_{gen}}} = \omega_n$$

So the solution of the complementary function is given as (C_1 and C_2 are constants):

Equation 4.11 $$\theta_{cf} = C_1 \cdot \sin(\omega_n \cdot t) + C_2 \cdot \cos(\omega_n \cdot t)$$

Now try a particular integral of the form $(A.t+B)$

Equation 4.12 $$\theta_{pi} = A \cdot t + B$$

By comparing coefficients:

Equation 4.13 $$\frac{T_{rated}}{J_{gen}} \cdot \frac{t}{t_{ramp}} = \frac{K_{shaft}}{J_{gen}} \cdot (A \cdot t + B) \rightarrow \frac{-T_{rated}}{K_{shaft} \cdot t_{ramp}} = A \text{ and } B=0$$

So the overall response of the shaft to an infinite ramp is given as:

Equation 4.14 $$\theta(t) = C_1 \cdot \sin(\omega_n \cdot t) + C_2 \cdot \cos(\omega_n \cdot t) - \frac{T_{rated}}{K_{shaft} \cdot t_{ramp}} \cdot t$$

Now considering that at $t = 0$, $\theta = 0$ gives that $C_2 = 0$ as all other terms would be zero.

Then consider that at $t = 0$, $d\theta/dt = 0$:

Equation 4.15 $$0 = \omega_n \cdot C_1 \cdot \cos(\omega_n \cdot 0) - \frac{T_{rated}}{K_{shaft} \cdot t_{ramp}} \text{ so that } C_1 = \frac{T_{rated}}{\omega_n \cdot K_{shaft} \cdot t_{ramp}}$$

Hence the general solution giving the response of the shaft to an infinite ramp in torque is given as:

Equation 4.16 $$\theta = \frac{T_{rated}}{K_{shaft} \cdot t_{ramp}} \cdot \left(\frac{1}{\omega_n} \cdot \sin(\omega_n \cdot t) - t \right)$$

In order to find the response of the shaft to a finite ramped-step function, it is possible to consider two opposing ramp functions offset in time as shown in Figure 4.10. Hence, the solutions to the two opposing ramps can be superposed.

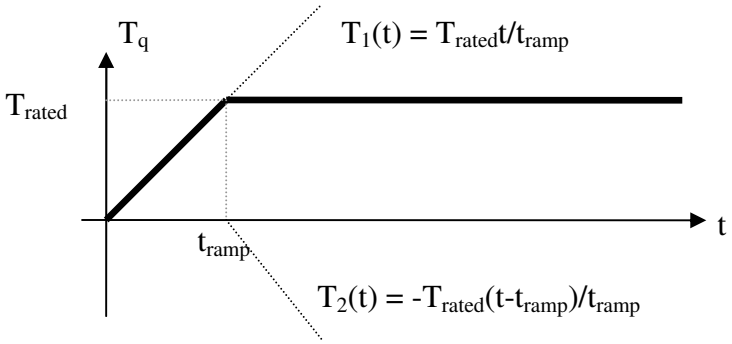

Figure 4.10: Composition of a Ramped-Step Function

Equation 4.17 $$\theta_2 = \frac{-T_{rated}}{K_{shaft} \cdot t_{ramp}} \cdot \left(\frac{1}{\omega_n} \cdot \sin(\omega_n \cdot [t - t_{ramp}]) - [t - t_{ramp}] \right)$$

Hence, the overall response is given as:

Equation 4.18 $$\theta_T = \frac{T_{rated}}{K_{shaft} \cdot t_{ramp}} \cdot \left(\frac{1}{\omega_n} \cdot \{\sin(\omega_n \cdot t) - \sin(\omega_n \cdot [t - t_{ramp}])\} - t_{ramp} \right)$$

And in order to minimise the oscillations, it is desirable to avoid oscillations in $d\theta_T/dt$:

Equation 4.19 $$\dot{\theta}_T = \omega_T = \frac{T_{rated}}{K_{shaft} \cdot t_{ramp}} \cdot (\cos(\omega_n \cdot t) - \cos(\omega_n \cdot [t - t_{ramp}]))$$

From standard trigonometric relationships this can be re-written as:

Equation 4.20 $$\omega_T = \frac{-2 \cdot T_{rated}}{K_{shaft} \cdot t_{ramp}} \cdot \left(\sin\left(\frac{2 \cdot \omega_n \cdot t - \omega_n \cdot t_{ramp}}{2} \right) \cdot \sin\left(\frac{\omega_n \cdot t_{ramp}}{2} \right) \right)$$

To avoid sinusoidal oscillation in ω_T, the stationary points provide the speed maxima by differentiating Equation 4.19:

Equation 4.21 $$\alpha_T = \frac{d\omega_T}{dt} = \frac{-\omega_n \cdot T_{rated}}{K_{shaft} \cdot t_{ramp}} \cdot (\sin(\omega_n \cdot t) - \sin(\omega_n \cdot [t - t_{ramp}]))$$

This can again be simplified by standard trigonometric relationships:

Equation 4.22 $$\alpha_T = \frac{-2 \cdot \omega_n \cdot T_{rated}}{K_{shaft} \cdot t_{ramp}} \cdot \left(\cos\left(\frac{2 \cdot \omega_n \cdot t - \omega_n \cdot t_{ramp}}{2} \right) \cdot \cos\left(\frac{\omega_n \cdot t_{ramp}}{2} \right) \right)$$

Now to avoid shaft oscillations it is necessary minimise α_T after the step to zero, which can be achieved provided that the following condition is met:

Equation 4.23 $\omega_n \cdot t_{ramp} = n \cdot \pi$ and n is an odd integer.

This shows that the magnitude of the shaft oscillations is critically dependent on the ramp rate of the step. Figure 4.11 shows that the theoretical peak amplitude of the shaft oscillation, in response to a ramped step in torque, follows a sinc function with discrete minima. This illustrates that provided the torque is ramped down on the generator at the correct rate, it is theoretically possible to eliminate the dominant shaft oscillations.

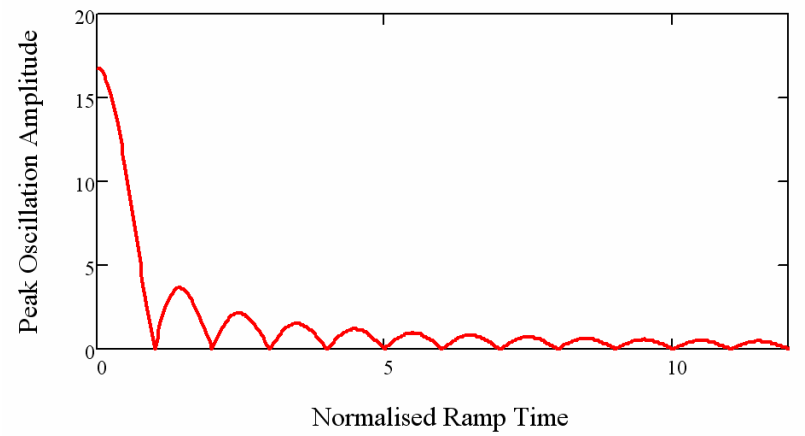

Figure 4.11: Amplitude of shaft oscillations following a ramped reduction in torque

This controlled ramped reduction in torque can be achieved during a grid fault by controlling the ramp rate of the generator's *q*-axis current after the onset of the fault. This is designed to force power into the DC link at the onset of the fault, whilst gradually ramping down the torque of the generator such that shaft oscillations are minimised and PMG peak voltage is kept within limits. This power that is pushed into the DC link following the onset of the fault would be diverted by the chopper into the DBR.

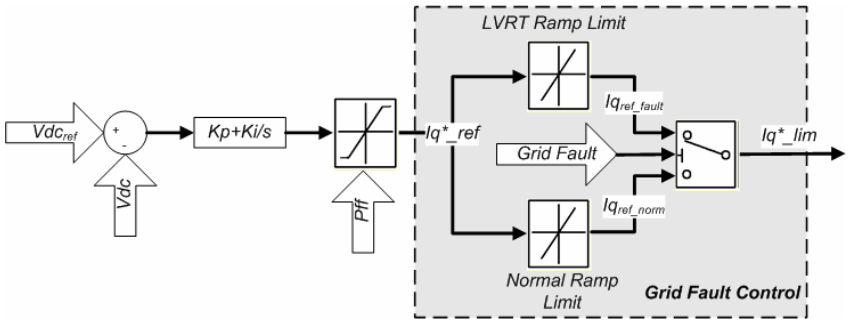

Figure 4.12: Converter Control for a Ramped Chopper

Figure 4.12 shows how the current controller on the machine bridge of the power converter can be modified to force the current (and therefore torque) to fall at a specific

ramp rate. The grid fault causes the feed-forward power limit and the DC link controller to work together to rapidly reduce the torque reference on the machine bridge, however, slower ramp limits are applied during the fault than during normal operation. This ramp limit is set according to the idealised ramp time described in Equation 4.23 and as *Iq*_ref* is reduced much faster than this limit, the set-point sent to the current controller (*Iq*_lim*) is limited to change at the specified ramp rate.

This modification to the control method has been implemented in the wind turbine converter model and simulated. Figure 4.13 shows the results. The energy absorbed by the DBR is reduced by 60% compared to the case with a fully rated DBR. This improvement would permit existing turbine designs to ride-through multiple consecutive faults, or for a smaller DBR and chopper to be used in future designs that only have a single fault requirement.

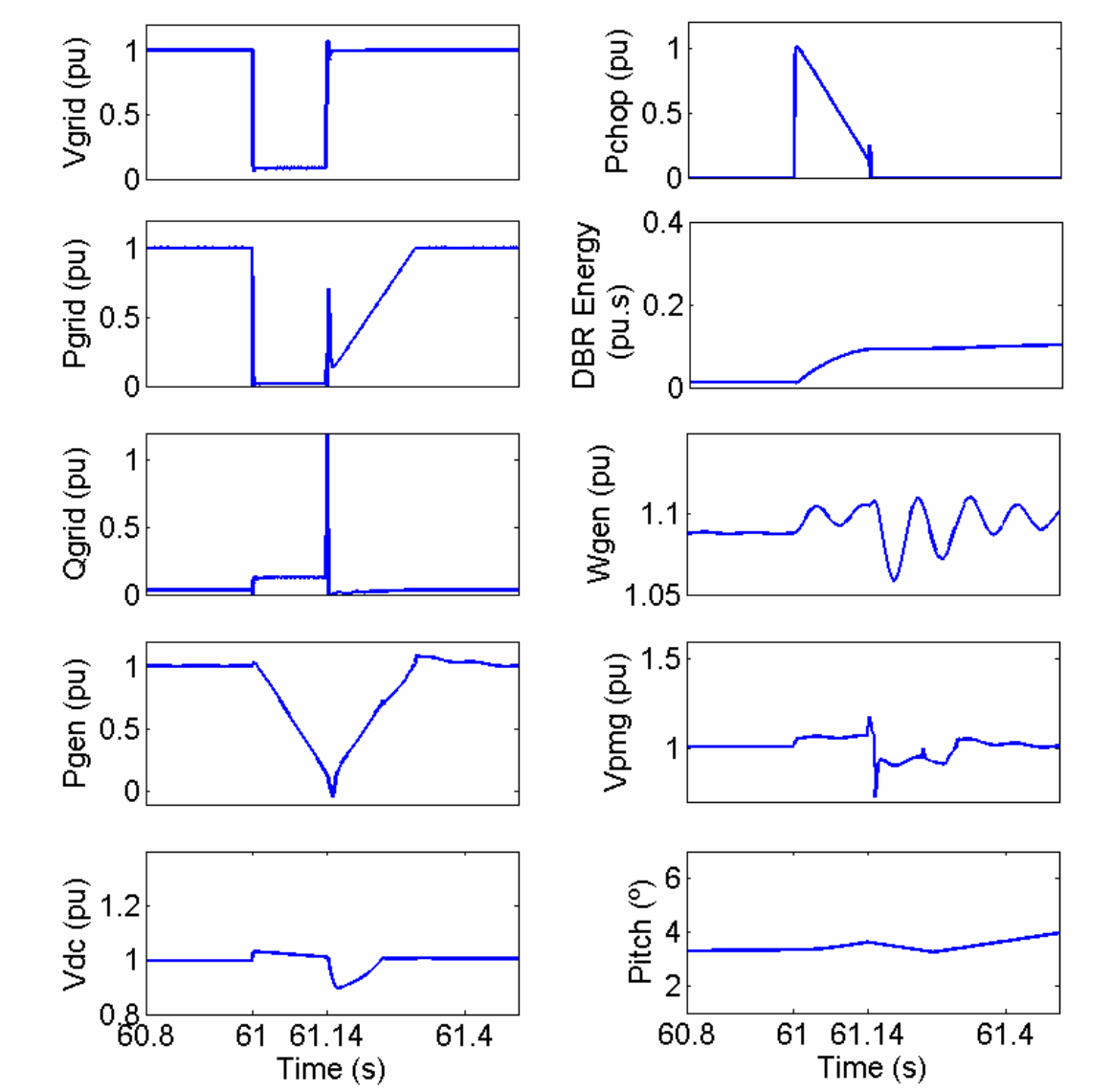

Figure 4.13: Fault Ride-through of a PMG with Ramped Chopper

The ramped DBR method has also made considerable improvements to the magnitude of the speed oscillations, which are around 0.015pu peak to peak during the fault and 0.045pu peak to peak in the worst case after the fault. This is compared to amplitude of 0.19pu peak to peak without a DBR and chopper. Hence, the oscillations are negligible compared to the case without a chopper. In fact the shaft is near transient free following the ramped reduction in torque at the onset of the fault, with the majority of shaft oscillations being excited by the release of the DC link controller to higher ramp rates as the fault clears. As the DC link controller regains control there is a rapid 0.15pu change in the generator torque (see Pgen plot at 61.14s). This slight step is also visible on the plot showing power through the chopper switch (Pchop), however, the power to the chopper broadly follows the intended profile, by absorbing the power imbalance between the network and machine bridges. The slight step in torque when the grid recovers is primarily responsible for the excitement of the shaft and it may be possible to improve on this response. The transient spike in output power that coincides with the fault recovery (Pgrid at 61.14s) draws power from the DC link causing it to fall suddenly at the same time that the DC link controller is released from the ramp limits. This transient therefore causes the transient in torque and removing this would allow an even smoother response from the machine bridge and shaft.

The result of minimising the speed oscillations and gradually reducing torque on the PMG is to significantly reduce the transient voltages that the power converter has to control on the generator side (Vpmg). This is achieved by reducing the peak speed and thereby reducing the rate of change of generator flux, which reduces the open circuit EMF of the generator.

Overall, this novel control adaption makes a contribution to improving the performance of direct-drive PMG systems under grid faults. The initial outcome of this work has been implementation of a generic design rule for new direct-drive PMG systems to ensure that they are equipped with chopper rated for full power for at least ½s. However, further work in this area would include verifying the control performance when a wind turbine reaches type testing. Additionally, the control strategy could be investigated further in the context of other mechanical modes rather than just the fundamental shaft oscillation.

4.2.6 Reduced Order Model

One of the side effects of deploying a chopper and DBR is to improve the decoupling between the machine bridge and the grid. The chopper ensures that the machine does not have to be exposed to any fast transients caused by grid events and that the DC link stays

within its target limits. This has led Conroy and Watson [86] to show that models of wind turbines with PMGs, full converters and choppers can be simplified. Their approach is only for transient studies and hence the machine side power can be represented as fixed by a constant current source feeding the DC link. The control and modelling of the network side bridge remains unchanged, thus ensuring the correct grid behaviour is represented. However, this approach is not appropriate for longer timescale studies where wind variability is relevant.

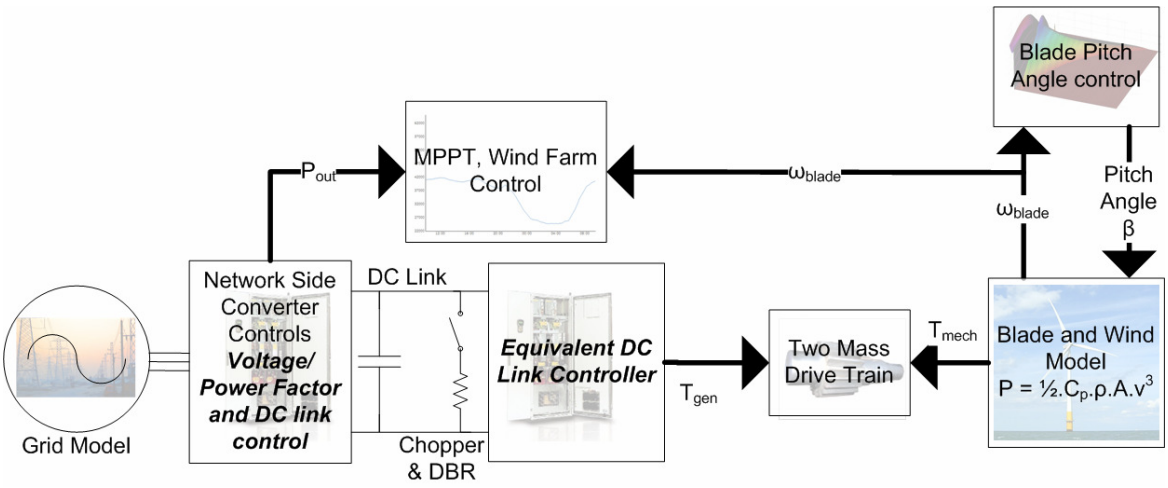

Figure 4.14: Reduced Order Model Design

Here Conroy and Watson's simplified approach has been built upon. The fast dynamics of the machine bridge are no longer relevant, hence it is not necessary to represent the machine or the inner current loops of the machine bridge. Instead, it can be noted from Figure 4.2 that the DC link voltage controller directly controls the *q*-axis current, which in turn aligns with torque. Ignoring fast dynamics, this DC link voltage controller is therefore indirectly, but proportionately controlling the generator torque. Hence, in a per unitised model, the per unit *q*-axis current reference is numerically identical to the per unit electromagnetic torque exerted by the generator on the shaft. Hence, the machine and much of the machine bridge control can be removed to leave a hybrid simplified model that retains sufficient fidelity for fast timescales whilst removing some of the complexity associated with the machine bridge. This is shown in Figure 4.14.

Figure 4.15 shows the comparison of the full model, which includes the machine model and machine bridge representation, and the simplified model discussed above. It is evident from these two plots that the grid side outputs of the simplified model are near identical to the more detailed model case. However, it should be repeated that this is only true for the case with a chopper and DBR decoupling the two bridges.

This hybrid reduced order model is often used in subsequent sections that address frequency response and inertia. Whilst even simpler models are possible for frequency response studies, this model accurately reflects speed changes which might otherwise influence PMG voltage, particularly with fast inertial response.

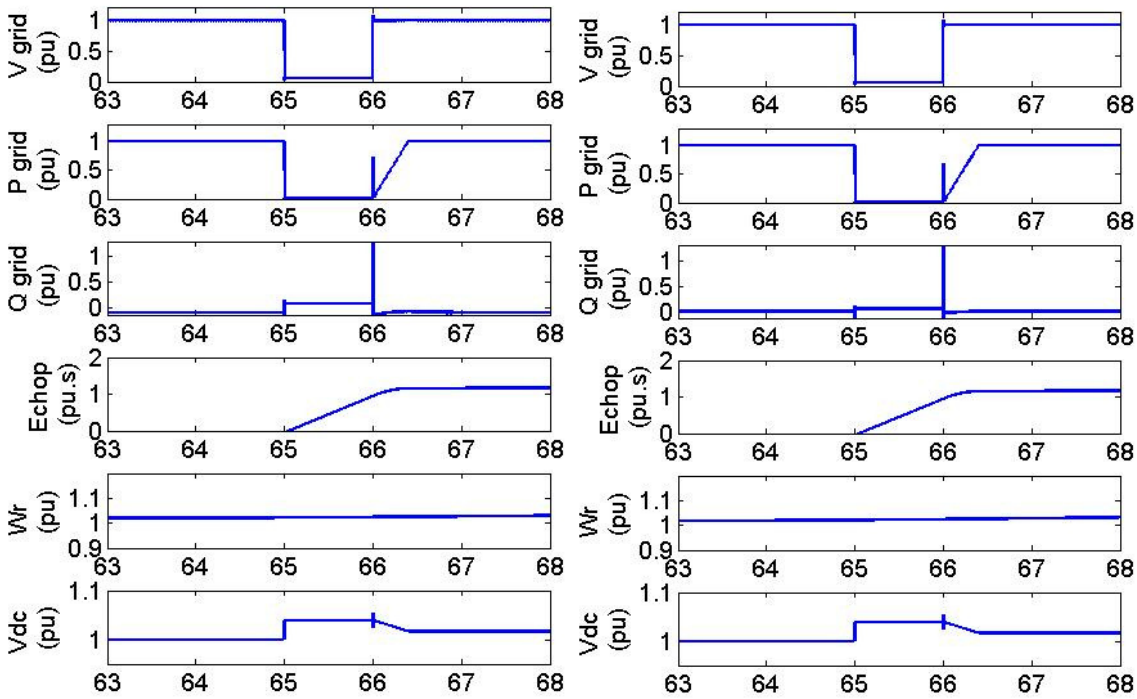

Figure 4.15: Fault Ride-through Simulation Comparison of PMG (Right) and Reduced Order (Left) Models

4.3 Frequency Response

The instantaneous balance between supply and demand on the transmission system is maintained through the system frequency. Conventional steam turbine synchronous generator based power plants provide a fast response to changing frequency by releasing or storing energy in their rotational inertia and steam drum before their slower governor and boiler action increases or decreases their output power to return system frequency to its target.

Full converter wind turbines are specifically designed to vary machine frequency independently to network frequency so that the blades can be rotated at the optimal aerodynamic speed rather than being fixed to the system frequency. However, this acts to decouple their physical inertia from the grid and means that frequency response capability must be built into their control systems to compensate.

Conventionally, if system demand exceeds supply then the system frequency falls and a synchronous generator would release an inertial contribution as its rotational kinetic energy falls, thus aiding the stability of the system. Conversely, if the system supply

exceeds demand then the system frequency rises above nominal and energy is stored in the synchronous generator's rotational inertia. This intrinsically stabilising contribution of synchronous generators helps to ensure that major deviations in system frequency are extremely rare.

Severe frequency disturbances, such as that illustrated in Figure 2.22, are usually the consequence of one or more large power stations tripping. Unscheduled power station trips cause a sudden generation shortfall which has to be rapidly covered by other power stations on the system, or else by flexible demand. Given that power electronic interfaced wind turbines do not intrinsically provide the same service as conventional generators, the subject of frequency response is of interest to system operators globally.

4.3.1 Grid Code Requirements

Parts of the following two sub-sections of the thesis, covering frequency response and synthetic inertia, have been written up for Wind Energy by Banham-Hall et. al. [87]. *This article is currently being updated following review.*

The GB transmission system is a comparatively islanded system with a high credible loss of generation due to large individual nuclear generators. Furthermore, with plans to meet the greater part of the UK's 2020 targets with large offshore wind farms, it is unsurprising that the GB Transmission System Operator (TSO) has been at the forefront of investigations into the capability and impact of wind turbines on system frequency.

The approach National Grid [78] has taken is in line with their general principle of treating all generators connecting to the grid equally. Hence, wind farms connecting to the transmission system must be technically capable of providing the same service as conventional generators. This technical capability is checked for compliance when the wind farm is commissioned, by a series of compliance tests.

4.3.1.1 Droop

The key frequency response related requirement currently mandated in GB Grid Code is the requirement to provide droop response and is shown in Figure 4.16. A wind farm must be capable of operating such that it can regulate up or down its output power in direct proportion to the magnitude of the deviation in system frequency from the nominal 50Hz target. This response should be directly proportional with only a limited dead-band permitted around the 50Hz nominal frequency. A droop of 3-5% should be attainable, which in turn relates back to the speed of a synchronous generator. A droop of X% implies that a hypothetical 100% load step on that generator would cause a change in

speed of X%. Hence a 3-5% droop implies a change in power of between 40-66% per Hertz deviation from the nominal frequency.

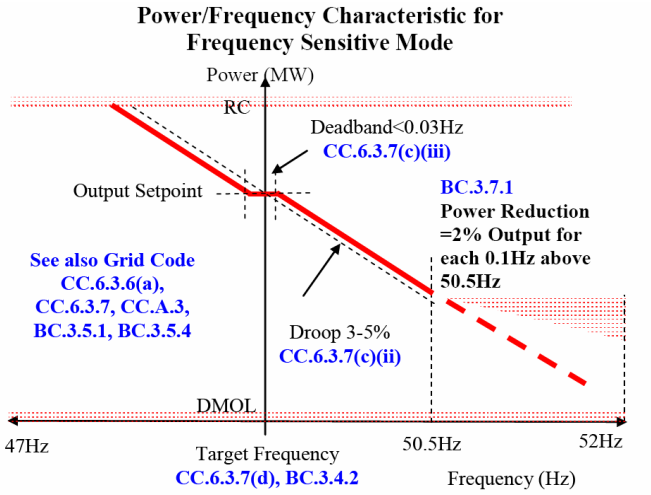

Figure 4.16: GB Requirement for Droop Control from National Grid [78]

Clearly, a wind farm cannot indefinitely increase its power output in line with a droop requirement unless it is operating at an output power lower than the available wind power. Additionally, it would be economically undesirable to operate wind farms at lower than their maximum output just to provide frequency response, when other power plants can provide this capacity. Therefore the requirement of Figure 4.16 is only relevant when a generator is selected for Frequency Sensitive Mode (FSM). When a generator, such as a wind farm, is not selected for FSM it can operate under the less stringent requirements for Limited Frequency Sensitive Mode (LFSM). Under LFSM, the wind farm is only required to regulate down its output in response to a frequency above 50.4Hz. It is thereby allowed to operate at the maximum available power unless there is a major system over-frequency event.

The split in requirements between FSM and LFSM highlights a key difference between the GB regulatory framework and the economic reality. Wind farms being built have to be technically capable of providing FSM operation and are tested for it; however, they typically price themselves out of providing this service and invariably operate under LFSM.

The technical requirement to provide droop response from a wind farm has to be enhanced to take into account the variable nature of the wind resource. In contrast to a conventional generator, which would operate at a fixed output under normal operation, a wind farm would operate according to the variable available wind power. Figure 4.17, from National Grid [78], shows the GB Grid Code requirement on wind farms providing frequency response, this requires that when they are selected for FSM, they reduce their output

below the variable available power (Pavail) to a lower *fixed* output, known as the Capped Committed Level (CCL), and regulate according to system frequency from that level. The generator must also then supply a discretely updated measure of the maximum available power, known as the Maximum Export Limit (MEL), which informs National Grid of the magnitude of the (varying) level of reserve held by the wind farm.

Figure 4.17 shows that with variable wind speed it is understood that the available power could drop sufficiently to compromise response. This is shown on the dark blue output between about 17 minutes and 24 minutes, where the output reverts to tracking the maximum available power. This highlights a distinct feature of the implementation of the GB droop response requirement; it is based on a variable reserve approach, but ideally targets a fixed output.

Figure C.2 Expected Frequency Response with Reducing Intermittent Power Source

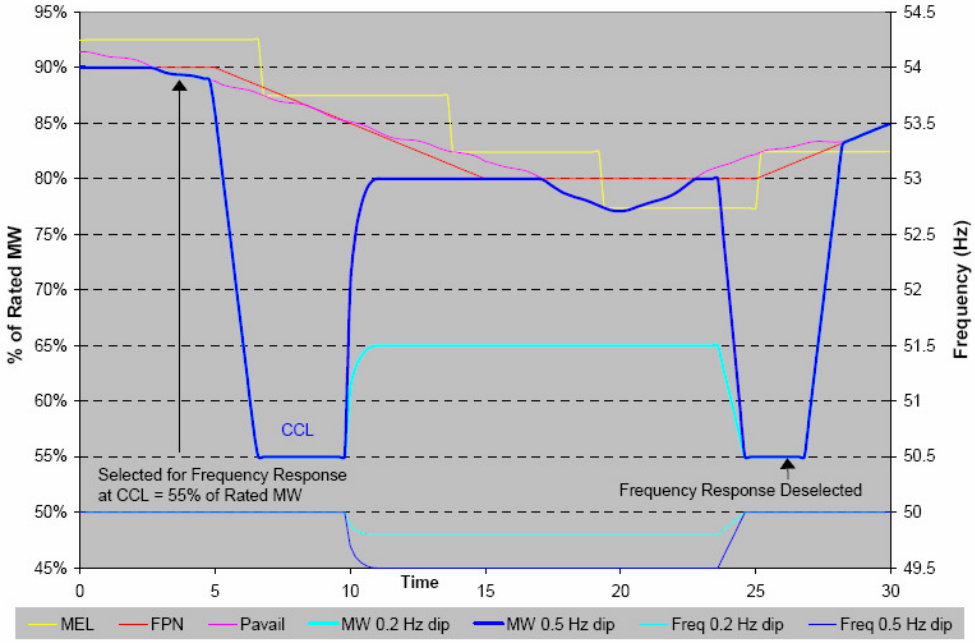

Notes:
The Maximum Export Limit (MEL), is declared to National Grid as a Balancing Mechanism parameter effectively equivalent to 'Pavail' which should be updated whenever the 'Pavail' changes by more than 5% or 5MW. The Final Physical Notification (FPN) is the generated power profile submitted to National Grid for a ½ hour period before gate closure. Gate closure is one hour ahead of real time. The Capped Committed Level (CCL) is the power level at which a Power Park Module operates when selected for frequency response.

Figure 4.17: Implementation of Frequency Response with an Intermittent Resource taken from National Grid [78]

The Danish approach to providing frequency response capacity is the reverse of the GB case, the Danish system operates a fixed reserve, variable output requirement [88]. This is typically known as "Delta-control" and requires a generator to operate at a fixed margin or "Delta" below their maximum available power. The droop response then operates relative

to the varying output of the wind farm. This type of response is illustrated, compared to the GB approach, in the FSM period of Figure 4.18 (P_{delta}).

4.3.1.2 Response Types

The droop requirement dictates the magnitude of the steady state change in power output that a wind farm should provide in response to a frequency deviation. However, following a major loss of generation the speed of response is also critical. As such the market, from which FSM services are procured, is divided into three different types of response. Of these three, "Primary" and "Secondary response" govern the increase in power output in response to a reduction in grid frequency and "High response" governs the reduction in power output in response to a rise in grid frequency.

Primary response is the fastest type of frequency response currently procured for the GB grid. The magnitude of response is measured 10 seconds after a frequency deviation and should be maintained for 30 seconds according to National Grid [78]. Although the measurement is made at 10 seconds it would usually be expected that a generator would start to provide additional power output within 2 seconds of the frequency deviation. The aim of primary response is to stabilise the frequency within operational limits.

Secondary response is slower response that is measured according to the minimum increase in power supplied between 30 seconds and 30 minutes after a frequency deviation. Its purpose is to start the process of restoring system frequency whilst allowing time for the TSO to modify generation profiles to make up for the generation shortfall. Both primary and secondary response would be expected to be supplied relative to a fixed output level.

High frequency response is the response to a system over-frequency event and is measured 10 seconds after the frequency event. In contrast to Primary and Secondary response, High frequency response has no time limit specified, however, it would usually only be required for a maximum of half an hour before National Grid's Balancing Mechanism adjusted generation profiles to compensate for the imbalance. Also in contrast to the low frequency response capabilities, the High frequency response controller must be active at all times, albeit it would only respond when frequency is significantly above target when in LFSM. When operating in LFSM, the wind farm's output would be variable, therefore, but if the frequency exceeds the limit (50.4Hz) and High response is required, the wind farm would regulate its output relative to its power output immediately prior to the frequency exceeding 50.4Hz. This control is known as Balance control and is

illustrated alongside the other types of control discussed here in Figure 4.18. It should be noted from this illustration that in the event that the available wind power falls, excess response may be provided by the wind farm, which would revert to tracking the (lower) available power.

In addition to the frequency response controllers, it is possible National Grid may constrain the output of a given wind farm to a maximum level. This is typically an expensive option for National Grid, and generates negative headlines such as The Telegraph's [89] "Wind farm paid £1.2 million to produce no electricity". This was due to the constraint payments made to Scottish wind farms for not producing power. Nevertheless, the control, known as "Absolute Limit" control is implemented in the frequency controller and shown in Figure 4.18.

Overall, methods of providing frequency response have been implemented by wind farm operators, which have been successfully tested against the compliance tests of GB Grid Code by Horne [90]. Different control methods that can be used to provide frequency response are discussed in section 4.3.2.

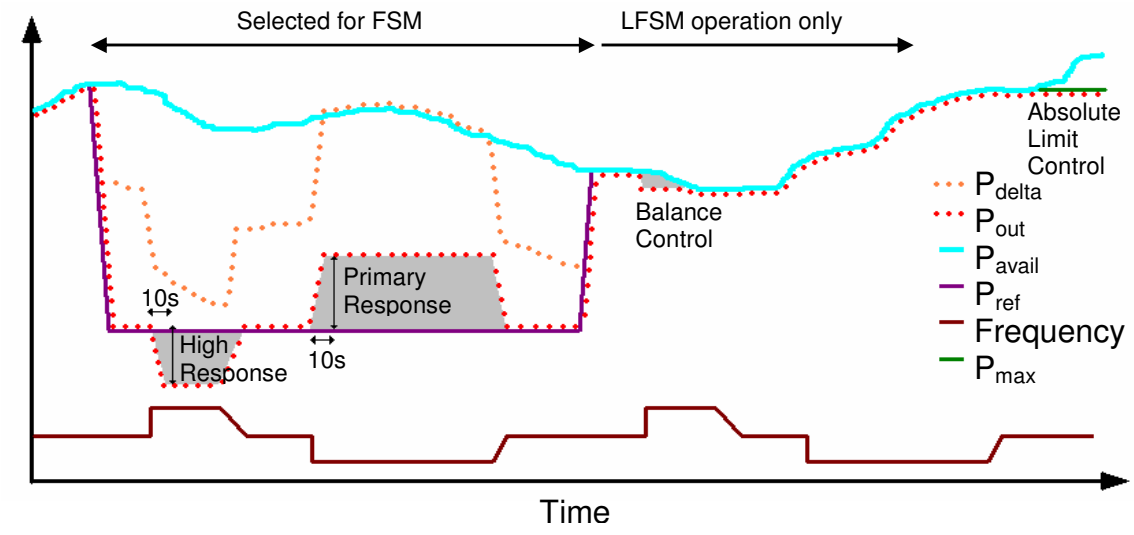

Figure 4.18: Frequency Response Types

4.3.2 Control Methods for Frequency Response

In order for a wind turbine to hold power reserve for frequency response, it is ultimately necessary to reduce the aerodynamic power from the blades. Figure 3.3 shows that in order to achieve this, for a given wind speed; a wind turbine controller must either change the pitch angle, or else change the speed of the blades. Whereas the pitch angle to coefficient of performance relationship is a monotonically decreasing function for any given Tip Speed Ratio (TSR); both acceleration and deceleration of the blades, relative to the optimal speed, leads to a decrease in power output. However, deloading a turbine by

deliberately slowing the blades down below the optimal speed would lead to slow response times due to the slow acceleration of the wind turbine required to return the turbine to the optimal operating point. It is therefore desirable to either operate on the right hand side of the peak in Figure 3.3 or to use the blade pitch to control output.

Holdsworth, Ekanayake and Jenkins [91] were the first to consider the provision of inertial and frequency response from wind turbines in depth. Their analysis compared the capabilities of an FSIG with a DFIG, showing the natural inertial response of the FSIG and comparing it with the lack of inherent response from the DFIG. They then proceed to demonstrate how inertial response and frequency control can be added to the wind turbine controller. Their contribution to synthetic inertia will be considered in section 4.4.1. Here, however, their proposals for provision of frequency response are considered. They propose a frequency response strategy that applies droop control on the converter torque set-point which is matched by a second droop characteristic that trims the minimum pitch angle of the blades. This range of pitch angle variation is shown to give a maximum 20% change in power output and is demonstrated through various different, but constant, wind speed simulations.

Section 3.5.2.2 showed that the direct speed controlled wind turbine optimised power capture by controlling the wind turbine blades to the optimal rotational speed. Therefore, in order for a direct speed controlled wind turbine to hold margin for frequency response it is necessary to deload the turbine through a change in pitch angle. This can be achieved with the wind turbine controller shown in Figure 4.19.

For this method of frequency control it is necessary to ensure that the power output of the wind turbine changes, but that the speed stays close to optimal. This allows the wind turbine to respond to a frequency deviation with all its power reserve whilst only changing the blade pitch angle and not speed. Hence, the controller of Figure 3.17 must set the optimal speed, when in FSM only, according to the estimated available power rather than the measured output power. This means that the margin held by the wind turbine when in frequency responsive mode is subject to the same error as the estimated available power. This error would be partially reduced by averaging many turbines' output.

Under this method of frequency response, the pitch controller acts to regulate the measured power output of the wind turbine to the set-point by using a PI controller (rather than the droop method used in Holdsworth, Ekanayake and Jenkins). The power reference is taken from the estimate of the available wind power and modified to hold a reserve and respond to any changes in frequency. For example if the available power in the wind is

2MW, a turbine is to hold a 300kW margin and the system frequency is 50Hz, the pitch angle controller will increase the pitch angle until the measured output power is 1.7MW.

The capability to provide primary frequency response by pitch control is considered further by modelling and simulation in section 4.3.3.

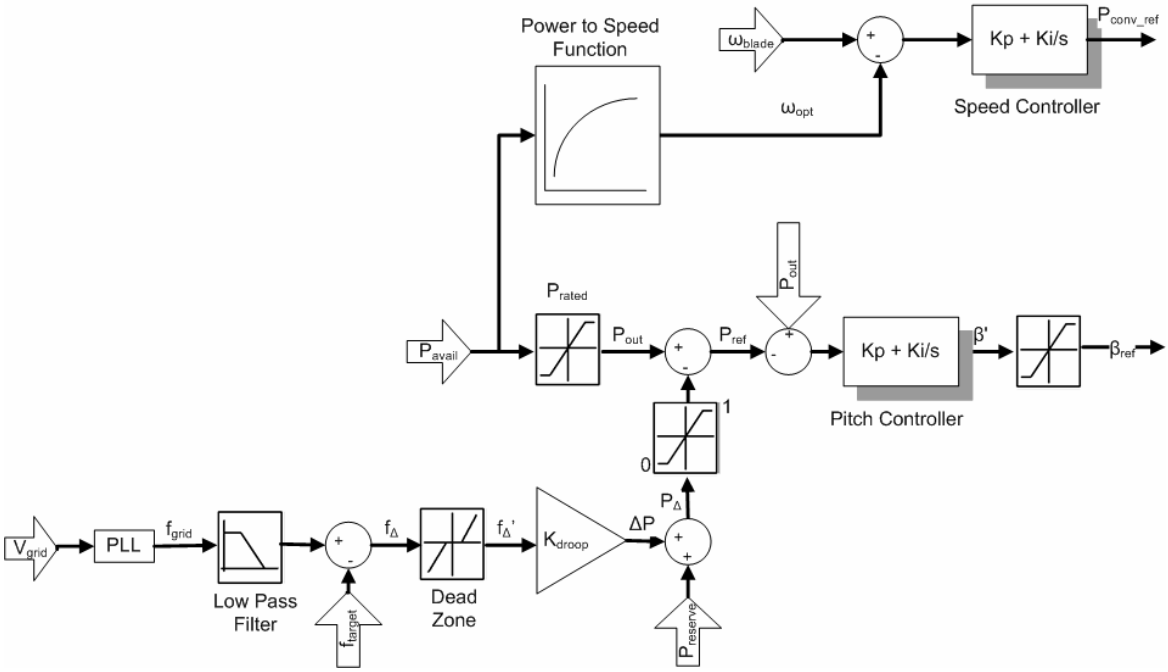

Figure 4.19: Primary Frequency Response by Pitch Control

The simple droop control of pitch angle proposed by Holdsworth, Ekanayake and Jenkins works under steady wind conditions and the control of pitch angle for frequency response is necessary for the direct speed controlled turbines. However, under intermittent wind conditions, neither technique is ideal for meeting the fixed output, variable reserve requirements of the GB Grid Code. Furthermore, the pitch controller has to deal with the continuously variable aerodynamic power.

An alternative approach, which works well with indirectly speed controlled wind turbines, is to modify the power generated directly. Section 3.5.2.1 showed how the rotor speed of a wind turbine could be used to set the optimal power or torque set-point for the generator. This torque (see Figure 3.12) or power (see Figure 3.14) set-point is then fed to the power converter controller.

Ekanayake, Jenkins and Strbac [92] have shown that frequency response reserves can also be attained by directly modifying the torque set-point of a DFIG or full converter wind turbine. This is done by subtracting a term from the optimal torque or power set-point. In Figure 4.20 this is shown as a modification to the P_{avail} reference point. P_{delta} is the margin held for response. The sample and hold block is triggered to hold whenever the frequency

exceeds the nominal limit (50.4Hz in LFSM) so that "Balance control" can be implemented. Otherwise, the power reference to the power converter is modified by the available power, response holding and any deviation in frequency. Note that in order to meet the specific requirements of GB Grid Code with regulation from a fixed output level, the controller's P_{avail} signal is held constant for a settlement period (30 minutes) based on a forecast; whereas under a "Delta control" arrangement it continuously varies.

A change in the power reference of the power converter leads to a change in the torque on the generator. This in turn leads to a change in the speed of the generator and blades. If the wind turbine is operating in rated wind speeds or higher, this change in speed will lead onto a change in the blade pitch angle of the turbine.

This frequency control method has the advantage that response times are only limited by the dynamics of the power converter and the ability to accurately measure system frequency. Given that system frequency measurement typically provides a noisy signal, the frequency controllers are equipped with low pass filtering on that frequency measurement, but given the response requirement of 2 seconds, this filter does not pose a problem for primary response. The disadvantage of this method from a commercial perspective is a patent by Delmerico and Miller [93], of General Electric, covering some of the necessary components and pre-dating Converteam's acquisition by GE.

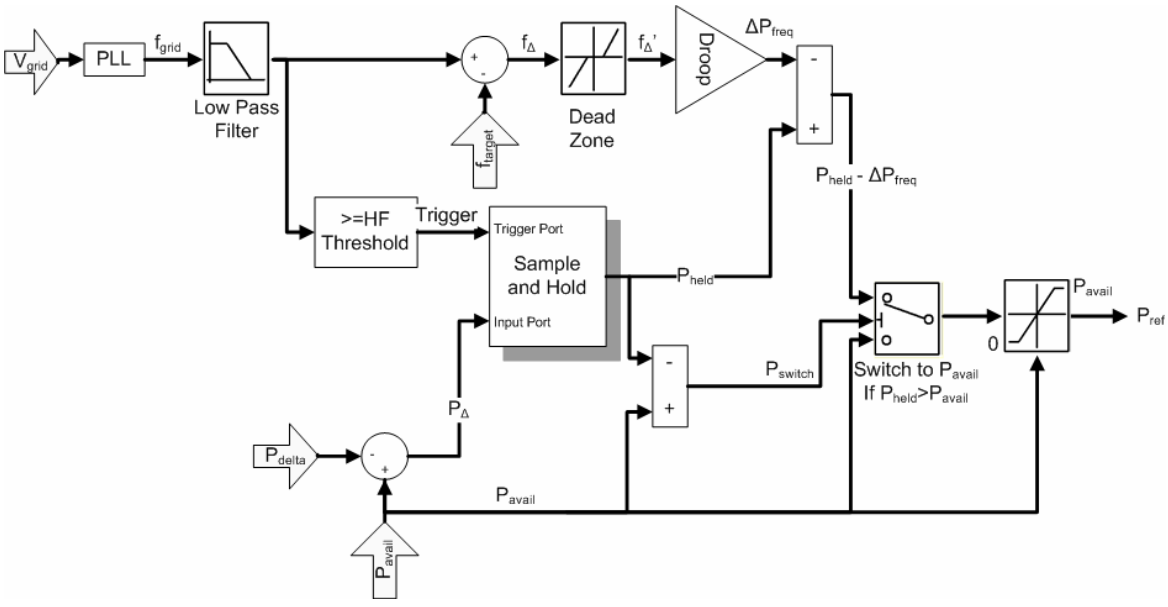

Figure 4.20: Primary Frequency Controller Using Converter Power Reference

The power converter control operates to implement the required torque on the generator. It does this regardless of the aerodynamic effect any speed change is having. Conroy and Watson [94] have shown, with work that included an inertial controller, that drawing too much power from the blades, which leads to an excessive deceleration, can cause unstable

operation and ultimately contribute to a frequency collapse. Even if collapse in the speed of the turbine is avoided, Tarnowski *et al.* [95] have shown that the recovery periods following periods of significant over-production can be of long duration and require significant power reductions.

Operation of a power converter interfaced wind turbine, with a power reserve for frequency response, in below rated wind conditions can lead to an acceleration of the blades to a higher than optimal TSR. Tarnowski's starting point was a turbine operating at the optimal rotational speed, such that over-production leads to worsening TSRs. However, a plant operating in FSM according to Figure 4.20 can store additional energy as kinetic energy under below rated wind speed conditions, thus potentially avoiding the under-production recovery periods associated with frequency response from an optimal starting speed. This has been investigated by Banham-Hall *et al.* [96] and Teninge *et al.* [97].

Figure 4.21 shows a one-shot controller to provide additional power output from stored rotor kinetic energy. First the estimated available power is used to provide an estimate of the optimal speed of the turbine. Tarnowski's [95] research, in conjunction with Vestas, derives the available power estimate from an estimate of the prevailing wind speed as is done here. The energy stored in the rotor can then be calculated for the current operating speed (ω_b) and the optimal operating speed (ω_{opt}). The difference between these two values is the energy available for over-production, which can contribute to an additional power response for the Primary response period (T_{prim}). This additional power capacity is sampled and held in the event of frequency falling below a fixed level (f_{target}) and added to the power converter's set-point to release a one-shot power increase.

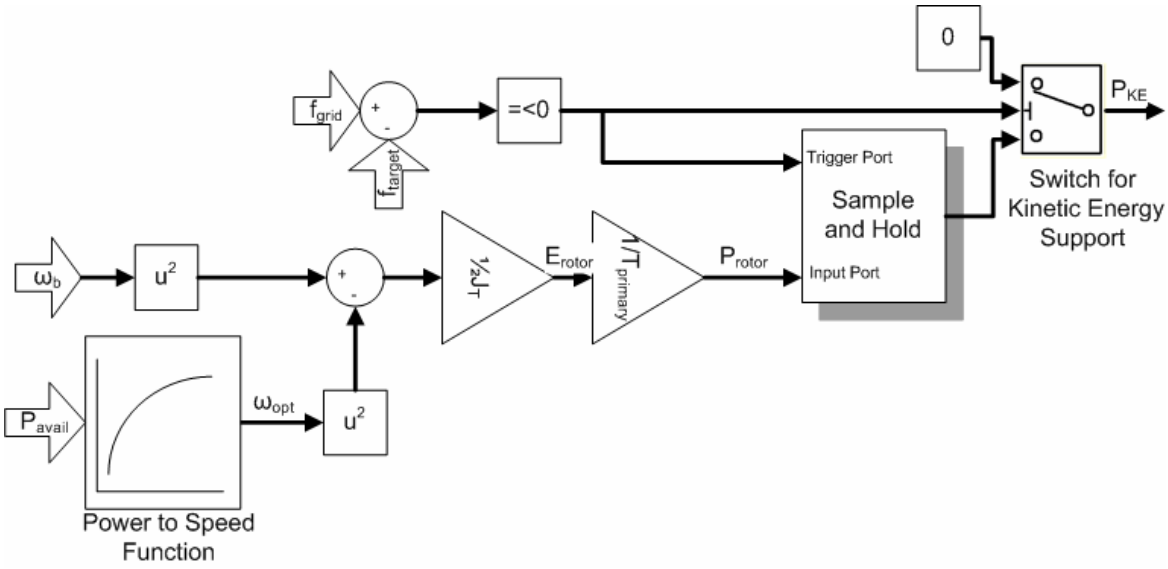

Figure 4.21: Frequency Response Controller for Temporary Over-production

4.3.3 Frequency Response Capability

Figure 4.22 shows a comparison of the high frequency response of wind turbines, using the pitch and power regulation strategies, under constant wind conditions. The left hand plot shows a case with low wind speed. The right hand plot considers the case where the wind speed is above rated, but the wind farm is operating in FSM and therefore holding a margin for both high and low frequency response. In both cases the response to a 0.5Hz frequency step at t=80s is evaluated, which corresponds to one of the more severe compliance tests for the GB Grid Code.

In both cases it can be seen that the frequency response method that directly adjusts the power converter set-point leads to an instantaneous and proportional change in the power output (Pturbine). The power response from the pitch regulated turbine is slightly slower, as it depends on the dynamics of pitching mechanism; however, a stable new power output level is achieved within 2 seconds.

In the low wind case, the power reserve held on the power reference regulated case has led to the turbine operating at above optimal rotational speed; furthermore, the pitch controller has intervened to ensure turbine speed does not exceed the design rating. However, the rapid reduction in the converter's power reference in response to the frequency change allows the turbine to accelerate (Wr), as the generator torque is lower than the blade torque in both cases. The change in blade pitch angle is then slow to catch up, as the turbine's acceleration is slow. In contrast, the pitch regulated turbine is operating at optimal speed throughout both scenarios. In order to maintain the optimal speed and provide the required power reduction, the pitch controller has to change the blade pitch much faster and is limited initially by the maximum pitch rate of the turbine. The pitch controller is slightly under-damped to optimise the speed of response in this implementation.

A side effect of operating the direct speed controlled turbine at optimal speed throughout the scenario is that the corresponding PMG voltage is lower, as the open circuit voltage of the PMG is reduced. Furthermore, the PMG is not exposed to the slight voltage transient that occurs for the power reference regulated case under high wind conditions, which is due to a sudden torque reference change.

Figure 4.23 shows the comparison of these turbine controllers, plus the one-shot additional energy controller, under a low frequency deviation. This time the frequency is ramped down by 0.8Hz over a 10 second period, again reflecting a severe test under the GB Grid Code.

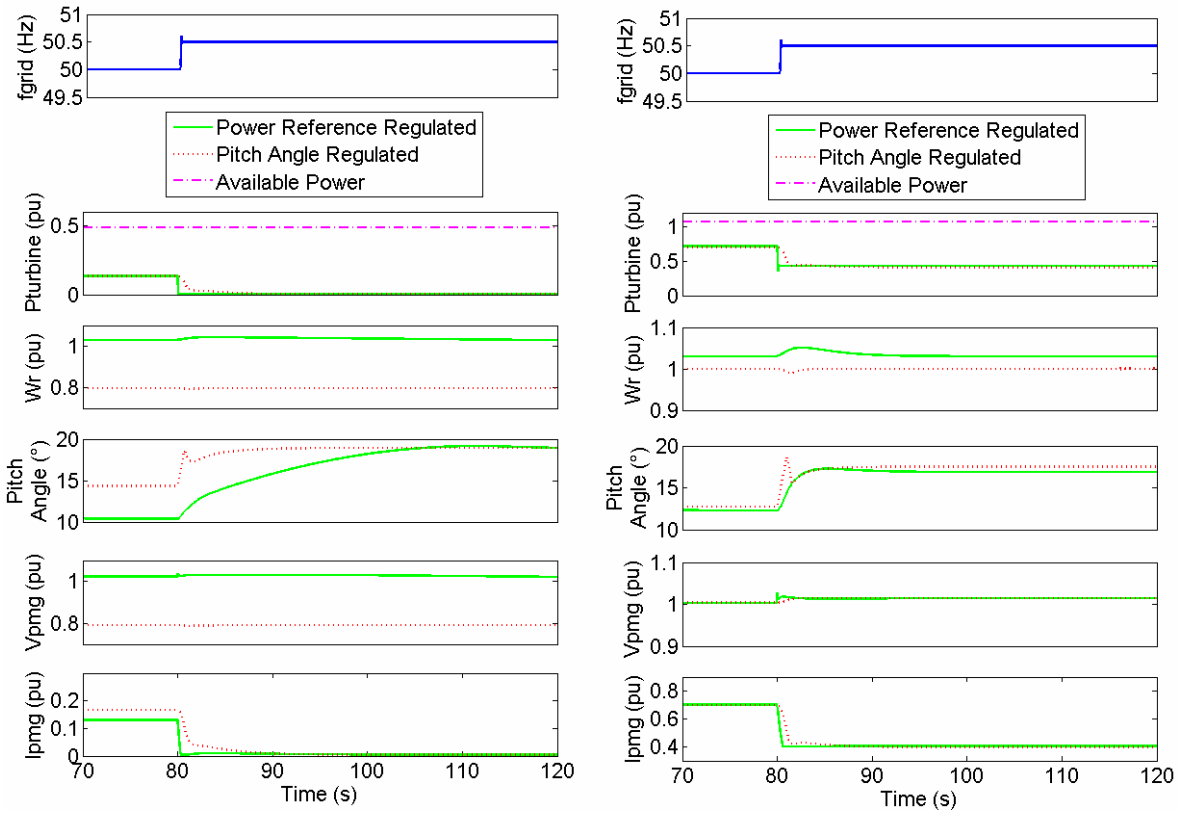

Figure 4.22: High Frequency Response Comparison under low wind (left) and high wind (right)

As with the high frequency response case, when the frequency response is driven by the pitch controller it is unsurprisingly somewhat slower than the power converter driven response. The response settles some 2.5 seconds later in the low wind case. The one-shot controller is activated right at the start of the frequency deviation and leads to a step increase in output power from the wind turbine (Pturbine) that lasts for 20 seconds.

For the low wind speed case, the direct speed controlled turbine, with pitch regulated power output, operates throughout the scenario at the optimal rotational speed for the wind speed. This is in contrast to the deceleration of the power reference regulated turbines, which start at an above optimal speed. In the case with the one-shot controller, the turbine decelerates back to the optimal speed much more quickly, as the kinetic energy stored in the blades is being actively used in the additional power output contribution. The standard power reference regulated case experiences a slower deceleration as power output only exceeds the power capture due to the relatively smaller deviation in *Cp* from optimal.

The one-shot controller is not applicable to the high wind case as the rotor will be operating at rated speed and therefore is below the optimal rotational speed and at rated torque. In this scenario the direct speed controlled turbine's constant speed approach can be seen to be of some value. The faster power response of the power regulated case comes

at the expense of a significant blade speed transient. The power difference between the power reference regulated case and the pitch reference regulated case has to be supplied from the kinetic energy of the blades, leading to a 6% drop in turbine speed. This sub-optimal speed recovers as a result of an undershoot in pitch angle, which allows the turbine speed to be restored to target. For different wind conditions, however, this speed transient could lead to a period of under-production, compromising the turbine's frequency response.

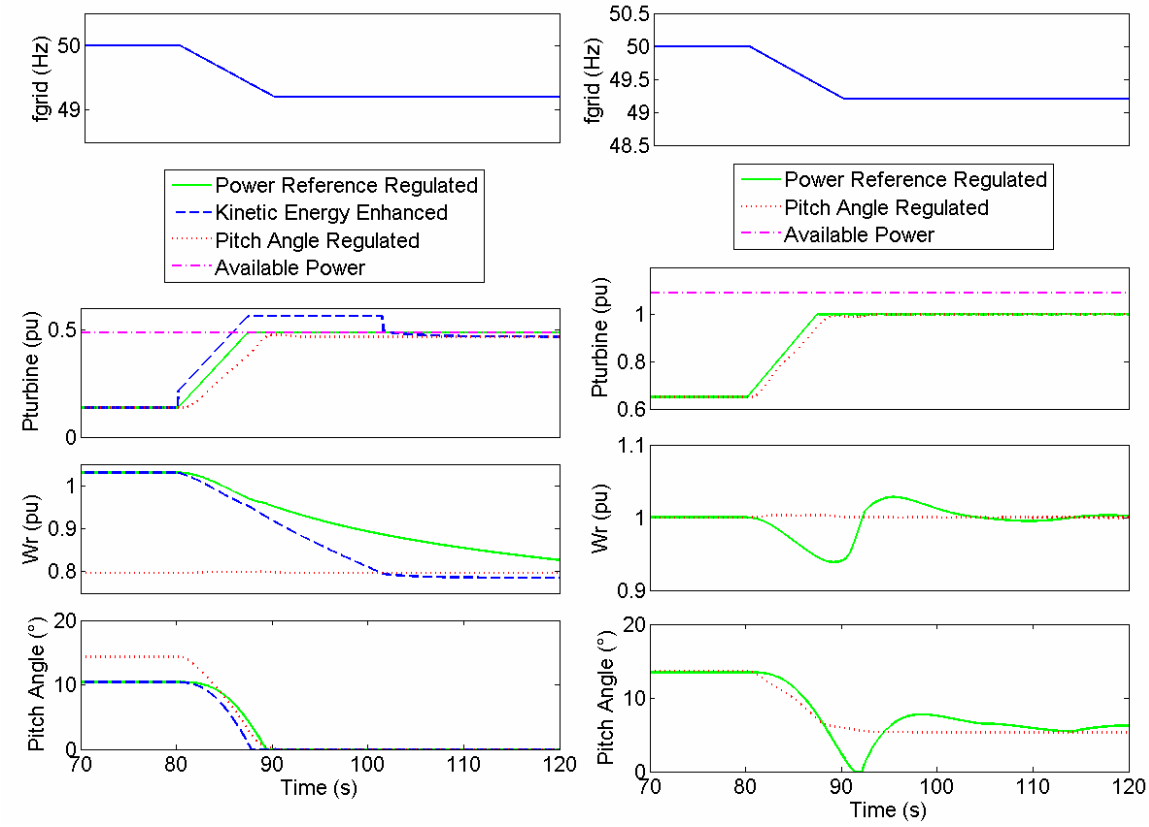

Figure 4.23: Low Frequency Response Comparison under low wind (left) and high wind (right)

Figure 4.24 shows a longer timescale study which includes variable wind speed for investigating the high frequency response performance of a wind turbine using the power reference regulated approach. This scenario demonstrates the behaviour of the absolute power limit (set at 0.95pu) and the balance controller. The scenario wind speed has been selected such that it varies around the rated wind speed (13m/s) of the wind turbine. The frequency is ramped up by 1Hz at t=200s.

From this variable wind speed study the smoothing effect of the rotor's inertia can be seen on the power output from the turbine. The turbulent wind field leads to much slower variations in the turbine's speed. These slow variations in turbine speed slowly move the turbine's operating point according to Figure 3.15, effecting a change in the power output. When the turbine is operating at rated speed and the wind speed rises, the turbine pitch

controller responds to limit the blade rotational speed. This pitch response is filtered by the slowly varying rotational speed too.

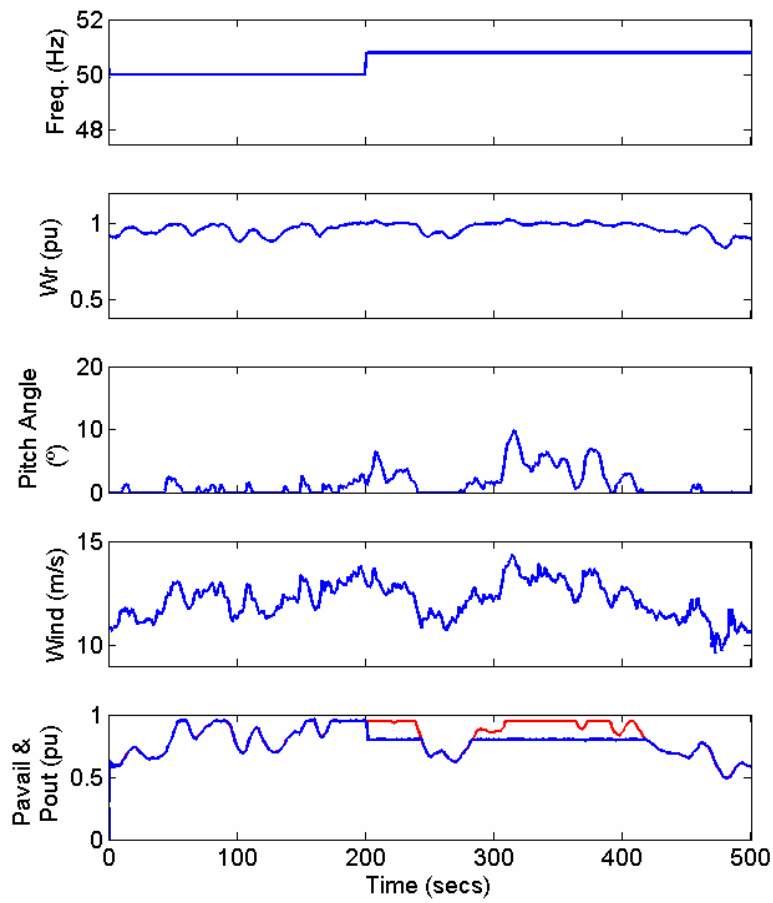

Figure 4.24: High Frequency Response in Variable Wind (available power shown in red, with output power in blue)

In this example, the turbine is operating only in LFSM, and hence only responds when the frequency has exceeded 50.4Hz with a "Balance control" response. Prior to the frequency deviation the wind turbine is tracking the available power (red) and outputting the maximum power possible. At the moment that the grid frequency rises, the wind turbine output is at 0.95pu, the Balance controller samples and holds this power output value and deloads relative to it to 0.8pu. The wind turbine's power output cannot now exceed 0.8 pu unless the frequency falls. However, when the available power drops below 0.8pu, the wind turbine can revert to tracking the available power in the wind, such as occurs in the simulation at around 260 seconds. This reversion to tracking available power cannot compromise the response but may lead to additional response, which helps to restore system frequency.

Figure 4.25 shows the challenges of providing low frequency response from a fixed output level. The wind farm is initially deloaded to a fixed output level (0.6pu), however, the available power varies sufficiently to cause the farm controller to have to revert to

tracking the available power for a period (around t = 100s). Furthermore, although the frequency response to the low frequency step at t = 200s leads to a predominantly smooth output from the wind farm, over the period considered here, the wind varies sufficiently to reduce the response for a period. The response is actually briefly eliminated by the reduction in available power at t = 390s.

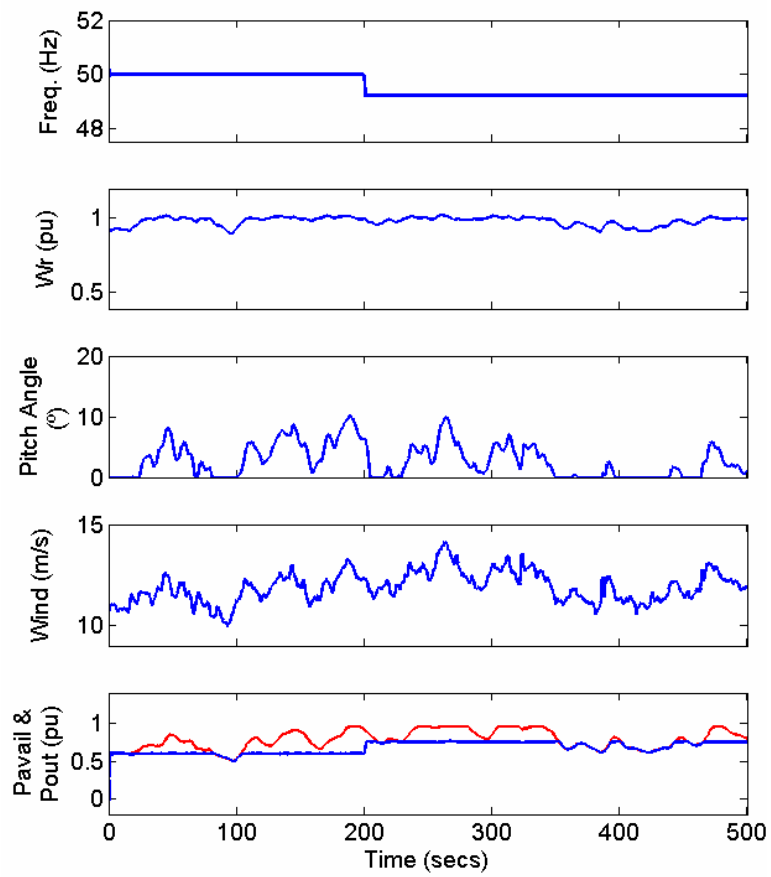

Figure 4.25: Low Frequency Response in Variable Wind with GB Requirements (available power shown in red, with output power in blue)

This shows the particular challenge of providing a firm response margin for secondary response time scales when the wind speed is close to the turbine's ratings. Small fluctuations in the wind speed cause significant changes in the output power, greatly affecting and potentially compromising the margin available for response. To compensate for this, the wind farm would have to deload itself by a greater margin prior to any frequency event, thereby incurring a greater economic penalty.

The alternative "Delta control" approach does not have this drawback, as shown in Figure 4.26. Under this control strategy the wind farm can track the available power with a fixed margin prior to the frequency deviation. Then, following the frequency fall, the wind farm can be increased up to a maximum of the available power. The wind farm then reverts to tracking the available power to provide maximum output.

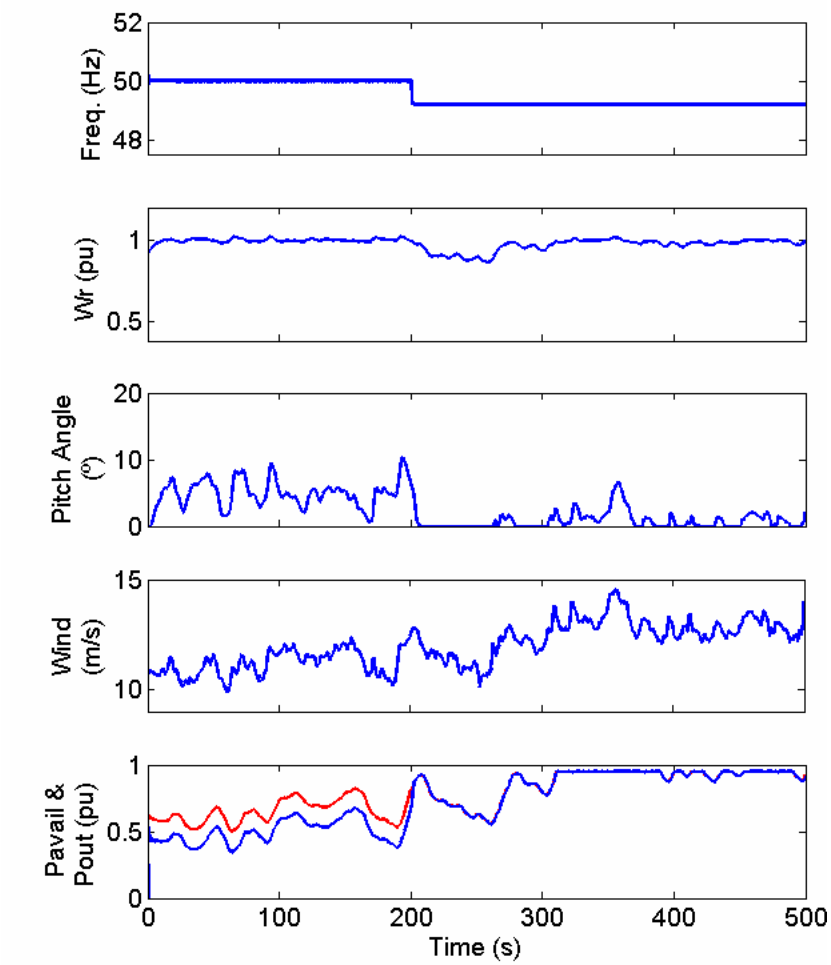

Figure 4.26: Low Frequency Response in Variable Wind with Delta Requirements (available power shown in red, with output power in blue)

In this scenario the wind speed rises and therefore the effect of wind intermittency is to contribute to meeting the generation gap. The problem with this control method would be highlighted by falling wind speed. In that event, the additional power provided by the use of the Delta margin could be offset by a loss of power due to reduced available power in the wind. Overall therefore, Delta control solves the challenge of predicting the necessary deload for reliable frequency response, that the GB requirements lead to, but potentially causes a further problem for system operators as real response capacity depends on the variability of the prevailing wind conditions.

Despite the differences between delta control and the GB requirement to regulate power output from a fixed level, it can be seen that the wind turbine control systems themselves can be modified to allow wind farms to hold power reserves. These power reserves can be delivered within the timescales required for primary response, although the mechanical systems of the wind turbine may continue responding for a considerable time afterwards. Wind farms can also contribute high frequency response and a balance controller has been presented that ensures optimal response from a wind farm in LFSM. The technical

challenges of providing droop type response from directly or indirectly speed controlled turbines can be met with appropriate control strategies.

Whilst this section has shown that it is technically feasible for wind farms to hold frequency response reserves, it has only touched on the economic implications. Holding reserves for low frequency response implies spilling wind energy and incurs a significant opportunity cost. Whereas today's conventional generators can benefit from significant fuel savings whilst holding reserves, there is no such compensation for wind power. Hence, the economic viability of wind for this application, on all but a few high wind occasions per year, is likely to be questionable.

The Grid Code requirements for provision of frequency response currently incur a technical burden on wind farms. They have to meet the technical requirements of the code. However, given the questionable economic implications of providing frequency response from wind power, it is worth considering what other options are available in order to meet the frequency response requirement. The second half of this thesis will address this issue.

4.4 Synthetic Inertia

Section 4.3 has shown that the frequency response capability of power converter interfaced wind turbines differs substantially from conventional synchronous generators. Along with section 2.5, it has been shown that the inertial response of grid connected generation could substantially change in the coming years. The frequency response capability of wind turbines and wind farms to provide primary, secondary and high frequency response has been investigated in the previous section and is already clearly mandated in the GB Grid Code with specific guidelines that cover technical requirements on wind farms. This section specifically covers the initial inertial response to changing frequency.

4.4.1 Grid Code Developments

It is notable that the procurement mechanism for frequency response of the GB TSO only considers time periods of 10 seconds and longer. This is reflective of the inherent inertial effect that conventional plant's synchronous generators and rotating machinery provides to the grid today, arresting the rate of change of frequency and helping stabilise the system. As the future grid is likely to incorporate more power electronic interfaced equipment, it is unsurprising that specification of an inertial component was considered in

the first draft of the European harmonised Grid Code [98] from the European Network of Transmission System Operators for Electricity (ENTSO-E).

Thus far only Hydro-Quebec [99] have implemented a Grid Code requirement for a synthetic inertial response, requiring manufacturers to have an equivalent H constant of at least 3.5 seconds.

The capability of wind turbines to provide inertial response has been the subject of consultation between National Grid [100] and manufacturers. Concern centred on the recovery period of wind turbines after they have provided an inertial response and whether the measurement of system frequency could be accurate and fast enough to provide the desired response. Perhaps as a result of these uncertainties, the latest working copy of the European code has removed this requirement according to ENTSO-E [101]. In its place ENTSO-E has proposed a faster response (6 seconds) from primary response, with the aim of avoiding the need for synthetic inertial response. It is in the context of this regulatory uncertainty that this work explores the capability of wind turbines to provide a synthetic inertial response.

4.4.2 Control Methods for Providing Inertia

An analysis of the change in kinetic energy of a synchronous machine's rotor in response to a frequency change led to Equation 2.12, which showed that power released by that synchronous machine would be broadly proportional to the derivative of frequency. On this basis Holdsworth, Ekanyake and Jenkins [91], Morren *et al.* [102] and Morren, Pierik and de Haan [103] considered the kinetic energy of DFIG wind turbines and proposed a control strategy based on emulating this. These papers inform the general derivation here.

The kinetic energy of the rotating parts of a wind turbine is given as:

Equation 4.24 $$KE = \frac{1}{2} \cdot J \cdot \omega^2$$

Differentiating the kinetic energy with respect to time provides the power output profile from energy stored in the rotor according to:

Equation 2.12 $$\frac{d(KE)}{dt} = \frac{1}{2} \cdot J \cdot 2\omega \cdot \frac{d\omega}{dt} = J \cdot \omega \cdot \frac{d\omega}{dt}$$

Additionally, an inertial constant can be defined according to the turbine's kinetic energy and rated apparent power. This inertial constant determines the time for which a generator can supply rated power purely from its kinetic energy.

Equation 4.25 $H = \frac{J \cdot \omega^2}{2 \cdot S}$ which can be rearranged to $J = \frac{2 \cdot S \cdot H}{\omega^2}$ and substituted into Equation 2.12:

Equation 4.26 $P_{inertia} = \frac{2 \cdot S \cdot H}{\omega^2} \cdot \omega \cdot \frac{d\omega}{dt}$ which naturally simplifies in per unit terms to:

Equation 4.27 $\overline{P}_{inertia} = 2 \cdot H \cdot \overline{\omega} \cdot \frac{d\overline{\omega}}{dt} \approx 2 \cdot H \cdot \frac{d\overline{\omega}}{dt}$

Hence, the inertial controller derived from an analysis of the release of kinetic energy of the wind turbine has to respond to the rate of change of grid frequency. A controller that uses this strategy is shown in Figure 4.27 and adds a term to the turbine's power reference. This approach of modifying the power (or torque) reference of the turbine means that it is suited to use with the classical indirect speed control of turbines.

It is notable that the controller has to include some additional components other than the gain and frequency derivative. Any measure of grid frequency is subject to noise owing to voltage distortion, harmonics, poor PLL performance or voltage transients. Given that the measurement of grid frequency is subject to noise, the frequency derivative will be subject to spurious transient peaks in response to frequency measurement noise. To prevent these transients leading to transitory impulse power demands on the wind turbine, the measured frequency has to be pre-filtered by a low pass filter. Additionally, if this inertial controller were continually active it would add a stochastic term to the wind turbine's maximum power tracker, thereby potentially having a negative impact on wind turbine yield. Therefore, a dead band is also included, which in conjunction with the low pass filter, helps to ensure that the inertial controller is only sensitive under large sustained frequency changes.

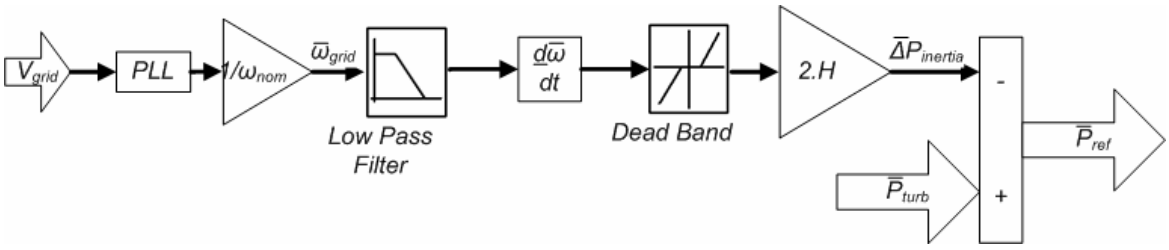

Figure 4.27: Inertial Control by Frequency Derivative

A comparison of the different inertial control methods presented here is conducted in section 4.4.3. Nevertheless it should be considered that the low pass filter and dead band combination have to be specifically introduced to avoid an overly sensitive response owing to noise on the frequency derivative and so that the controller only responds under large frequency deviations. Furthermore, whilst this control is suitable for the common

indirect speed controlled turbine, it would not be directly applicable to any future direct speed controlled versions.

A synthetic inertial controller can be derived for the direct speed controlled turbine by considering that the aim of an inertial controller is to release the kinetic energy from the rotating equipment as it slows down to a new operating point. Hence, the synthetic inertial controller can modify the speed set-point of the turbine, dependent on the magnitude of the frequency error, to invoke an inertial response. This would de-optimise the energy capture slightly, although even a frequency change to 49Hz would only lead to a 2% change in speed, so this effect is negligible. The benefit of this control approach is that the inertial set-point change is initiated by the magnitude of the frequency deviation and not by the rate of change of frequency. Hence the controller is less sensitive to frequency measurement noise. Furthermore, the speed of response is dependent on the dynamics of the speed controller rather than the bandwidth of the low pass filter used to filter the frequency in the derivative case. However, this controller still requires a dead band to ensure that small frequency fluctuations do not continually lead to transient power swings from the turbine as the speed controller's set-point changes.

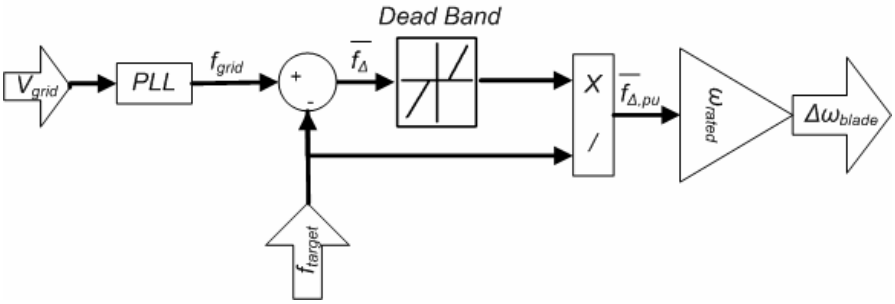

Figure 4.28: Inertial Control by Speed Control

Whilst the speed control method solves the problem of avoiding noise sensitivity to the frequency derivative, it can only be directly applied to the directly speed controlled turbine. Furthermore, its response is dependent on the bandwidth of the speed controller. It is shown in Figure 4.28.

A new alternative approach can be developed by considering the approach to providing inertia from an energy store described in Larsen and Delmerico [104]. Under their approach, an inertial controller directly modifies an energy store converter's firing angle, thereby modifying power output. However, a feedback loop effectively takes a derivative of frequency and filters it with a first order low pass filter, thereby indirectly taking a frequency derivative.

The controller developed here takes Larsen and Delmerico's approach of generating an angle from the system frequency but applies it instead to model a synchronous machine's response. The feedback loop is replaced by a model of the blades' deceleration. Section 2.5.3 suggested that changes in grid frequency actually caused the inertial response from a synchronous machine by leading to a load angle change. This load angle change in turn leads to a change in torque, which follows a sinusoidal path, according to section 2.5.1. Hence instead of taking the frequency derivative, an inertial controller can be developed by generating a synthetic change in load angle. This change in load angle is calculated by integrating the error between the nominal frequency and the instantaneous system frequency (note f_{nom} would normally be 1):

Equation 4.28 $$\Delta\delta_{inertia} = \omega_{nom} \cdot \int \left(\bar{f}_{grid} - f_{nom}\right) \cdot dt$$

This change in load angle has to be taken relative to an initial synthetic starting load angle (δ_{nom}), which is here taken to be $\pi/4$, although this value is somewhat arbitrary (see Figure 2.21). Hence, a new operating load angle is:

Equation 4.29 $$\delta = \frac{\pi}{4} + \omega_{nom} \cdot \int \left(\bar{f}_{grid} - f_{nom}\right) \cdot dt$$

This new synthetic load angle would lead to a relative change in torque, from the initial load angle (δ_{nom}) to the new load angle (δ), of:

Equation 4.30 $$\bar{T}q_{out} = \frac{Tq_2}{Tq_1} = \frac{\sin\delta}{\sin\delta_{nom}}$$

This ratio can then act as a torque (or power) reference multiplier, increasing the output of the turbine as and when the frequency falls and decreasing it when the frequency is high. This leads to the "Torque Multiplier" output in Figure 4.29.

Thus far this approach has considered a hypothetical machine angle change between the nominal frequency and the instantaneous system frequency. In a synchronous machine, this angle change is stopped by the acceleration or deceleration of the machine such that its rotational frequency returns to matching the grid frequency. In order to emulate this part of a synchronous machine's behaviour, it is possible to model the turbine's speed response to the torque change and use this to form the feedback loop.

Equation 4.31 $$\bar{T}q = 2 \cdot H \cdot \frac{d\bar{\omega}}{dt}$$

Hence, the change in speed of the turbine can be modelled as:

Equation 4.32 $$\Delta\overline{\omega} = \int \frac{1}{2 \cdot H} \cdot \overline{T}q \cdot dt$$

This modelled change in the speed of the turbine then modifies the frequency reference point and closes the feedback loop. In parallel with this integral feedback is a small proportion gain contribution which improves the stability of the loop. Now, in the event of a frequency change, the controller estimates a change in a synthetic load angle and modifies the torque (or power) reference to the power converter. The power converter responds fast by changing the generator torque. The modelled speed of the turbine (in the inertial controller) then decreases and modifies the frequency reference until the load angle closes and the torque rebalances to its original value. Note that the real turbine speed is not used owing to unpredictable speed behaviour due to wind speed changes. Figure 4.29 shows this inertial response controller.

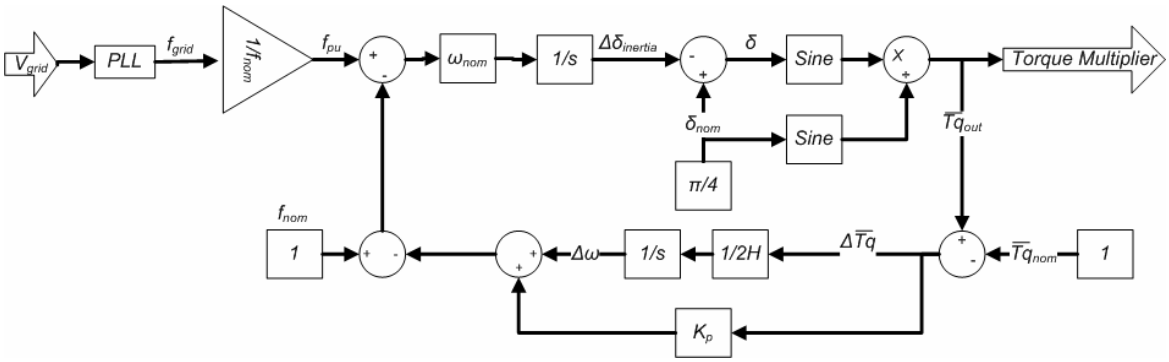

Figure 4.29: Inertial Control by Synthetic Load Angle

4.4.3 Inertial Response Capability

Figure 4.30 shows a comparison of the three different inertial methods in response to the 0.5Hz step increase in frequency. Whilst a step response would not be a realistic physical scenario on the power system, it serves to distinguish the response of the different control methods by highlighting the filter and derivative effects. The top plot shows the measured frequency after the PLL but before the low pass filtering stages of the controllers, however, the actual frequency applied was a pure step at t = 80s. The wind conditions were constant and below the rated wind speed. In all three cases, the droop controller was also active.

The transient power to the grid (Pgrid) shows the benefits and shortcomings of the different control methods. The method relying on the frequency derivative shows both a noisy response and a slight delay of around 150ms before the inertial response is initiated. The delay is partly induced by the low pass filter, whilst the noise is a response to the overshoot in measured frequency from the PLL, which to an extent persists even after filtering. Given the fast change in frequency measured, the response is sharp and short

lived from this controller, effectively only achieving a slight improvement over a fast droop response.

The speed controller method achieves a faster response than the frequency derivative method and is clearly less noisy. However, the power output profile is solely determined by the dynamics of the speed controller, so the inertial response lasts for only around 300ms before the inertial contribution is finished and the power profile follows the droop response. This droop response is only provided at the slower rate at which the blade pitch mechanism can respond, leaving a time lag between the end of the inertial response and the droop response reaching the same level.

The response of the synthetic load angle controller is extremely promising, responding with no time lag and showing little noise sensitivity. The high rate of change of frequency leads to an overshoot, relative to the steady state droop response, before the feedback loop closes the synthetic load angle and brings the inertial response contribution back to zero.

The frequency derivative controller and the synthetic load angle controller both effect rapid changes in power output whilst leaving the slower turbine dynamics to respond. This change in power output leads to the generator torque being reduced and the blades gradually accelerating. As the blades reach the maximum speed the pitch controller begins to increase the blade pitch angle in order to decrease *Cp*. This is in contrast to the speed controlled approach, where the pitch controller and speed controller work together to change the turbine operating point which then leads onto a change in the output power. This difference means that the speed controlled turbine continues to operate at the optimal speed, but the other two methods accelerate to a higher than optimal rotational speed.

Figure 4.31 shows the inertial response (no droop) to the GB system event discussed in section 2.6.2. Here, the response of the synthetic load angle controller and the frequency derivative controller appear similar, with the speed controller slower. However, close inspection of the frequency derivative output shown in Figure 4.32 shows the improved noise rejection of the synthetic load angle method. The frequency measurement noise, combined with a finite update rate of the power control on the power converter leads to significantly less smooth power output from the power regulated control.

It is also notable, that the inertial response causes a speed change from the power reference and synthetic load angle regulated turbines. This speed change in turn leads onto a reduction in the turbine's power reference (Po/p) (which then has the inertial term added) according to the cubic relationship of Figure 3.15. This change in operating point

reduces the inertial response and eliminates it prior to the frequency stabilising. This ultimately leads into the recovery period, which can be seen as the turbines slowly regain speed for up to half a minute after the frequency deviation. Whilst this recovery period can be delayed (by triggering the balance controller on falling rate of change of frequency), this serves to highlight the concerns that National Grid have had over the recovery of wind turbines following an inertial response contribution.

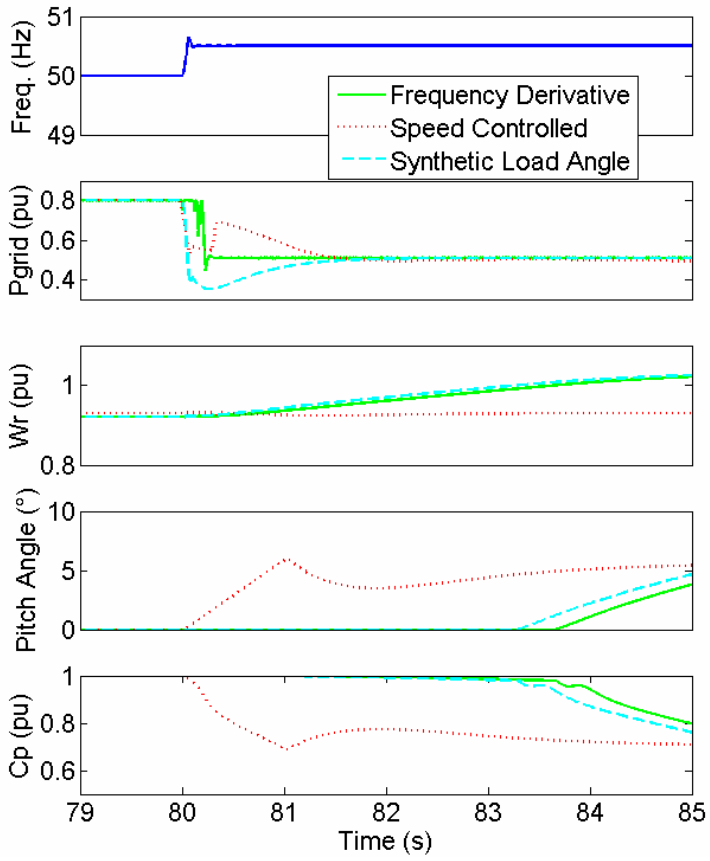

Figure 4.30: Inertial response to a high frequency step

The speed controller modifies the speed set-point for as long as the grid frequency is low; the speed recovery in this case is much slower, matching the frequency recovery of the grid. However, the dynamics of the speed controller ensure that the inertial response is also delivered slightly slower. Nevertheless, following delivery of the inertial power contribution, the controller only recognises a change in speed of the turbine as a slight de-optimisation of *Cp* across the flat peak of Figure 3.3 instead of the cubic outcome of the other two controllers. This ensures that the power recovery period is insignificant compared to the other two cases.

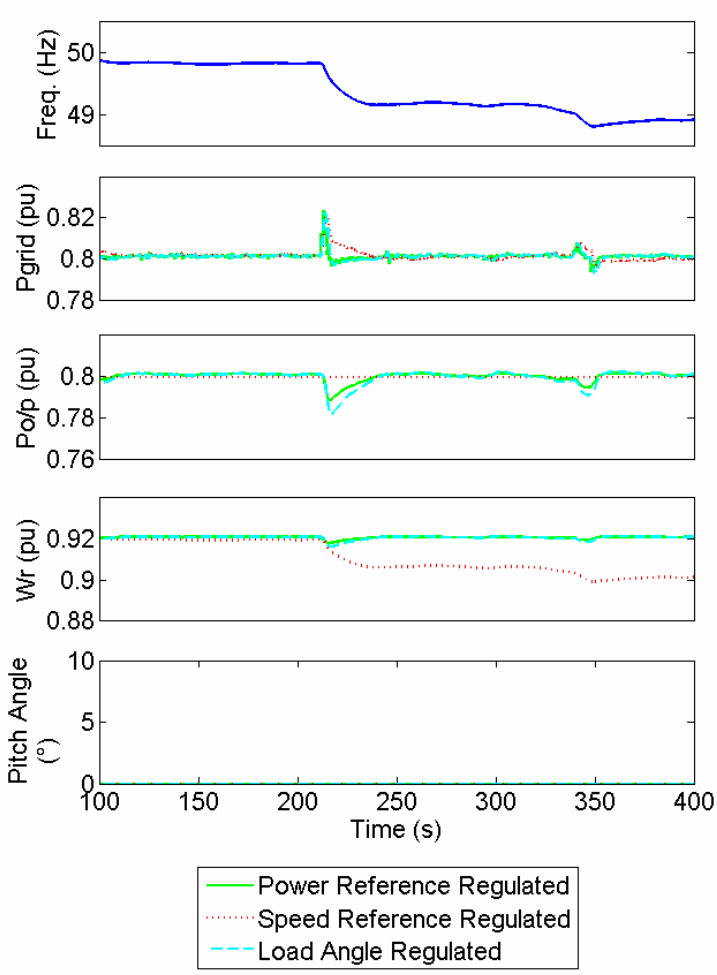

Figure 4.31: Inertial response simulation to 27th May 2008 frequency profile (low wind)

In this scenario the wind speed was deliberately modelled at constant speed, but slightly below the rated wind speed of the turbine. This ensured that the speed changes of the turbine occur at the steepest part of the operational curve in Figure 3.15, maximising the differences in the performance of the controllers.

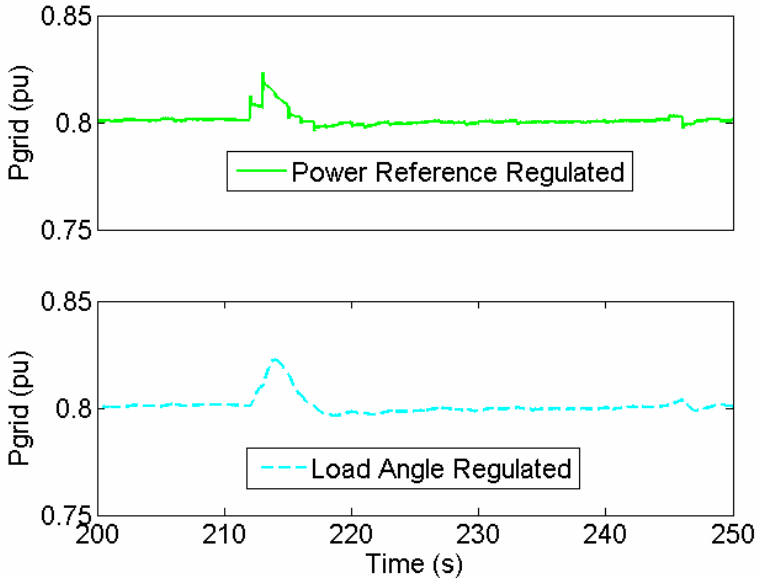

Figure 4.32: Expanded view of Figure 4.31

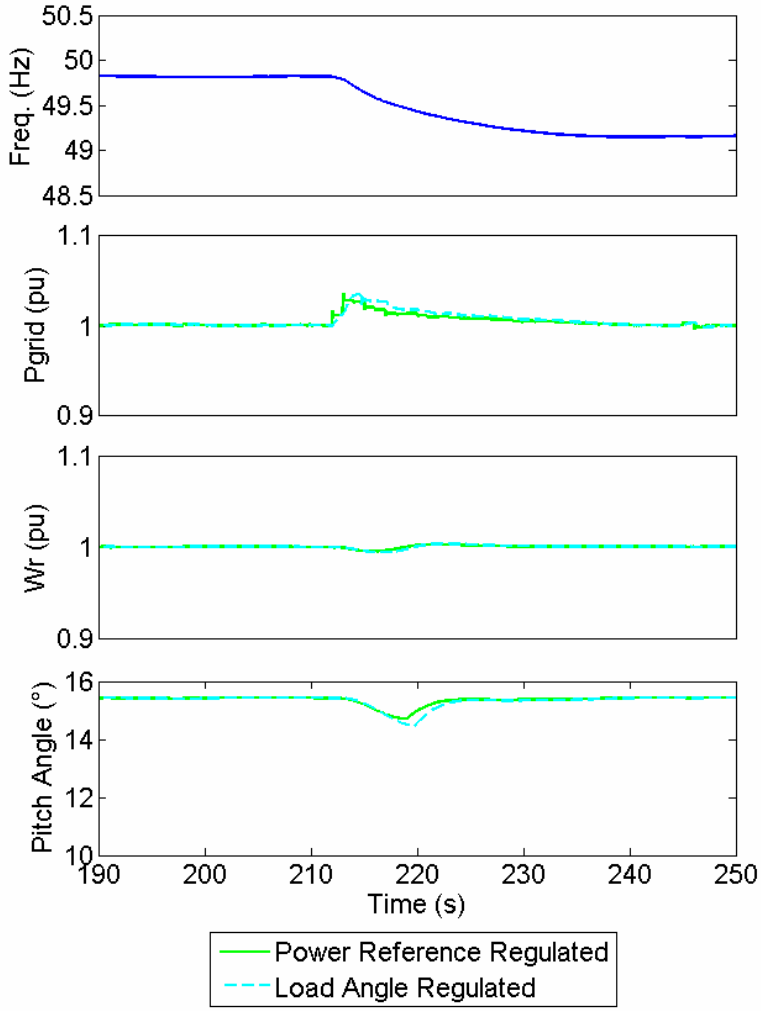

Figure 4.33: Inertial response simulation to 27th May 2008 frequency profile (high wind)

In contrast to the case with the wind speed just below rated, the inertial response to the frequency change at 210 seconds with above rated wind conditions is shown in Figure 4.33 and this illustrates that under high wind conditions the recovery period is eliminated. The response is not compromised by a change in the available power as the pitch angle controller responds to the slight change in turbine speed by reducing the pitch of the blades, thereby temporarily increasing *Cp* and allowing the turbine speed to recover to rated rotational speed.

The inertial response simulations have shown the benefit of using a synthetic load angle approach to providing inertial response. This offers fast response with less noise sensitivity than the traditionally proposed frequency derivative method. There are several other alternative methods of providing inertial response. Manufacturers such as Enercon [105] have proposed one shot controllers that output either a set percentage increase in power output (*i.e.* 10% extra for 10 seconds above the varying output) or a set power output (*i.e.* 100% output for 10 seconds). Others such as Vestas [106] have proposed controllers that follow the frequency derivative method.

Initial GB TSO engagement with manufacturers, to address inertia, raised two concerns; first the recovery periods of wind turbines and second the sensitivity and design of controllers reliant on taking the derivative of a noisy frequency signal. This work has shown that it is possible to devise inertial controllers that are less sensitive to frequency noise whilst offering a fast response. To complete the evaluation of this controller's capabilities it would be necessary to address National Grid's first concern and investigate the recovery period of multiple different turbines from different manufacturers when providing this service. National Grid [100] has consulted with manufacturers, whilst considering the system needs, on limitations and capabilities of wind turbines' inertial emulation. This is perhaps a better forum for addressing aspects that depend on manufacturer specific designs.

4.5 Summary

A novel converter control adaptation has enabled full converter PMG wind turbines to ride through grid voltage transients with only a minimally rated chopper, whilst a modification to the wind turbine controller has permitted demonstration of response to grid frequency transients with a noise insensitive synthetic inertial response.

This chapter has covered the development of control schemes for wind turbines with full converters to meet the requirements of modern Grid Codes. It has illustrated the challenge presented by grid faults and used type test data to validate a complete wind turbine model. This validated wind turbine model then forms the basis for further investigation of the impact of grid events on turbine behaviour. Section 4.2.4 looks specifically at the fully fed direct-drive Permanent Magnet Generator identifying its speed-voltage relationship and high stator reactance as new challenges for GFR compliance. The developed models are then applied to improving this GFR behaviour, leading to a novel ramped chopper control scheme in section 4.2.5. This control scheme allows PMGs to ride-through grid faults with minimal shaft oscillation and stator over-voltage, whilst permitting a smaller chopper and brake resistor than conventional schemes.

Beyond the challenges of GFR, the chapter moves on to examine the frequency response capabilities of wind turbines. It shows the key requirements in Great Britain in section 4.3.1 and highlights how these have been applied in the context of the intermittent wind resource. Section 4.3.2 builds on and extends existing knowledge to develop control strategies for conventional indirect speed controlled turbines and then novel strategies for direct speed controlled turbines. Further it shows how wind turbine's rotors can store

some kinetic energy for short term additional response when operating with a power reserve in low winds. The operation of these controllers is demonstrated in section 4.3.3.

Synthetic inertial response is one area not currently covered by GB Grid Code, however, as section 4.4.1 shows; there are developments on a European and international scale which may see it included. Concern has been raised over the ability of a synthetic controller to be sufficiently fast and noise insensitive when driven by a noisy frequency signal, therefore alternative approaches are taken offering better performance than straightforward derivative based controllers. This is presented alongside an inertial controller for the directly speed controlled turbine in section 4.4.2, with simulations of these controllers demonstrating the new controllers' improved behaviour in section 4.4.3.

5 Energy Storage Development

5.1 Introduction

Chapters 2 to 4 have covered the large scale development of wind power on the GB power system. They have addressed the emerging challenges for the power system, the development of models for further power system study and the technical capabilities of wind turbines and farms to meet some of the requirements of Grid Codes. Chapters 6 and 7 will address the complementary capabilities of Vanadium Redox Flow Batteries to wind farms and the economics of their development. This chapter acts as a bridge between these two subjects, highlighting the opportunities, technologies and applications of energy storage on the power system.

Wind farms have been shown to be capable of complying with the requirements of frequency response under Grid Codes. However, this technical capability comes at a significant economic cost owing to spilt wind. Section 2.7 explores whether this dichotomy between capability and cost will lead to a split in power system development between generators providing bulk energy and energy storage systems providing balancing services. There is a strong intuitive link between increasing intermittent power providers, such as wind farms, and a perceived need for energy storage, so this section introduces the question of whether energy storage would be a better provider of balancing services than wind farms.

In view of the potential opportunities for energy storage technologies to be applied as wind power scales up, section 5.2 explores the different energy storage options. A critical evaluation of the energy storage technologies addresses the strengths and weaknesses of each technology. This is followed by an economic analysis of the typical costs of different storage systems in section 5.3, which breaks down the technologies based on their power costs and energy costs. The technical and economic comparisons identify that the Vanadium Redox Flow Battery (VRFB) has the potential to be complementary to wind power in power system applications.

Given the interest in the VRFB, section 5.4 introduces the technology, its historical development and further details surrounding its potential application to the power system.

5.2 Energy Storage Technologies

Chapter 4, in part, addressed the frequency response requirements placed on wind farms. It showed how wind farms could meet the technical requirements of the code, but also briefly highlighted the economic implication of spilling wind to provide frequency response reserves. This cost, which could be placed on wind farms, presents a potential opportunity for energy storage systems. There are a multitude of energy storage technologies available with different strengths and weaknesses, this chapter therefore sets out to find the correct technology to address this market need.

As a result of the array of different technologies there are many reviews from academic sources such as Chen *et al.* [107] or Ibrahim, Ilinca and Perron [108] as well as from government sources illustrating the range of interested parties:

- The UK's Department of Trade and Industry (DTI) [109]
- The US's Electric Power Research Institute (EPRI) [110]
- The International Council on Large Electric Systems [111]
- The European Parliament's committee on Industry, Research and Energy (ITRE) [112].

The Electricity Storage Association [113] takes an advocacy role in promoting the benefits of all different storage technologies on the power system. These sources, plus technology specific references inform the analysis of different technology options which is included in this chapter. Further numerical data, which underpins the technology comparison, is shown in appendix 9.2, which also lists the references from which the data was sourced.

5.2.1 Pumped Hydro

Pumped hydroelectric storage takes advantage of specific geographical locations where natural or artificial reservoirs exist with a significant height difference. Energy is stored in the potential energy of water pumped into the upper reservoir. In a market based system pumping typically takes place during low demand and low price periods, with the system generating during peak demand hours. Typical round trip efficiency of these schemes is around 75% or less, meaning that significant price differentials must exist in order to allow economically viable operation purely from energy time-shifting.

The GB system is supported by a significant facility at Dinorwig in Wales, rated at 1.8GW. The greater part of all the energy storage on the GB grid is found at Dinorwig,

which has been running since 1981. It has impressive dynamic properties for such a large system, being able to reach full output power in only 16 seconds from a spinning start or 75 seconds from a standing start. This allows it to earn revenue from the market for Short Term Operating Reserves.

Pumped hydroelectric storage is a mature technology with many large scale, long duration plants in long term operation around the world. Nevertheless, the highly site specific nature of this storage type has been shown to lead to highly variable economics according to Deane, Gallachóir and McKeogh [114]. There are some opportunities for further development of pumped hydroelectric storage in Europe, however, due to the specific geological features required, these developments are limited.

Pumped hydroelectric projects are typically expensive undertakings, whilst their long lives, of upwards of 50 years, ultimately ensure that they payback, it has been suggested by Kazempour *et al.* [115] that newer technologies such as Sodium Sulphur batteries may represent better investment opportunities. Furthermore, the long payback periods associated with pumped hydroelectric may deter new investment.

Advantages	Disadvantages
Very high power ratings (GW) possible	Limited locations possible
Large energy capacity (GWh) possible	High capital cost
Good economics in the right sites	May require land use change
Long cycle life	Very low energy density
Moderate round trip efficiency	

Table 5.1: Advantages and Disadvantages of Pumped Hydroelectric Storage

5.2.2 Compressed Air Energy Storage

Like pumped hydroelectric storage, Compressed Air Energy Storage (CAES) requires specific geological features, such as salt caverns. Energy is stored as a pressure increase of gas within a sealed cave or feature and is usually then pre-heated by natural gas prior to expansion. Operation is typically similar to pumped hydroelectric, with off-peak compression of gas for use during peak periods; however, the slightly lower efficiency (~70%) of CAES requires a greater price differential. Furthermore, often caverns suitable for CAES are also ideal for natural gas storage for the gas network, limiting GB development opportunities.

Advantages	Disadvantages
High power ratings (100's MW) possible	Specific geological sites only
Moderately high storage capacity (100's MWh)	Sites compete with natural gas storage
Proven at large scale	Low energy density
Long cycle life	Poor round trip efficiency

Table 5.2: Advantages and Disadvantages of CAES

Two large scale CAES facilities have been developed, 100MW at McIntosh, U.S.A. and 290MW at Huntorf, Germany. These have been operating for two and three decades respectively, showing that CAES plants typically have longer lifetimes than battery technologies. This also shows that CAES is a relatively mature technology and is the only storage technology, other than pumped hydroelectric, to offer GW and GWh scale technology today.

5.2.3 Conventional Batteries

There are multiple traditional cell batteries, based on different chemistries, with varying strengths and weaknesses. Divya and Østergaard [116] have addressed the specific features of cell battery technologies and flow batteries (see section 5.2.4) for application in the power system and concluded that batteries such as Vanadium redox batteries are more likely to be used on a large scale than traditional lead acid batteries. Dufo-López, Bernal-Agustín and Domínguez-Navarro [117] have also looked at these technologies for application in conjunction with Spain's wind power and concluded that there would need to be a subsidy for batteries to become viable in that context, but that Sodium Sulphur batteries represent the best technology choice. With such differing views, this section outlines the different battery types.

5.2.3.1 Lead Acid

Lead acid is the oldest of the battery technologies for utility scale energy storage, having been around for over 140 years. Following the Californian renewable energy boom of the 1970s, there was much interest in Lead Acid batteries for system support. That interest re-emerged for renewable power smoothing in the late 1990's. However, the major advances in higher power and energy density batteries, due in part to the need for portable power in the communications industry, have led to Lead Acid batteries being technologically surpassed.

Advantages	Disadvantages
Mature technology	Limited depth of discharge
Lower capital cost than other batteries	Very limited cycle life
	Low specific energy
	Poor round trip efficiency
	High environmental cost
	Power and energy ratings inter-linked

Table 5.3: Advantages and Disadvantages of Lead Acid Batteries

5.2.3.2 Nickel Cadmium

Nickel Cadmium is the most common Nickel based battery chemistry, having been developed in the early 20th century. It was a common rechargeable battery type until being overtaken by Nickel Metal Hydride in the 1990's and then by Lithium based batteries. Cadmium is a toxic and heavy metal with a significant environmental impact. Recent changes to EU environmental legislation have outlawed the use of Nickel Cadmium batteries in all but a few specific applications. As such Nickel Cadmium batteries are unlikely to be deployed further in EU power systems.

Advantages	Disadvantages
Mature technology	High capital cost
High charge and discharge rates achievable	Limited cycle life
Low maintenance	Power and energy ratings inter-linked
	High environmental impact
	Poor round trip efficiency

Table 5.4: Advantages and Disadvantages of Nickel Cadmium Batteries

5.2.3.3 Sodium Sulphur

Sodium Sulphur batteries are one of the leading technologies seeing deployment in power systems today and have been pioneered since 1983 by Tokyo Electric Power Corporation and NGK in Japan. These batteries use a molten salt technology, whereby a high temperature (typically >300°C) is necessary for battery operation. This technology can achieve improved round trip efficiency compared to older battery technologies, however, the battery must be continually heated, leading to some self-discharge losses even when not in use. Additionally, the batteries typically have a long warm up time if they are to be activated from cold and there are health and safety concerns owing to battery temperature.

Sodium Sulphur batteries do offer high energy density and a very high short term overload capability. Advertised round trip efficiencies are typically approaching 90%, however,

Xcel Energy's Himelic and Novachek [118] have reported on the recent trial of a Sodium Sulphur battery in the U.S.A. and found round trip efficiency varied from 68 to 79%.

Advantages	Disadvantages
Very high energy density	Continuous heating required
High theoretical round trip efficiency	Limited cycle life
High short term overload capability	Power and energy ratings inter-linked
Rapidly approaching maturity in large scale	

Table 5.5: Advantages and Disadvantages of Sodium Sulphur Batteries

5.2.3.4 Sodium Metal Halide

Sodium metal halide batteries are an alternative form of molten salt battery, again requiring high temperatures for operation. The most common form is the Sodium Nickel Chloride battery (also known as the Zebra battery), owing to its operation at 245°C versus around 400°C for other variants. General Electric moved into the development of this type of battery following their acquisition of Beta. They have recently developed a facility with a target to supply up to 900MWh of these batteries per year meaning that this battery type is moving rapidly towards maturity for commercial applications. It is yet to be seen whether this technology will be deployed for power system applications as there is a significant market for telecommunications infrastructure.

Compared to Sodium Sulphur batteries, Sodium Metal Halide is safer under over-charge or over-discharge conditions but it does not achieve as high energy or power density.

Advantages	Disadvantages
High energy density	Continuous heating required
High theoretical round trip efficiency	Limited cycle life
Short term overload capability	Power and energy ratings inter-linked
Rapidly approaching maturity in large scale	

Table 5.6: Advantages and Disadvantages of Sodium Metal Halide Batteries

5.2.3.5 Lithium Ion

Small scale Lithium ion batteries have developed rapidly over the last two decades, due mainly to the rapidly expanding communications industry and the consequent need for portable power sources. Their high energy density makes them ideal for such applications. However, safety issues, particularly if the cells are over-charged, punctured or deeply discharged, and difficulty dealing with heating and life times when scaled up means that their use for large utility scale systems has developed more slowly. Nevertheless, 2011

saw the deployment of a Lithium Ion based battery storage facility by UK Power Networks at Hemsby, Norfolk, UK according to Lang *et al.* [119]

Advantages	Disadvantages
High energy density	Significant safety risks associated
Very high round trip efficiency	Expensive
Technology development driven by communications and potentially automotive industries	Difficult to scale
	Limited Lithium supplies
	Power and energy ratings inter-linked
Maturing – commercial trials started	

Table 5.7: Advantages and Disadvantages of Lithium Ion Batteries

5.2.3.6 Metal Air

Metal air batteries have long held the promise of extremely high energy density, making them ideal for mobile applications and were investigated by militaries in the 1960s. Typically air provides oxygen for the cathode reaction contributing to their high energy density when compared to cells that contain all electrolytes. IBM are developing a Metal Air battery but don't anticipate commercialisation until 2020.

Advantages	Disadvantages
Very high energy density	Very limited cycle life
Very high power density	Difficulty with electrical recharging
	Low round trip efficiency
	Immature technology

Table 5.8: Advantages and Disadvantages of Metal Air Batteries

5.2.4 Advanced Redox Flow Batteries

Ponce de León *et al.* [120] distinguish redox flow batteries from conventional cells by the nature of the energy stored. Conventional cell batteries store energy within the battery's electrode structure, whilst flow batteries store energy in the form of reduced and oxidised species which are then circulated through the reaction cell. Fuel cells are different again, storing energy in the reactants that are external to the cell. This section looks at the various different redox flow battery types considered by Ponce de León *et al.*

In general redox flow batteries have the following advantages and disadvantages compared to conventional batteries:

Advantages	Disadvantages
Independently variable power and energy ratings	Less mature technology
Longer cycle life	Lower energy density
High efficiency	
Capable of fast mechanical recharge	
Modularity	

Table 5.9: Advantages of Redox Flow Batteries compared to conventional batteries

5.2.4.1 Bromine Polysulphide

Bromine Polysulphide flow cells were the basis for the technology demonstrator by Regenesys at Little Barford in the UK and are based on the following redox couple.

Equation 5.1 $3 \cdot Br^- - 2 \cdot e^- \leftrightarrow Br_3^-$ where $E^{\ominus} = 1.09V$

Equation 5.2 $S_4^{2-} + 2 \cdot e^- \leftrightarrow 2 \cdot S_2^{2-}$ where $E^{\ominus} = -0.265V$

Unfortunately, as the demonstrator and subsequent review by the Department of Trade and Industry [DTI] [121] proved, it was very difficult to avoid membrane breakdown and cross-contamination of the active species. In this redox flow cell the electrical balance is achieved by transfer of Sodium ions across a selective membrane. The relatively similar size of the Sodium ions to the other electro-active species in this reaction cell mean that it is highly prone to cross-contamination. This cross-contamination in turn necessitates complete replacement of the chemicals and punctured membrane.

Advantages	Disadvantages
UK experience gained through Little Barford demonstrator	Risk of H_2S (gas) evolution
	Cross-contamination almost inevitable
Low cost chemicals	Sulphur deposition on electrodes
	Poor round trip energy efficiency

Table 5.10: Advantages and Disadvantages of the Bromine Polysulphide Redox Flow Battery

5.2.4.2 Zinc-Bromine

The Zinc Bromine flow cell is another flow cell system to have received widespread research and development interest. It relies on the following redox couple:

Equation 5.3 $3 \cdot Br^- - 2 \cdot e^- \leftrightarrow Br_3^-$ where $E^{\ominus} = 1.09V$

Equation 5.4 $Zn^{2+} + 2 \cdot e^- \leftrightarrow Zn$ where $E^{\ominus} = -0.76V$

The many advantages of this redox couple have been outweighed by practical experience with unbalanced rates of reaction leading to system polarisation and breakdown as well as

Zinc deposition on the electrodes during charging. These practical difficulties have left Zinc Bromine systems some way short of theoretical potential. Nevertheless, ZBB Energy Corporation has been developing these systems and is now marketing systems up to 125kW.

Advantages	Disadvantages
Good energy density	Low cycle life
Highly reversible	High self-discharge
Low cost reactants	High cost electrodes
Higher cell voltage	Poor energy efficiency

Table 5.11: Advantages and Disadvantages of the Zinc-Bromine Redox Flow Battery

5.2.4.3 All Vanadium

Concerns resulting from the difficulty of avoiding cross-contamination of electrolytes in other flow battery systems have led to a significant focus on the Vanadium Redox Flow Battery (VRFB). This type of flow battery uses the same chemicals, Vanadium dissolved in Sulphuric Acid, on both sides of the cell stack, and this means it is relatively robust against cross-contamination. Furthermore, the fast kinetics of the Vanadium reactions leads to higher efficiency than other flow cells. The redox reaction is based on the following couple:

Equation 5.5 $VO^{2+} + H_2O - e^- \leftrightarrow VO_2^+ + 2 \cdot H^+$ where $E^{\Theta} = 1.00V$

Equation 5.6 $V^{3+} + e^- \leftrightarrow V^{2+}$ where $E^{\Theta} = -0.26V$

Prudent Energy has been involved in the commercialisation and sale of VRFBs, deploying GE Energy's power conversion business' power converters, including projects in China and California.

Advantages	Disadvantages
Long cycle life	Low energy density
Membrane failures aren't catastrophic	Membrane costs currently high but falling fast
High efficiency	
Can be mildly over-charged	Energy capacity cost is linked to Vanadium cost
Fast response time	

Table 5.12: Advantages and Disadvantages of Vanadium Redox Flow Batteries

5.2.4.4 Others

In addition to the utility scale flow batteries mentioned, there are Zinc-Cerium and Iron-Chromium systems. Zinc-Cerium offers the promise of an environmentally benign system with higher voltage and current density than other flow cell systems. This system is being

developed by Plurion in Scotland and is at an early stage of development. Further Deeya Energy is developing energy dense Iron-Chromium flow cells but targeting them at smaller scale applications, such as telecommunications and defence, rather than utility power use.

5.2.5 Thermal Storage Systems

An alternative to storing potential energy or chemical energy is to store energy thermally either in a cryogenic store, or a hot thermal store. Many such systems are in use in order to displace Heating, Ventilation and Air Conditioning (HVAC) loads at times of peak demand, but these typically do not convert the stored heat energy back to electricity for use. Resistance heating or refrigeration are used to heat or cool the store and a heat engine can be used to recover the energy. The bulk storage medium can typically be a low cost material ensuring that the underlying cost of materials in a thermal energy store is low. Thermal storage systems normally have limited round trip energy efficiency although Isentropic [122] claim to have improved upon typical efficiency levels with a hot gravel storage system designed to achieve efficiencies in excess of pumped hydroelectric. However, self-discharge is typically higher than battery storage systems.

Advantages	Disadvantages
Long cycle life	Low round trip efficiency
Potentially low cost	Requires extreme temperature stores
Scalable	Relatively immature for power grid applications
Environmentally Inert	

Table 5.13: Advantages and Disadvantages of Thermal Storage Systems

5.2.6 Flywheels

Flywheels store energy as kinetic energy in a rotating mass. Composite materials permit high speeds allowing greater kinetic energy storage; however, overall energy capacities are limited. Flywheels are well suited to power applications where high specific power and peak output capacity are key parameters. High self-discharge means that flywheels are not suited to storing energy for long time periods.

Beacon Power's flywheels were amongst the first of the 'new' energy storage technologies to be deployed on the grid, with projects in New York and California in the USA according to Lazarewicz and Ryan [123]. The 20MW project in New York State is one of the biggest power quality applications of storage in the world. However, it is likely that flywheels will be limited in scope to the short time-scale frequency regulation market,

where in time they will be overtaken by other energy storage technologies that provide a wider range of services to the grid.

Advantages	Disadvantages
High specific power	Low specific energy
Economically mature	High self-discharge
High cycle life	Small unit capacities
High round trip efficiency	
Environmentally benign	
Fast response time	

Table 5.14: Advantages and Disadvantages of Flywheels

5.2.7 Supercapacitors

Supercapacitors store energy in the form of an electrostatic field. They offer very high specific power, but very low specific energy in comparison to other energy storage technologies. However, they have been proposed by Muyeen *et al*. [124] to smooth power fluctuations from wind power due to their high speed of response and low standby losses. For very short term power smoothing, the high specific power allows a compact and cheap system, whilst the low specific energy is not a constraining factor. For longer term storage Supercapacitors are not an option, due to their low energy density and high self-discharge.

Advantages	Disadvantages
Very high specific power	Very low specific energy
Very high cycle life	Moderate self-discharge
Excellent round trip efficiency	Power and energy ratings inter-linked
Fast response time	Wide operational voltage range

Table 5.15: Advantages and Disadvantages of Supercapacitors

5.2.8 Superconducting Magnetic Energy Storage

Superconducting Magnetic Energy Storage (SMES) stores energy in a magnetic field created by high circulating currents in infinitely low impedance high temperature superconducting materials. The lack of moving or chemical components promises very long cycle lives. However, cryogenic cooling of the superconducting components ensures that these devices have a significant ancillary load causing low round trip efficiency. The high cost of superconducting wire and associated ancillaries ensures that the energy capacities of these systems are typically low.

Advantages	Disadvantages
Very high specific power	Very low specific energy
Very high cycle life	Moderate self-discharge
Excellent round trip efficiency	
Fast response time	

Table 5.16: Advantages and Disadvantages of SMES

5.2.9 Hydrogen

A study of energy storage would be incomplete without reference to the alternative viewpoint of using hydrogen as the energy vector in place of electricity. Hydrogen's energy density, along with the gradual advance of fuel cells, is particularly attractive for vehicular applications due to the high specific energy capacity. The challenge in these applications is ensuring the successful and safe storage of hydrogen at high pressures.

A key challenge facing hydrogen for power system applications is that when electrolyser fuel cell efficiencies are taken into account, the round trip efficiency of a hydrogen based system is currently too low (<50%). Such a low round trip efficiency means that it cannot be economically viable in all but a few niche applications. Furthermore, currently the bulk of Hydrogen is created by steam reforming Methane, with associated CO_2 emissions.

Advantages	Disadvantages
High specific energy	Very low round trip efficiency
Potentially environmentally benign	Requires high pressure storage
	High capital cost
	Hydrogen currently derived from fossil sources

Table 5.17: Advantages and Disadvantages of Hydrogen

5.3 Energy Storage Economics

The success or failure of different energy storage options will ultimately come down to their commercialisation and economics. This section relies on the data available in appendix 9.2 in order to compare the different economic strengths and weaknesses of the different energy storage options.

5.3.1 Power Costs

Figure 5.1 shows the comparative cost of installed power capacity. As expected, high power density technologies such as flywheels, SMES and supercapacitors can be seen to have favourable costs per installed kW. These technologies are well suited to applications

where a short duration pulse of energy is required, but owing to high self-discharge and very low energy density are not applicable to longer timescale applications. It is notable that the high power density storage technologies can offer a lower cost of installed capacity than the mature energy storage technologies of CAES and pumped hydroelectric.

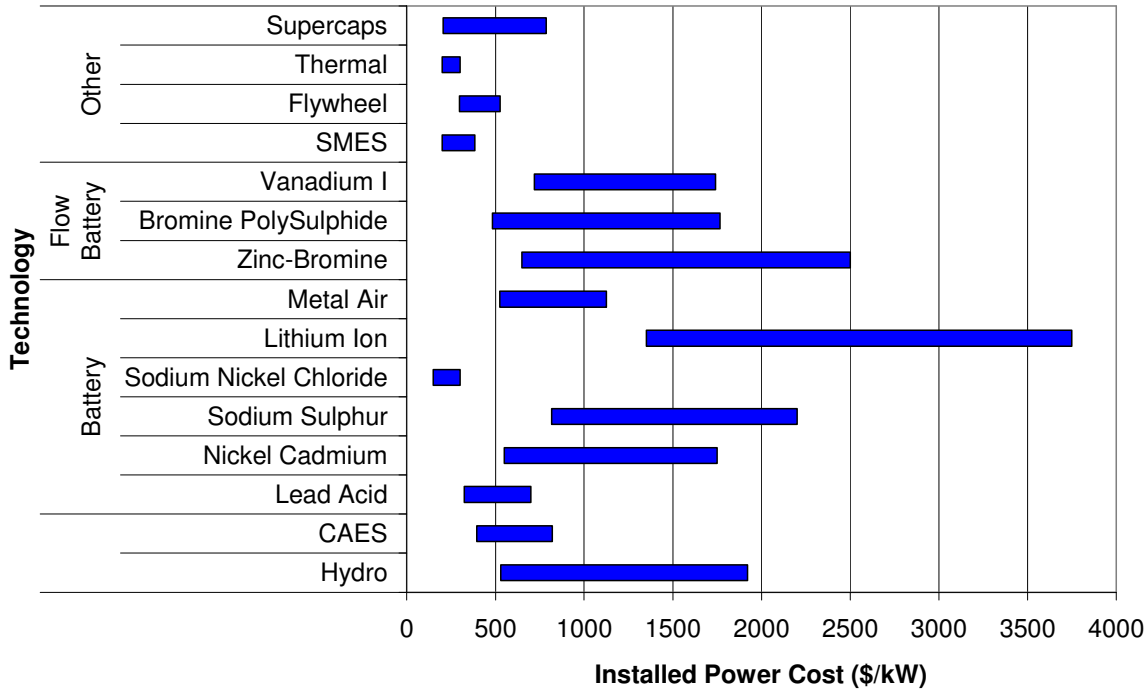

Figure 5.1: Indicative Range of Power Capacity Costs for Energy Storage Technologies

Amongst the technologies that have moderate or high energy density, the Sodium Nickel Chloride battery is shown to have a favourable power cost of the commercialised technologies. Thermal energy storage can also be seen to hold the potential of low cost power capacity, however the principle developers of these systems (e.g. Highview Power, Isentropic Ltd.) appear to be at an earlier stage of development than the other technologies considered here.

5.3.2 Energy Costs

Figure 5.2 compares the cost of the different energy storage technologies for increased energy storage capacity. This highlights one of the shortcomings of the three power dense technologies (SMES, flywheels, supercapacitors) in that they have the highest installed energy costs of all the technologies considered. Furthermore, their low energy density would lead to unfeasibly large systems for long duration energy storage applications.

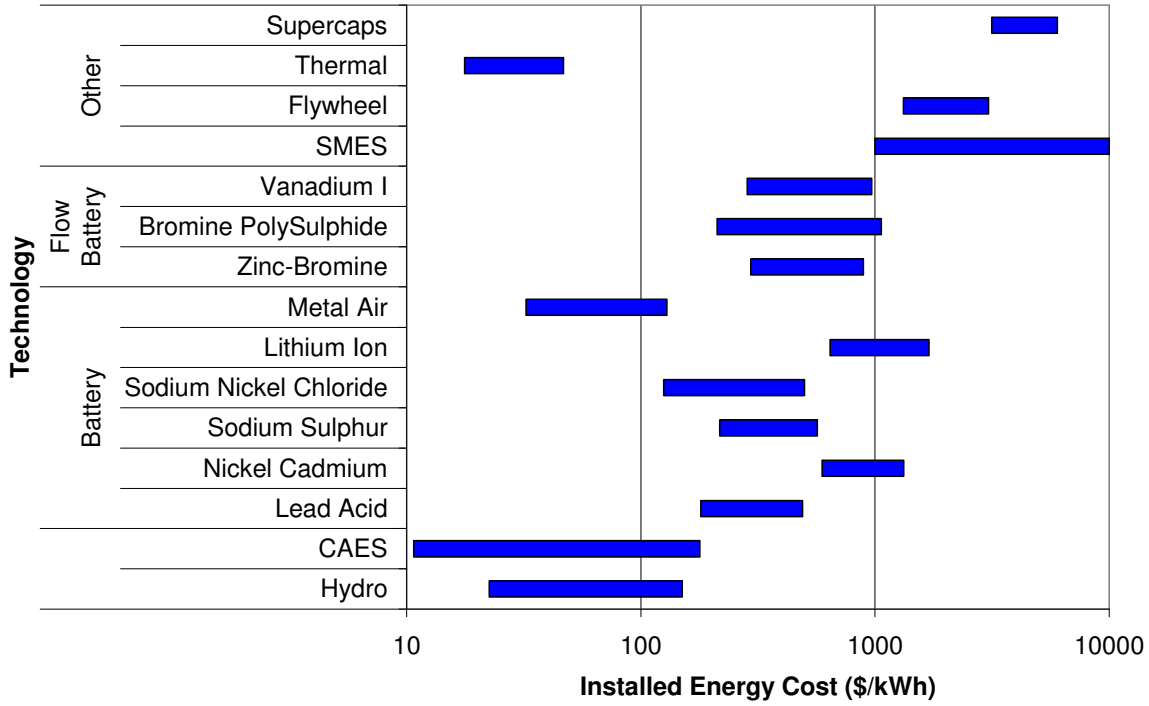

Figure 5.2: Installed Energy Capacity Costs

Once again thermal energy storage can be seen to hold promise, with a relatively low cost of installed energy capacity that is anticipated to be competitive with CAES and Hydroelectric systems. Metal air batteries, which are similarly experimental, can be seen to offer a low cost of energy capacity but are hindered by their very short cycle life capacities.

CAES and pumped hydroelectric systems can be seen to typically have installed energy costs that are lower than the various commercialised battery technologies. Depending on site geology, the installed energy costs of CAES and pumped hydroelectric can be significantly lower than all but the projected cost of thermal energy storage.

5.3.3 Economic Comparison

The capital cost of an energy storage system is defined by its installed cost of power capacity and installed cost of energy capacity. The capital cost of a system does not, however, define the economic merit or otherwise of a system. Different technologies have significantly different lifetimes and efficiencies, which directly affect the revenue they can expect to earn and recover the capital costs from. Figure 5.3 shows a comparison of the different technologies' round trip efficiencies and shows that cycle life expectations vary from just a couple of hundred cycles (Metal air batteries) to around 100,000 or more (SMES, supercapacitors, flywheels).

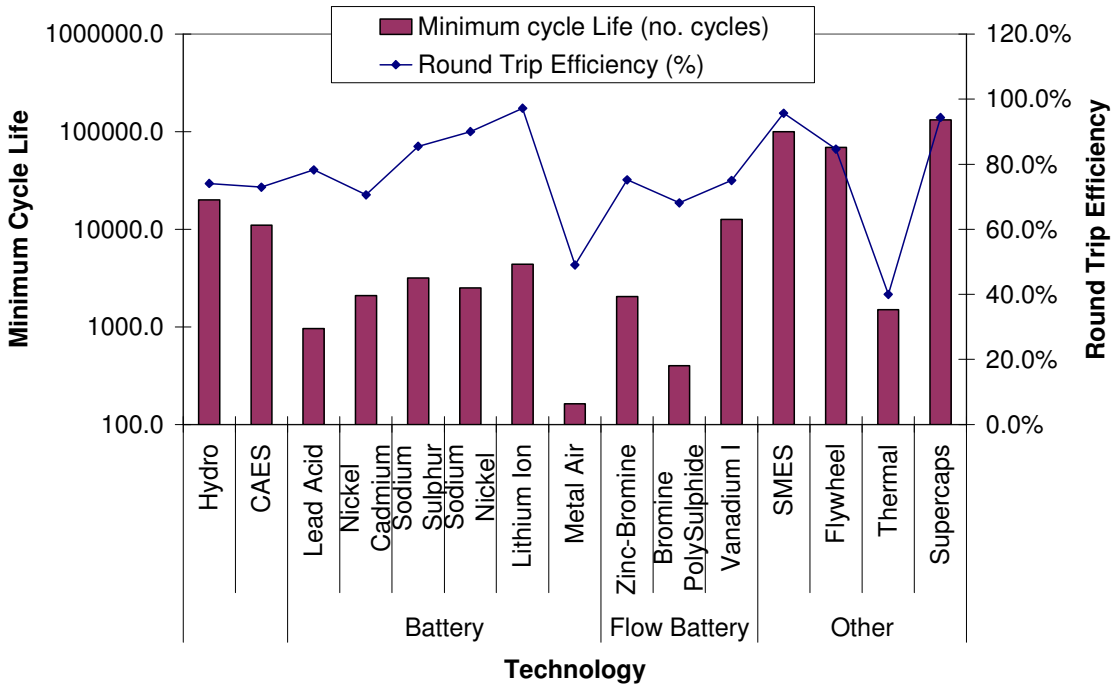

Figure 5.3: Energy Storage Technologies' Cycle Life and Efficiency

In order to reasonably compare the different technologies it is possible to consider the capital cost spread over the cycle life of the system. This provides a comparable metric to the cost of generation from an alternative source and is a method used by the Electricity Storage Association (ESA).

Equation 5.7 $$\Pi_{effective} = \frac{\Pi_{kWh\_installed}}{n_{cycles} \cdot \eta_{round\_trip}}$$ where $\Pi_{kWh\_installed}$ is the capital cost of installed energy capacity (£/kWh), $\Pi_{effective}$ is the effective generation cost (£/kWh), η_{round_trip} is the efficiency and n_{cycles} is the storage technology's cycle life.

This effective generation cost from an energy store can be compared to the typical costs of generating from conventional power plants. Parsons Brinckerhoff [125] in 2006 produced a report "Powering the Nation" detailing the typical range of power generation costs in the UK, Parsons Brinckerhoff [126] then provided an update to that report in 2010 to bring the costs into line with recent experience. A comparison of the different effective generation costs from energy storage technologies is shown in Figure 5.4. The estimated costs from conventional generation are shown in Figure 5.5. It should be noted that the effective generation cost is a simple calculation and does not discount the value of future revenue, whilst the "Powering the Nation" reports considered a 10% discount rate. The high capital cost of storage systems, combined with their reliance on future revenue, would undoubtedly have less favourable costs on a discounted basis. However, without knowing the application of the energy store, its lifetime can not be assessed, therefore an

appropriate discounting strategy can not be defined. Nevertheless, it can be seen, that when the effective generation cost is considered, some energy storage solutions can be seen to potentially offer competitive costs. Furthermore, in chapter 7 a full economic analysis of the VRFB battery in a specific application with a wind farm is considered. This does apply a discounting strategy and therefore extends the analysis conducted based on reasonable lifetime assumptions.

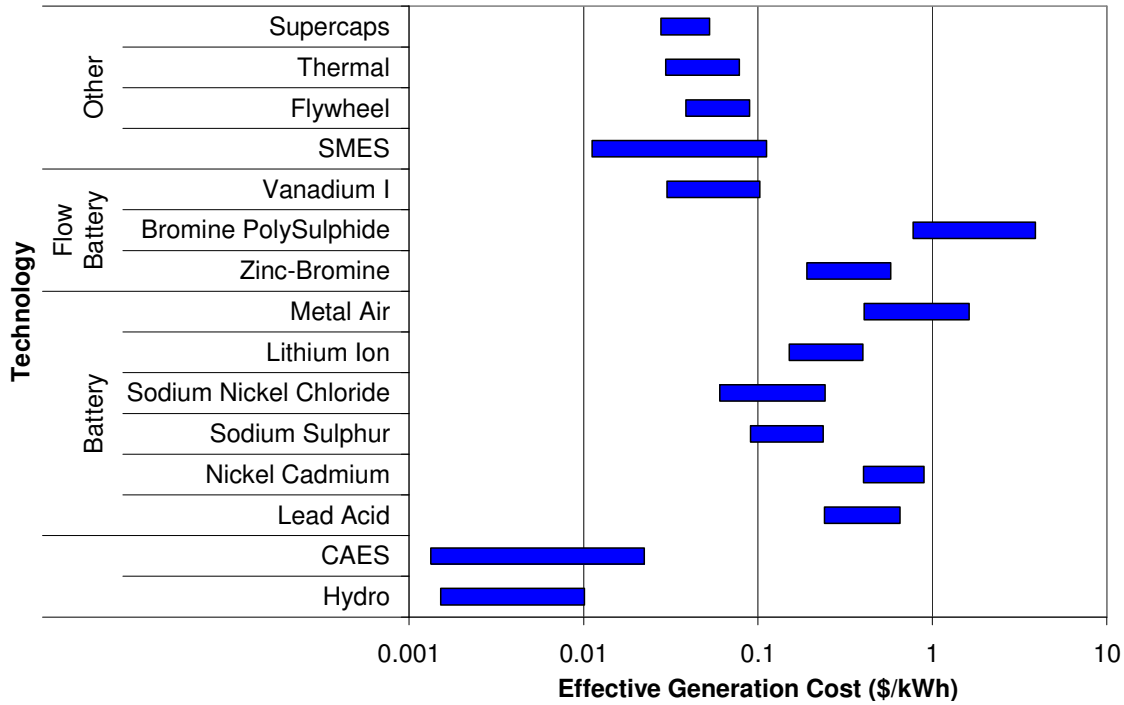

Figure 5.4: Effective Generation Cost of Storage

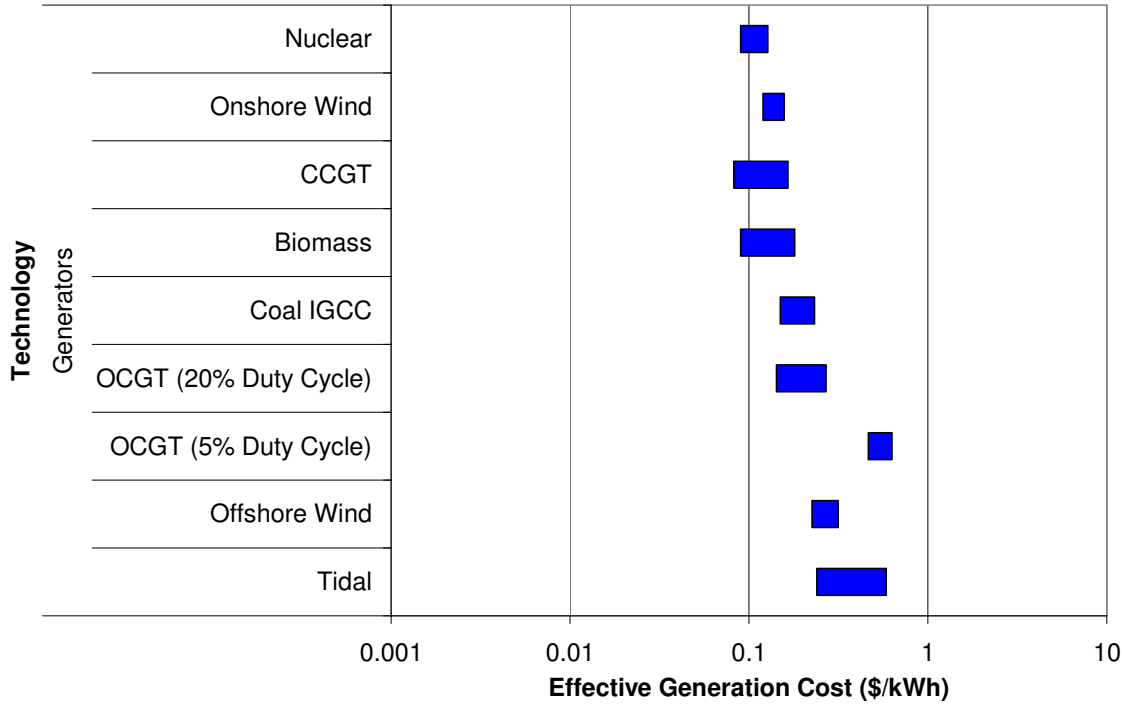

Figure 5.5: Generation Costs from Parsons Brinckerhoff [125], [126]

Amongst the different energy storage technologies, CAES and pumped hydroelectric still stand out as the best options economically. However, their requirement for specific geological sites limits their further development. The power dense technologies (SMES, flywheels, supercapacitors) are competitive for power applications but would be unfeasibly large for high energy capacity projects. This leaves the VRFB competing with thermal energy storage for widespread adoption. The VRFB holds a commercialisation advantage with a number of systems already in deployment, particularly in Japan. Amongst the conventional battery technologies, the two high temperature technologies (Sodium Nickel Chloride and Sodium Sulphur) lead the way. However, their effective generation cost is increased by their currently limited lifetimes. Overall it is worth tracking the developments in thermal energy storage systems as large scale prototypes are developed and following high temperature batteries' life time developments. Nevertheless the Vanadium Redox Flow Battery will be considered further and in particular for application in conjunction with wind power in section 5.4.

5.4 Vanadium Redox Flow Battery Development

5.4.1 Historic Development

The invention of the Vanadium Redox Flow Battery (VRFB) is attributed to the work of Skyllas-Kazakos *et al.* [127] at the University of New South Wales, Australia. Kear, Shah and Walsh [128] have recorded the development of the VRFB in detail since then, showing that whilst the technology originated in Australia, developments since have focussed on Japan. Sumitomo Electric Industries hold the license for Japan and have developed at least 16 installations of up to 4MW, 6MWh capacity. Japan's battery facilities have benefitted from access to the national feed-in-tariff for renewable energy generation.

Kear, Shah and Walsh also show that recently research interest has increased in China following Prudent Energy's purchase of VRB Power Systems in 2009. China itself has burgeoning wind and solar sectors which Prudent will undoubtedly try to complement. Furthermore, Chinese transmission grids are operating at greater than 95% capacity in many urban areas.

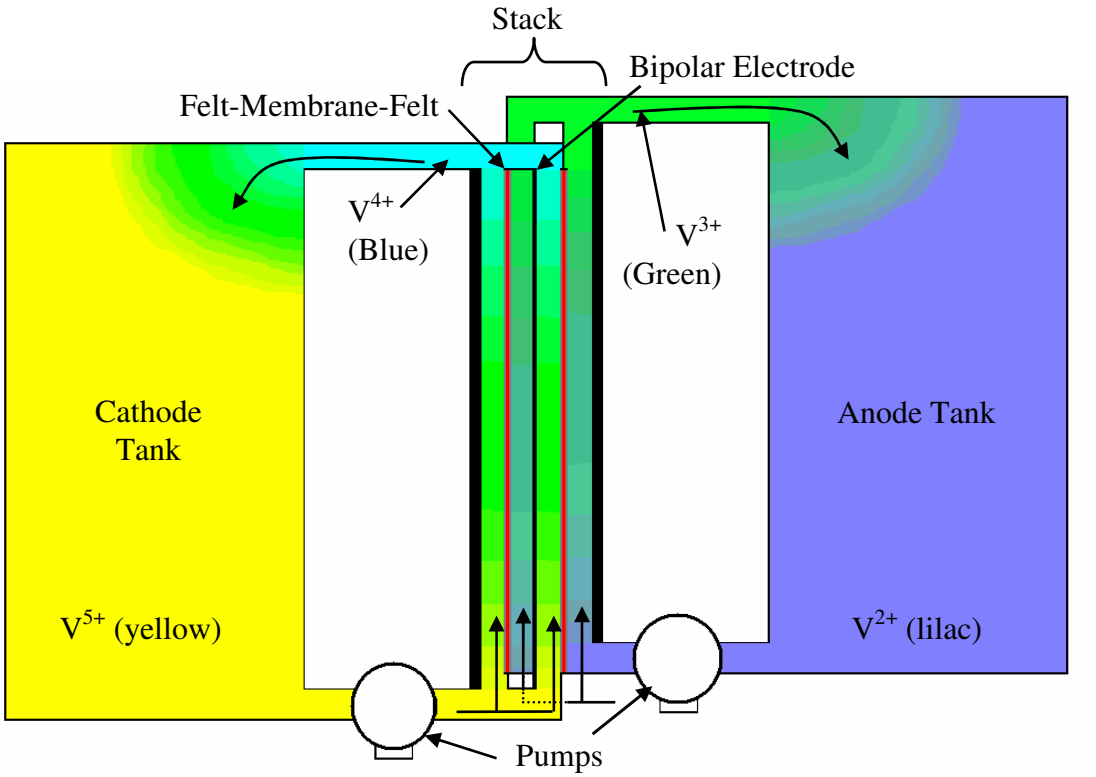

Figure 5.6: The VRFB System

Beyond transmission level applications, Cellstrom GmbH (Austria) markets a smaller scale VRFB for Uninterruptible Power Supply (UPS) applications. In the UK, Renewable Energy Dynamics Technology Ltd. (REDT) is marketing VRFB systems in the range 30kW to 150kW.

A typical VRFB consists of two tanks, the cathode tank where V^{4+} and V^{5+} ions are stored in a solution of mild Sulphuric acid, and the anode tank where V^{2+} and V^{3+} are stored, again in Sulphuric acid solution. When the system is primed for operation, these solutions are pumped continuously through the stack. If the system is to be shutdown for a significant period of time, the stack is prepared and the pumps switched off. The two solutions are separated in the stack by semi-permeable membranes. These membranes are permeable to hydrogen ions but not the other soluble ions. The flow of current is controlled by the DC voltage applied across the stack. Application of a voltage below the equilibrium voltage will discharge the VRFB, whilst higher voltages charge it. The basic chemistry will be explored in more detail in chapter 6. Figure 5.6 provides an overview of the VRFB system and highlights that the four different Vanadium ion solutions have different colours. Here the picture illustrates a fully charged system just beginning to discharge.

Typical VRFB performance characteristics are given in Table 5.18, based on appendix 9.2.9. Key to the VRFB's economic merit is its capability for a high cycle life, which is a critical precursor to application in frequency response services.

Characteristic	Low range	High range
Energy Density (kWh/kg)	0.02	0.04
Cycle Life (No. of full cycles)	>12,000	
Age (years)	10	20*
Round Trip Efficiency (%)	70	85
Power Cost ($/kW)	600	2500
Energy Cost ($/kWh)	200	400

Table 5.18: VRFB Performance Metrics (* with membrane replacement at 10 years)

5.4.2 Present Application

Prior to the financial crisis, Tapbury Management Ltd. *et al.* [129] were planning a large scale VRFB deployment on the Sorne Hill wind farm in Ireland. The purchase of VRB Power Systems by Prudent Energy in 2009 appears to have ended this interest; however, it shows an underlying interest in storage technologies. Furthermore, Ireland's grid with low interconnection capacity and increasingly high wind power penetration is perhaps a microcosm of where the mainland GB grid is heading.

Elsewhere, Prudent Energy and GE Energy Power Conversion recently deployed a 500kW, 2MWh battery in China according to Gray and Sharman[130].They also have a large scale industrial project in California, showing the rising international interest in flow batteries and energy storage in general. The challenge is to advance the technology to megawatt scale deployments.

5.4.3 Future Advances

One of the limiting factors of the VRFB today is that it has relatively low energy density. This means that tanks must be large and that pumps have to run at higher speed to ensure that the electrolyte circulation is sufficient to support high powers. This higher pump speed in turn leads on to higher ancillary loads and lower round trip efficiency. In recent years the VRFB's originators, Skyllas-Kazacos *et al.* [131], have turned their attention to solving these twin problems. They propose using Vanadium Bromide in both half cells, which has the potential to almost double the energy density, opening up mobile applications.

Alongside development of alternative chemistry, Skyllas Kazakos *et al.* have also been investigating the performance of the original VRFB with lower cost membrane material.

The round trip efficiency of 80% reported suggests that this research is proving effective. Both research streams suggest the continued development of the VRFB towards widespread commercial application.

5.5 Summary

The Vanadium Redox Flow Battery has been shown to be well suited to meeting the requirements of smoothing wind output, time shifting energy and providing fast frequency response services.

Chapter 4 showed the technical control methods that allow wind farms to contribute to frequency control of the National Grid. However, despite the technical capabilities in this area, the economic case is unfavourable. Section 2.7 showed that this could present an opportunity for energy storage. The expected increase in required GB frequency response holdings combined with the loss of responsive plant is anticipated to lead to a significant shortfall which could be filled with energy storage. Furthermore, this section shows that there are a number of storage companies looking at the opportunities that frequency response markets will provide globally. Nevertheless, realistic commercial application of energy storage is likely to depend on aggregation of benefits and this section suggests the combined aggregation with providing energy time shift to peak demand periods.

Section 5.2 then critically analyses the different energy storage technologies available, leading on to an economic comparison in section 5.3. This shows that high power density energy storage technologies (SMES, flywheels, supercapacitors) offer a competitive solution in low energy applications, but that in higher energy capacity applications the optimal solutions are the Vanadium Redox Flow Battery and thermal energy storage systems.

Section 5.4 shows that the VRFB has been widely applied today, but also that there is significant research that may lead to improvements in its commercial viability in future. As such it is worthy of detailed consideration.

6 Modelling of Vanadium Redox Flow Batteries

6.1 Introduction

Chapters 3 and 4 of this thesis developed models and control strategies that enhanced full converter wind turbines' capability to meet the requirements of Grid Codes. This work included control methods allowing a wind turbine to provide frequency response reserves and power regulation up and down in response to system frequency changes. However, they also illustrated that the margin for low frequency response, from intermittent wind resources, is critically dependent on the prevailing wind conditions. Furthermore, whilst improved control methods to allow synthetic inertial response were presented, there remain concerns over the capacity of wind turbines to recover following a period of temporary over-production.

The limitation on the capability of wind power to secure the frequency stability of the GB transmission system potentially presents an opportunity for energy storage. Chapter 5 therefore explored the different energy storage technologies available and their applicability to providing frequency response services and operating with wind power. It highlighted the potential of the Vanadium Redox Flow Battery (VRFB) to operate across different time-scales and compliment wind power and the power system, whilst being a commercially favourable option. Chapter 6 therefore focuses on the VRFB and its integration into the power system.

First, a model of the VRFB, appropriate for power system representation, is developed in section 6.2. A model of the power electronics representing the interface between the VRFB and the grid is then developed in section 6.3. The representation of the VRFB is shown to be valid by comparison with published data in section 6.4, whilst simulations are used to demonstrate the effectiveness of the VRFB controller in section 6.6. Overall, the chapter presents a novel simplified model of a flow battery for use in power system applications. Incremental changes to the power converter grid fault control schemes are then developed based in part on knowledge from the grid integration of wind turbines, but novel in application with energy storage. Finally, the controller, developed for management of the VRFB state of charge and frequency reserves, shows how energy storages' many potential applications can be managed in a single controller.

6.2 VRFB Electrochemical Model

VRFB energy storage would be integrated with the grid through a power electronic interface as illustrated in Figure 6.1. Therefore to a first approximation, from a power system perspective, the energy store can be considered to be an ideal current source behind an inverter. However, this would neglect the VRFB's round trip efficiency, state of charge or finite energy storage and power capacities, which are critical to the economic provision of frequency response reserves. In order to accurately assess the VRFB's capability for operation with a wind farm it is necessary to develop a model of the VRFB which simply represents these features for power system application. Section 6.2.1 investigates the typical level of detail in a full representation of a VRFB before section 6.2.3 extends the existing literature on simplified models in order to meet the minimal requirements for the power system model.

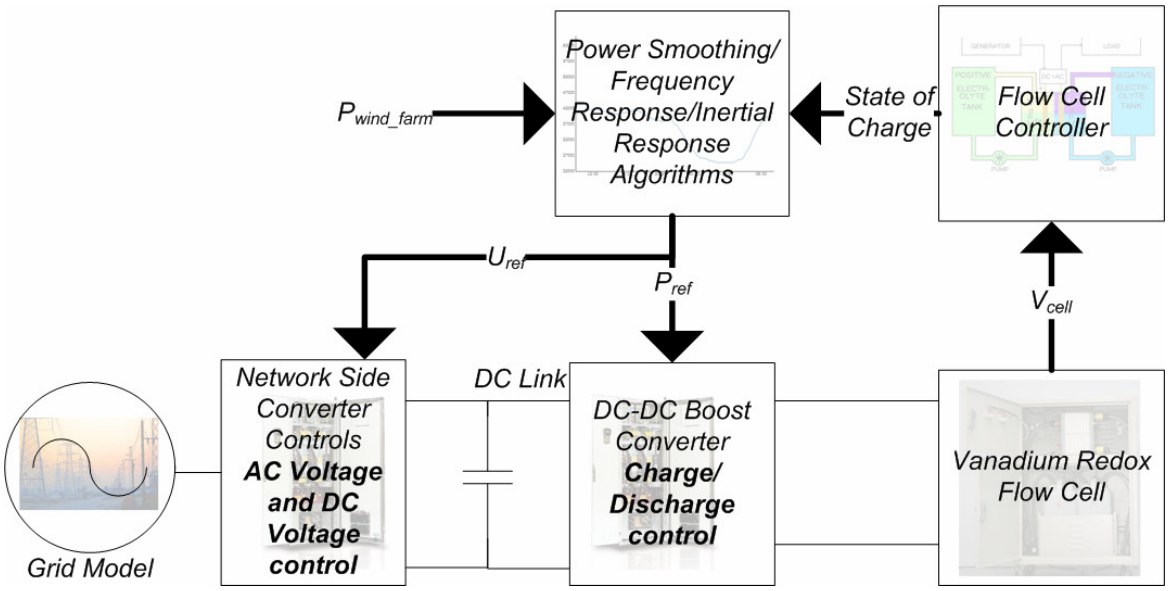

Figure 6.1: Summary of VRFB Integration

6.2.1 Fully Detailed

The University of Southampton has long been at the forefront of the UK's interest in flow batteries and in conjunction with Brunel University were involved in the Regensys project discussed in section 5.2.4. Shah, Watt-Smith and Walsh [132] from this group have presented the first significant work on modelling the fundamental behaviour of a VRFB. Their work aimed to provide a model that assisted commercialisation of flow batteries by minimising the required laboratory tests associated with long term effects such as membrane fouling and electrolyte stability.

In order to investigate these effects, their model relies on fundamental chemical behaviour and equations and was validated against a small scale VRFB. However, it relies on a

complex representation of the transport and circulation of the charge carriers, focussing on the relationship between the coupling of fluid dynamics and electrochemical phenomena. As such, this approach to modelling of the VRFB is unnecessarily complex for a power system representation. However, Shah, Watt-Smith and Walsh's work does demonstrate that the chemistry defining a VRFB's electrical behaviour is ultimately governed just by the two reaction equations:

Equation 5.5 $VO^{2+} + H_2O - e^- \leftrightarrow VO_2^+ + 2 \cdot H^+$ where Eo = 1.00V

Equation 5.6 $V^{3+} + e^- \leftrightarrow V^{2+}$ where Eo = -0.26V

This work has been replicated by You, Zhang and Chen [133] and described as a simple model, however, it leads to a model that is applicable to a single cell, with voltage of approximately 1V and negligible energy storage capacity. For power system application, typically at least fifty cells are stacked in series in order to give a reasonable output power level with a higher voltage whilst the current is kept lower. Consequently, this model is inappropriate for a power system model, but does demonstrate that a simple approach just representing the electrical output, but based on the underlying chemical equations, but assuming ideal fluid dynamics, ought to be possible.

6.2.2 Fully Simplified

When considering an energy store, modelled to the simplest possible degree, it may be considered to be a high value capacitance connected to the grid through a power electronic converter. The capacitor may have maximum and minimum permissible voltage levels which set the maximum and minimum state of charge. Any energy stored or discharged from the capacitor then causes a change in voltage owing to the underlying Equation 6.1.

Equation 6.1 $E = \frac{1}{2} \cdot C \cdot V^2$

Such an approach is useful where the technology of the energy storage medium is irrelevant to the simulations being conducted. However, it is at best limited to a static representation of a system's round trip efficiency and therefore is not appropriate for applications where the energy losses are of interest. As the VRFB efficiency is considerably lower than unity and is also dependent on the power output, a more detailed model for representing the VRFB is beneficial.

6.2.3 Power System

Blanc [134] has studied the modelling of VRFBs extensively and in his thesis builds up the complex chemical theory in chapter 2 before developing a simplified model in chapter

3. His model depends only on the physical parameters of the system and outputs the voltage across the VRFB; it depends on the following parameters:

- The initial electrolyte and acid concentrations.
- The tank volumes.
- Electrolyte flow rate.
- Ambient temperature.
- The number of series cells.
- The system current.

This makes it more relevant to power system application, particularly if the flow rate and temperature are constant. Figure 6.2 shows the outline of the structure of Blanc's model.

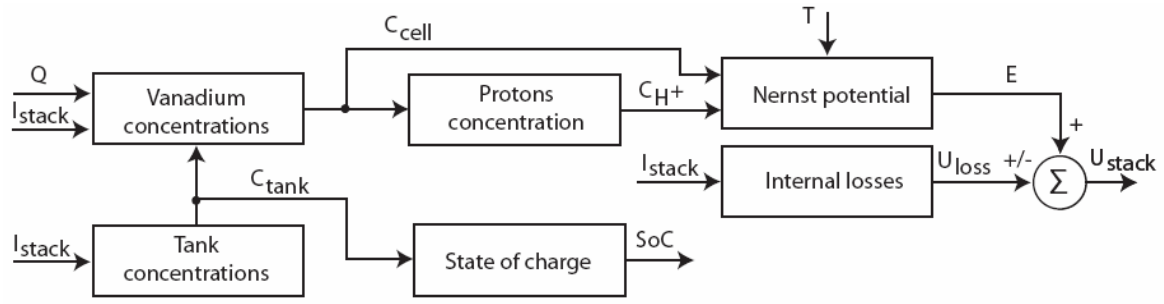

Q	- Electrolyte flow rate (l/s)	C_{cell}	- Electrolyte cell concentration (mol/l)
I_{stack}	- Cell current (A)	SoC	- State of charge
C_{tank}	- Electrolyte tank concentration (mol/l)	C_{H+}	- Hydrogen ion concentration (mol/l)
T	- Ambient temperature (K)	U_{loss}	- Internal voltage loss (V)
U_{stack}	- Output voltage (V)	E	- Open circuit potential (V)

Figure 6.2: Mathematical Model of VRFB from Blanc [134]

This model structure can be readily understood in conjunction with the physical system shown in Figure 5.6.

- First, the "Tank concentrations" of the Vanadium ions can be derived directly from the current and initial ion concentrations. This is done according to the general formula in Equation 6.2, where the concentration of V^{2+} and V^{5+} rise with positive current (charging) whilst the concentration of V^{3+} and V^{4+} fall and *vice versa* for negative current (discharging).

  Equation 6.2 $$\left[V^{x+}\right]_{tc} = \left[V^{x+}\right]_{init} \pm \frac{1}{F} \cdot \int I_{stack} \cdot dt$$

  This equation uses the current integral to calculate the change in charge based on the law Q = It. $[V^{x+}]$ represents the concentration of the $x+$ Vanadium ions, $[]_{tc}$ represents the instantaneous tank concentrations and $[]_{init}$ initial values; F is the

Faraday number, which is in C/mol and converts the change in individual charge numbers (Q) to a change in molar concentration; finally, I_{stack} is the VRFB current.

- The tanks contain the vast majority of the entire electrolyte in the system for a large VRFB; hence, measurement of the concentration of the Vanadium ions in the tanks allows a reasonably accurate measurement of the system's state of charge. In practice this information can be inferred from the voltage of an open-circuit test cell connected across the tanks, however this measurement can directly use calculated concentrations in the power system model. Hence, the "State of charge" (SoC) block calculates the charge level according to Equation 6.3 and as the membrane is assumed ideal, both half cell SoC's should balance.

Equation 6.3 $$SoC = \frac{[V^{2+}]}{[V^{2+}]+[V^{3+}]} = \frac{[V^{5+}]}{[V^{4+}]+[V^{5+}]}$$

- The actual "Vanadium concentrations" in the stack will differ from the tank concentrations, as beyond the physical input point of the pumped electrolytes to the stack, the reaction will be proceeding and ion concentrations changing. To a first approximation the stack (or reaction) concentrations can be modelled as the mean of the input (≡ Tank) and output concentrations. The change in Vanadium concentration through the stack is itself a function of the fluid flow rate and the VRFB current according to Equation 6.4.

Equation 6.4 $\Delta[V^{x+}] = \frac{N_{cell} \cdot I_{stack}}{F \cdot Q}$ where N_{cell} is the number of series cells and Q is the fluid flow rate in mol/s.

Hence, the stack concentration can be represented as:

Equation 6.5 $$[V^{x+}]_s = \frac{1}{2} \cdot \left(2 \cdot [V^{x+}]_c \pm \frac{N_{cell} \cdot I_{stack}}{F \cdot Q} \right)$$ where $[]_s$ is the average stack concentration.

- Equation 5.5 shows that as the VRFB is charged, H^+ ions are liberated, pushing up the "Protons concentration" and hence acidity of the electrolyte. This in turn influences the equilibrium voltage of the cells. However, this equation shows that the acid concentration climbs linearly with the increase in $[V^{5+}]$, meaning that the acid concentration can be readily calculated from its initial condition and the concentration change in $[V^{5+}]$.

- The "Nernst potential" calculates the electrode potential of the reaction under equilibrium conditions according to the effective stack concentrations of the

participating ions and the standard potential. This potential is multiplied up by the number of cells in series according to Equation 6.6.

Equation 6.6 $$E = N_{cells} \cdot \left(E^{std} + \frac{R \cdot T}{F} \cdot \ln\left(\frac{\left[V^{5+}\right] \cdot \left[H^{+}\right]}{\left[V^{4+}\right]} \cdot \frac{\left[V^{2+}\right]}{\left[V^{3+}\right]} \right) \right)$$

E^{std} is the standard potential produced by this reaction under equilibrium conditions. R is the gas constant (8.31J/K.mol) and T the ambient temperature, which is here assumed to be constant at 293K owing to the likelihood that large installations would be temperature controlled.

- The reaction in a VRFB will be driven away from equilibrium by the stack voltage; this is dealt with in Blanc by the "Internal losses" block. This block modifies the equilibrium electrode potential according to the various internal resistances (membrane, electrodes and bulk fluid) and the activation over-potentials associated with the energy of activation of the reaction and the circulation of ions. Rather than mathematically calculating these losses, here these losses have been modelled in the resistance and diode elements of the physical model as shown in Figure 6.3, these values have then been tuned to match the output voltage profile and round trip efficiency characteristics.

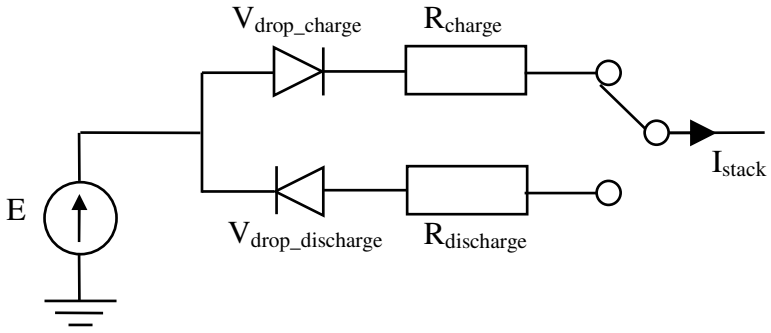

Figure 6.3: VRFB Physical Model

This electrochemical model represents the combined output of the VRFB, which itself consists of a number of series cells. This feeds into a DC-DC boost power electronic converter for connection to the DC link of an inverter and through to the grid.

6.3 Electrical System Model

Equation 5.5 and Equation 5.6 show that under standard conditions, the potential across a VRFB is only around 1.3V. Figure 5.6 also showed that bipolar electrodes may be used in the cell stack, effectively allowing multiple cells to operate in series. This series operation permits the VRFB's voltage to reach around 200V today with a target to double this,

leading to lower currents for power applications. Nevertheless, this voltage is DC, not AC, and too low for optimal grid integration.

Arulampalam *et al.* [135] have proposed the integration of a battery energy store onto the DC rail of a STATCOM for power quality improvement on a wind farm. According to Smith, Hayward and Lewis [136] some wind farms require STATCOMs in order to meet the reactive power requirements at the grid connection point, this option therefore provides an optimised solution for the integration of energy storage with wind power. However, as Arulampalam *et al.* were focussed on the stability improvement of the wind farm, they did not consider the voltage requirements for connecting the battery onto the DC rail or else may have considered higher voltage battery technologies.

6.3.1 Step-up Converter

Figure 6.1 shows that the VRFB is connected through a DC-DC converter, which raises the DC voltage level, before supplying the DC link of an inverter. Use of this DC-DC converter allows connection to the grid with the same power converter topology as is used for a wind turbine. This in turn permits minimal modification in order for the VRFB's power converter to be compliant with the rigours of Grid Codes.

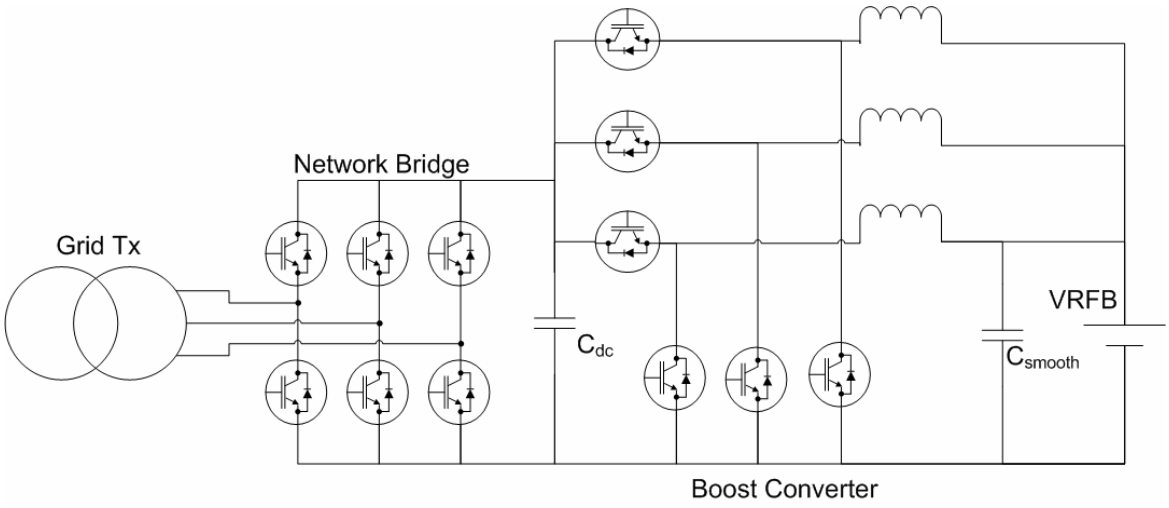

Figure 6.4: VRFB Power Converter Interface

Figure 6.4 shows the configuration of the network side inverter and the boost converter. It illustrates that the standard two-level converter used for wind power applications can have the 'machine bridge' reconfigured such that the three IGBT phases act in parallel through independent smoothing reactors to supply the controlled voltage across the VRFB. This parallel operation of the IGBT phases allows the high current, low voltage operation of the VRFB to be met as it turns the circuit from a three phase rectifier into a single phase boost converter with current capacity three times that of a single IGBT. Note, however, a smoothing capacitor is required across the VRFB to ensure the controlled voltage quality.

There are, however, limitations of this circuit including the high device count, owing to the paralleled operation of IGBTs within the boost converter. This is currently necessary, owing to the low operating voltage (~200 to 400V) of the largest VRFB systems, as the IGBTs are limited by current capacity. Additionally, the three parallel IGBTs have to be matched by three parallel smoothing inductors, leading to a hardware system that uses standard components but is not topologically optimal. The typical AC side voltage is ~400V, necessitating a step up transformer for connection to the grid.

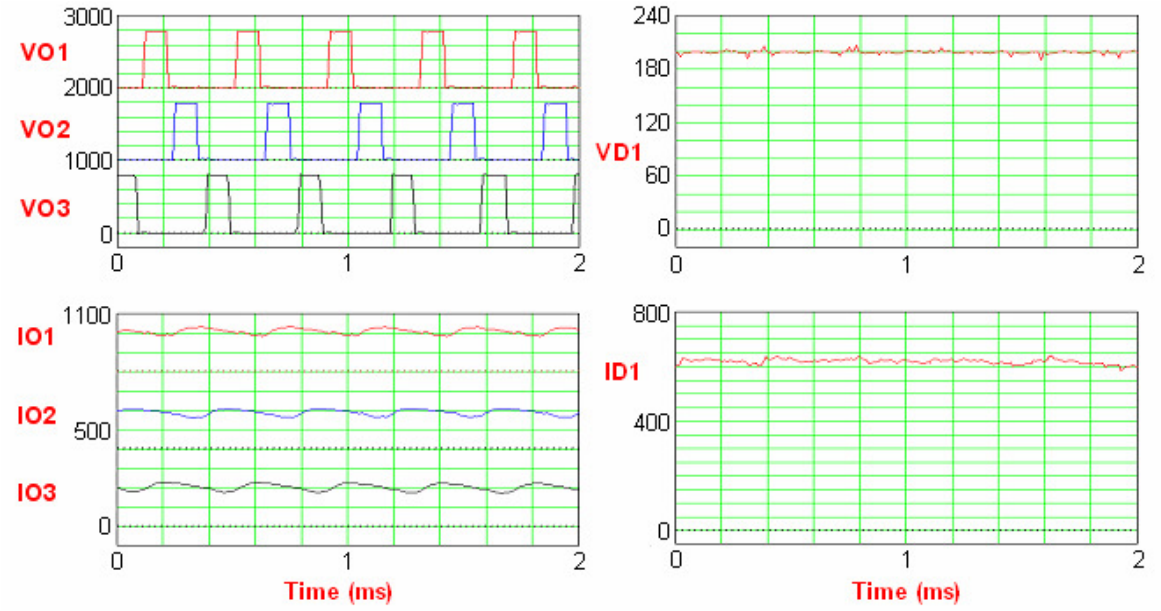

Figure 6.5: VRFB Boost Converter Performance from Gray and Sharman [130]

Figure 6.5 shows the output voltage and current from a VRFB and is taken from Gray and Sharman's [130] presentation on a Prudent Energy and GE Energy development in China. This shows that the ripple in the output voltage is minimal and is at a high frequency compared to the VRFB's response time. The current output can be seen to have a slight residual ripple from the three phase displaced currents through the smoothing inductors despite the smoothing capacitor, but again this is minimal and does not adversely affect the VRFB's operation.

Overall, as VRFBs currently represent bespoke project developments, there is a need to avoid new product development and this circuit has been shown to permit the minimal modification of a wind turbine converter and reuses a hardware system that has been extensively proven in the field.

6.3.2 Power Converter Model

As with a wind turbine, representing the DC-DC boost converter, common DC link and network side inverter with switching models of the IGBTs would lead to a slow and

cumbersome model. Therefore, as in that case, it is proposed to use ideal voltage source representation of the IGBT bridges and to couple them mathematically using power balance calculations. This representation is shown in Figure 6.6 and allows a significantly faster simulation model than full detail would permit.

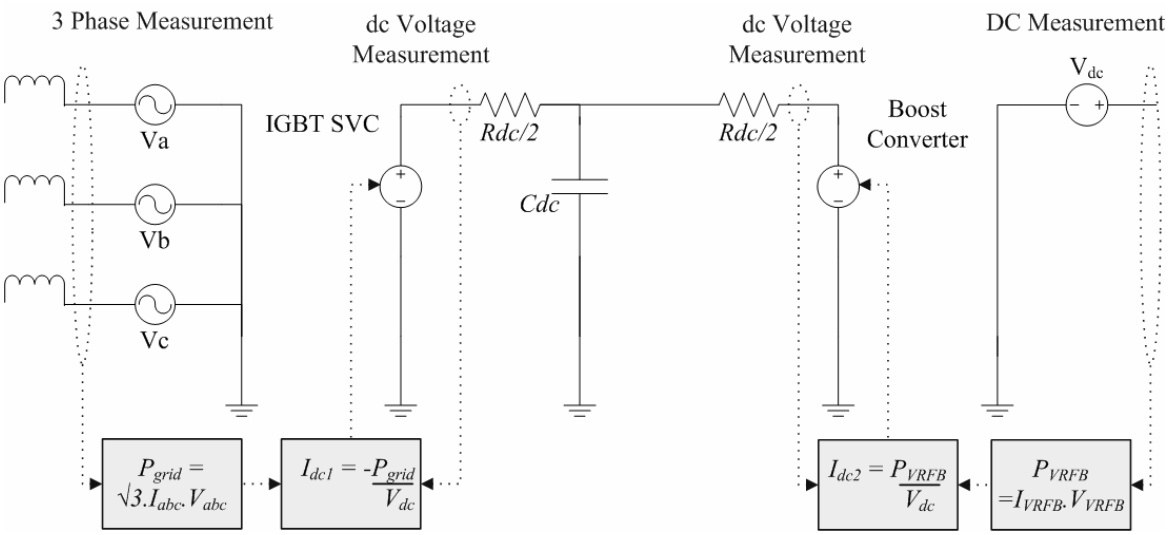

Figure 6.6: Simplified Model of the Boost Converter and IGBT SVC

6.3.3 Ancillaries

The VRFB has a significant ancillary load predominantly providing power to the pumps that circulate the electrolyte through the stack. These pumps represent a significant constant power drain on the VRFB as the low energy density of the electrolytes means that they must be circulated at relatively high flow rates to ensure the ion concentrations in the stacks are optimal. Additionally power must be provided to the associated control circuits. The development described by Gray and Sharman [130] had a 500kW power rating so was of significant size compared to earlier demonstration work, the ancillary load provided a constant power draw of approximately $1/6^{th}$ of the total rating. This value is used here for the ancillary loading as it is anticipated that larger installations will exceed this performance and hence it provides a conservative middle-ground between the high ancillary loads of current small installations and the potential to lower this with very large installations.

6.3.4 Wind Farm

Connecting energy storage with wind farm level reactive power compensation equipment, as proposed by Arulampalam *et al.* [135], presents one obvious location for energy storage within a wind farm. Such a scheme might be configured as in Figure 6.7, with a VRFB operating at an improved 400V DC and connecting to the grid at 690V. The example presented represents an offshore wind farm, as these wind farms will certainly be large

enough to be captured by the frequency response requirements of Grid Code (these offshore wind farms are typically greater than 50MW capacity or even larger) according to National Grid [78].

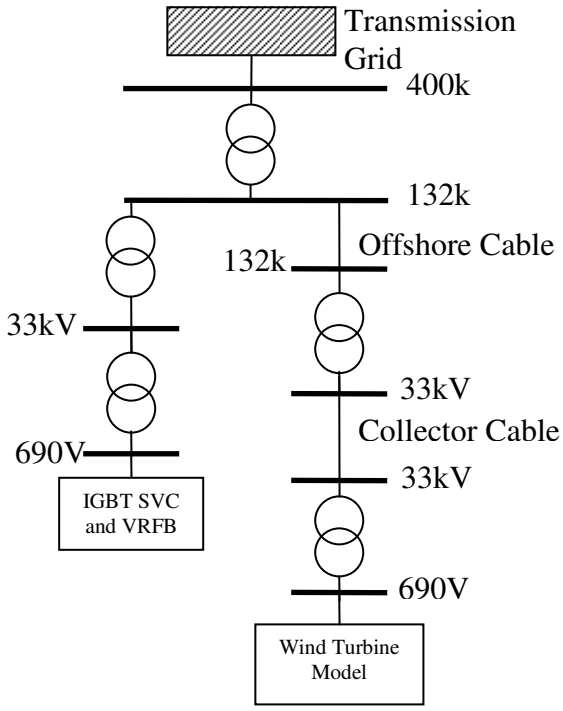

Figure 6.7: Integrated VRFB and Wind Farm Single Line Diagram

6.4 Model Validation

As with the wind turbine model, new components of the flow battery model have been validated. Bindner *et al.* [137] have conducted an extensive long-term practical evaluation of a small scale (15kW, 120kWh) VRFB by Prudent Energy and published significant results. Some of the key results presented there are used to validate the VRFB model developed here. As the VRFB systems are modular systems, relying on modules of this size to build larger systems, validation of the electrochemical stacks model against this data gives a good approximation to likely performance of much larger systems.

6.4.1 Software

The flow battery model has been implemented in both DIgSILENT PowerFactory and Matlab-Simulink. The Matlab-Simulink model is better suited to modification and tuning of the power converter and state of charge control loops, however, it is too slow to allow long time scale studies with a high energy capacity VRFB. As an alternative, the model has also been implemented in DIgSILENT PowerFactory which allows longer time-scale studies and ready integration with the earlier developed model of a wind turbine to represent a complete wind farm with energy storage. The model outputs have been

compared to confirm that they match and the validation plots shown here are from the DIgSILENT model.

6.4.2 Flow Battery Voltage

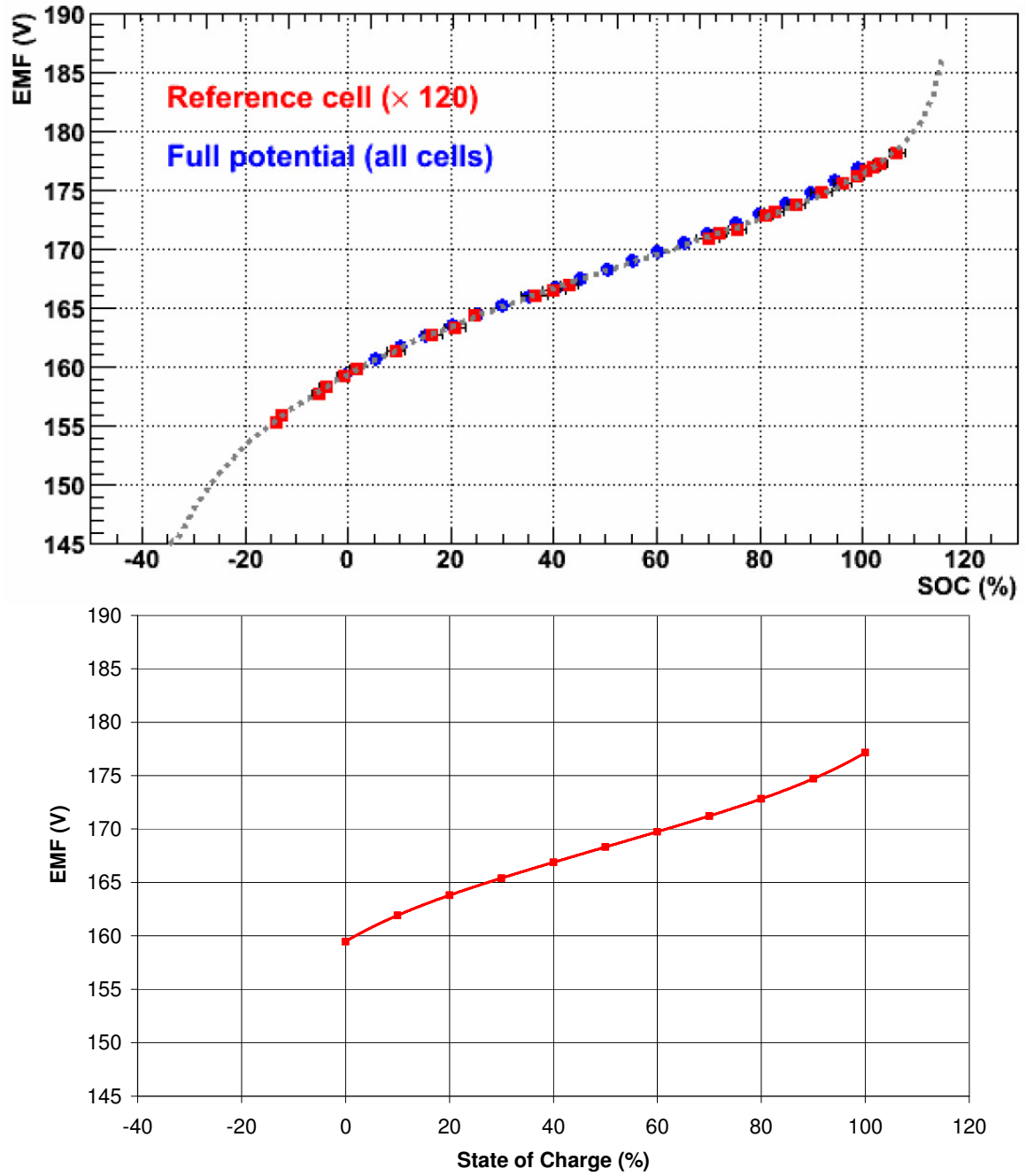

Figure 6.8: VRFB Voltage according to Bindner *et al.* [137] (Top) and Model (Bottom)

Figure 6.8 shows the DC open circuit voltage across the VRFB at various different state of charge levels. The top plot shows the reported results from Bindner *et al.* The maximum and minimum states of charge (SOC) reported here are outside of the nominal operating range (<0% and >100%) representing a load level beyond that of the battery's normal operational limits. Bindner *et al.* state that this is due to the difference between the SOC

reported by the battery (which is an interpolation of various data points and is shown in the plot) and the theoretical state of charge as calculated from the state of the battery.

The application of the VRFB to providing frequency response services with a wind farm is likely to involve repeated charge and discharge cycles, as such; it is not acceptable to allow the state of charge of the flow battery to exceed the nominal operating range as this would rapidly degrade the VRFB's lifetime. Furthermore, as the voltage drops, the constant power current increases, hence at low states of charge the current for rated power would be at a maximum. The power converter would be optimally sized for rated power capacity at the lowest nominal state of charge; hence, at the low end of the range the power converter's current limit would lead to reduced output power. Hence, the battery's reported state of charge would be used in order to ensure operation within the designed limits of SOC. This means that the model needs only replicate the voltage profile in the nominal state of charge operating range and not the extended range.

As a result of some of the underlying assumptions in simplifying the VRFB model, the physical molar concentrations of Vanadium ions do not directly correspond to the concentrations applied in the Nernst equation to calculate the open circuit potential. As a result, the five underlying concentrations (four Vanadium ion concentrations and the acid concentration) have been tuned to optimise the match between the VRFB output and the model output; this is a quick manual process that only affects the initial concentrations and not the magnitude of changes in concentration of the various ions. Figure 6.8 shows the result of a tuned electrochemical model across the normal state of charge range for the VRFB. The validation plot shows that the slight non-linearity in the voltage profile has been replicated and that at all states of charge the open circuit voltage is well within 3% of the expected value and is normally within 1.5%.

This voltage to state of charge profile also highlights the current output variation that can be expected from the VRFB. As the power converter will operate to ensure that the battery provides a constant power output, the boost converter current will increase by more than 10% as the battery state of charge drops from its rated level.

The non-linearity in the voltage profile also helps to show the benefits of a limited operating range. As the SoC approaches full charge, the voltage increases more steeply, hence the power converter voltage rating would have to increase significantly to provide a limited additional capacity for operation at higher states of charge. Conversely, as the SoC reaches the lowest nominal level, the voltage drops more severely, indicating that the power converter's current rating would have to increase substantially to provide limited

additional power capacity from lower states of charge. Overall, the optimal system will be developed and the model agreement has been shown to be acceptable based on less than 3% difference in the model and output voltage across the entire operating range.

6.4.3 Round Trip Efficiency

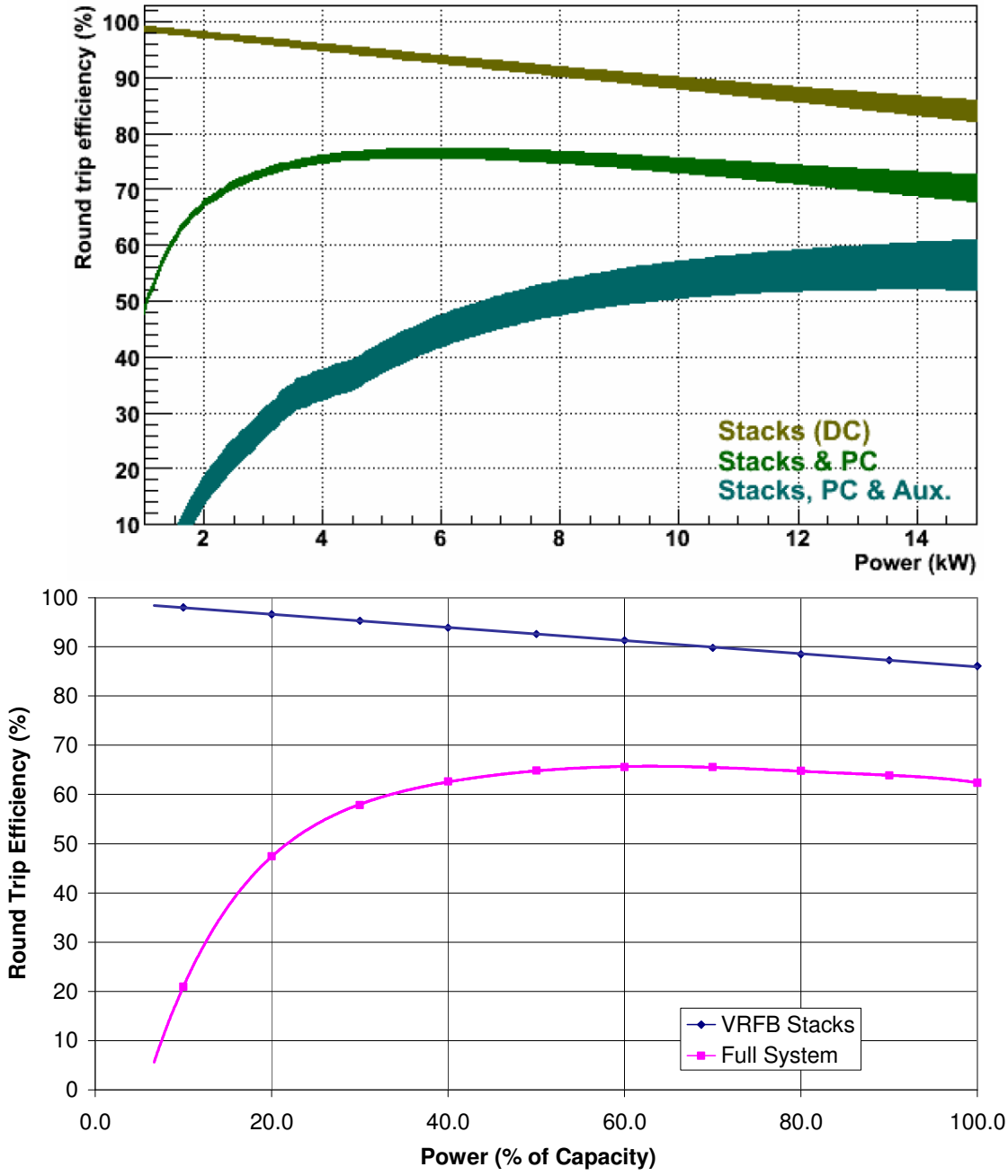

Figure 6.9: Energy Store System Round Trip Efficiency according to Binder *et al.* [137] (Top) and Model (Bottom)

The top plot in Figure 6.9 shows the practical efficiencies achieved with constant power charge and discharge cycles. The two plots' x axes have been approximately aligned to allow quicker cross referencing. The gold coloured plot shows the round trip efficiency from the electrochemical part of the flow battery system (stacks, membrane and stack concentration changes). This agrees well with the modelled round trip efficiency, shown

by the blue line in the lower plot. This validates the efficiency of the electrochemical part of the model.

Bindner *et al.* noted the low efficiency of the power converter in their installation (<85% round trip). This in part is due to its smaller scale (15kW) when compared to the systems typically supplied for commercial applications. However, their power converter also suffered very poor response times, suggesting that the design was poor. Furthermore, the total auxiliary load on the 15kW system represented a higher proportion of rated output than would be the case for a larger scale system. As a result the electrical model represents the typical commercial system, with the ancillary load set according to that experienced for real applications where the load was approximately $1/6^{th}$ of the rated power. This leads to a higher round trip efficiency for the full system model of a large scale VRFB (lower plot, magenta) than the measured round trip efficiency on the small scale demonstrator (top plot, blue). This is in line with claims that the efficiency of VRFB systems will improve with scale but is still lower than the average 70-85% range projected in Table 5.18, which is the range widely predicted in the literature.

The overall round-trip efficiency plot illustrates the need to consider the dynamic efficiency. The non-linearity in efficiency means that in a real world application, particularly in conjunction with an intermittent resource such as wind power, the instantaneous losses will vary widely. Overall, this representation of round trip efficiency will provide an accurate projection of likely VRFB commercial performance.

6.5 Converter Control System

Parts of the following two sub-sections of the thesis, covering control of energy storage and wind farms, have been written up as a peer reviewed journal article and accepted for publication in IEEE Transactions on Power Systems by Banham-Hall et. al. [138].

The electrical interface to the grid has been shown to use the same hardware, but in a different topology, as a full converter wind turbine. However, whereas a wind turbine operates only as a generator, a flow battery can operate either as a generator or as a load. Furthermore, the flow battery has a finite energy capacity which must be managed in order to avoid over-charging or under-charging the battery. These differences mean that, whilst there is some cross-over with the control scheme of a wind turbine, some parts of the power converter control software must be modified.

6.5.1 Converter Control Scheme

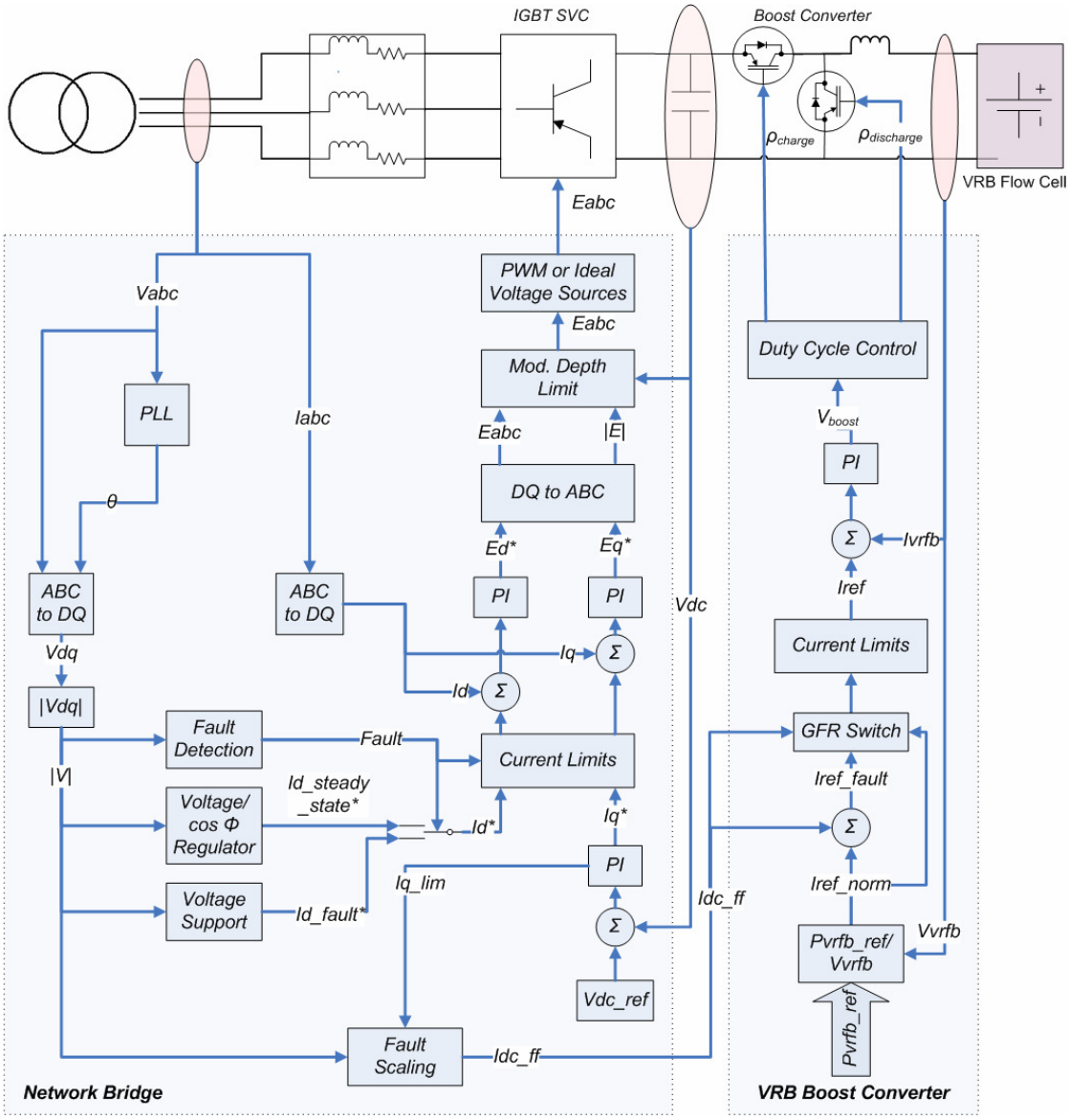

Figure 6.10: Power Converter Control for VRFB

It has already been discussed in section 6.3 that the VRFB would be connected to the DC link of a power converter. This power converter in turn could be essential for meeting a wind farm's reactive power control requirement. As such, the network bridge must be capable of operating independently of whether the battery is charging or discharging or even connected. This means that the network bridge controller must follow the conventional control scheme from section 3.5.1.1. The network side converter must be responsible for controlling the power converter's DC link voltage as well as the grid's reactive power requirement in order to ensure that the DC link stays within operational limits. This is clear in Figure 6.10 as the general structure of the network bridge control part is identical to the wind turbine application. Furthermore, by avoiding using the VRFB to control the DC link voltage, micro cycles and voltage noise will not lead to battery

degradation as the battery will only charge or discharge according to an external set-point and not grid disturbances.

The DC boost converter receives a single control reference as a power set-point from the battery controller. The controller in Figure 6.10 then converts this power reference set-point into a current reference for the flow battery and controls the VRFB voltage. By controlling the voltage relative to the chemical equilibrium voltage of the flow battery (see Figure 6.8) the current can be controlled. This power to/from the VRFB will be supplied to/from the common DC link, leading the network bridge's DC link controller to modify the power to or from the grid in order to maintain a constant DC link voltage.

Whilst it is necessary to control the DC link voltage from the network, the VRFB offers the potential to support the reactive power compensation capability of the network bridge under certain situations. With a conventional IGBT based SVC, when the grid voltage is very low (<15% of rated) the IGBT SVC is unable to draw sufficient real power from the grid to compensate the converter's ancillary load and switching losses, owing to the IGBTs' current limit. This means that the converter's reactive current capacity is reduced as a greater proportion of the converter's current rating is used for real power import to compensate losses. A typical example of this limitation would be the ability of the power converter to continuously supply reactive power into a severe low voltage fault (until the fault is isolated). The losses of the converter would lead to a falling DC link voltage until the converter's modulation depth limit is reached and it could no longer supply reactive current into the fault.

If an IGBT based SVC is equipped with an energy store the operational envelope of the power converter can be extended to allow supply of rated current at all voltages below unity with the energy store compensating for converter losses at low voltage. In order to achieve this, control of the DC link must pass from the network bridge to the boost converter under low voltage conditions.

Figure 3.13 shows the DC link controller block diagram, this controller typically works because an approximation can be made between the DC current and the AC *q*-axis current because of the per unit power balance between the AC and DC sides of the bridge, the inaccuracy in the approximation is then covered by the integral gain of the controller:

Equation 6.7 $\sqrt{3} \cdot V_l \cdot I_q = V_{dc} \cdot I_{dc}$

Equation 6.8 $I_q \approx I_{dc}$ as the modulation depth is nearly 1.

However, under grid faults, this power balance no longer stands as the AC side voltage is reduced and the modulation depth is very much less than unity. The power is reduced by a factor of (in per unit terms):

Equation 6.9 $$\frac{1-V_f}{V_f}$$

So, if the error in the DC link controller is scaled by the inverse of Equation 6.9 then the power balance will approximately hold.

This can be achieved with the feed-forward shown in Figure 6.11, which acts to modify the VRFB current reference. The feed-forward operates on I_{q_lim}, the DC link controller wind up, and scales it such that at very low voltages the feed-forward is greater (V_f is the fault voltage). By operating on the wind-up of the DC link controller, the network bridge continues to maintain some control over the DC link voltage, within the bounds of the current limit of the power converter.

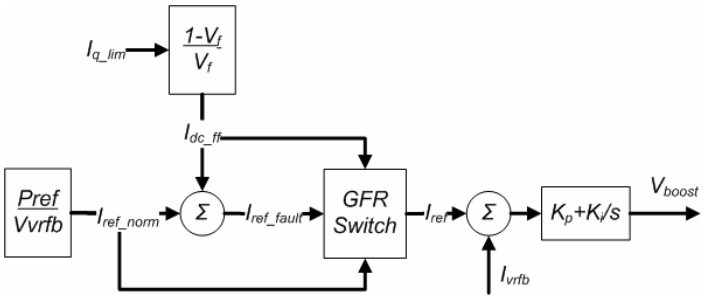

Figure 6.11: Low Voltage Ride-through Controller

6.5.2 Grid Fault Ride-through Simulations

Figure 6.12 shows the response of the system to a zero voltage grid fault on the primary side of the VRFB system's transformer, with the retained voltage (Vg) measured across the secondary. Prior to the grid fault the energy store was charging and therefore acting as a load. At the onset of the fault (t=16s) the power output (P) of the system is rapidly reduced to zero as the entire current capacity of the network bridge is provided for reactive current output. Note in this example that the base power used is the power rating of the VRFB, which itself is rated at half the apparent power rating of the IGBT SVC. The network bridge reactive current (Id) therefore increases to rated current at the onset of the fault. The suppressed network voltage means that the total reactive power (Q) provided is well below the rated limit. The successful operation of the DC link control feed-forward can be seen as the VRFB stops charging (Pvrfb) and discharges slightly to compensate the ancillary load thus helping to maintain control over the DC link (Vdc). The fast response

of the VRFB means that the transient change in DC link voltage is minimised and would not cause a problem for the power converter.

When the fault recovers, a significant transient is seen in reactive power owing to the increase in voltage and rated current output before the reactive current reference is reduced. This in turn leads to a transient in the real power output as the current controller regains control over the *d* and *q* axis currents. However, overall the VRFB when operating as a load is shown to ride-through the fault and ramps power back to its original state once the system has recovered from the fault, but the control is slightly under-damped.

The fault simulated is well beyond Grid Code limits (4s as opposed to 140ms), but it serves to illustrate the benefit that the DC link control provides to the operation of the power converter. Full reactive current output is maintained through the fault and the DC link voltage is controlled. The energy store is therefore acting to supply the converter's losses and prevent a DC link voltage fall.

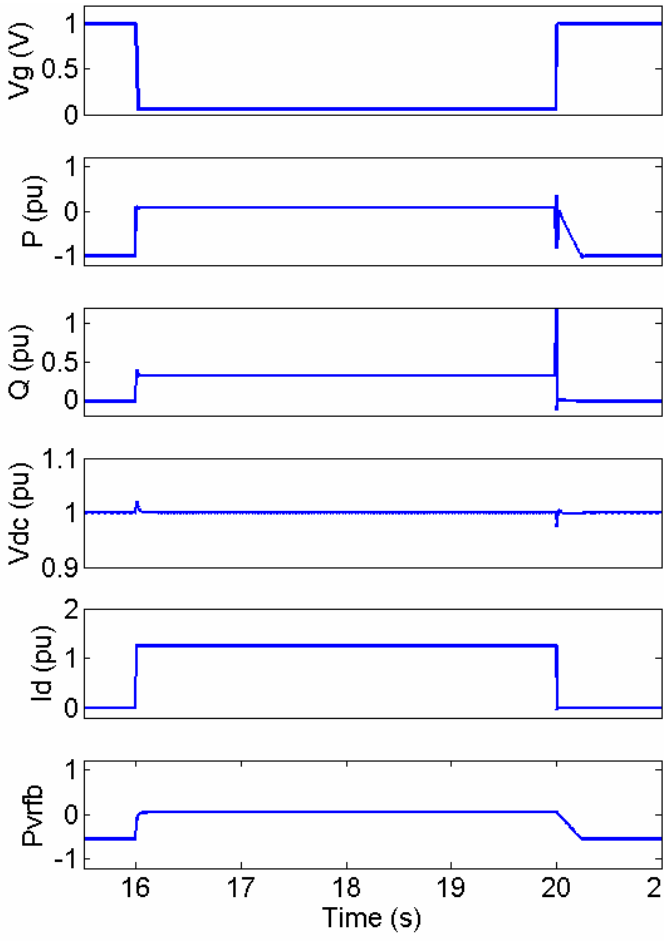

Figure 6.12: GFR of Energy Store as a Load

Figure 6.13 shows that the VRFB system also successfully rides through this fault when the flow battery is initially operating as a generator rather than a load. The performance of the system can be seen to be near identical, with only the DC link voltage transients

showing a significant deviation from the previous case, as the VRFB reduces its output but remains supplying the power converter through the fault.

The control strategy of the power converter has been shown to offer excellent dynamic control. The enhanced DC link control allows the power converter to provide reactive power through even the most severe faults, by transferring DC link control to the flow battery's boost converter. This would provide a further benefit over an independent IGBT based reactive power compensation device.

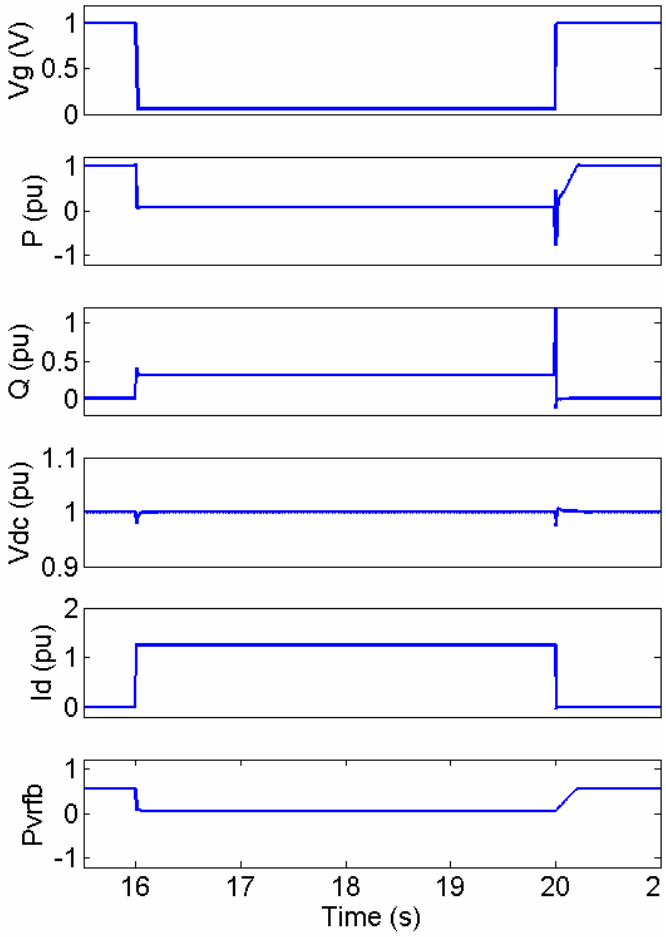

Figure 6.13: GFR of Energy Store as a Generator

6.6 Wind Farm and VRFB System Control

Figure 6.14 shows that the natural arrangement for connection of a VRFB with a large, transmission level AC connected, wind farm. This arrangement has also been proposed by Wang *et al.* [139] who consider a wind farm of FF-PMG type wind turbines with a VRFB for power smoothing. As is the case in their application, the power converter offers both real and reactive power support to the grid. However, Wang *et al.* do not consider the control of the battery state of charge and show only the simulation of a smooth output power profile over a relatively short time period, furthermore, they do not consider the frequency response capability.

This configuration of wind farm and VRFB allows the store to aggregate several benefits:

- The VRFB can be used to smooth wind power output and compensate for forecast errors to ensure that the wind farm meets its production target.
- The VRFB can offer frequency response services to the grid on behalf of the wind farm, thus earning additional revenue and avoiding the need for the wind turbines to offer this service.
- The energy generated by the wind farm can be stored at times of low demand and price and released at times of high price (arbitrage).

To take advantage of these opportunities, the control scheme must be designed in such a way as to ensure that the Grid Code requirements for frequency response, the market requirements for energy trading and the battery's state of charge are all optimally controlled.

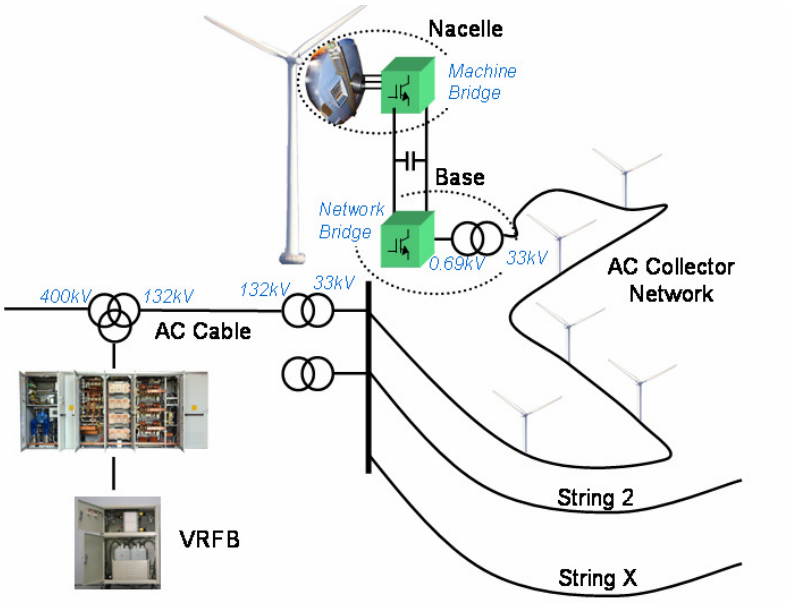

Figure 6.14: VRFB Integration with a Wind Farm

For the purposes of modelling the VRFB a single typical offshore wind farm design has been modelled with a VRFB in DIgSILENT PowerFactory, according to the diagram in Figure 6.7. The wind farm is sized at 300MW and is represented by a single lumped turbine model, which is driven by real wind speed data from the large Horns Rev offshore wind farm. A variety of different power and energy rating VRFBs have then been modelled at the onshore connection point. This model forms the basis for simulations of the energy store behaviour in this chapter and in the multiple scenarios run as part of an economic analysis in chapter 7.

6.6.1 Output Smoothing

Section 3.5.3 described the role and purpose of a wind farm main controller and described how such a scheme can help to ensure that a large scale wind farm can offer the functions of a conventional power plant. Such a centralised controller acts as an aggregator of the wind turbines' output, receiving a measure of their available power and dispatching real and reactive power (or voltage) operating points to the turbines. In normal operation such a scheme would typically track the available power for the whole wind farm to maximise output. The wind farm's intermittency is then typically accommodated by the electricity supplier with the wind farm holding a power purchase agreement for the whole wind farm's output [140]. The electricity supplier currently then balances wind's intermittency with other generators, however, as wind power's contribution to the UK grid expands this may become impossible and wind generators will themselves become exposed to the cost of their imbalance.

If the wind farm is equipped with an energy store, such as a VRFB, its control can be integrated with the wind farm main controller to minimise the imbalance between forecast output and actual output. In this work, the wind farm main controller generates a simple persistence forecast, whereby the output at a certain time in the future is assumed to be the average of the output over the recent past, as in Equation 6.10, according to the method of Bludszuweit, Dominguez-Navarro and Llombart [141]. This method is comparable to more complex forecasting techniques over short time horizons.

Equation 6.10 $\overline{P}_{forecast}(t+k\,|\,t) = \frac{1}{T} \cdot \sum_{i=0}^{n-1} P(t - i \cdot \Delta t)$ where T is the total time period averaged, k the time into the future that the forecast is for, Δt is the time step of the samples and n the number of discrete power measurements to be averaged.

Based on the forecast output the wind farm would then have a contracted output power profile for a given half-hour settlement period. Thus the wind farm can be dispatched to track the available power whilst the VRFB is dispatched to output the difference as shown in Figure 6.15 according to Equation 6.11.

Equation 6.11 $P_{ref\_VRFB} = P_{forecast} - \sum_{n=1}^{N} P_{avail,n}$

The VRFB would not be likely to be sized to accommodate a 100% error in forecast output. In fact the natural limit on the VRFB size could be affected by the power converter, which for meeting reactive power requirements at the wind farm's connection point would have a maximum apparent power rating equivalent to 33% of the wind farm's

real power rating. Hence there will be times when the VRFB is operating at maximum charge or discharge rate and the wind farm is still subject to imbalance, nevertheless overall imbalance would be significantly reduced.

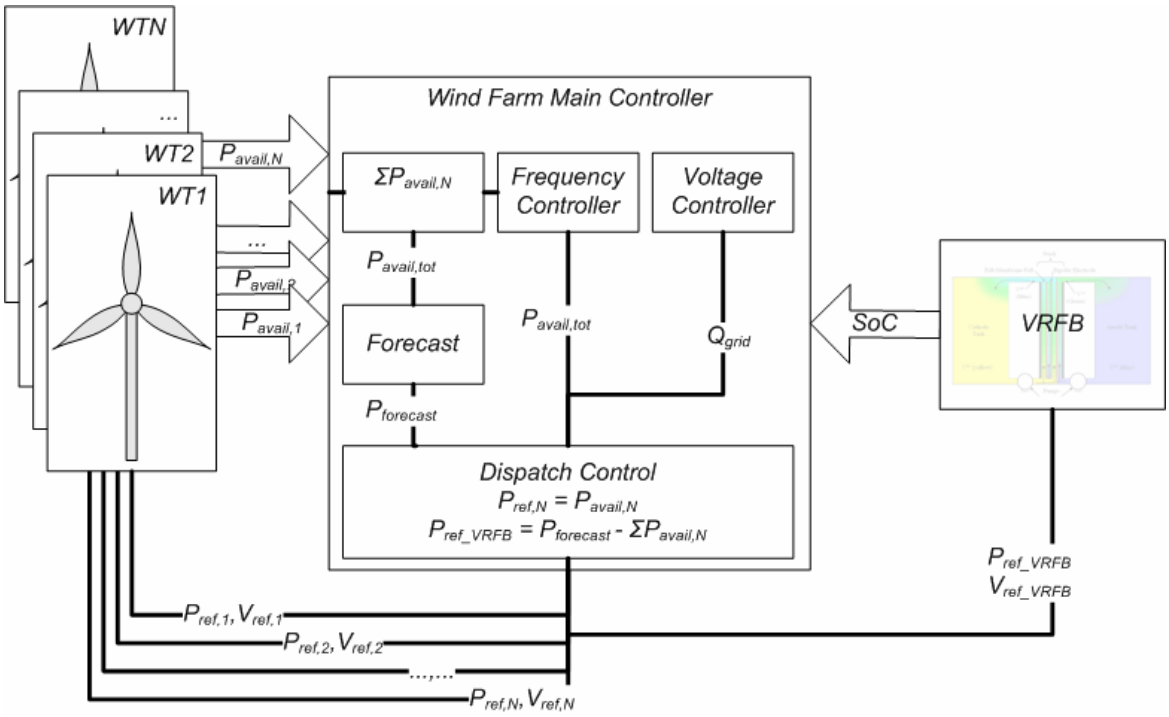

Figure 6.15: Wind Farm Main Controller with Integrated Storage

6.6.2 Frequency Response

One of the key purposes of providing output power smoothing would be to comply with the requirements for offering frequency response, as outlined in section 4.3.1. These requirements mandate that a generator operating in FSM must regulate their output from a fixed output level (the CCL). Discussions with National Grid have highlighted that this level, in future, would be likely to be updated each settlement period (currently 30 minutes). Without an energy store, a wind farm in FSM would be required to spill wind in order to hold a margin for frequency response but would only be likely to receive balancing mechanism payments equivalent to their firm, reliable holding, else National Grid could dispatch an alternative supplier for an economic advantage. Wind farm operators set their acceptable prices for offering such services when they bid into the market. If National Grid had few alternatives, as wind dominates the system, then this would likely lead to significantly higher balancing costs as the system operator would have to compensate the wind farm for lost Renewable Obligation Certificates (ROCs) at times when wind power dominates supply.

By contrast to the stand alone wind farm, for a wind farm with an energy store, the output of the combined farm could be controlled to a constant output based on the persistence

forecast of Equation 6.10 for a period of half an hour. The power capacity of the energy store can then be used for providing frequency reserve and for achieving a constant output power for a given settlement period.

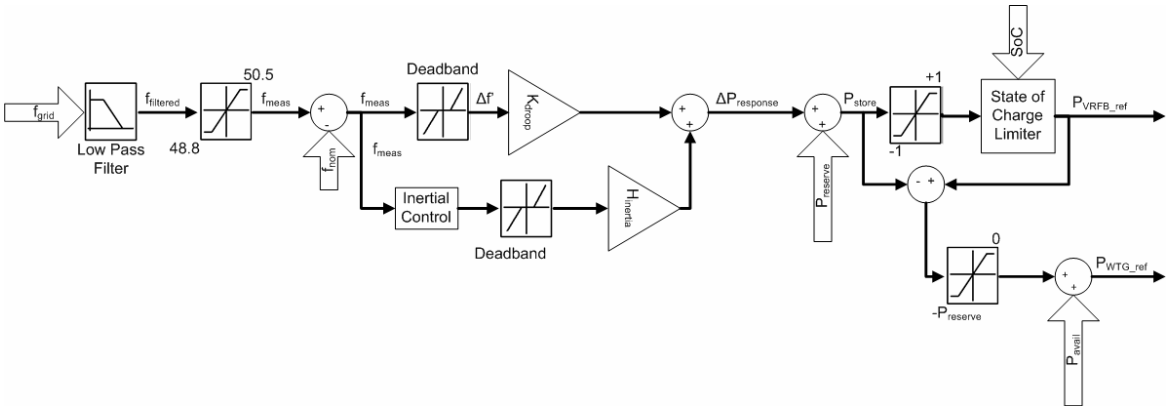

Figure 6.16: Controller for Shared Frequency Response Capability between a Wind Farm and an Energy Store

In addition to the requirement to regulate power output under FSM from a fixed output, section 4.3.1 also showed that whilst low frequency response can only be applied up to the available reserve held, the high frequency requirements aren't limited in this manner. The wind farm could effectively be required to regulate its output down to zero under a high frequency event, as they typically have no minimum operating level equivalent to the level at which a conventional plant would trip. Clearly a partially rated VRFB could not absorb all the wind farm's power and therefore the typical frequency controller of Figure 4.20 has to be modified such that if the charging power limit of the VRFB is reached owing to a high frequency event, the output of the wind farm is regulated down instead. This modification is shown in Figure 6.16.

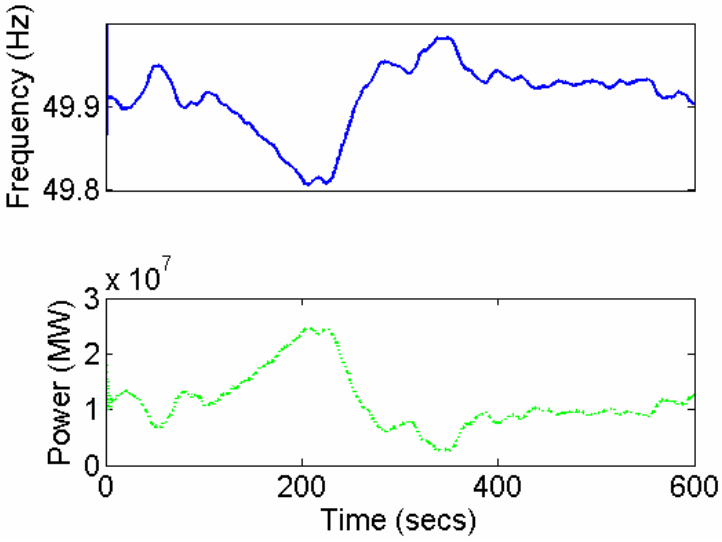

Figure 6.17: Fast Frequency Response from VRFB

The VRFB is capable of rapid response to frequency changes; Gray and Sharman [130] demonstrated that the output could be reversed from full charge to full discharge in around a mains cycle (20ms). This rapid response has been reflected in the energy store model's tracking of a typical grid frequency signal when in FSM. This is shown in Figure 6.17. The VRFB output can be seen to give a proportional response, with no discernable lag, to the error in frequency from the target (50Hz). This demonstrates one of the key advantages of the VRFB, in that whilst it is capable of long time scale energy storage it is also capable of fast response for applications such as frequency response.

The frequency controller shown in Figure 6.16 shared the responsibility for providing high frequency response between the wind farm and the energy store. The operation of this controller under a high frequency ramp is illustrated in Figure 6.18, for the purposes of illustration the wind speed has been modelled as constant.

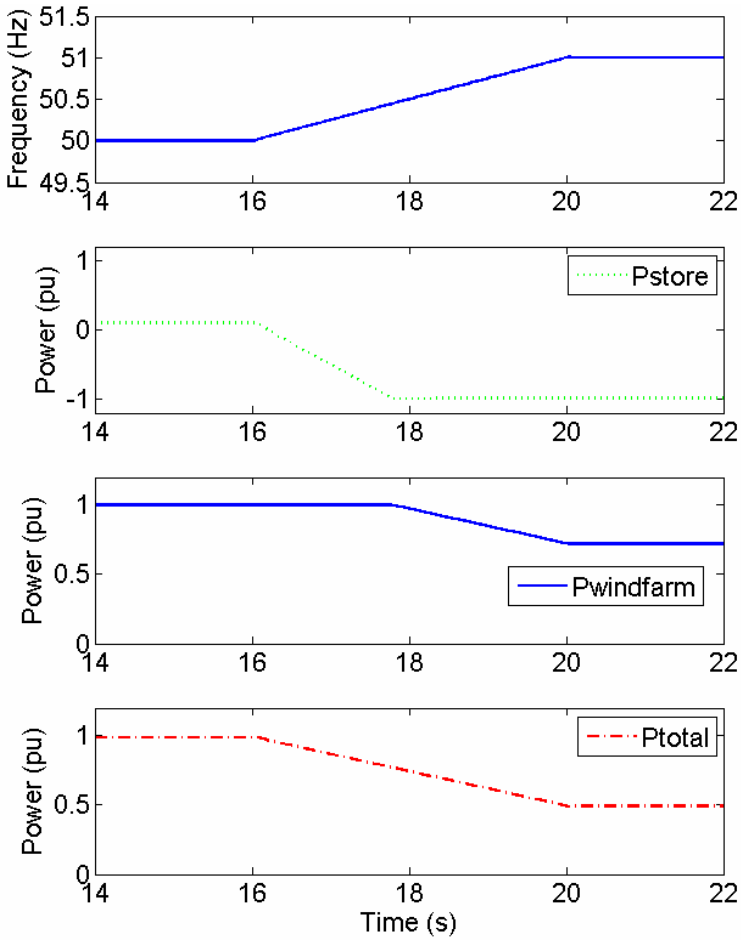

Figure 6.18: High Frequency Response from a Wind Farm and VRFB

The key point to note from the simulation is that the energy store's power (Pstore) is modified preferentially; therefore as the system frequency is normally near to the target of 50Hz, the energy store will accommodate most high frequency deviations, excepting the severe cases. When the frequency does rise significantly, such that the energy store

reaches its maximum charging rate, the wind farm's power output (Pwindfarm) begins to be regulated down but this action would very rarely be required. The overall response (Ptotal) is a seamless ramp of constant gradient, which itself was defined by the controller's droop setting. (Note the base powers of the VRFB and wind farm are different leading to the different gradients on their individual plots).

Incorporating an energy store for this particular application will have increasing benefit in avoiding having to spill wind power as the proportion of wind power on the GB system increases.

Operation of the VRFB to provide low frequency response services can take several different forms. Figure 6.19 to Figure 6.21 illustrate the behaviour of the energy store, providing frequency response services but without responsibility for smoothing the wind farm's output. In each case the energy store would add a fixed margin to the variable output of the wind farm, thereby creating a "Delta Control" response (see section 4.3.1) from the combined wind farm and energy store. Whilst this combined response would not be in line with the present specifics of GB Grid Code, these three simulations are illustrative of the way that energy storage and wind power can work in tandem to provide frequency response services.

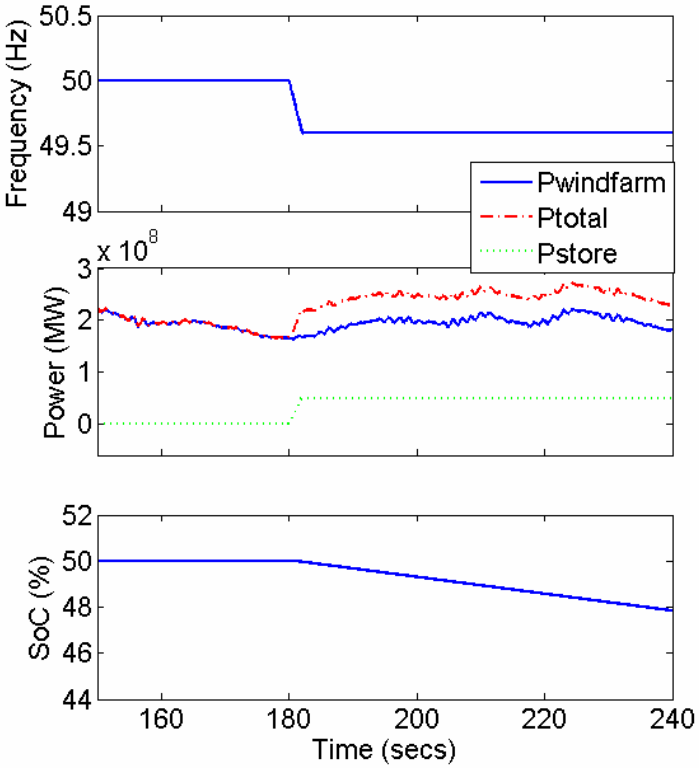

Figure 6.19: Generator Control for Low Frequency Response

Figure 6.19 shows the case where the energy store is holding equal high and low frequency response margin. In this case, when the frequency is close to the target of 50Hz,

the energy store idles, neither charging nor discharging. Both high and low frequency response reserves are equal to the rating of the VRFB. When the frequency falls, as it does in this scenario, the VRFB can increase its output (Pstore), from zero, up to the maximum rating of the battery. This increases the combined plant's output, but that output is still variable. Furthermore, the battery will begin to discharge, so the energy stored must be sufficient to provide for a continuous output until the system frequency is restored or other plant can come online (i.e. to last at least to the end of the half hour balancing period).

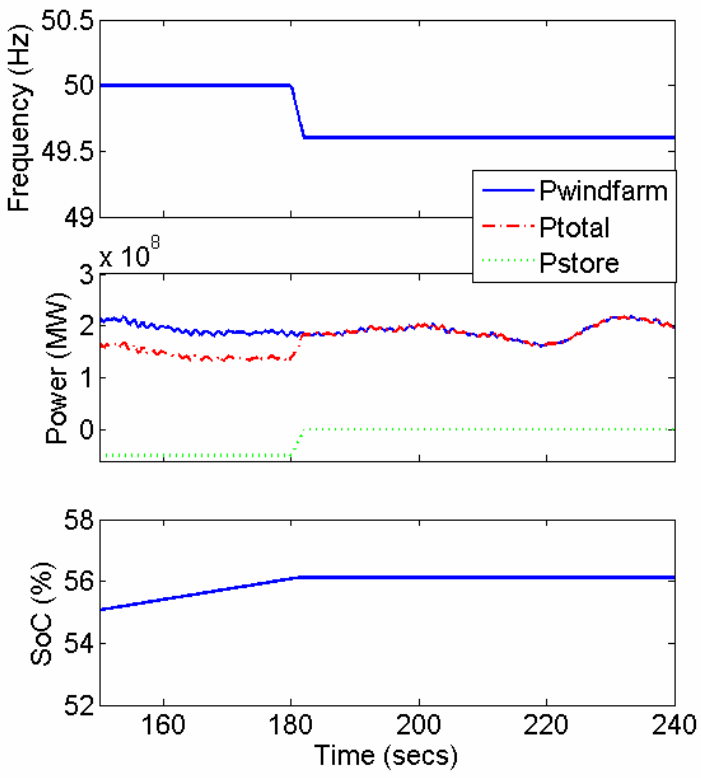

Figure 6.20: Load Control for Low Frequency Response

An alternative approach is shown in Figure 6.20, which could be used when an energy store is charging. In the event that the system frequency falls, the charging rate of the energy store could be reduced, thereby helping the system balance by reducing the total load. A by-product of this control method is that the VRFB can offer twice its rated output capacity as low frequency response whilst it charges. However, in order to offer high frequency response the wind farm output would have to be put at risk of being spilt as the VRFB cannot accommodate a reduction in power output by charging faster.

Figure 6.21 illustrates a greater frequency deviation, where the capability of the VRFB to swing from acting as a load on the system, to generating is illustrated. Once again however, it must be reiterated that in order to offer any high frequency response margin, the wind farm's output must be put at risk.

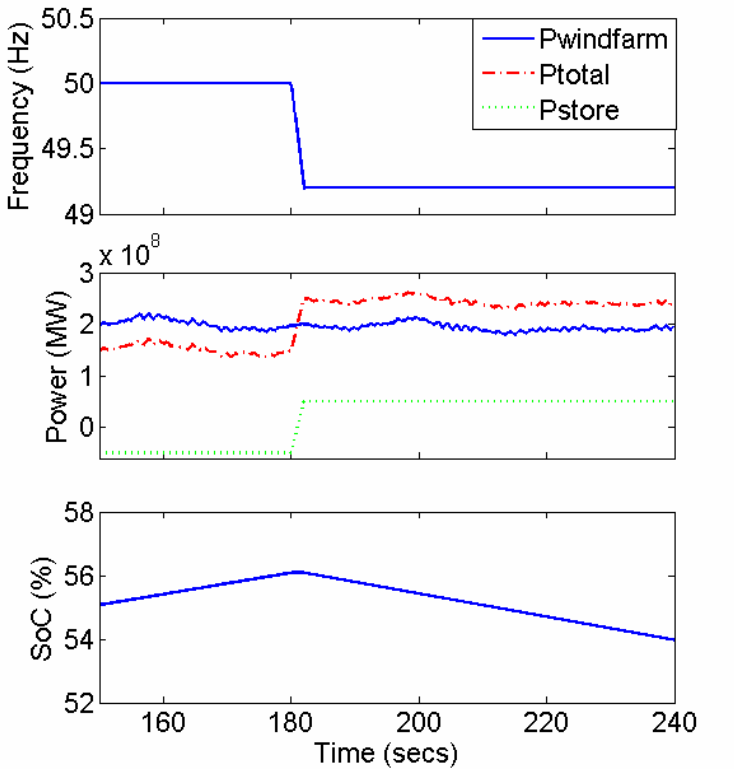

Figure 6.21: Bipolar Control for Low Frequency Response

The GB regulations for frequency response stipulate that the output variation must be relative to a fixed power output level. Figure 6.22 therefore shows the behaviour of this frequency controller when the smoothing controller of section 6.6.1 is active. As can be seen, prior to the frequency deviation, the VRFB power (Pstore) absorbs the fluctuations in the wind power output (Pwindfarm) allowing a constant output power to the grid (Ptotal). When the frequency falls, the mean of the VRFB output increases so that the total grid power increases.

This example illustrates the challenge of operating from a constant power output. Towards the end of the scenario (t>230s), the wind falls sufficiently far that the total output power from the wind farm and energy store combined is no longer flat. This illustrates that whilst the initial output is flat, the reserve margin held would be variable dependent on the prevailing wind conditions. Furthermore, as a consequence of the smoothing power, the state of charge variation is not predictable, meaning that it must be independently controlled to ensure that the battery does not exceed its state of charge limits.

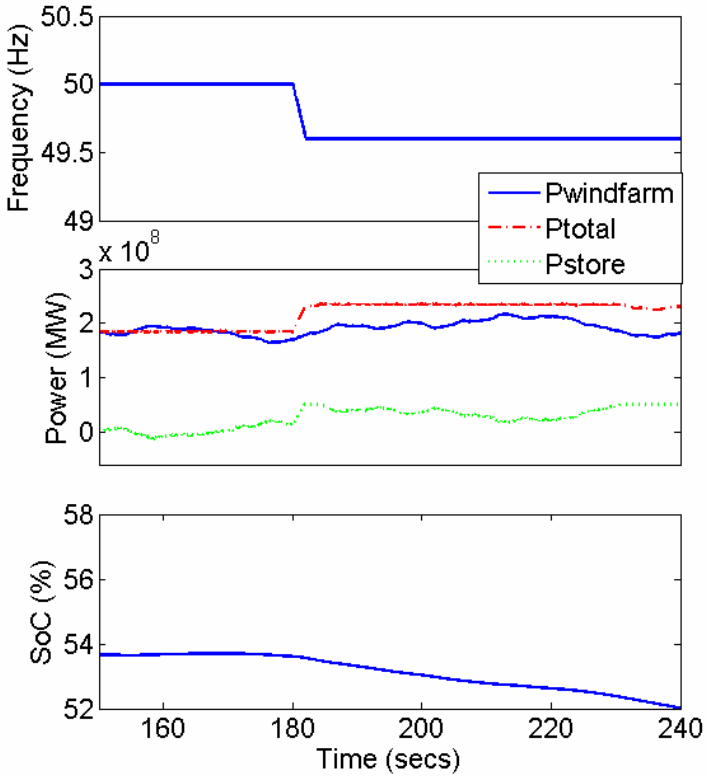

Figure 6.22: Frequency Response and Power Smoothing

6.6.3 State of Charge

It has been highlighted that the state of charge of the VRFB will have to be controlled. Yoshimoto, Nanahara and Koshimizu [142] have developed a controller for regulating the state of charge of a VRFB installed to smooth a wind farm's output in Japan, although without frequency response capability. This is the largest installation of a VRFB globally and the VRFB effectively acts such that the output of the combined system is low pass filtered compared to the raw wind power so the VRFB absorbs fast fluctuations. However, whilst this state of charge control is effective, it is essentially a continuous time modification to the power output of the combined system. If this were applied here, this would lead to a variable power output within a settlement period, which would contravene the GB frequency response requirement to regulate from a fixed output level, and lead to consequent imbalance.

As an alternative to continuous time management of the state of charge of the VRFB, it is proposed to manage the state of charge by updating the power output profile (or Final Physical Notification, FPN) for the next settlement period to be submitted. This FPN has to be submitted an hour ahead of the relevant half hour settlement period. It is therefore proposed to use a fuzzy logic supervisor to control the battery's state of charge by modifying the forecast output for the wind farm and VRFB for a given settlement period an hour ahead. Use of fuzzy logic for controlling energy storage on a wind farm was

proposed in Brekken *et al.* [143], however, there the energy store was purely for smoothing wind output and had no other purpose, hence the state of charge reference was constant and the controller was continuous acting. The controller proposed for this more complex situation is shown in Figure 6.23.

The fuzzy logic controller is designed such that it depends on both the state of charge itself and the planned change in the state of charge reference. Hence, if the battery is scheduled to charge or discharge for arbitrage purposes, the controller accounts for this. In total each input variable is defined to have three states.

- The state of charge is defined as either low, near to its target value or high; where near to target is defined by a range of ± 20% relative to the target value.
- The rate of change of the state of charge reference is defined to be discharging, charging or holding; where holding corresponds to a planned change in SOC of less than 5% per hour.

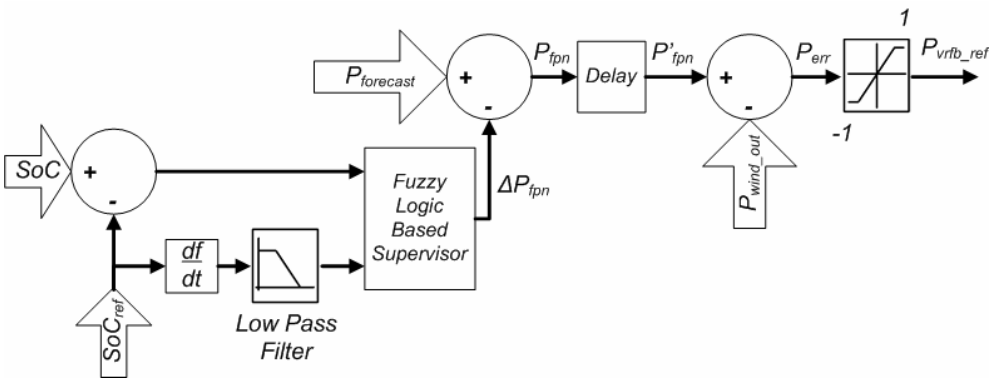

Figure 6.23: Integrated Fuzzy Logic Based Wind Farm and Store Controller

The membership functions of the normalized input and output variables are shown in Figure 6.24 and the inference table, Table 6.1, shows the fuzzy rules. These nine rules are a consequence of the two, three-state inputs. The outputs have been defuzzified according to Mamdani's centre of gravity approach. It should be noted that different input combinations have different rules but potentially the same output. For example, if the state of charge was near to its target but the planned change in that state of charge target is negative (to discharge), then the rule states that this should lead to a slow discharge. Likewise, if the state of charge was high, but the planned change in the state of charge was to stay constant, then the rule also states that this should lead to a slow discharge of the VRFB.

The controller has been designed with a view to ensuring that there is sufficient energy capacity in the battery to absorb significant over or under-production from the wind farm.

Hence, if the battery becomes over-charged relative to the reference, and the reference is set to hold energy, it will attempt to slowly discharge to ensure there is sufficient energy margin to absorb a high wind period.

The state of charge controller is only permitted to use 80% of the power capacity of the VRFB, thus guaranteeing some power capacity margin for frequency response. Further, by capping the average rate of charge and discharge, the VRFB can be operated more efficiently by minimizing Ohmic losses as can be seen from Figure 6.9.

		SoC		
		Low	Near Target	High
Planned SoC Change	Discharge	N: Neutral	SD: Slow Discharge	FD: Fast Discharge
	Hold	SC: Slow Charge	N: Neutral	SD: Slow Discharge
	Charge	FC: Fast Charge	SC: Slow Charge	N: Neutral

Table 6.1: Integrated Fuzzy Logic Controller

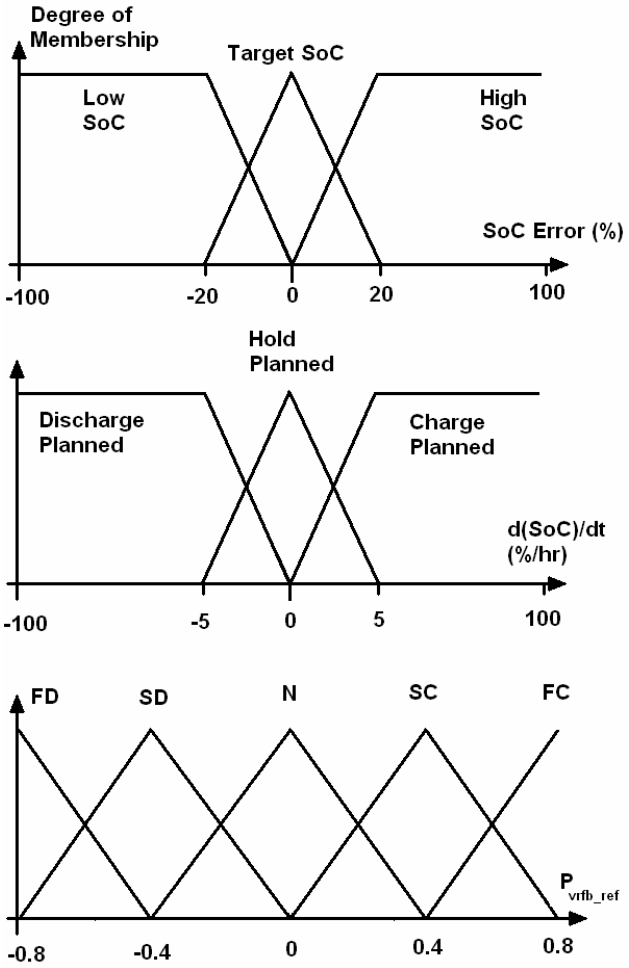

Figure 6.24: Degree of Membership of the Input (Top & Centre) and Output (Bottom) Functions

6.6.4 Arbitrage

It can be desirable to charge the VRFB at times of low prices and to sell at times of high prices, or in essence to provide arbitrage services. The state of charge controller has therefore been designed in order to accommodate a changing state of charge reference. As the state of charge is based on the integral of the power output of the VRFB, power exchange for arbitrage can be scheduled by varying the state of charge reference of the VRFB. When charging the change in the state of charge reference should be defined as:

Equation 6.12 $$\Delta SoC_{ref} = \frac{1}{E_{rated}} \cdot \int P_{charge} \cdot \eta\left(P_{charge}\right) \cdot dt$$ where E_{rated} is the rated energy capacity of the storage system, P_{charge} is the desired charging power and $\eta(P_{charge})$ is an estimate of the one way efficiency of the VRFB at the selected charging power. This means that an *a priori* estimate of the efficiency profile for the VRFB is required, but this can be obtained from the data behind Figure 6.9.

The case is similar for when the VRFB is to be scheduled to discharge, although now the state of charge reference would be scheduled to reduce. This is illustrated in Equation 6.13. Errors in the open loop setting of the state of charge schedule are then covered by the fuzzy logic state of charge controller.

Equation 6.13 $$\Delta SoC_{ref} = \frac{1}{E_{rated}} \cdot \int -P_{discharge} \cdot \eta\left(P_{discharge}\right) \cdot dt$$

6.6.5 Integrated Controller

The integrated control of the wind farm and energy store is illustrated in Figure 6.25 for providing the range of control functions outlined in section 6.6.1 to section 6.6.4.

By scheduling the state of charge reference point (SoC_{ref}), the planned energy stored in the battery can be indirectly controlled, whilst allowing power fluctuation smoothing to take priority. A forecast is used to predict the wind farm's output ($P_{forecast}$) during the next balancing period to be submitted. The state of charge controller then alters the next FPN to be submitted, in order to schedule a charge, discharge or neither (ΔP_{SoC}), to maintain the battery's state of charge near target. Any deviations between this modified power production schedule (P_{FPN}) and the actual wind farm output (P_{WF_Grid}) are then combined with any power demands from the frequency controller (ΔP_{freq}) to set the power demand for the VRFB (P_{VRB_Ref}). However, if the battery's power demand exceeds the maximum charging rate (1pu) then the wind farm reference (P_{WF_Ref}) is modified as well.

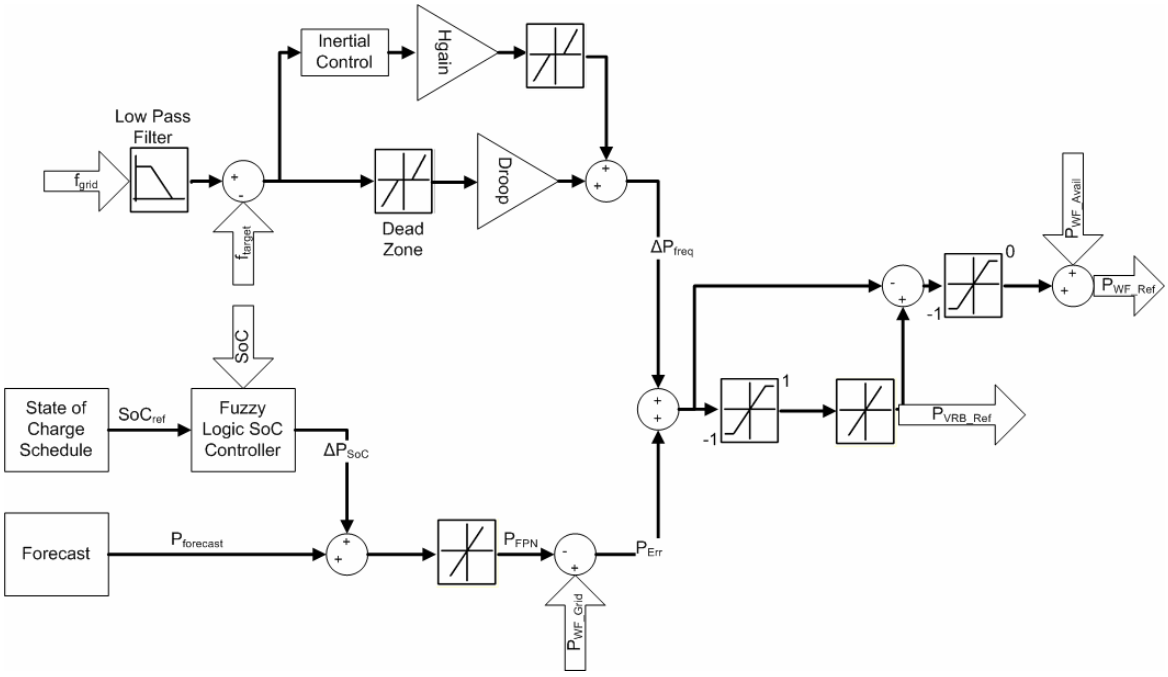

Figure 6.25: Integrated Power Smoothing and Frequency Response Control including, top to bottom, inertial response, droop response, state of charge management, forecasting and wind smoothing

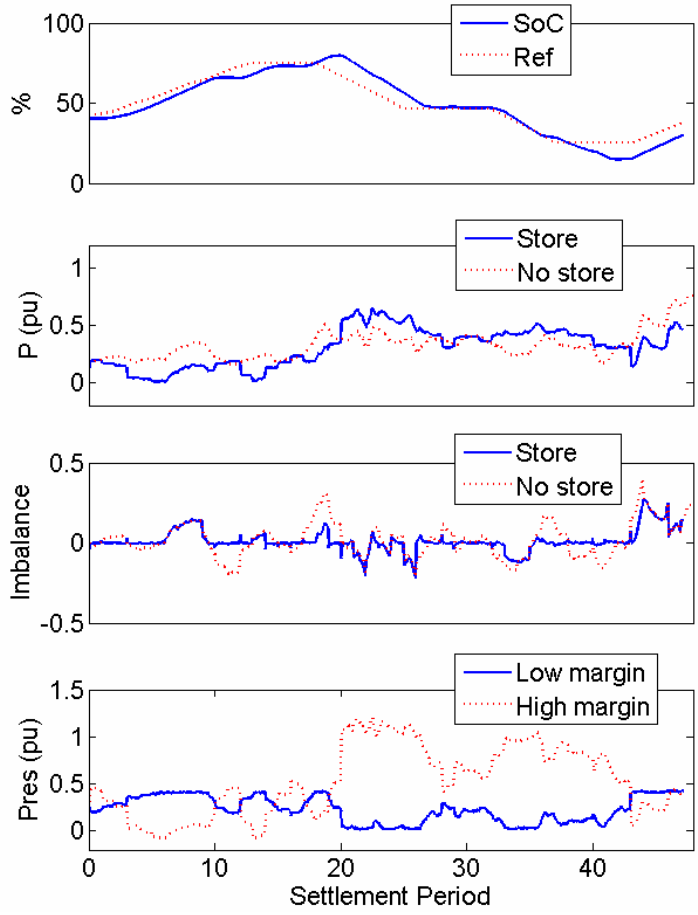

Figure 6.26: Performance of Integrated Wind Farm and VRFB Controller

Figure 6.26 shows the operation of the integrated controller for the wind farm equipped with a 25% (75MW) store rated for 6 hours output at maximum power. The plots' x axes are defined in terms of the settlement periods (1/2 hour periods, hence 48 per day). From

the top plot, it can be seen that the SoC control clearly operates well, with the SoC broadly following the reference set for it. The SOC does not track perfectly as the battery uses power capacity to smooth the wind farm's output and reduce its imbalance of actual power output to scheduled power output.

The second plot compares the output of the wind farm with a store, with that of a wind farm alone (P). The wind farm attempts to maintain a constant output in each half-hour balancing period, with a 1 minute ramp between periods. This is in order to additionally provide a stable base power output for frequency response, however, extreme gusts and lulls can still lead to some imbalance (albeit at a reduced level) as shown in the third plot (Imbalance). This imbalance is undesirable from a power system perspective and would be penalised by having to be covered by the wind farm operator purchasing the shortfall at above the typical market rate or selling an excess at reduced price. Nevertheless, this penalty does not necessitate sizing an energy store to cover any possible imbalance, as this would lead to a store of equal capacity to the wind farm, with much of that capacity rarely used.

The store is scheduled to charge at night (SoC ref increases), which is reflected in the lower output from the combined wind farm and store during this period when compared to the wind farm alone. This stored energy is then released during the morning and evening peaks, by scheduling the SoC reference to fall.

Finally, the fourth plot down shows the maximum power reserves (Pres) available at any given time for either high or low frequency response. During the periods when the energy store is discharging, to take advantage of the day-night price differential, little or no low frequency response capability is available. However, during these periods the system typically has higher inertia due to more synchronized plant and the requirement for frequency response reserve is lower and more marginal plant would be online. Conversely, at night time, the margin for high frequency response capability is lower, as the store is charging and therefore does not have margin to regulate the plant output downwards. However, the ability of the energy store to swing from charging to discharging means that significant low frequency response capability is held. As the response capability is specified against a fixed output level, the volume of response available can be seen to continuously vary as the wind speed varies.

Overall, the figure illustrates that the innovative integrated controller presented here can be used to aggregate some of the multiple benefits of an energy store. The novel state of charge controller can also be seen to correctly manage the battery capacity and

successfully time shift energy from night to day time peaks. Meanwhile the smoothing capacity of the battery is used to meet the GB frequency response technical requirements as the combined system holds a variable reserve for increasing or decreasing combined output power.

6.7 Summary

This chapter revolves around the development of an integrated controller for the operation of a VRFB in tandem with a wind farm to provide frequency response services, energy time shifting, wind smoothing and battery state of charge management.

This chapter began (in section 6.2) by developing a simple electrochemical model of a Vanadium Redox Flow Battery, that model has sufficient accuracy to represent output voltage and round trip efficiency, whilst avoiding the complexity of a full representation of the fluid dynamics of a flow battery. This flow battery must be integrated with the grid through a boost converter and an inverter. The modelling techniques for representing these components are drawn from earlier modelling work on wind turbines and adapted for use with the energy store.

This modelling work led to a simple energy store model that is applicable to power systems study whilst allowing the viability of the VRFB to be assessed. The model has been validated against published data in section 6.4.

The energy store's power converter control is principally drawn from a wind turbine application but is further developed in order to enhance the response to grid faults, by a novel feed-forward in section 6.5. This allows the energy store to ride-through grid faults when generating or consuming power and also support the reactive power capability of the inverter supplying the grid.

Finally, an innovative controller is developed that allows an energy store to aggregate the benefits of operating with a wind farm, providing frequency response services and time-shift of the renewable energy output to peak price periods. At the heart of this control is a novel fuzzy logic controller for managing the state of charge of the VRFB. The performance of this controller is verified with simulations using real wind speed data and the previously validated models.

7 Frequency Response Economics

7.1 Introduction

The power system modelling work described in previous chapters has led to validated models of wind turbines and Vanadium Redox Flow Battery energy storage systems. This in turn led to the development of control methods for providing frequency response from stand alone wind farms or wind farms equipped with flow battery energy storage. These chapters had a particular focus on the technical capabilities of these technologies to provide fast response to frequency changes on the power system. Nevertheless, whilst they addressed the technical capabilities, both applications were left with key questions. Would the cost of curtailing wind to provide reliable frequency response be too high? Would the revenues from a flow battery energy store ever be sufficient to provide an attractive return given their additional capital cost?

This chapter attempts to bridge this gap and to address the economic aspects of providing frequency response from wind power and energy storage. A series of wind scenarios, as described in section 7.2, are used by the DIgSILENT model of a 300MW wind farm with a variety of different capacity VRFB energy stores associated. Section 7.2 also describes how the outputs from this power system model interface with MathCAD and Excel models and data which when combined create an economic model in order to assess the revenues and returns provided by the store.

Whilst the electricity market structure is introduced in section 7.2, its functions and markets, which impact on frequency response revenues, are described in greater detail in section 7.3. This section also describes the key calculations in the MathCAD model that provide the assessment of revenues from the wind farm and energy store. These calculations ultimately provide the revenue inputs to a discounted cash flow analysis and the range of appropriate discount rates is considered here.

The financial impact of adding an energy store to a wind farm's revenues is discussed in section 7.4, as well as the relative contribution of the different revenue streams. A novel method of maximising the revenues from an energy store providing frequency response, whilst putting a wind farm's output at minimal risk is introduced. This contributes to a discussion of the advantages and disadvantages of integrating the energy store with the wind farm by comparing the revenues to the case of an independent energy store. These revenue calculations lead into the net present value assessment of such energy storage projects in section 7.5. Finally section 7.6 considers the implications of this analysis and

what the alternatives for frequency response provision are, whilst linking energy storage to its potential environmental benefits.

7.2 Economic Modelling Methodology

The economic model depends on the outputs from the DIgSILENT model of a 300MW wind farm enhanced by energy stores with a variety of different ratings. This power system model is supplied with a series of ten different wind scenarios, each covering a single day, the selection of these scenarios is described in more detail in section 7.2.2. These wind inputs lead onto a persistence forecast, as described in section 6.6.1, which is modified for battery state of charge management and such that the wind farm is scheduled to hold a (variable) frequency response power reserve. This modified output forms the basis for the power output forecast (FPN) which is used later in the economic model, alongside actual output power, to assess imbalance.

The raw wind speed data drives the power system model of the wind farm and energy store, resulting in a power output profile. This model also provides a profile of the spare power capacity of the generator to regulate up or down power output, primarily through modifying the energy store's charge rate. Hence, overall the power system model passes three main outputs to the economic model: the contracted (or forecast) power profile, the actual output power profile and the reserve capacity for high and low frequency response. The interconnection of this model with the economic model is shown in Figure 7.1.

The economic model draws in data from Microsoft Excel as well as the power system model. Electricity market price data, balancing mechanism prices and frequency response market prices have all been collated in Excel spreadsheets. Historical data has been used to inform three different economic scenarios based on low, mid and high forecasts for the different prices. The data sources and projections used are described in detail in sections 7.3.2 to 7.3.4.

The economic model itself draws on the outputs of these ten different wind scenarios from the power system model, together with the three different price scenarios for power system revenues. It independently calculates the different revenue (and cost) streams for traded energy, imbalance, frequency response and ROCs before conducting a net present value analysis based on three different projections for possible costs of the flow battery installation.

By incorporating three different economic scenarios the uncertainty associated with the projection is accounted for through the range of possible different economic developments.

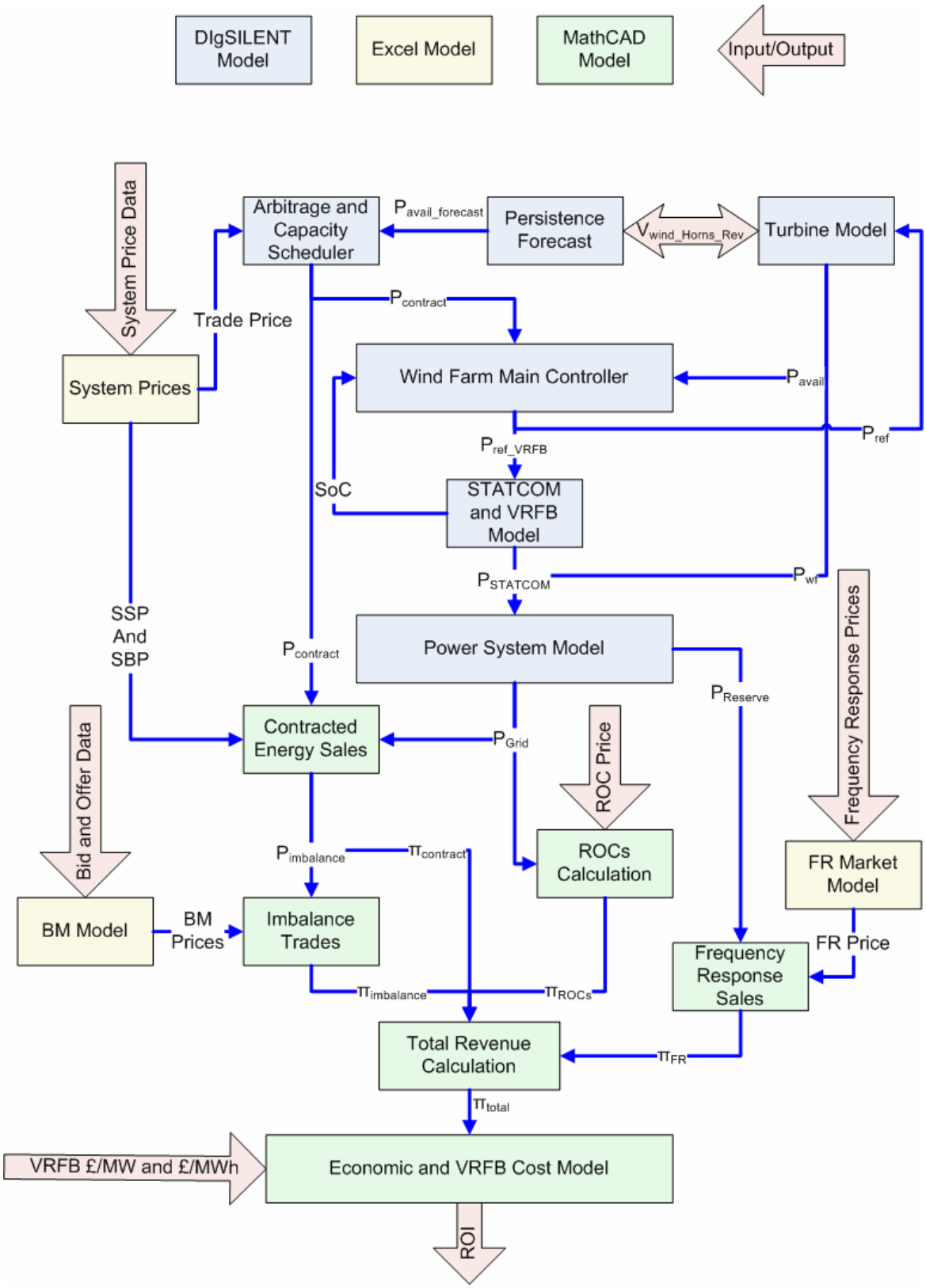

Figure 7.1: Economic Modelling Methodology

7.2.1 Electricity Market Structure

Figure 7.2 illustrates the present structure of the GB Electricity market according to National Grid [144]. It is essentially an energy only market, where participants buy and sell energy (in MWh) for delivery in a specific half hour period (herein known as a "settlement period") in the future. Such trades can take place from any time in advance up until 24 hours before the scheduled settlement period. In reality, historically, the so called "Big Six" suppliers typically internally supplied much of their demand such that the actual amounts traded through the market are small. However, this situation is liable to change.

Following the arrangement of contracts in the futures market, the short term bilateral exchange allows participants to modify their traded positions up to an hour ahead of the start of a given settlement period. At gate closure, the participants must then notify National Grid of their power production schedules (FPNs). This final hour allows National Grid time to balance the system and deal with any constraints.

National Grid's task to balance supply schedules with the demand forecast for a given settlement period is achieved by accepting Bids and Offers in the Balancing Mechanism. Participants can "Offer" to increase their output or decrease demand relative to their FPN in exchange for receiving a payment (£/MWh), conversely, they can "Bid" to decrease output or increase demand in return for paying a different price.

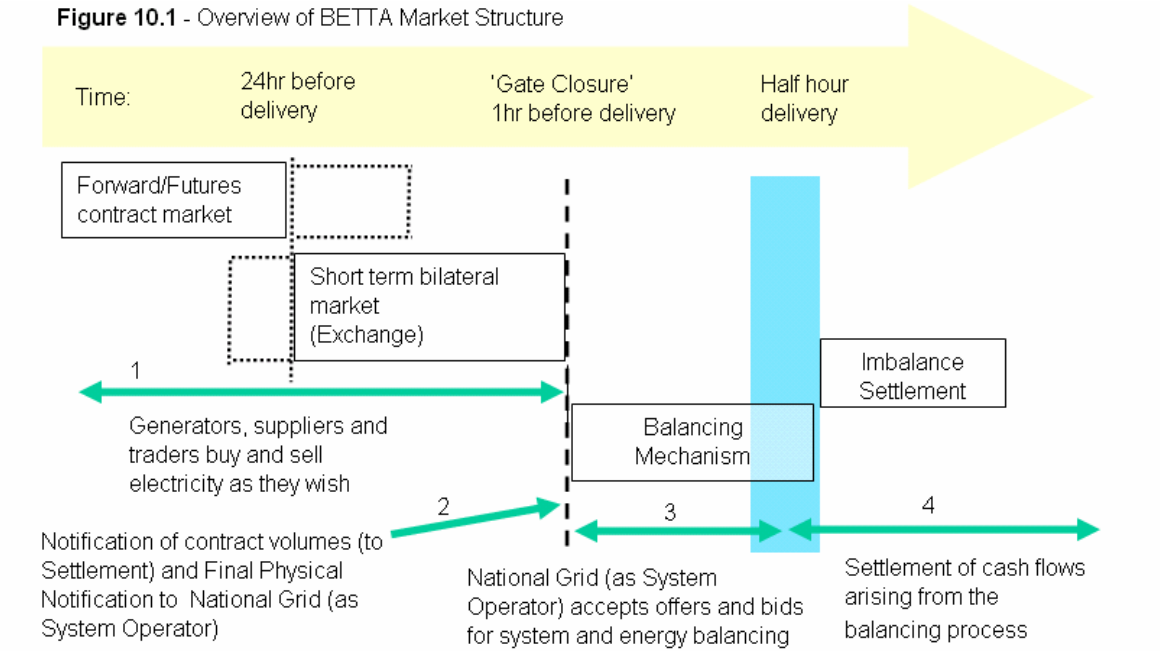

Figure 7.2: Electricity Market Structure according to National Grid [144]

National Grid, which is the "for-profit" system operator acts as counterparty to these trades. Susteras, Hathaway, Caplin and Taylor [145] have shown the range of different means by which National Grid can balance the system and have discussed the incentive

scheme by which National Grid retains a share of profit made through being incentivised to optimise the balancing services, or can be punished for any losses. Whilst there are other options than the Balancing Mechanism available to National Grid, they highlight that these represent only a minority of operations in comparison to the bids and offers.

This balancing mechanism should ensure that at the start of a given settlement period the supply schedule meets the forecast demand level. As well as ensuring the match between forecast supply and demand, the balancing mechanism is also used to ensure that there is sufficient headroom and footroom on frequency responsive plant to meet the requirements of Figure 2.23.

During each settlement period, active frequency responsive plant ensures the continuous match between actual supply and demand outturns. Any significant forecast errors or supply shortfalls are then met over longer time-scales through use of Short Term Operational Reserves (STOR) and fast starting units. Following the conclusion of a settlement period the system operator then retrospectively settles the imbalance payments.

7.2.2 Scenario Analysis

A scenario based approach has been used to assess the economic benefit of adding a VRFB to a wind farm. Under this approach it is necessary to ensure that the scenarios tested cover the true range of expected operating conditions. The wind data, which in turn sets the power output from the power system model, has been extracted from several months of measured data from Horns Rev offshore wind farm. Analysing the complete data set would have required excessive simulation time from the power system model; therefore a subset has been used. However, the subset is reflective of the underlying data set, particularly for the following parameters:

- Overall Capacity Factor: appropriate selection of data led to an equivalent estimation of the wind farm's energy yield.
- Power Output Fluctuation: the scenarios analysed reasonably represent the variability of the power output that the full wind farm produced.

The capacity factor is relatively straightforward to compare by finding the average output of the complete dataset and comparing it to the average output of the scenarios chosen. This comparison shows a capacity factor of 0.43 for the complete dataset, versus a capacity factor of 0.42 for the sub set, which is well within the bounds of variability in capacity factor found between different wind farms. This high capacity factor is indicative of an excellent offshore wind resource.

The subset consists of data from ten periods of one day selected from the complete dataset. Using a smaller subset inherently means that the histogram of power fluctuations is not as consistent for the scenarios subset as for the full dataset. However, Figure 7.3 shows the comparative histograms of five minute power ramping incidents for the full data set and the subset, with the subset appropriately scaled to reflect its lower number of data points. These histograms are broadly comparable, with the extremes of ramping reflected reasonably well (i.e. the worst case scenarios will be represented in the analysis). However, it should be noted that these scenarios have a slightly higher representation of rapid reduction in output power compared to the original dataset, and a lower representation of extremely fast increases in power output. Nevertheless, overall the scenarios selected are reasonably reflective of the range of operation that an offshore wind farm and energy storage system would encounter.

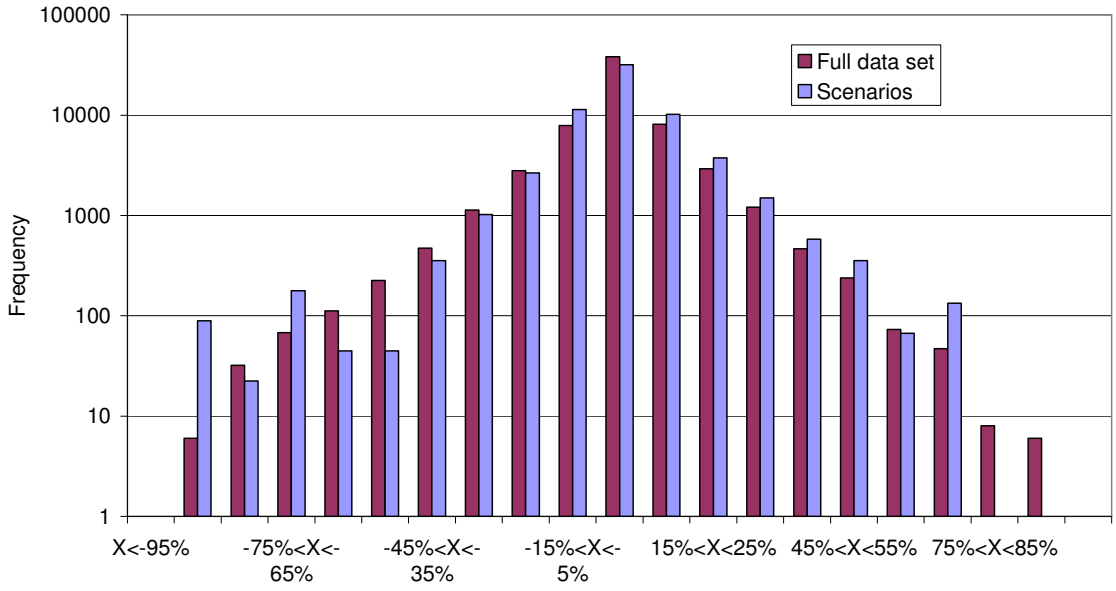

Figure 7.3: Horns Rev Wind Speed Data Subset Comparison, histogram of forecast errors for an hour ahead FPN (the x axis shows the % error in forecast to actual output as a percentage of total wind farm rating)

The different wind scenarios used are shown in Figure 7.4, and illustrate that there are prolonged periods with both high and low wind speeds as well as a range of scenarios with high levels of turbulence reflected in the output power profiles (for example days 3 and 5). Additionally, some start the 24 hour period at very low output and ramp up considerably (day 2), whilst others do the opposite (day 1 and day 6), thereby challenging the output scheduling.

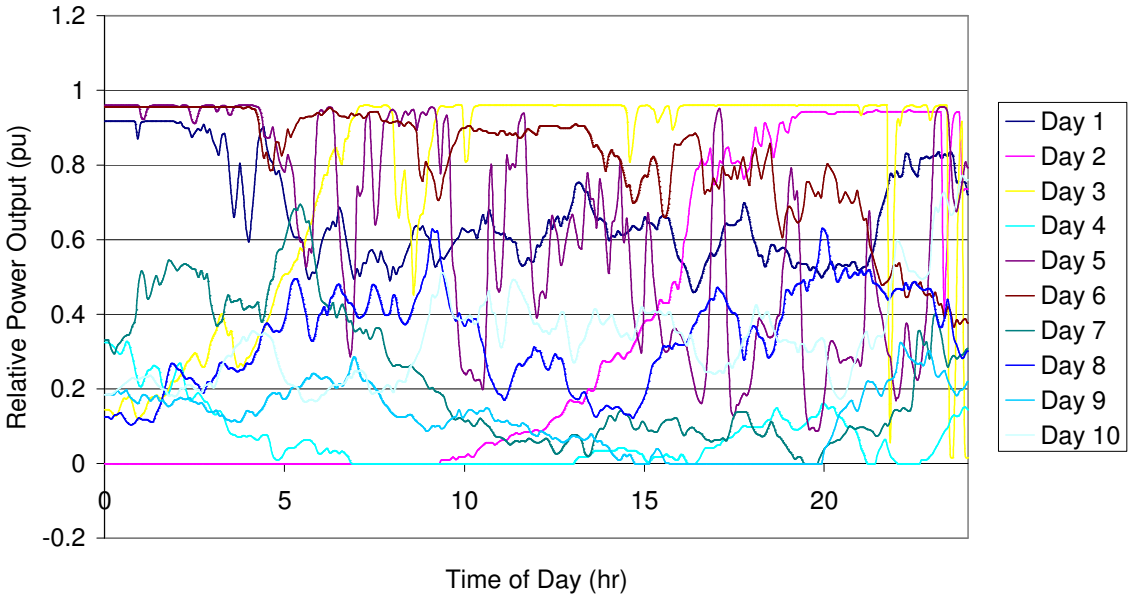

Figure 7.4: Wind Speed Scenarios

7.2.3 Energy Store Capacity

Bludszuweit and Dominguez-Navarro [146] suggest that sizing an energy store to cover wind farm forecast errors can be done probabilistically. Essentially they propose calculating the required energy capacity by integrating the error between historic forecasts and actual power output, whilst allowing a certain proportion of "unserved energy". However, this methodology is only applicable to compensating for forecast errors.

Korpaas, Holen and Hildrum [147] consider instead a mixed probabilistic approach combined with scenarios to test the sizing of the store, additionally they incorporate the effects of a varying electricity market spot price on the storage operation. However, their work does not consider diurnal pricing leading to arbitrage opportunities and considers short term power regulation, such as for frequency response, as a cost. These differences are primarily due to its focus on the Nordpool market, which has significant hydroelectric resources and a different market structure.

Brekken *et al.* [143] have proposed sizing a Zinc-Bromine flow battery energy store using a scenario approach. In their work they consider power and energy ratings at 0.1pu steps relative to the wind farm rating, before increasing the resolution of their study to find the optimal solution. Their work was focussed purely on avoiding imbalance penalties in the Bonneville Power Authorities' region of western U.S.A. and whilst the optimal sizes depend on different economics the general approach of using different energy store sizes is useful.

In order to assess the different possible sizes of energy store, six different power ratings have been selected and for each different power rating, four different discharge times have

been simulated. The power ratings have been selected as a varying proportion of the wind farm's output power. The smallest rating considered is 10% of the wind farm's output, which is the minimum size to meet the frequency response requirement of GB Grid Code. The largest size considered is 33% of the wind farm's power, which equates to the largest conceivable size of the wind farm's IGBT SVC and therefore the point at which the power electronic interface cost would start to significantly increase. 33% corresponds to the Grid Code mandated reactive power capacity to achieve a ±0.95 power factor at the grid connection point.

The four energy ratings have been defined according to a number of hours discharge at full power output. This means the energy rating for the 1 hour discharge case with a 20% store is twice that of the 10% case. The relative energy ratings of the store can be seen in Table 7.1.

		Discharge Time at Full Power				
		No Store	1 hour	3 hours	6 hours	10 hours
Store Power Rating	No Store	0	N/A			
	10%	N/A	0.1	0.3	0.6	1
	15%		0.15	0.45	0.9	1.5
	20%		0.2	0.6	1.2	2
	25%		0.25	0.75	1.5	2.5
	30%		0.3	0.9	1.8	3
	33%		0.33	1	2	3.3

Table 7.1: Energy Store Power and Energy Ratings

The wind farm itself is considered to be 300MW (to be of similar size to UK round 2 offshore projects). Hence, energy store power ratings vary from 30MW to 100MW. The size of the wind farm and consequently the energy stores are reflective of the fact that providers of frequency response in the UK must offer a minimum of 10MW response to access the market. It is anticipated, however, that any demonstrations or prototype projects would have to be significantly smaller.

7.2.4 Discounted Cash Flow Analysis

As the primary cost of an energy storage facility would be the initial capital cost of the technology, whilst the revenue would accrue over time, it is appropriate to consider the economic case on the basis of a Discounted Cash Flow (DCF) analysis. This allows the future revenues to be converted to a Net Present Value (NPV) using an interest rate to accommodate money's time value and to a lesser extent, risk. The NPV of a future year's revenue (π_n) is given in Equation 7.1, where i is the percentage interest rate applied and n is the number is years into the future.

Equation 7.1 $$\pi_{NPV} = \left\{ \frac{100}{(100+i)} \right\}^{n} \cdot \pi_{n}$$

Where the scenario analysis implicitly assumes that the future revenues will be equal in any given year, the total revenue over a period of N years can be calculated from the sum of a geometric series according to Equation 7.2.

Equation 7.2 $$\Pi_{NPV} = \sum_{n=1}^{N} \pi_{NPV} = \frac{\pi_{1} \cdot \left(1 - \left\{ \frac{100}{(100+i)} \right\}^{n} \right)}{1 - \left\{ \frac{100}{(100+i)} \right\}}$$

As the expected life of a VRFB is around 20 years, with a membrane replacement after 10 years, this is the time frame used for the DCF. The interest rate used strongly influences the outcome of a DCF analysis and this rate in turn may depend on several factors according to Aston [148]:

- The prevailing bank interest rate.
- The return an equivalent investment could make.
- Returns to shareholders.
- A premium for a project's risk.

The interest rates applied, along with the costs of operating a VRFB are discussed further in section 7.3.

7.2.5 Market Reform

The widespread deployment of wind power on the GB power system could have a significant impact on the electricity market. James Cox [149] of Pöyry Consulting has highlighted the significant price volatility that could be seen during periods of high and low wind. Periods of low wind and high demand could lead to particular stress on the system, leading to a particular concern for DECC over the market's structure. As the electricity market currently operates as an energy only market, there is a perceived risk that it is not sufficiently flexible to provide a return on investments in peaking capacity which may be used only rarely to cover low wind, high demand periods.

Owing to the concerns that the GB electricity market will not deliver security of supply, DECC [150] have been consulting on modifying the existing market through the addition of a capacity mechanism. This would act as an additional revenue stream for providers of firm capacity, such as energy storage. Hence, whilst this work attempts to estimate the

revenue that an energy store could earn under today's market arrangements, it should be recognised that due to proposed reforms these estimates are subject to some uncertainty.

7.3 Economic Data

7.3.1 Renewable Obligation Certificates

The UK wind industry is currently supported through the Renewables Obligation Certificate (ROCs) scheme, where a power supplier must source a rising share of electricity from renewable sources. Wind farms are issued with these certificates for each MWh of energy produced. These certificates can then be traded in a market and the typical revenue, per MWh generated, is often higher for this revenue source than for a wind farm's traded energy.

Equation 7.3 $$\Pi_{ROC} = \left(\int_{t=0}^{t=T} P_{grid} \cdot dt \right) \cdot \overline{\pi_{ROC}}$$ Where Π_{ROC} is the total revenue and $\overline{\pi_{ROC}}$ is a long term average price for ROCs, both in £/MWh.

The challenge when assessing the revenue ROCs generate is not in the mathematical assessment, which is shown in Equation 7.3, but in understanding the regulations as to what is and what is not eligible for ROCs, and therefore the impact an energy store would have.

For an offshore wind farm, the ROCs are metered offshore and the energy store would be likely to be located onshore, hence any energy transferred to and from the store is independent of the ROCs regime. This has benefits as it is simple and the round trip losses of the energy store do not lead to ROC losses. This is inline with the present definitions of ROCs which are only available for specific, named, technologies, and this list excludes storage.

The onshore case is less clear as the ROCs could be metered either side of the energy store's connection. When the energy store is included, this means that any round trip energy losses would lead to lost ROCs and therefore have a negative impact on the wind farm's overall revenue. Owing to the lack of clarity around what is and isn't eligible for ROCs, whilst they are included in the economic assessment, two different cases are assessed: including ROCs at 1ROC/MWh and excluding them.

7.3.2 Energy Price and System Price Data

In order to assess the revenue from the energy yield of the wind farm, a simplifying assumption has been made, that the energy is traded at the average of the system buy and

system sell price. This is the same underlying assumption used by Collins, Parkes and Tindal [151] in assessing the value of advanced forecasting techniques for British power markets. This assumption implicitly assumes that the economic penalty for over or under-estimation of the wind power forecast is equal and that the system prices are reflective of the actual market price paid in the forward/futures market (see Figure 7.2). If this assumption is not made, the high probability of wind power missing its production schedules, relative to that of a dispatchable fossil fired plant, means bidding strategies would become important for maximising revenues thereby significantly complicating matters.

These system buy and sell prices for every settlement period can be downloaded from the Elexon reporting website (www.bmreports.com). One year's data from March 2010 to February 2011 has been collated and has been approved for use here by Elexon.

Figure 7.5 shows the annual price averages and variation across the settlement periods, with settlement period 1 corresponding to 00:00 to 00:30 each day. This price profile clearly illustrates the impact of energy use on the price. During the night hours energy use is low, leading to lower system price, however, as the day begins energy use and the corresponding price ramps up. The price stays high during the morning work hours before declining in the afternoon. The biggest peak of the day is seen during the evening peak, as domestic demand for heat, light and appliances leads to high demand. Following this peak, demand gradually declines.

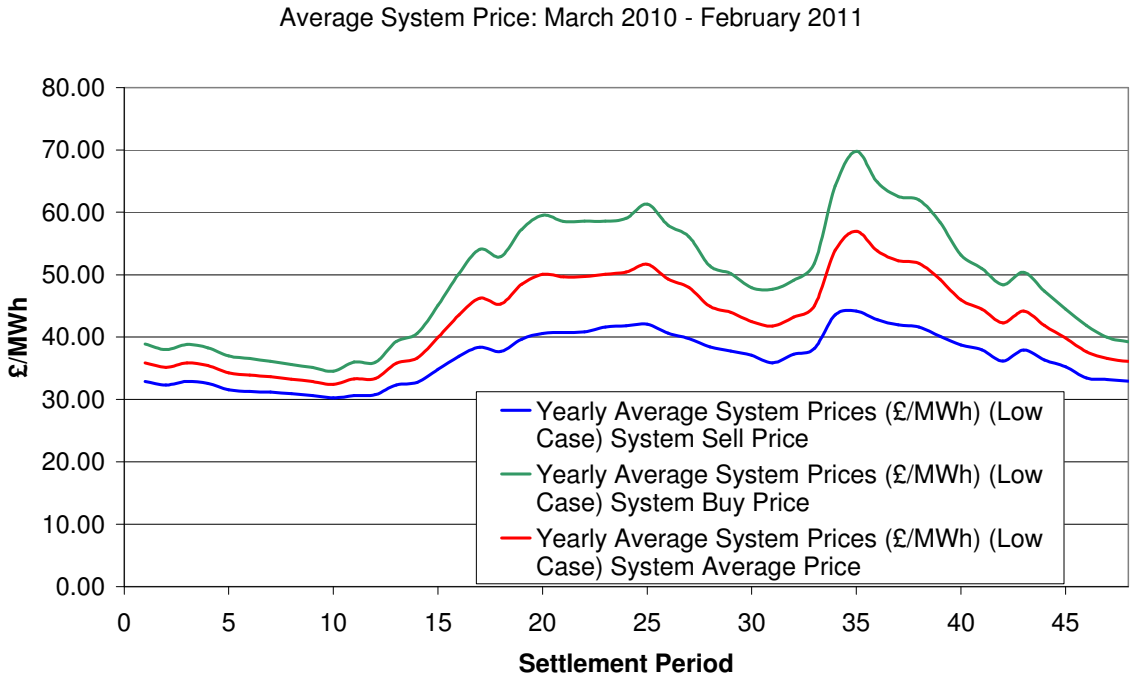

Figure 7.5: Average System Buy and Sell Prices for March 2010 to February 2011

The revenue from traded energy is derived by assuming that the forecast will be perfect and therefore the entire forecast energy yield is sold. The price is derived as the average of the system buy and sell prices and revenue is calculated as shown in Equation 7.4.

Equation 7.4 $$\Pi_{sales} = \sum_{SP=1}^{48} \left\{ \left(\int_{t=0}^{30\,\min} P_{ccl} \cdot dt \right) \cdot \left(\frac{\overline{\pi_{SBP\,SP}} + \overline{\pi_{SSP\,SP}}}{2} \right) \right\}$$ Where P_{ccl} is the power production schedule (MW), $\overline{\pi_{SBP\,SP}}$ is the long term average system buy price for the settlement period SP and $\overline{\pi_{SSP\,SP}}$ is likewise the long term average system sell price for a particular settlement period.

The error in the power production forecast is accounted for by the separate imbalance calculation(see next section). Furthermore, the scheduling of the battery state of charge inherently takes account of day-night arbitrage, as P_{ccl} will be modified to be higher during the periods with higher prices.

OFGEM [152] have presented an analysis of projected development in electricity costs up to 2025, called "Project Discovery". According to their analysis electricity prices are likely to rise by approximately 14% under a central projection or 24% under a worst case. Today's system prices form the basis of the "Low" case for the economic forecast, with these rates of increase being used to adapt the system price profile to give "Mid" and "High" priced alternative scenarios for comparison.

7.3.3 Imbalance

The costs associated with deviating from a contracted FPN during a settlement period fall on a wind farm through the System Buy Price (SBP) and System Sell Price (SSP). If the wind farm is short of its projected output then it must pay for the energy shortfall at the (usually higher) SBP. If the wind farm overproduces relative to the forecast then it will only receive the lower SSP. Bathurst and Strbac [153] have shown how using an energy store to avoid these costs and maximise revenue can lead to added value for a wind farm, however, their analysis focuses on revenues and not costs nor the likelihood that a system would pay back.

The revenue associated with the imbalance payments is calculated according to Equation 7.5 for periods where the wind farm's output is above the contracted level and Equation 7.6 when it is below.

Equation 7.5 $$\Pi_{SSP} = \sum_{SP=1}^{48} \left\{ \left(\int_{t=0}^{30\,\min} \left(P_{grid} - P_{ccl} \right) \cdot dt \right) \cdot \overline{\pi_{SSPSP}} \right\}$$

Equation 7.6 $$\Pi_{SBP} = \sum_{SP=1}^{48} \left\{ \left(\int_{t=0}^{30\,\min} \left(P_{grid} - P_{ccl} \right) \cdot dt \right) \cdot \overline{\pi_{SBPSP}} \right\}$$

The total revenue/cost associated with the imbalance of the wind farm is therefore the sum of these two components as in Equation 7.7.

Equation 7.7 $$\Pi_{\mathrm{Im}\,balance} = \Pi_{SSP} + \Pi_{SBP}$$

7.3.4 Frequency Response Market

7.3.4.1 Balancing Mechanism Payments

As indicated in section 7.2.1, the balancing mechanism is used by National Grid to avoid constraints and match the planned balance between scheduled supply and forecast demand on the power system. It may also be used to adjust the FPN of plant to create "headroom" for low frequency response or "footroom" for high frequency response. Hence, even with a system where supply and demand are scheduled to balance during a settlement period, National Grid may end up accepting bids on some plant and equal offers on others in order to ensure that their frequency response margins (see Figure 2.23) are met.

The offer price relates to an increase in generation and therefore needs to cover additional fuel use plus profit; hence, the offer price is typically loosely tied to the cost of marginal plant on the system. Bids relate to a reduction in power output and therefore ought to lead to fuel savings. However, the bids will be made at a level less than the contracted price that the supplier has received, such that they typically recover their profit, whilst accounting for fuel savings. Hence, whilst offers are only ever positive values, a bid may be negative, implying that a generator requires a net payment to reduce its output. Overall the balancing mechanism prices, which are updated for each settlement period an hour ahead of delivery, add a cost to the provision of frequency response that is reflective of the short term market conditions.

The cost of the balancing mechanism payments made to change the output on frequency responsive plant are available through National Grid's [154] market information data on commercial (or "Firm") frequency response. This data has been collated over a twelve month period (March 2010 to February 2011) and averaged to find the incremental cost of frequency response attributable to the balancing mechanism. This can be seen in Table 7.2.

Incorporating the bid and offer data into the calculation of energy store revenue, introduces an element of value, rather than revenue. Currently an energy store, would not require a deload to provide frequency response services and therefore would only directly access the holding payments. However, it is assumed that it could tender higher holding payment prices and still be selected in the market as that would lead to an overall optimisation of the response holding.

7.3.4.2 Holding Payments

The balancing mechanism reflects near real time frequency response pricing, but only covers plant which require an FPN change in order to create headroom or footroom. In addition to the revenue from the balancing mechanism, there is a separate market for frequency response which operates monthly covering all relevant plant. Participants in this market indicate the price (£/MWh, where a MWh here is a measure of potential to deliver energy, not actual energy delivered) that they require in order to hold margin for primary, secondary or high frequency response. National Grid [155] publishes details of the monthly prices paid for plant to hold frequency response.

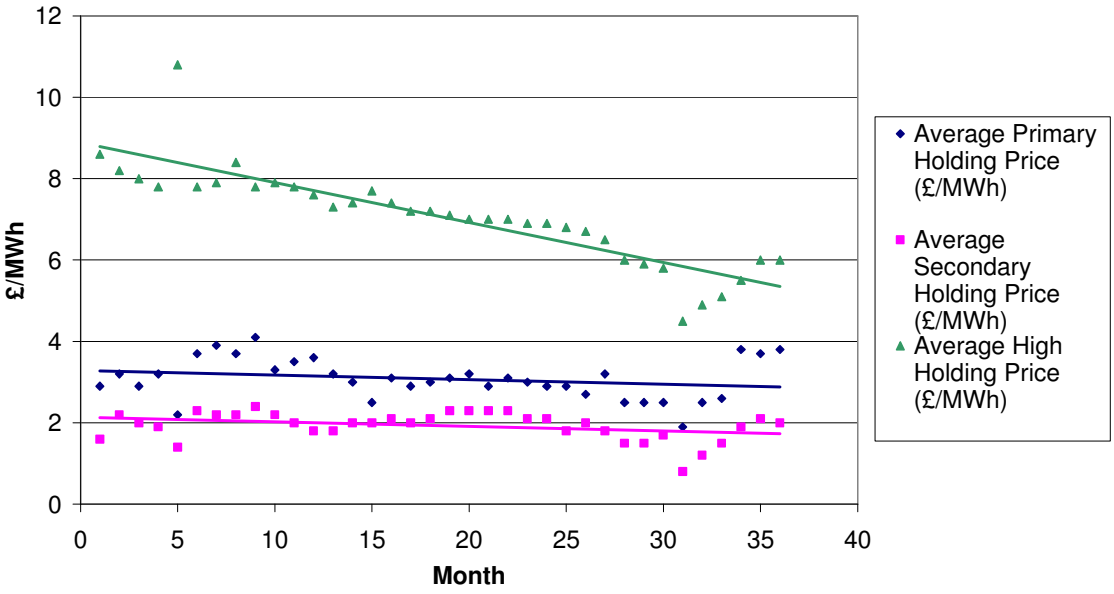

Figure 7.6: Mandatory Frequency Response Market Price Evolution over a 3 year period March 2008-February 2011)

As the development of the frequency response market is a result of the relatively recent deregulation of the electricity industry, prices are still evolving. Figure 7.6 attempts to illustrate the trend in these prices over time. This shows a strong negative trend for high frequency response, until, towards the end of the period for which data was available, prices stabilised and perhaps even slightly increased. The development in price for primary and secondary response is less dramatic, with prices little changed over the period.

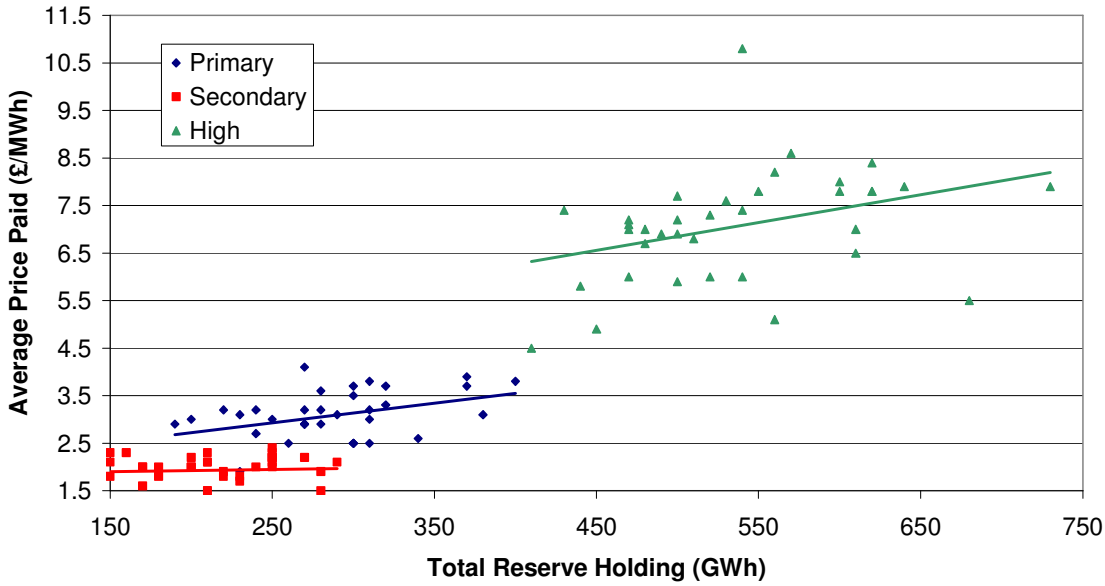

Figure 7.7: Mandatory Frequency Response Market Price to Holding Volume Relationship

Figure 7.7 shows that the prices paid for response have not just developed over time, there is a correlation between the holdings that National Grid purchase for a given month and the price paid on average. This is particularly relevant because the projected increase in requirement for primary and secondary response (Figure 2.23) would therefore suggest a developing trend towards higher prices.

7.3.4.3 Response Payments

Provision of response, whether reduction in power output in response to a high grid frequency, or increase in power output following a frequency fall would lead to a change in the fuel usage of a conventional fossil fuel fired power station. As a result, frequency responsive plant is compensated, retrospectively, according to its response energy to frequency deviations. However, these response payments are typically small in comparison to the payments previously discussed and typically average out to nearly zero. Hence, the contribution of response payments to the economic case has been ignored with National Grid's confirmation that this is a reasonable simplification.

Scenario	System Prices	Balancing Mechanism (£/MWh)		ROCs (£/MWh)	Frequency Response Holding Prices (£/MWh)		
		Bids	Offers		Primary	Secondary	High
Low	As today	5.4	2.2	45	3.0	2.0	7.0
Mid	+14%	6.2	2.5	50	4.0	2.5	7.0
High	+24%	6.7	2.7	55	4.5	3.0	7.5

Table 7.2: Economic Scenarios

Table 7.2 illustrates the three different scenarios that have been considered for the economic analysis of the energy store. The "Low" case takes prices that are approximately

the same as today, whilst developments in the energy market and frequency response market are modelled separately in the three scenarios owing to differing impacts of wind's deployment.

Equation 7.8 to Equation 7.10 show how the revenues from frequency response are calculated based on the margins held and the different pricing mechanisms.

Equation 7.8 $$\Pi_{High} = \left(\int_{t=0}^{30\,\min} (P_{ccl} - P_{sel}) \cdot dt \right) \cdot (\pi_{Hold\_high} + \pi_{Offer})$$ Where P_{sel} is the minimum possible combined output (MW), which may be negative; π_{Hold_high} is the payment for holding power available to withdraw MWh of energy as needed (£/MWh); π_{Offer} is the system wide average offer payment required to create the footroom for high response (£/MWh).

Equation 7.9 $$\Pi_{Low} = \left(\int_{t=0}^{30\,\min} (P_{mel} - P_{ccl}) \cdot dt \right) \cdot (\pi_{Hold\_prim} + \pi_{Hold\_sec} + \pi_{Bid})$$ π_{Hold_prim} and π_{Hold_sec} are the payments for holding power available to deliver MWh of energy as needed (£/MWh) within primary and secondary timescales; π_{Bid} is the system wide average bid payment required to create the headroom for low response (£/MWh).

Equation 7.10 $$\Pi_{FR} = \Pi_{High} + \Pi_{Low}$$

7.3.5 Arbitrage Scheduling

Figure 7.5 illustrates that there is a significant potential revenue opportunity from buying energy at the low night time prices and selling it into the day time peak periods. Figure 7.8 represents a simplified analysis of the absolute maximum revenue that could be derived from arbitrage, capacity firming and frequency response combined under today's prices. The frequency response payments have been derived from the residual power margin held for either low or high frequency response after the arbitrage charging or discharging takes priority. The arbitrage revenues been generated by ordering the settlement periods by average system price and assuming if only 1 hour is allocated to arbitrage that buying would take place (at the SSP) in the lowest priced settlement period and selling in the highest (at the SBP). The use of the system buy and sell prices implicitly incorporates the maximum benefit from capacity firming.

For an energy store with 6 hours capacity, buying would take place in the 12 lowest priced settlement periods and selling in the 12 highest. Where the efficiency is less than 100%, the number of settlement periods that the energy store can sell into profitably is reduced.

This places a rough upper limit on the amount that can be earned from different energy store ratings through arbitrage. Also on the plot is again a rough estimate for the combined value of frequency response without arbitrage, illustrating that in the 60-75% round trip efficiency band, as this plot shows the maximum combined revenue, arbitrage may only add incrementally to the frequency response revenues.

Dependent on the energy storage capacity of the VRFB under consideration, the arbitrage scheduler uses this plot, in conjunction with the ordered settlement period prices to generate a schedule as to whether to use capacity for buying selling or holding energy. This introduces some imperfection into the controller as Figure 7.8 is based on approximate values and relies on long term average system prices, but this is reflective to some extent of real world operation.

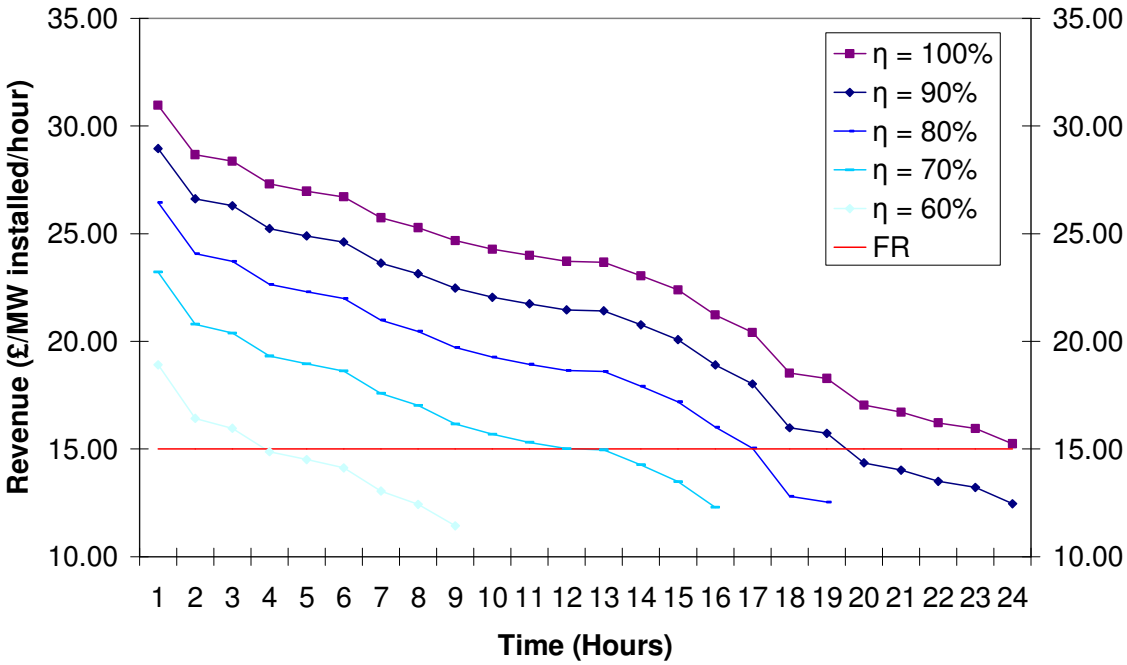

Figure 7.8: Comparison of Arbitrage and Frequency Response Revenues, the first hour represents charging in the cheapest half-hour period and discharging into the single peak half hour period, with longer charge/discharge periods shown moving right on the x axis

Figure 7.8 includes many assumptions and was generated to assess whether the aggregated benefits of different revenue streams from the energy store could produce meaningful revenue. It provides an upper bound on the possible revenue from arbitrage as the full differential between the minimum system sell price and the maximum system buy price is unlikely to be realised. Overall, it indicates that aggregating benefits in this manner is likely to provide some improvement over a single purpose energy store, even with limited round trip efficiency. The scenario analysis provides a more accurate assessment of the potential aggregated revenues.

7.3.6 VRFB Costs

The principle costs associated with the VRFB are the capital costs, both the energy cost ($/kWh) and the power capacity cost ($/kW). Figure 5.1 provided the indicative range of costs of power capacity according to current literature, whilst Figure 5.2 provided the indicative range of current energy capacity costs, again based on the available literature. Lewis and Sharman [156] have presented on the costs of VRFBs highlighting their benefits for longer term energy storage. Their analysis of Prudent Energy and GE Energy's system estimated the power cost at around $1700/kW and the energy cost at $300/kWh. These form the central estimate for costs as outlined in Table 7.3, with the higher and lower estimates based around this central projection.

Kear, Shah and Walsh [157] have conducted an extensive analysis of VRFBs considering commercialisation and current costs. Their analysis estimates that a typical VRFB installation would require a membrane refurbishment after 10 years operation and that this cost would be in the order of 15% of the initial capital cost.

Scenario	Power Cost ($/kW)	Energy Cost ($/kWh)
Low	1200	200
Mid	1700	300
High	2200	400

Table 7.3: Cost Scenarios for the VRFB

Kear, Shah and Walsh [157] include a significantly higher estimate of operations and maintenance costs than Bindner [137], whose installation has required no maintenance over several years operation. Here an operations and maintenance cost of the VRFB is assumed to be around 0.5% of the capital cost per year.

7.3.7 Discount Rate and Sensitivity Analysis

Under a DCF analysis, the discount rate used significantly affects the results of the study. Oak Ridge [158] have conducted a study on deploying used batteries in power systems, under their central case a discount rate of 4% has been used. This is low compared to a typical discount rate but reflects current low interest rates and a relatively low risk project. As the analysis here includes scenarios covering low, mid and high end estimates of revenues, it is reasonable that the discount rate should not include a significant risk component, as this is reflected in the different scenarios; instead basing it on alternative returns is reasonable. However, this is still based on an American project and should be compared to the discount rates appropriate for renewable energy generation projects in

general in the UK. Oxera [159] have conducted an extensive survey of discount rates that are applicable to low carbon power generation projects. Furthermore, they estimate that appropriate policy support could lead to discount rates that are 2-3% lower by 2020 for supported technologies. Figure 7.9 illustrates the range of discount rates that are typical today and are expected to be typical in 2020 with appropriate government support.

In view of these typical rates, and recognising that the risk weighting is largely reflected in the different scenarios addressed, 4% can be seen as a reasonable low end estimate for use in the analysis, where the realistic time frame for deployment of large scale energy storage is closer to 2020. However, a sensitivity analysis is included where rates of 8% and 12% have been used to stress test the results under significantly higher rates of interest.

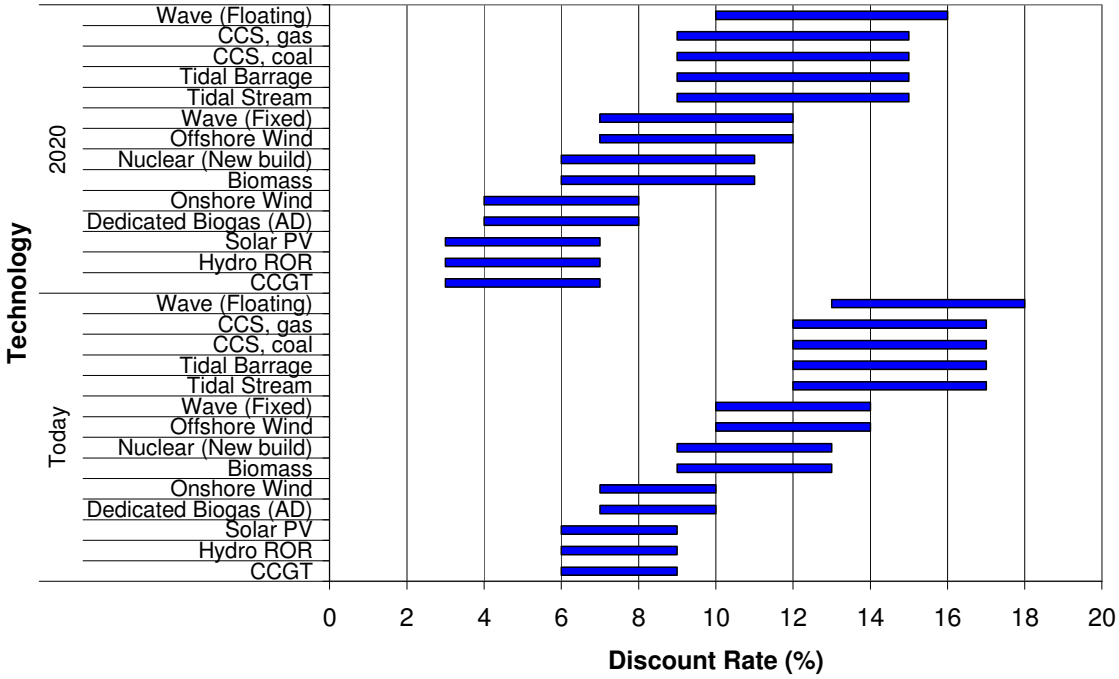

Figure 7.9: Oxera, 2011 discount rates today and 2020 for typical low carbon sources

7.4 Energy Storage Revenues

This section considers the benefits that an energy store can bring to a wind farm purely in terms of its impact on revenues. It begins by considering the case where the energy store is integrated with the wind farm and therefore responsible for smoothing the wind power in order to meet the requirement to provide frequency response from a stable output level. It then moves on to considering the case where the energy store is entirely independent of the wind farm before introducing an optimal arrangement.

7.4.1 Integrated Energy Store Revenues

The annual (undiscounted) revenues from the wind farm with an energy store can be compared to the case without a store. This allows an assessment of the incremental revenue that the energy store provides over and above that of the wind farm alone. The resulting incremental annual revenues for the three economic scenarios are plotted in Figure 7.11 through Figure 7.13. The finite number of scenarios considered in the analysis means that the results for each different store size do not provide totally smooth plots, which would be possible only with a very large scenario pool. The intermittency and variability of the wind, combined with different arbitrage capabilities of each of the different energy ratings, mean that the power profile of the energy store varies significantly between the various store sizes, even under the same wind profile.

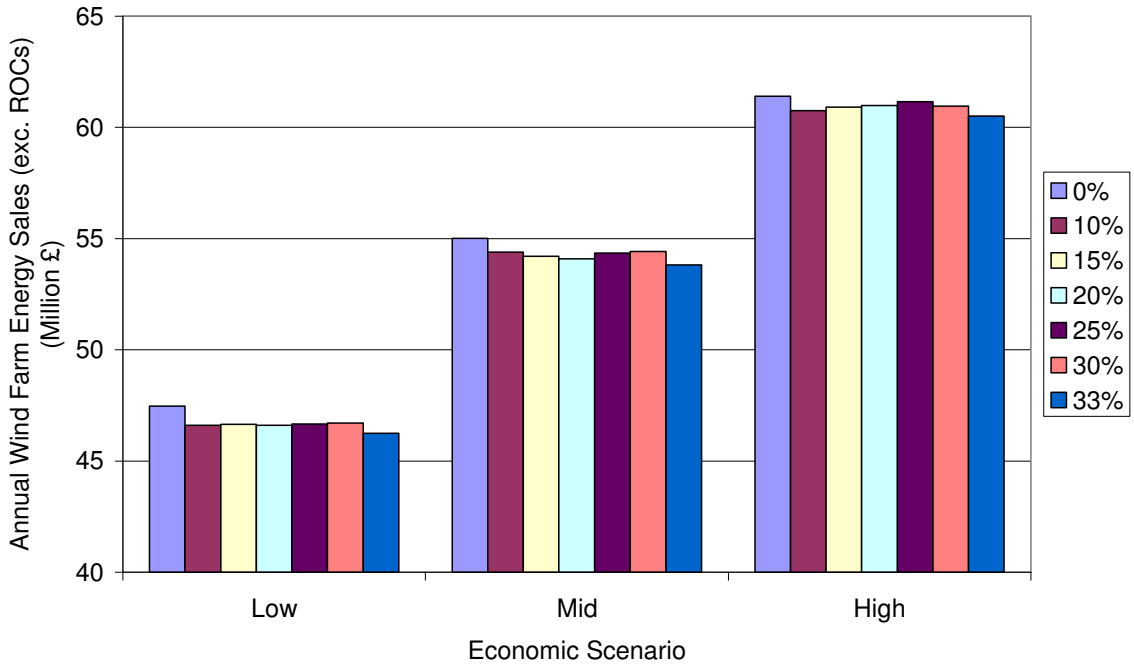

Figure 7.10: Traded Energy Revenues, excluding frequency response, for the different power capacities considered

As the efficiency of the VRFB varies depending on the power input/output; this leads to significantly different energy losses between the different scenarios. These energy losses lead to lost sales and may lead to lost ROCs, which can only be compensated for by selling the remaining energy at a higher price. However, as Figure 7.10 illustrates, the time shifting of energy to higher prices and the increased certainty of delivery are insufficient economic levers in any of these scenarios to compensate for the lost energy in the energy store. This is because the VRFB's round trip efficiency of around 65% (an approximate average) is insufficient, at today's typical power price variation and imbalance penalties, to operate purely for arbitrage and power smoothing. Frequency response revenues become the critical revenue stream. However, the capacity of the

energy store to provide frequency response is limited because much of the power capacity is required to provide wind smoothing, which in turn leads to a loss owing to the round trip losses.

It can be seen from Figure 7.11 through Figure 7.13 that the ROCs have a significant impact on the outcome of the analysis. If the energy store were located 'behind the meter' then any round trip energy losses would also lead to lost ROCs and therefore lost revenues. However, if the energy store is independent, such as for an onshore energy store with an offshore wind farm, the ROCs would still be allocated to the wind farm and the only loss is due to the lower traded energy sales.

Overall, the addition of an energy store can be seen to normally increase the revenue from a large wind farm even under the low case. However, these results suggest that the greater the power capacity of the energy store the better the revenues, owing to the increased proportion of the power capacity available for frequency response and arbitrage over power smoothing. This suggests that an independent energy store may be preferable as all its power capacity could be used for the higher value applications of arbitrage and frequency response.

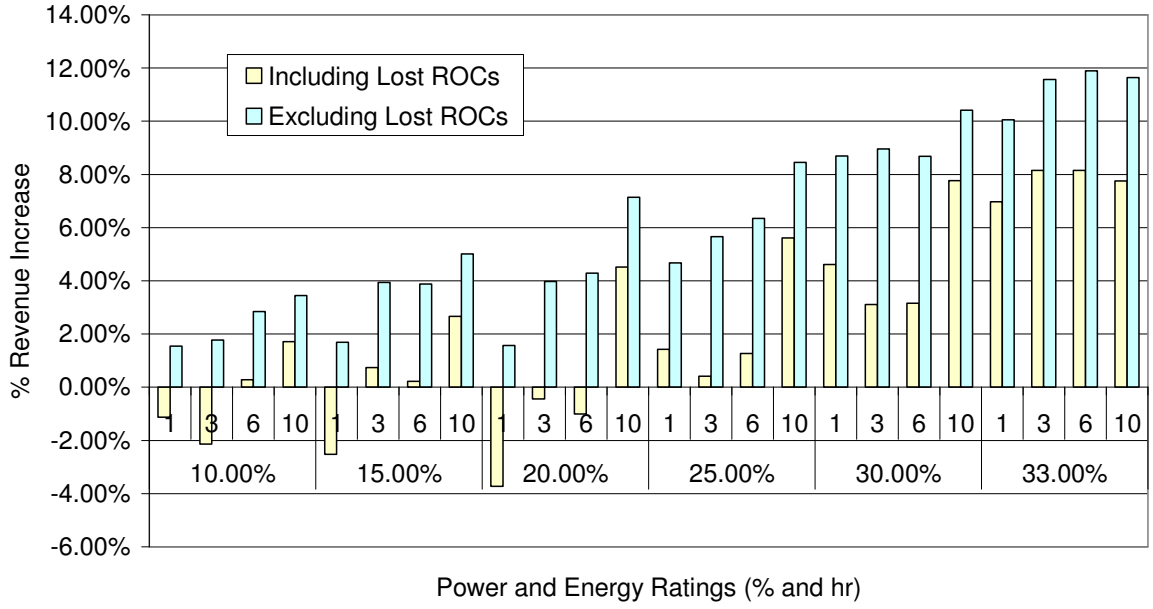

Figure 7.11: Low Case - Incremental Revenue

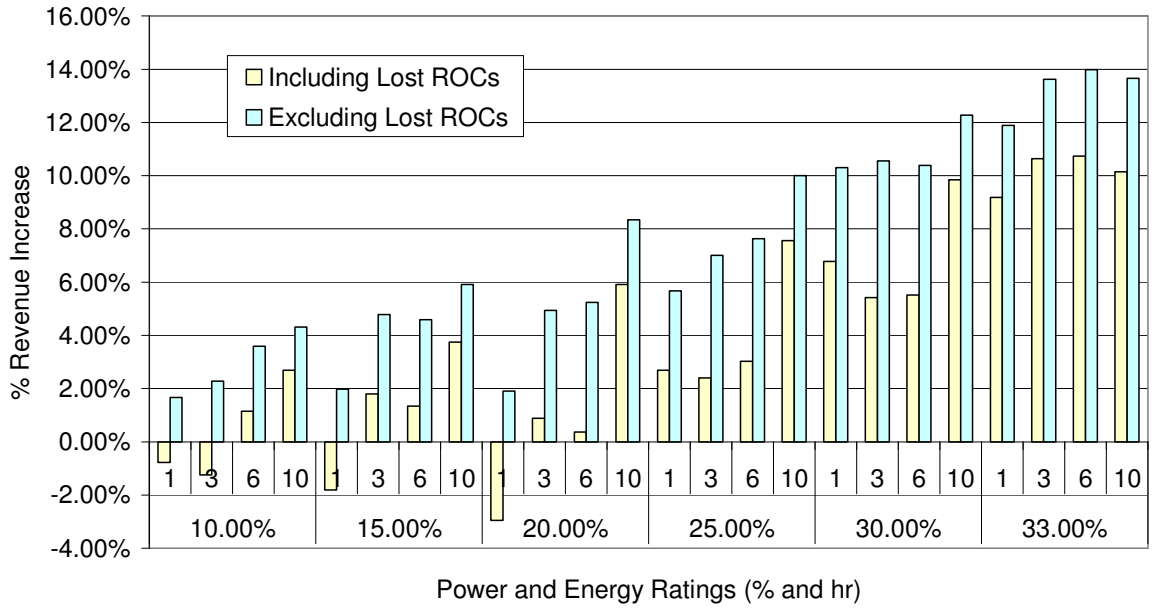

Figure 7.12: Mid Case - Incremental Revenue

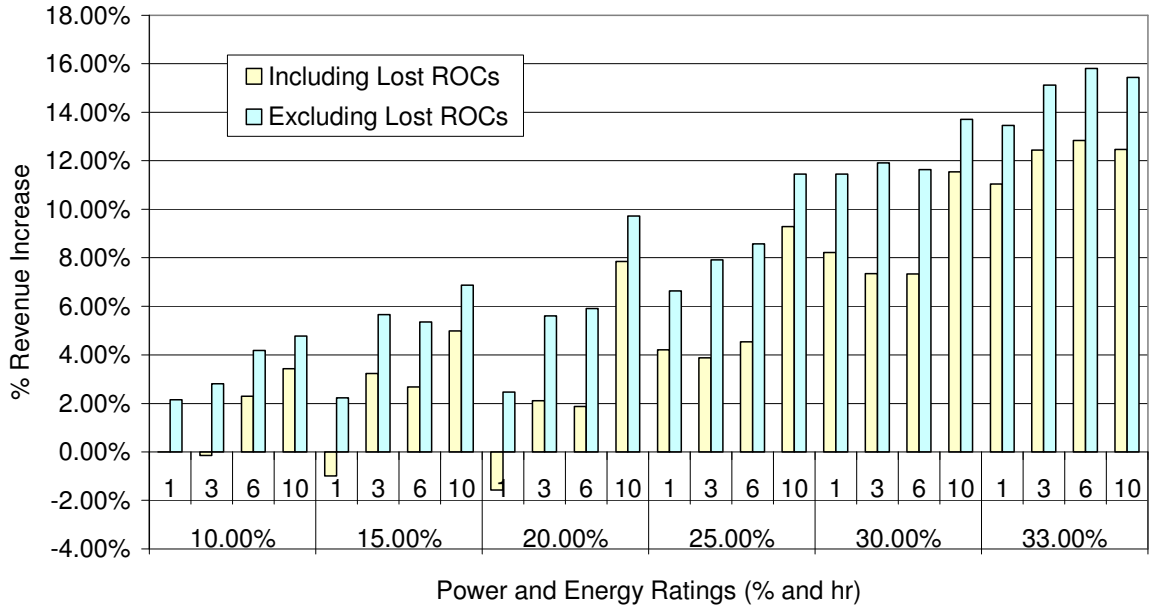

Figure 7.13: High Case - Incremental Revenues

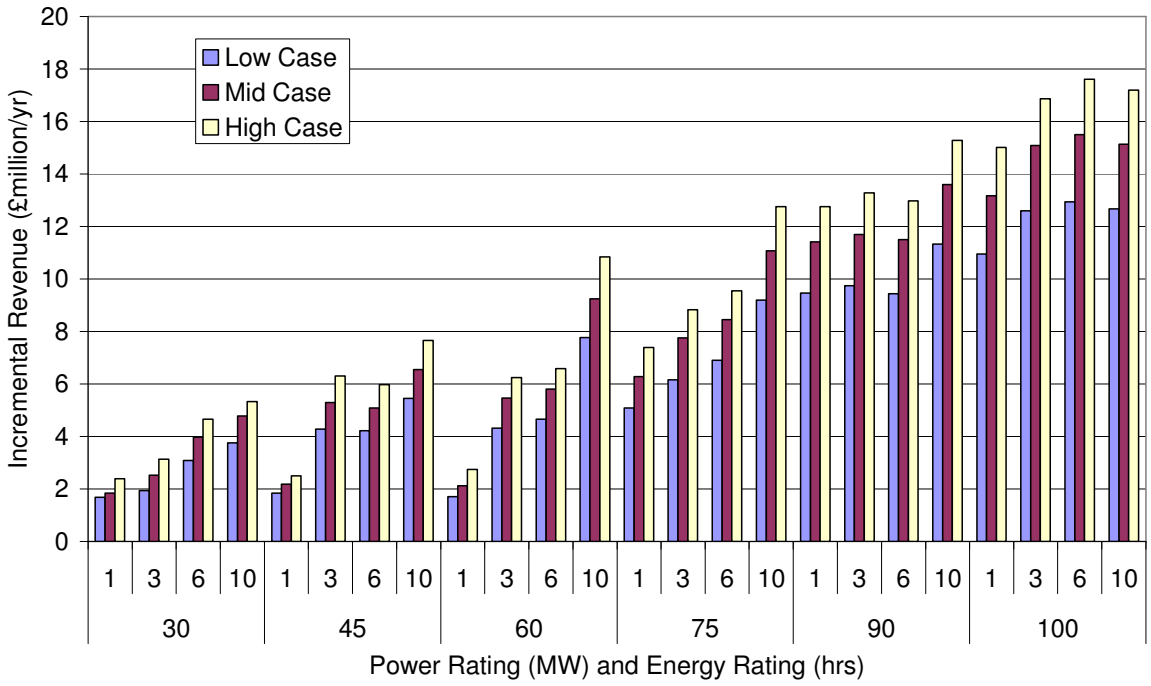

Figure 7.14: Incremental Revenues (Excluding ROCs) in £ for different power and energy rating batteries

As a very simple comparison, the results above suggest that the addition of an energy store would ultimately lead to an increase in annual revenue of at a minimum £1.7million for a 30MW store. Likewise a £17.6million increase for a 100MW store is possible. This is equivalent to a yield of around £57/kW/yr to £176/kW/yr. As Figure 7.10 shows that the energy trading actually leads to a net loss, this incremental revenue is entirely ascribable to the value derived from frequency response.

It is possible to provide a quick validation that the results here are of the right order by considering the comparison to the published value of frequency response from electric vehicles derived by Ricardo and National Grid [160]. The annual value of an electric vehicle for providing frequency response, which is assumed to be not available during peak periods, is estimated to be £600 for a 3kW system to £8000 for a 50kW system. This equates to £160/kW/yr to £200/kW/yr, and this is for a system that is assumed to be unavailable during rush hour, which is typically close to peak power demand periods. Conversely, Short [161] looked into the economic value of providing frequency response from dynamic demand in 2004 and concluded a 50W system would provide a benefit of around £3 per year, which equates to £60/kW/yr.

This shows that the results of this study are inline with the dynamic demand case and are also of a similar order to those from electric vehicles. In fact the estimates are perhaps on the low side, which is in part due to conservative projections and in part owed to the

specifics of operating with a wind farm which will be covered further in subsequent sections.

7.4.2 Independent Energy Store Revenues

The previous section has demonstrated the difficulty of incorporating a VRFB energy store with a wind farm, owing to the low revenue that is earned for providing a predictable, flat output, which is a pre-requisite for providing frequency response. Therefore, this section assesses whether it would be viable to use a VRFB in isolation purely for the purpose of providing frequency response. Using an energy store in isolation has the advantage that it can offer its full power capacity for frequency response without having to smooth the wind. Conversely, it has the disadvantage that it cannot be used in conjunction with the wind farm's high frequency response capability to offer greater combined response.

The revenue from an independent energy store is much more readily calculated than that from a store integrated with a wind farm, as its output is not compensating for wind's variability. Payments are dependent only on the average frequency response payments and the cost of power to supply the ancillaries of the VRFB.

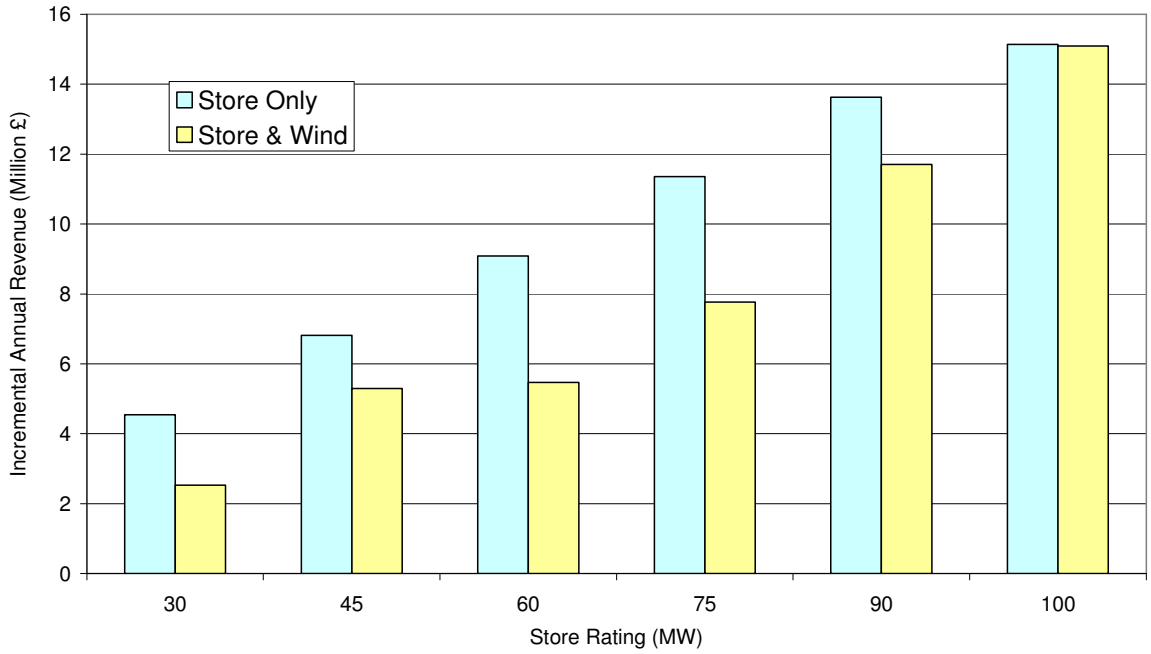

Figure 7.15: Comparison of revenues from an independent energy store and a store operating with a wind farm (under the "Mid" scenario)

Figure 7.15 shows the comparative revenues of a VRFB operating in tandem and independently from a wind farm, the comparison uses the "Mid" scenario, with 3 hours capacity. It is clear from this plot that at low size relative to the wind farm, the store is better off as an independent entity, as the power required for smoothing the wind output

reduces the capacity available for frequency response. However, as the wind farm's store becomes relatively larger, the revenues approach those of the independent store; the cost of smoothing the wind is compensated for by the increased frequency response payments and the ability to use the wind farm's capacity to offer greater high frequency response capacity.

This shows that under some circumstances there is an economic advantage to being able to combine wind power's high frequency response capability with the energy store's ability to provide low frequency response and simultaneously charge up under low price periods for later high price dispatch. This fits in with the fact that Figure 7.8 suggests that even for a relatively inefficient energy store, the combined total revenues including arbitrage are greater than the frequency response revenues for some settlement periods. However, when the wind farm is integrated with the energy store, the cost of smoothing the wind output to meet the frequency response technical requirements typically diminishes this benefit. The next section therefore considers how an energy storage system and wind farm could operate to maximise mutual benefits, whilst avoiding the challenge of having to smooth the wind.

7.4.3 Affiliated Energy Store Revenues

This optimisation of the operation of a combined energy store and wind farm is the subject of a patent application [162].

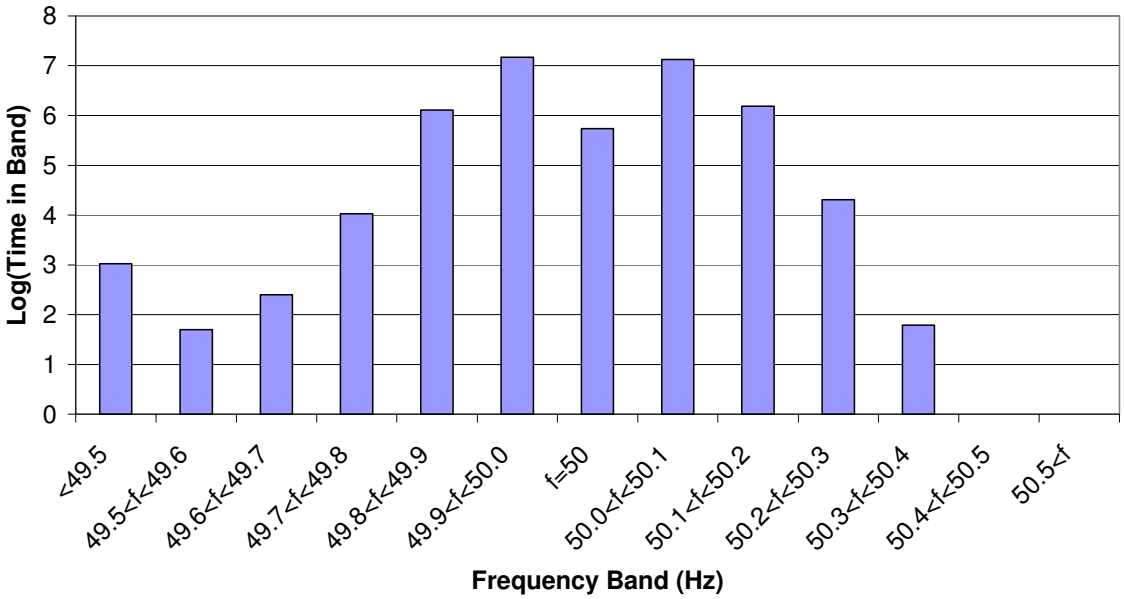

Figure 7.16: Grid Frequency Distribution for 2008 courtesy of National Grid

Section 7.4.1 demonstrated that an energy store could increase the revenue from a wind farm. However, the round trip losses of the VRFB and the typically low differential between system prices combined meant it could not provide increased revenue from

power smoothing, which itself was a prerequisite of providing frequency response services. Section 7.4.2 therefore considered whether an independent energy store would have higher revenues, as it would have no requirement to provide wind smoothing. Whilst it was found that this was the case under some circumstances, it also found that the frequency response revenues were diminished as the energy store could not use the wind farm's capacity to offer additional high frequency response services. This section considers an optimal configuration of a wind farm and energy store, here called an "affiliated" energy store.

Figure 7.16 shows the distribution of the power system's frequency during the year 2008. Noting the logarithmic axis, it highlights that the frequency spends the vast majority of the time very close to the target of 50Hz. Figure 4.16 illustrated that the response to a deviation in frequency, from 50Hz, by a frequency responsive plant should be proportional to the magnitude of the frequency deviation. Hence, the vast majority of the time, the limits of the frequency response reserve are not used. Whilst Figure 7.8 suggested that for several settlement periods each day an energy store could earn higher revenue from combining arbitrage with frequency response provision. It is possible to provide both arbitrage and margin for frequency response; during the time period that the VRFB is charging it has the capacity to offer low frequency response equivalent to Equation 7.11, whilst the high frequency response would be capped by Equation 7.12. The corollary of this is that when the store is discharging into peak demand periods, it could offer no response, but would be earning higher revenues from the value of its energy.

Equation 7.11 $P_{Low} = P_{Charge} + P_{Rated}$ where P_{Rated} is the energy store's rated power, P_{Charge} the charging power and $P_{Windfarm}$ is the wind farm's output.

Equation 7.12 $P_{High} = \left(P_{Rated} - P_{Charge}\right) + P_{Windfarm}$ where $\left(P_{Rated} - P_{Charge}\right)$ is the "residual capacity" of the VRFB to charge at a faster rate.

Operating the VRFB in this manner would put the wind farm output at risk of being spilled, if high frequency response greater than the residual capacity of the VRFB is required, then the wind farm would have to reduce its output. Reducing the wind farm's output would lead to lost revenue, primarily through the loss of ROCs. Therefore, when charging an energy store for later dispatch, there can be an economic gain from providing frequency response (through the frequency response payments) which must be traded off against the risk of lost ROCs revenue should high frequency response by required.

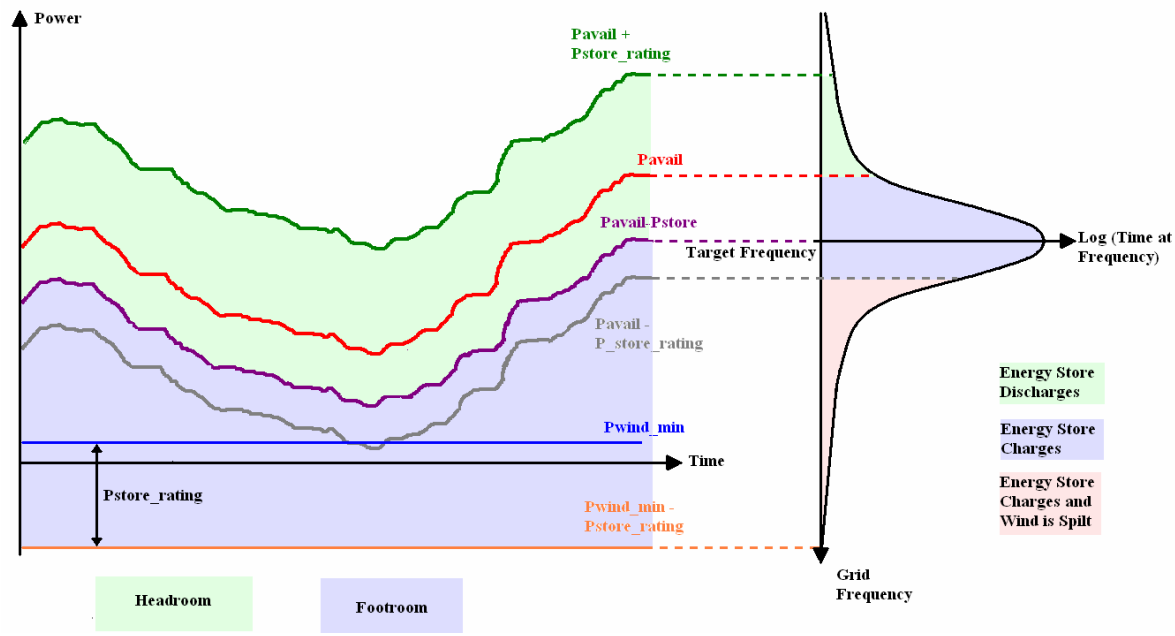

Figure 7.17: Optimal control of wind and energy storage in tandem

There is an optimal charging rate where the arbitrage and frequency response revenues are balanced against the risk of losing ROCs. This trade off is illustrated by Figure 7.17, when the frequency is exactly 50Hz, the combined output tracks below the available wind power and the energy store charges. If the frequency falls, the energy store can reduce its charge rate or even discharge, such that the total output power is the available wind power plus the energy store's rated power. If there is a small positive frequency deviation, the energy store would increase its charging rate, however, for a large positive frequency deviation, the wind farm would have to activate its balance controller and spill wind as well. The frequency distribution of frequency shows though that such high frequency events resulting in spilt wind are rare (the right plot in Figure 7.17 is a simplification of Figure 7.16).

Figure 7.18 considers the overall revenue that would accrue to a wind farm and affiliated energy store as a result of the increased frequency response payments from putting more of the wind farm's output 'at risk'. The left hand side of the peak shows a near linear initial rate of increase of revenue with increased charging rate, reflecting the very low probability of a high frequency event ever leading to spilt wind. However, the fall off in revenue as the charging rate exceeds the peak is rapid as the loss of ROCs dominates the increased frequency response revenues.

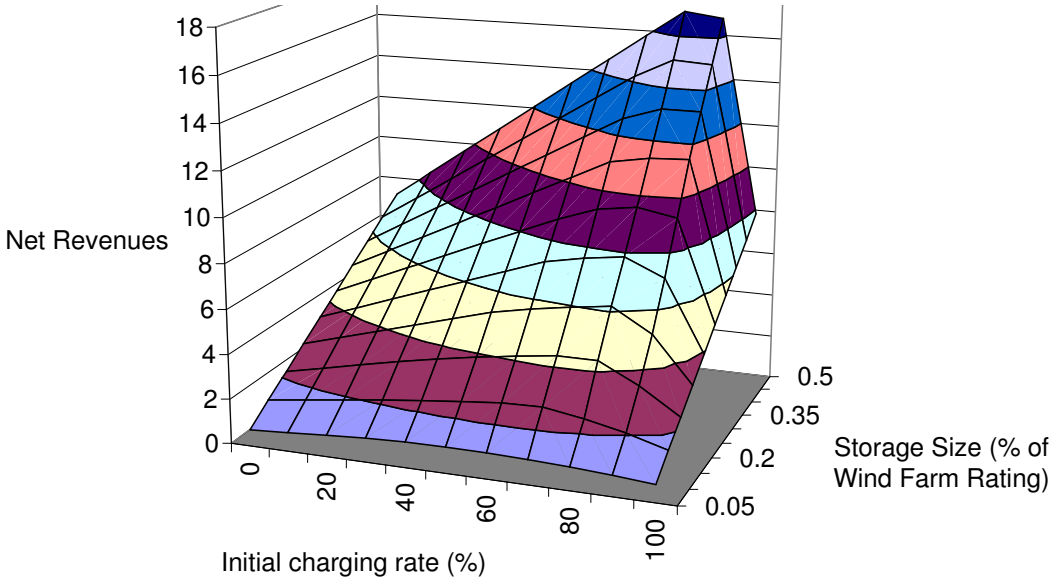

Figure 7.18: Optimal Charging Rate of an Energy Store with a Wind Farm

Figure 7.18 suggests that the optimal charging rate for maximum revenues is around 70% to 80% of the rated power capacity of the energy store. This leaves relatively little power capacity available for the high frequency response margin from the energy store before wind must be spilled; therefore it illustrates the steepness of the frequency distribution in Figure 7.16.

It should be noted, that this increase in frequency response capacity is only available whilst the energy store is charging. Owing to the finite capacity of energy storage, it will have a period of reduced frequency response capacity during its discharge period. However this period still generates high revenue as the store takes advantage of the energy price differential instead.

7.4.4 Arbitrage Impacts

Figure 7.19 illustrates the critical importance of round trip efficiency to the revenues from arbitrage of an independently operated energy store with 3 hours storage capacity. The practical round trip efficiency from today's VRFBs is around the breakeven point from arbitrage. However, this is well short of the theoretical efficiency possible from the VRFB (see Table 9.9) of around 85% for the full system. Hence, the results shown here are highly sensitive to small technological improvements to the VRFB's practical efficiency.

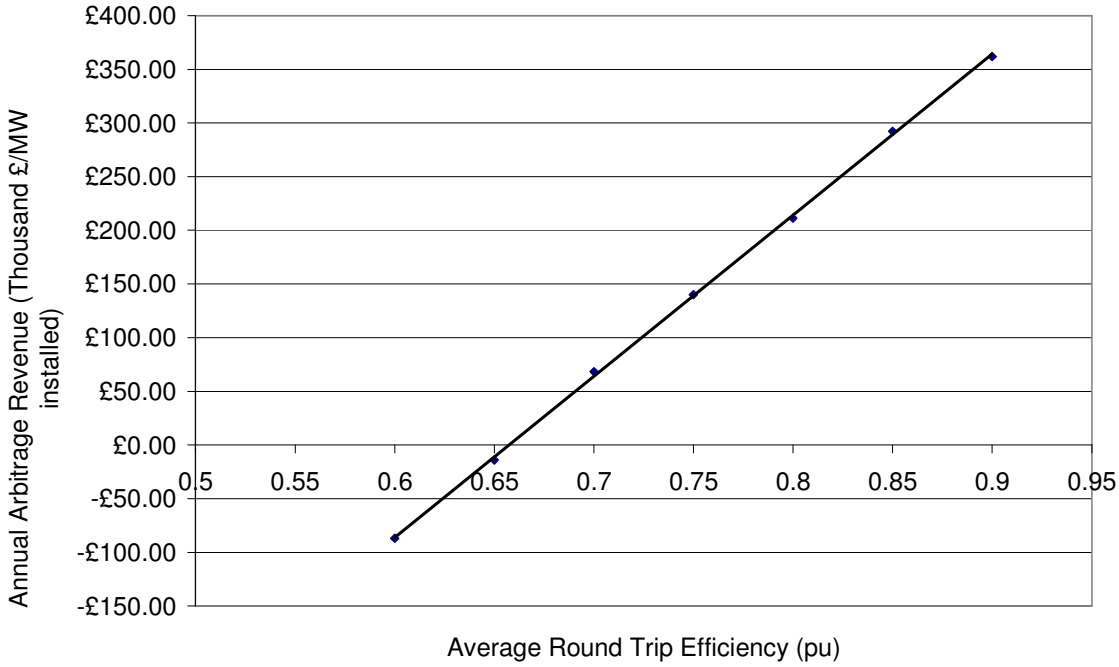

Figure 7.19: Potential Annual Arbitrage Revenues - Dependence on Round Trip Efficiency

7.5 Net Present Value

7.5.1 Integrated Energy Store

Incorporating the costs of the VRFB into the analysis allows the viability of this application to be assessed. Hence the Net Present Value (NPV) over a 20 year period with a 4% discount rate has been calculated for the various energy store capacities under the three economic scenarios.

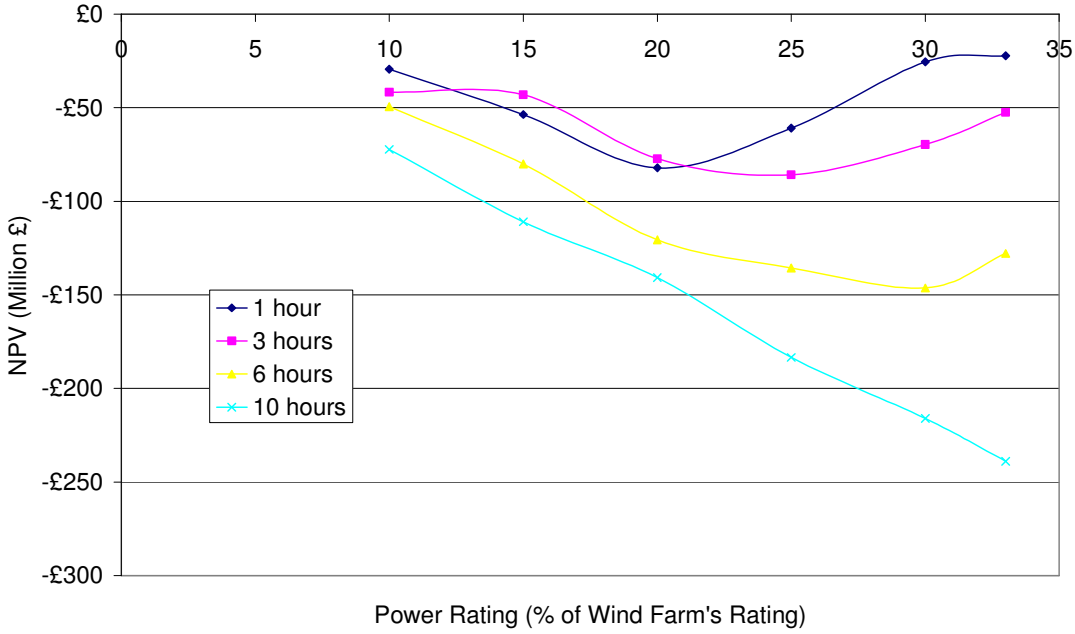

Figure 7.20: Net Present Value of VRFB over 20 year life under Low scenario

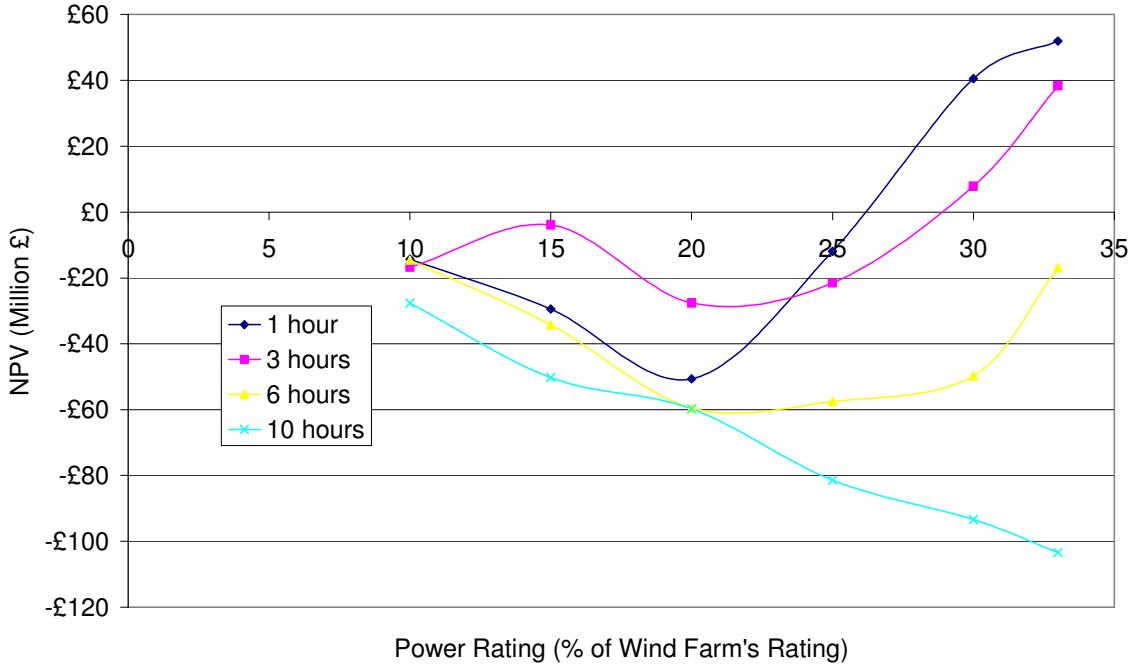

Figure 7.21: Net Present Value of VRFB over 20 year life under Mid scenario

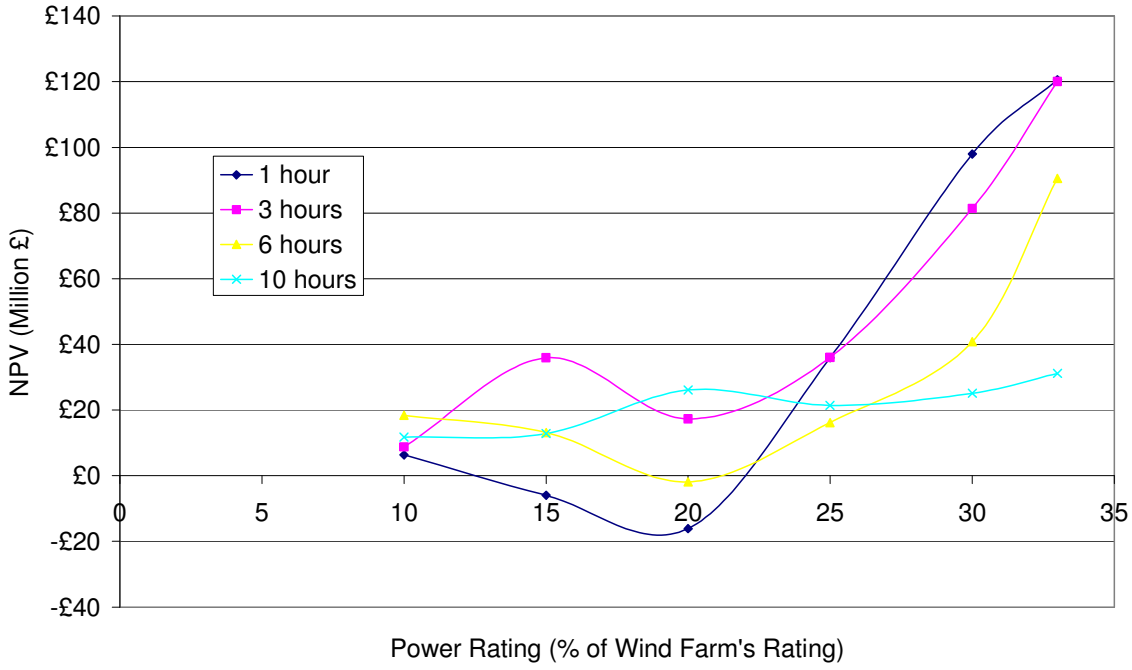

Figure 7.22: Net Present Value of VRFB over 20 year life under High scenario

The results are shown in Figure 7.20 to Figure 7.22. This illustrates that under current system prices and frequency response prices (Low scenario); the VRFB cannot provide an economically viable service, when in conjunction with a wind farm, as all NPVs are negative. However, under the forecasts for expected price increases (Mid scenario) or high price increases (High scenario), some of the high power, low energy rating systems show a significantly positive NPV.

Figure 7.8 demonstrated that the average differential price achieved with arbitrage decreases for longer term energy stores. This is due to there only being few peak price

settlement periods in each day (see Figure 7.5). Furthermore, in order to provide primary and secondary frequency response the energy store only needs to be rated for sufficient energy capacity to charge or discharge at full power for a single settlement period. Hence a store rated for full power for a single hour is sufficient (assuming it starts a settlement period at 50% SOC) to meet frequency response needs. Adding energy capacity is expensive and offering frequency response capacity accesses most of the value. This is the reason for low energy rating stores outperforming longer term stores; however, higher round trip efficiency would preferentially improve the economics of higher energy capacity stores by improving arbitrage economics.

The comparative benefit of higher power rating of the energy store is again owed to the relatively low benefit that can be derived from smoothing the wind power output. Higher power rating stores can dedicate a greater proportion of their energy capacity to providing frequency response reserves.

Power Rating (% of Wind farm MW rating)	Power Rating (MW)	Energy Rating (hrs)	Payback Period (years)		
			Low	Mid	High
10.00%	30	1	x	x	15
		3	x	x	15
		6	x	x	13
		10	x	x	16
15.00%	45	1	x	x	x
		3	x	x	9
		6	x	x	16
		10	x	x	17
20.00%	60	1	x	x	x
		3	x	x	15
		6	x	x	x
		10	x	x	16
25.00%	75	1	x	x	10
		3	x	x	13
		6	x	x	17
		10	x	x	17
30.00%	90	1	x	14	6
		3	x	19	9
		6	x	x	14
		10	x	x	17
33.33%	100	1	x	13	6
		3	x	15	7
		6	x	x	10
		10	x	x	17

Table 7.4: VRFB Deployment Payback Periods (x = Not paid back within 20 years)

The negative NPVs of the low case, even with this low discount rate, indicate that developing a project today would be extremely high risk and likely to deter investors. Even under the central scenario the returns are modest at best. As development of such a storage project would be highly capital intensive it is also of interest to compare the payback periods, which are shown in Table 7.4. These are discounted payback, rather than

simple payback periods, but the lack of a short term payback under the central scenario suggests that this would not represent a desirable investment. Whilst some ratings promise relatively short payback periods under the high scenario, this is likely to be insufficient to prove attractive unless price rises are at the upper end of forecasts.

7.5.2 Optimal Power Rating

Figure 7.23 shows the effect that increasing power capacity has on the total revenues of a combined wind farm and energy store. The broad trend is not a linear one, with increasing power capacity leading to greater revenue benefit for larger stores. This connects with the assertion that the storage facility would be better deriving revenue from frequency response and arbitrage, rather than through avoiding imbalance penalties. This in turn also corroborates the payback periods shown in Table 7.4, where the higher power capacity energy stores are the ones achieving the shorter payback periods.

The optimal power rating of an energy store, if it must be operated in conjunction with the wind farm, can be found by considering the traded energy sales. Figure 7.10 shows that under each of the 3 scenarios, the highest energy sales were achieved with an energy store rated at 25 to 30% of the wind farm's rating, aside from the case with no storage. Given the high capacity factor of the wind farm considered here, the lower of these values is therefore recommended as an approximate guide.

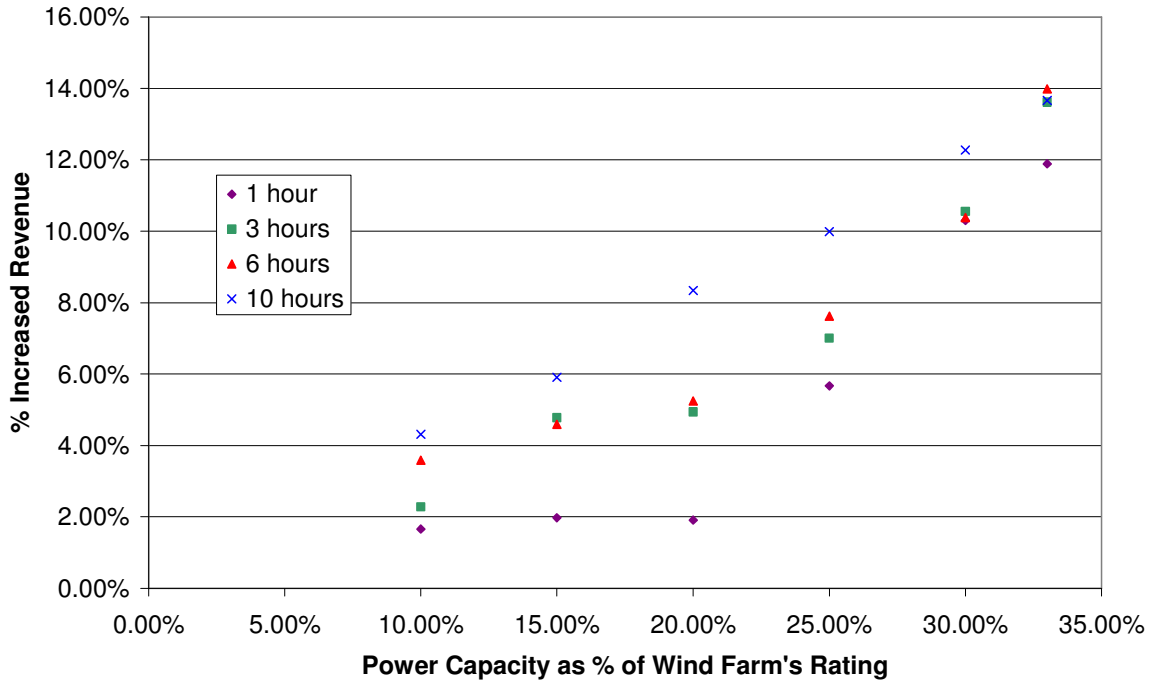

Figure 7.23: Comparison of VRFB's Benefit to a 300MW Wind Farm (Mid Case)

7.5.3 Optimal Energy Rating

Figure 7.24 through Figure 7.26 show the Net Present Value (NPV) of various different storage ratings assessed over 20 years, under the three economic scenarios. This illustrates the optimal energy store size, as the lower power ratings (10-20%) typically have higher (less negative) NPV at 3 to 6 hour ratings, whilst the larger power ratings typically have higher NPV at 1 to 3 hours. This is a consequence of the greater proportion of revenue derived by larger stores from frequency response services, which require only limited energy capacity. The high energy ratings at high power ratings are rarely required, whilst the high energy ratings at lower power ratings are frequently required for wind smoothing. This is because wind gusts and lulls of greater than 30% magnitude lasting an hour or more are orders of magnitude rarer than wind gusts or lulls of 10% magnitude lasting an hour (note the exponential scale of Figure 7.3). Large unforecast peaks and troughs in wind output tend to be transient in nature.

Overall, the trends of Figure 7.24 to Figure 7.26 suggest that the optimal energy rating of a VRFB in conjunction with a wind farm is likely to be around 3 hours or less at full power output. This is likely to shift to higher energy capacities as and when the round trip efficiency of these batteries improve, as lower differential market prices would become profitable for arbitrage. However, this corroborates Prudent Energy and GE Energy's modular system size which, whilst expandable, currently typically has a two hour rating as a base point.

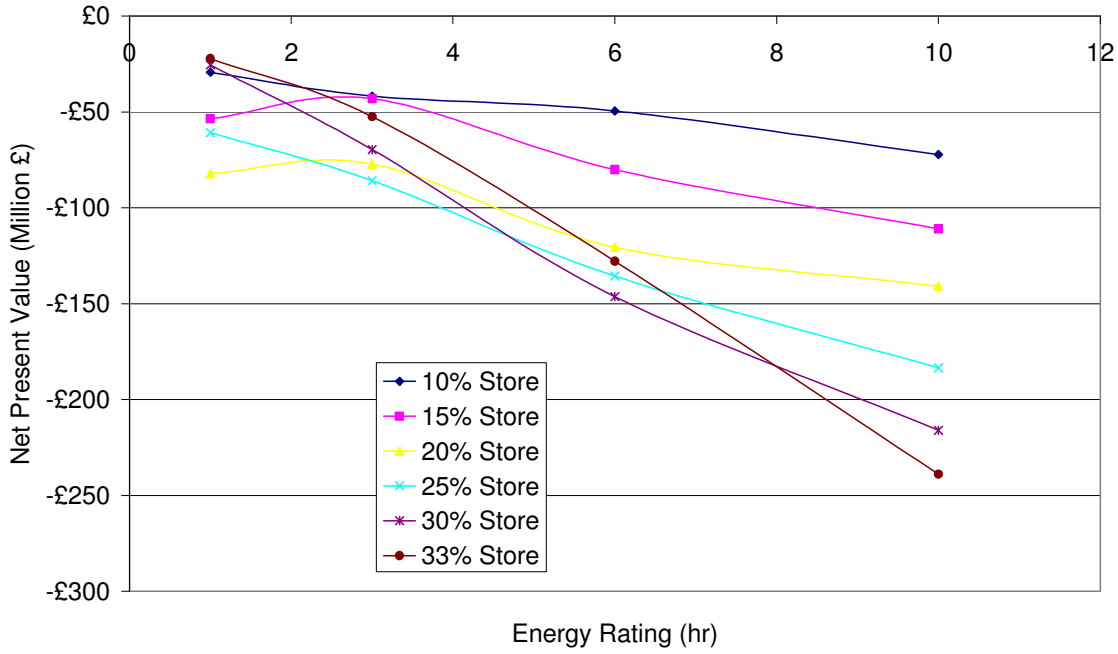

Figure 7.24: Net Present Value (20 year lifetime) of Different Power and Energy Rating Stores under Low Economic Case

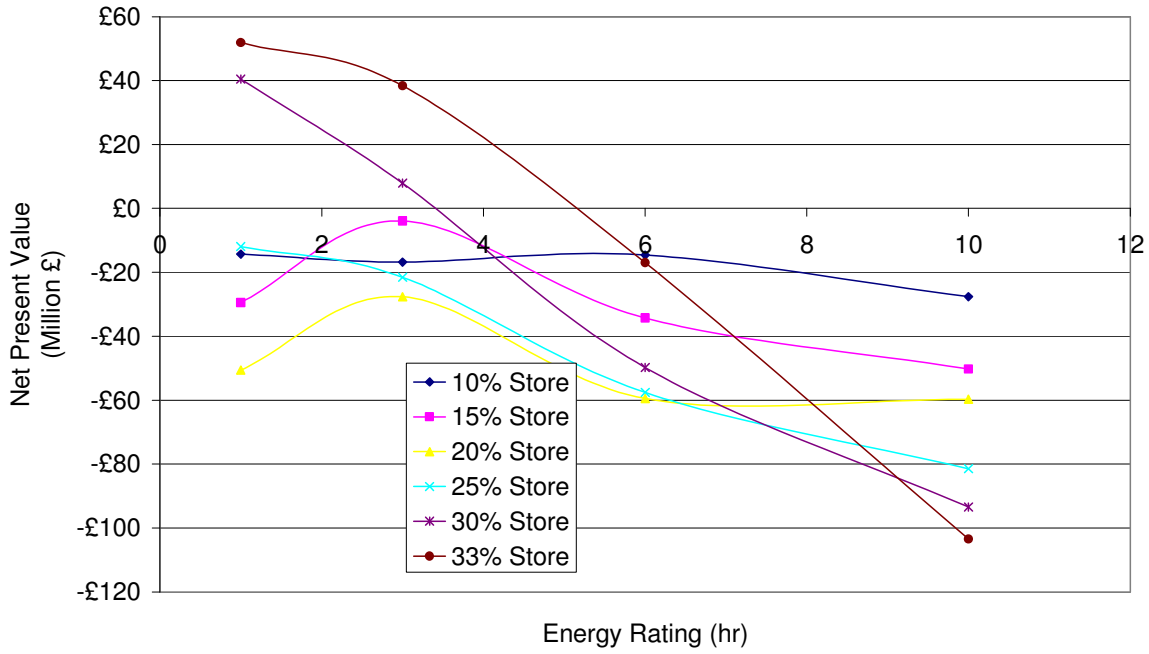

Figure 7.25: Net Present Value (20 year lifetime) of Different Power and Energy Rating Stores under Mid Economic Case

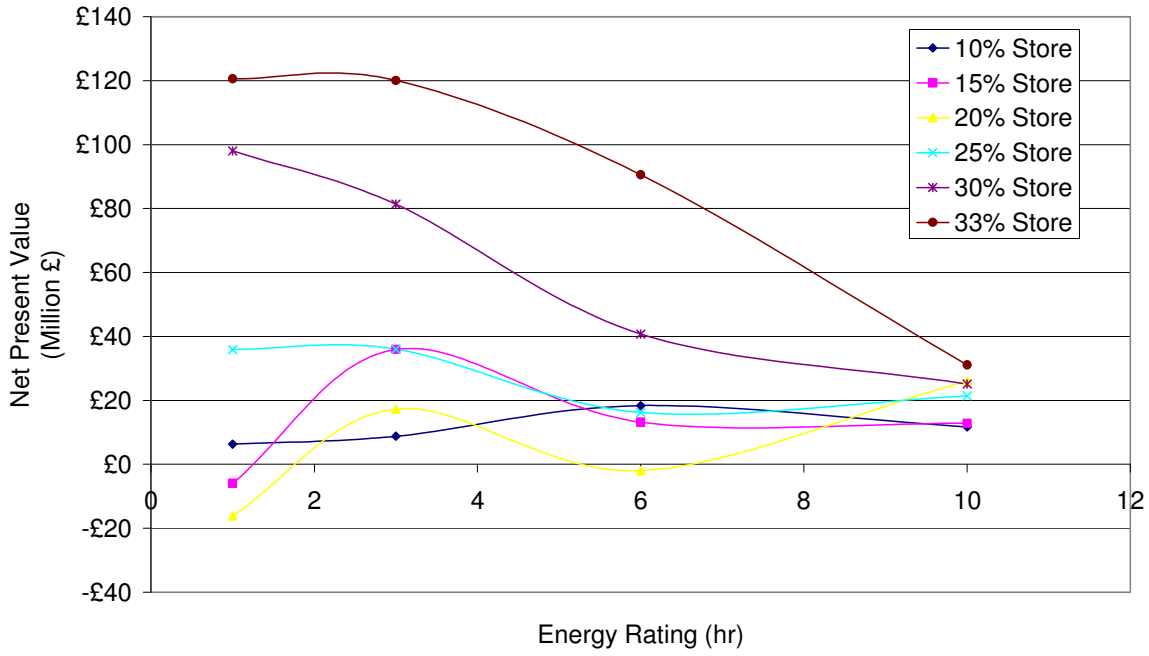

Figure 7.26: Net Present Value (20 year lifetime) of Different Power and Energy Rating Stores under High Economic Case

From the analysis, it is clear that 6 or 10 hours of storage capacity is unlikely to be viable in the near future, owing to the very low average differential price from arbitrage and the significantly higher capital cost of such a large capacity. However, it should be noted that a significant benefit of flow battery solutions is that the energy capacity can be adapted by addition or enlargement of the tanks of electrolyte at a comparatively low cost. This is achievable at a significantly lower cost than implementing a completely new system, as whilst the power cost of the VRFB is high compared to other technologies, the energy cost is comparatively low (see Figure 5.1 and Figure 5.2).

7.5.4 Affiliated Energy Store Revenues

Figure 7.27 shows the comparative NPVs of a 75MW VRFB, with 3 hours capacity, based on whether the energy store is fully integrated with the wind farm, as in section 7.4.1, fully independent as in section 7.4.2, or merely affiliated to a particular wind farm as in section 7.4.3. This shows the benefits of the affiliated method, which combined arbitrage with providing higher volumes of frequency response by offering additional high frequency response from the wind farm. This scheme offered a slight improvement over the independent energy store case, which in turn was significantly improved over the case where the energy store was integrated with the wind farm.

This plot illustrates that under the central projection, both the independent and the affiliated energy store have positive NPV, indicating that they would represent investments that would payback. However, none of the options offers a positive NPV under the low projection, raising the level of risk of developing such a project and deterring investment. This highlights the problem identified by the Electricity Market Reform; the capital cost of investing in storage or other assets for peak load operation is not supported by the energy only market. However, there is a new capacity mechanism proposed to solve this problem. Given that the NPVs, under the low projection, of the independent and affiliated energy stores are relatively small negative values, it is entirely possible that the capacity mechanism may provide sufficient support to energy storage to make such projects viable in the medium term.

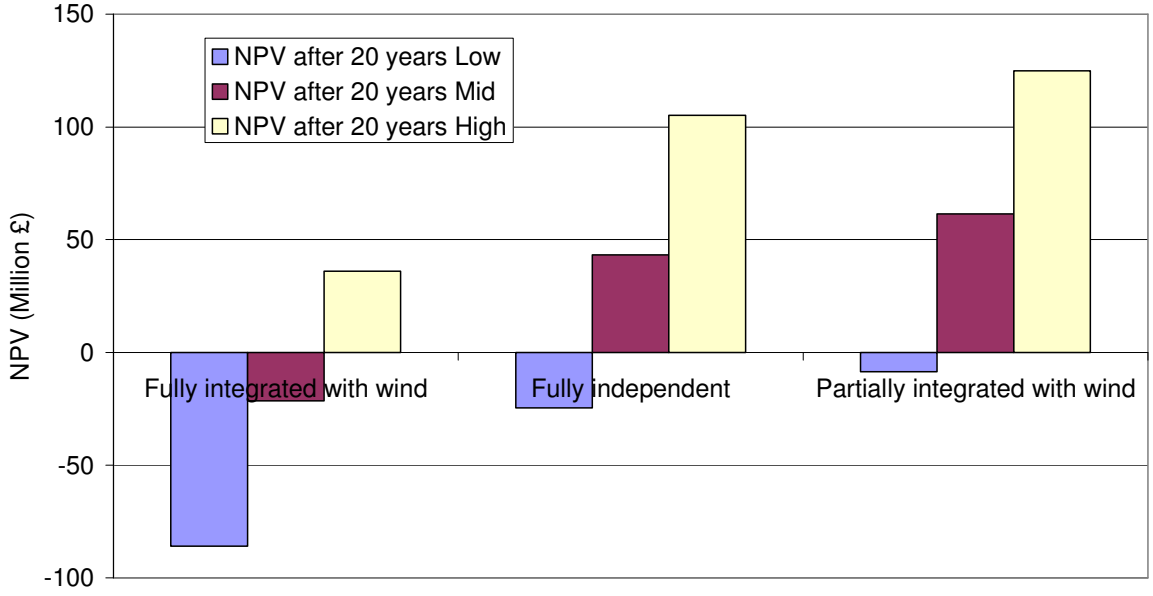

Figure 7.27: NPV Comparison of the Different Storage Integration Options (75MW, 3 hour store over 20 years)

7.5.5 Discount Rate Sensitivity

Table 7.5 to Table 7.7 show the sensitivity of the NPV calculations to discount rates. The three tables are all for a 75MW, 3 hour store but for the three applications of the energy store: integrated with a wind farm, totally independent and affiliated with a wind farm. As expected, the NPVs are highly sensitive to the discount rates applied, however, owing to the nature of compound interest, those cases with short payback periods suffer less than those with longer payback periods. This means that the cases with attractive payback periods of significantly less than 10 years only see a lengthening of payback period of 1-2 years with the higher discount rates. However, high discount rates do mean that the independent and affiliated energy stores would not pay back under central projections.

Discount Rate (%)	Net Present Value (Million £)			Payback Period (years)		
	Low	Mid	High	Low	Mid	High
4	-85.9	-21.5	36.0	x	x	13
8	-105.0	-50.0	6.2	x	x	15
12	-117.2	-63.1	-12.7	x	x	x

Table 7.5: Integrated Energy Store NPV Sensitivity to Discount Rate

Discount Rate (%)	Net Present Value (Million £)			Payback Period (years)		
	Low	Mid	High	Low	Mid	High
4	-24.6	43.3	105.1	x	14	7
8	-59.0	1.6	58.0	x	20	7
12	-80.9	-24.7	28.2	x	x	9

Table 7.6: Independent Energy Store NPV Sensitivity to Discount Rate

Discount Rate (%)	Net Present Value (Million £)			Payback Period (years)		
	Low	Mid	High	Low	Mid	High
4	-8.6	61.4	124.9	x	12	6
8	-47.1	15.3	72.9	x	16	7
12	-71.4	-14.0	39.9	x	x	7

Table 7.7: Optimal Energy Store and Wind Farm NPV Sensitivity to Discount Rate

7.6 Alternatives to Storage

The preceding analysis used reasonable projections for the cost of a VRFB, likely revenues in the energy and frequency response markets and appropriate discount rates to assess the NPVs of VRFB energy storage on the GB system. It has found that under the central projection, energy storage is likely to have positive net present value for providing

frequency response and arbitrage when operating as an independent store. This positive NPV can be improved if the energy store can affiliate itself to a wind farm and use the wind farm's capability for providing high frequency response to offer greater frequency response capacity when charging up for arbitrage.

The challenge for the VRFB is that the payback periods, combined with the lack of a guaranteed payback under worst case projections suggest that it may remain too risky an investment for this application alone. This assessment considered the open markets from which a storage owner could presently earn a return. The Electricity Market Reform may lead to higher payment for storage's firm capacity, which could in turn tip the economics in favour of storage. Failing this, a VRFB owner would have to be able to accrue the revenue from other benefits it could provide, such as constraint management or grid capacity upgrade deferral. These revenue streams are less accessible to an independently owned storage operator, however.

In view of the questionable economics of storage to provide frequency response services, it is worth briefly considering the alternatives.

7.6.1 Curtailment of wind power

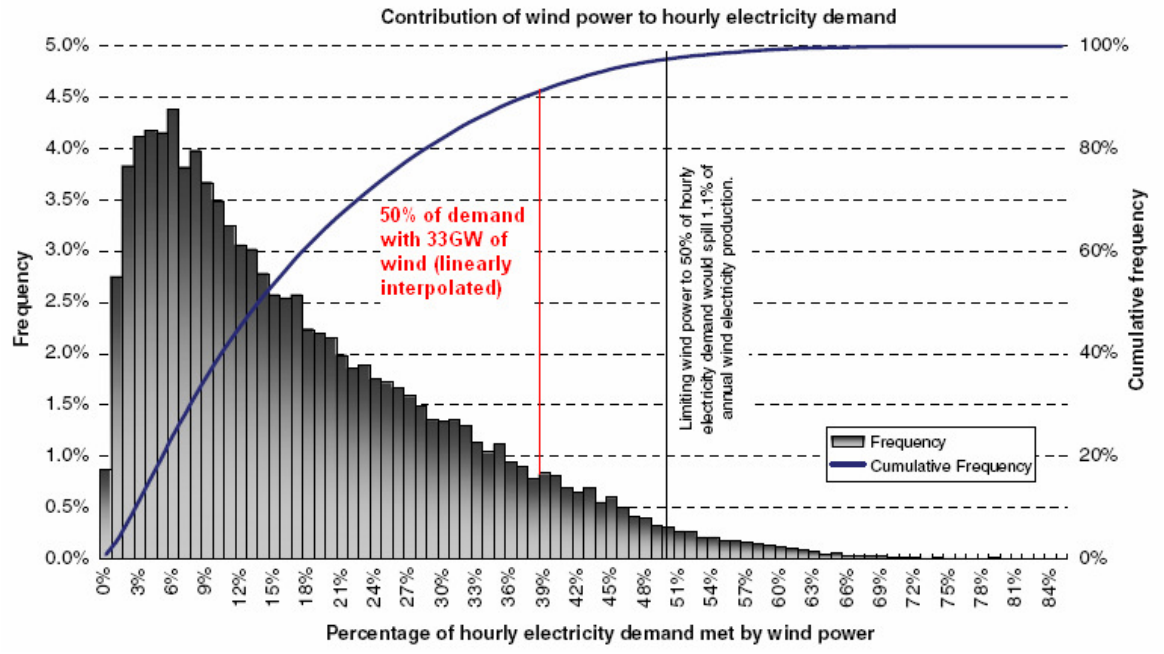

Figure 7.28: Plot of hourly electricity demand to percentage served by wind from Sinden [163] (red elements are superimposed and show the curtailment of energy if wind were curtailed at 50% of demand and 33GW were installed on the GB system, rather than Sinden's 25GW)

If energy storage does not provide frequency response services on behalf of a wind farm, it is likely that at times of high wind and low demand; the wind farm may have to provide the service instead. This implies a level of spilt wind as the turbines regulate output down in order to hold the margin required for frequency response. Sinden [163] has conducted

an extensive analysis using 33 years of wind data from 66 weather stations and compared this with demand data so as to assess the correlation between the two. He has shown that wind power has a weak positive correlation with demand in the UK, such that wind power's capacity factor during peak demand hours is around 30% higher than the annual average. Sinden has considered the case where the UK has 25GW of installed wind capacity and a peak demand of 60GW; he has shown the percentage of hourly energy served by wind, which is shown in Figure 7.28.

Sinden's work was based on 25GW of wind development in the UK. If this were scaled up to 33GW (see section 2.6.1) and Sinden's limit of wind power providing 50% of demand remained, then wind power plants could have to spill wind energy approximately 8% of the time to ensure their output does not exceed 50% of supply. This would lead to an annual energy loss of around 3%. This in turn would put a significant additional cost on wind farms, demonstrating the potential additional value of storage for managing this form of constraint.

7.6.2 Interconnection

Section 2.4.2 showed the ambition of the European Union to move to a more interconnected grid for Europe, to allow both a free market in electricity and to accommodate greater renewable energy deployment. In theory such interconnectors could provide the frequency response services required by the GB grid. However, the current operation of interconnectors is based almost entirely on the energy price differential between different countries. It would require an improvement in the economics of provision of frequency response in order for interconnectors to hold capacity purely for the purposes of frequency response margin. Such an improvement in these economics would in turn lead to a more favourable return on any energy storage developments as well.

7.6.3 Conventional Generation

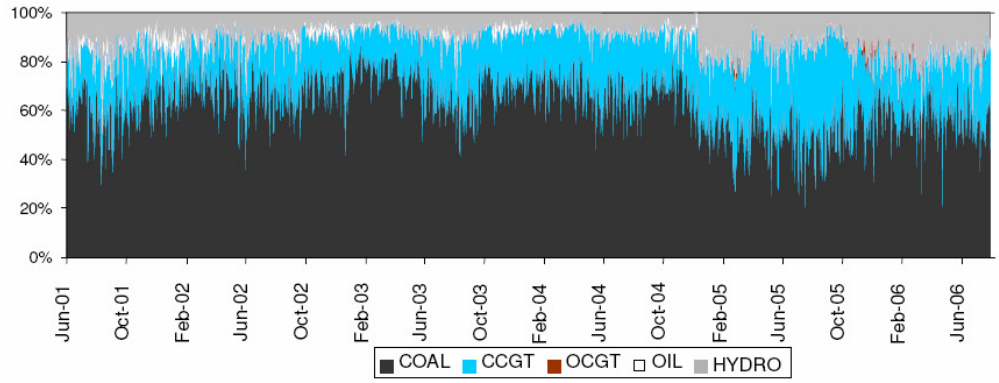

Figure 7.29: Frequency Response Instructions Distribution from Pearmine [164]

Frequency response is presently provided by part loaded conventional generation, traditionally predominantly coal fired as illustrated in Figure 7.29. However, as Coal plants are decommissioned due to the Large Combustion Plant Directive and concerns over CO_2 emissions, the principle conventional generation source that could fill the frequency response gap is Combined Cycle Gas Turbines (CCGT).

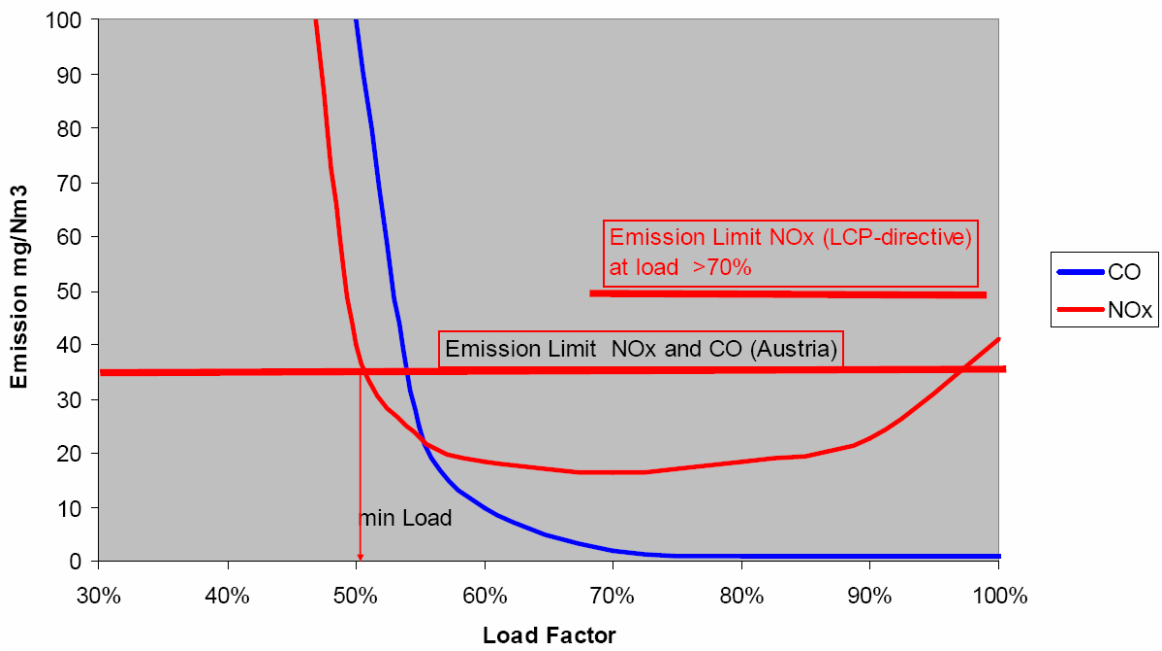

Figure 7.30: NOx and CO Emissions from CCGT Plant According to Tauschitz and Hochfellner [165]

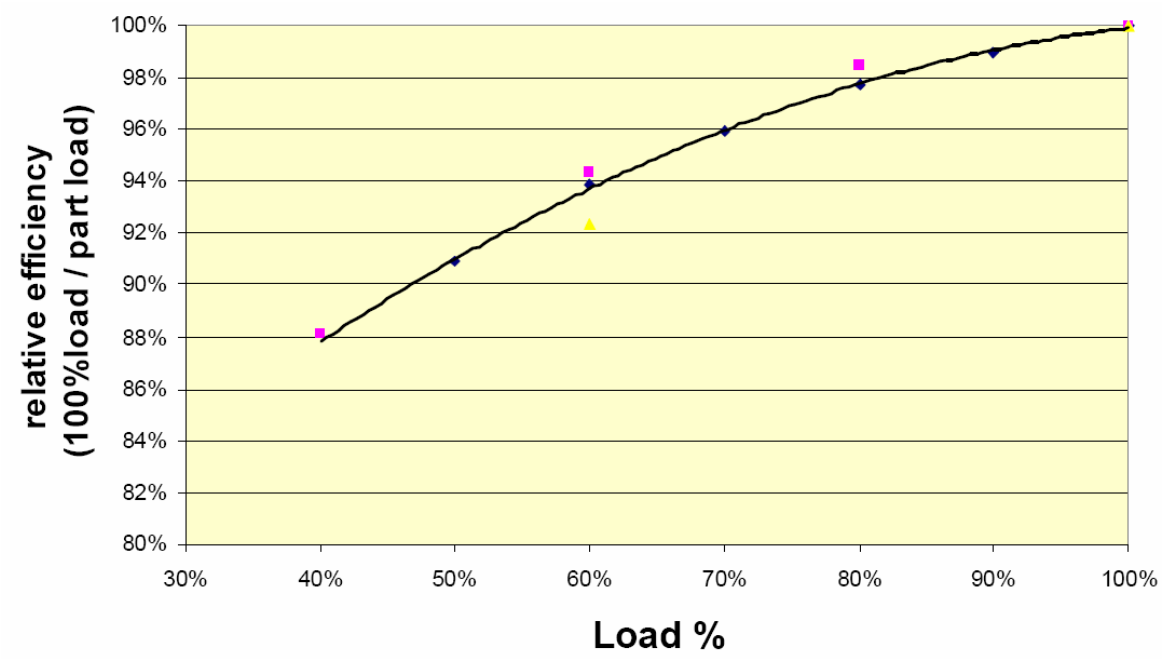

Figure 7.31: Part Load Efficiency of CCGT Plant According to Tauschitz and Hochfellner [165]

Tauschitz and Hochfellner [165] have shown that the typical efficiency of CCGT is significantly affected by operating at part load. Typically a CCGT can regulate its output power down to around 50% before the non-linear increase Nitrous Oxide (NOx) and

Carbon Monoxide (CO) emissions reach environmental limits. This is shown in Figure 7.30. Hence, in order for a typical CCGT to offer equal high and low frequency response capacity it would be regulated down to around 75% of maximum output.

Figure 7.31 illustrates that if a CCGT is regulated down to around 75% of its rated output it would reduce in efficiency by around 3%. Furthermore, according to Pearmine [164], such a fossil fuel plant could only be relied on to deliver 55% of its frequency response holding. Here the net effect on emissions is considered.

First, for simplicity it is assumed that CCGTs are operated to provide 600MW of low and high frequency response, based on Figure 2.23. Based on delivery of only 55% of this, the frequency response holding would have to be:

Equation 7.13 $P_{FR} = \frac{600}{0.55} = 1090MW$ where P_{FR} is the frequency response holding.

Assuming the CCGTs are operated at 75% output, this holding would be distributed across:

Equation 7.14 $P_{Tot} = \frac{1090}{1-0.75} = 4360MW$ of plant.

The Department of Energy and Climate Change [166] has created estimates of the Carbon Intensity of power generation in the UK, which is shown in Table 7.8.

Source	Carbon Intensity (χ) ($kgCO_2/MWh$)
CCGT	380
UK Average	550

Table 7.8: Carbon Intensity of Electricity Generation in the UK

Initially, prior to deloading to hold a low frequency response margin, the CCGT plant will have a CO_2 output of:

Equation 7.15 $m_{CO_2} = P_{Tot} \cdot \chi_{CCGT} = 4360 \cdot 380 = 1657 tonnes/h$

However, after the deload instruction, the frequency response holding would have to be replaced on the system. Here we consider two conditions, either that this is replaced by more CCGT plant coming online, or that the shortfall is picked up across all generators, thereby incurring the average Carbon intensity of the power system. Either way the total Carbon emissions are given as:

Equation 7.16 $m'_{CO_2} = \frac{(P_{Tot} - P_{FR})}{\eta_{CCGT}} \cdot \chi_{CCGT} + P_{FR} \cdot \chi$ where η_{CCGT} is the CCGT *relative* efficiency at that load from Figure 7.31.

If we assume CCGT plant fills the gap created by deloading this plant, the total CO_2 emissions now become:

Equation 7.17 $m^{CCGT}_{CO_2} = \frac{(4360 - 1090)}{0.97} \cdot 380 + 1090 \cdot 380 = 1695 tonnes/h$

Or if we assume an average mix of current power stations fills the gap, the total CO_2 emissions become:

Equation 7.18 $m^{Mix}_{CO_2} = \frac{(4360 - 1090)}{0.97} \cdot 380 + 1090 \cdot 550 = 1881 tonnes/h$

So the Carbon Intensity of providing 600MW of high and low frequency response holding can be calculated as:

Equation 7.19 $m^{FR}_{CO_2} = \frac{(m'_{CO_2} - m_{CO_2})}{600MW}$

For the CCGT only, and average power mix cases, this translates to a Carbon Intensity for holding frequency response equivalent to:

Equation 7.20 $\chi^{FR}_{CCGT} = \frac{(1695 - 1657)}{600MW} = 63 kgCO_2/MWh$

Equation 7.21 $\chi^{FR}_{Mix} = \frac{(1881 - 1657)}{600MW} = 373 kgCO_2/MWh$

This shows that providing frequency response from storage as opposed to deloaded CCGT plant could lead to substantial CO_2 savings. These savings are between 17% and 98% of the emissions saved from renewable energy displacing each MWh generated by CCGTs in the generation mix.

Currently onshore wind power receives 1 ROC per MWh and each MWh typically displaces a MWh from a CCGT plant thereby saving 380kg of CO_2. Offshore wind, a less mature technology although arguably more mature than flow battery storage, receives 2 ROCs per MWh with the same effect on total emissions. This analysis suggests that ROCs targeted at storage for frequency response could have a beneficial effect on total Carbon emissions.

The analysis shows a significant environmental benefit to providing frequency response from energy storage rather than conventional plant. It does not consider the environmental benefit of providing arbitrage from storage, thereby avoiding the need to have polluting peaking plants running during peak periods and hence reducing the average Carbon

intensity of UK generation. Instead, this final section is intended to promote discussion. On the basis of this analysis a targeted subsidy could both act to make storage economically viable and prove to be an effective means of reducing emissions. A Brunel Institute of Power Systems M.Sc. project will investigate this further.

7.7 Summary

This chapter has shown that VRFBs are close to being commercial viability for application on wind farms for frequency response.

This chapter has used the models and techniques described in the preceding chapters in order to assess the economics of providing frequency response from energy storage and wind power. Section 7.2 introduced the different scenarios that were to be applied to the power system models in order to generate power output and power reserve profiles from a wind farm with VRFB energy store. It also showed how this power system data integrated with an economic model reflecting the behaviour of the electricity market to generate revenue data from the power data.

Section 7.3 introduced the financial data behind the calculation of the different revenue streams, including frequency response, imbalance and traded energy market data. It also presented the different cost scenarios for the VRFB and introduced the discounted cash flow analysis scenarios that are used later in the chapter. Three different scenarios: low, mid and high, were introduced to reflect differing economic conditions.

Section 7.4 discussed the potential increase in revenues from the energy store, demonstrating that excluding the effect of lost ROCs (if applicable) the energy store could increase the total revenue of the wind farm in most scenarios. However, it also showed that integrating it with a wind farm led to lower revenues than independent operation owing to round trip losses in the VRFB outweighing reduced imbalance penalties from improved predictability. Against this it showed the advantage of being able to share responsibility for high frequency provision with the wind farm through access to higher holding payments. Hence, the concept of an affiliated energy store was developed which promised incrementally improved revenues.

The revenues from the energy store led into an assessment of the present value of different storage developments in section 7.5. Whilst this found that some cases produced positive present value under the central projection, none achieved this under the low revenue projection and payback periods were shown to be typically too long for an attractive investment under the central and high revenue projections.

If storage cannot provide frequency response, then it must be provided elsewhere and section 7.6 explores this. It shows that if wind farms are to provide frequency response then there will be a small but significant impact on energy yields. Furthermore, the section introduces the reasons why if conventional CCGT plant is increasingly the source of frequency response provision this leads to a negative environmental impact and higher CO_2 emissions. This illustrates that storage for frequency response can save CO_2 and should perhaps have a specific support mechanism to bring it to commercial maturity.

8 Conclusions and Further Work

8.1 Modelling of Wind Turbines

The UK has set itself ambitious targets to reduce the carbon intensity of the power generation sector over the coming decades. The specifics of the UK's subsidies, seabed geology and conservative approach to development mean that these targets are in large part likely to be met with widespread deployment of offshore wind farms. The development of the offshore wind resource is likely to present significant challenges to the power system's frequency stability owing, in part, to wind's intermittency.

Advances in both Grid Codes and power electronics have driven the wind industry towards increased use of full converter interfaced wind turbines. The power electronic interface decouples the generator from the grid system, offering flexibility through control, but removing the generator's natural inertial response from the grid. Active power control from large offshore wind farms is therefore an area of increasing importance to ensure the power system's future stability. The use of full converters in wind turbines permits a range of different control philosophies and physical systems as outlined below:

- In-direct speed control of the turbine (conventional) versus direct speed control (subject to some renewed commercial interest).
- Blade pitch control as a speed controller versus a power controller.
- Real power control on the grid side inverter versus real power control on the generator side rectifier.
- Permanent magnet generators versus electrically excited generators.
- Synchronous or asynchronous generators.
- Direct-drive or geared shaft systems.

This project has therefore delivered a suite of validated full converter wind turbine models. These have been used to investigate the implications of moving to direct-drive permanent magnet generator based wind turbines, and the effect of directly speed controlling a wind turbine, on the grid interface.

Direct speed control of the wind turbine, which offers a potential means of incremental improvement to the wind turbine's energy yield, is shown to require increased torque swings in order to improve the tracking of the optimal power coefficient. Furthermore, the

dynamic response is shown to largely depend on the torque limit and the speed controller performance.

Use of permanent magnet excitation in generators leads to an intrinsic link between speed and open circuit voltage, meaning that over-speed of a permanent magnet generator based wind turbine risks leading to excess voltages on the power converter. Whilst it is shown that voltage can be controlled by a pseudo field-weakening approach when the rectifier is switching with four quadrant operation, this control method is insufficient to protect the power converter from over-voltage in the event of a drive trip leading to uncontrolled diode bridge rectification. Furthermore, direct-drive shafts are shown to be at risk from mechanical oscillations at higher frequencies than the conventional geared shafts. Excitation of this mechanical resonance would risk imposing a transiently high generator speed with a corresponding over-voltage transient on the power converter.

The requirement to equip a PMG based wind turbine with a chopper and dynamic brake resistor has led to a decoupling of machine and grid dynamics. This led to the development of a simplified model of this type of wind turbine where the DC link controller on the machine bridge directly effected a torque on the shaft model. This removed the need to represent the generator and the majority of the machine bridge control thus increasing computational efficiency for longer time scale modelling.

8.2 Grid Connection of Wind Turbines

The mechanical resonance of a PMG shaft combined with its intrinsic voltage dependence on speed and high stator reactance are shown to lead to particular challenges under grid faults. An electrically excited machine can rely on field weakening to reduce terminal voltage and thereby avoid the power converter's maximum voltage limits under grid faults. However, the magnetic energy in the PMG's stator reactance must transfer to the power converter's DC link in order for the PMG's torque to be reduced during a fault; this inherently drives up the DC link voltage. With direct drive permanent magnet generators, this increase in DC link voltage has the potential to exceed the rated DC link voltage for the power converter. Furthermore, the rapid torque reduction could excite the shaft mechanical resonance and lead to a transient over-voltage on the power converter's stator connection. This demonstrates the importance of choppers and dynamic brake resistors for protecting the power converter of a PMG under grid faults.

Banham-Hall *et al.* [80] and section 4.2.5 described a novel, patented, adaptation to the generator bridge control in order to drive a ramped reduction in a PMG's torque under a

grid fault. This method, using a specific ramp rate, is shown to significantly reduce the amplitude of the resulting mechanical resonance. Furthermore, as the generator's torque is eventually removed, the brake resistor need only be rated at a reduced energy rating compared to a full chopper and brake resistor system.

The presence of a dynamic brake resistor, to slow the transient torque changes of a PMG wind turbine down, has been shown to permit a significant simplification of the model of a full converter PMG. The machine and rectifier can be removed, with the DC link voltage controller, which would normally set the rectifier's per unit real current reference, being used directly to set the per unit torque to the shaft model. This simplification produces a model that is faster in simulations and therefore beneficial for frequency response studies, which require a longer time-scale.

The GB Grid Code has implemented a requirement that necessitates all large (>50MW), transmission connected, wind farms to be capable of a proportional droop response to grid frequency disturbances. The power converter can deliver this response extremely quickly and with direct proportionality, however, the change in power output can then lead to slower mechanical changes from the wind turbine. Alternatively, the pitch control can be modified such that changes in the aerodynamic blade performance filter through to a change in turbine output power. This method offers slower response, but with no residual mechanical transients. Furthermore, the flywheel effect of the blades can be used to store energy when the wind turbine is operating in low wind speeds, this energy can then be used for temporary over-production following a frequency fall. These control methods were explored in section 4.3.

GB and European transmission system operators have floated the prospect of a requirement on transmission connected wind farms to provide a synthetic inertial response. This would require the turbine controller to restore the link between generator rotational kinetic energy and system frequency. Conventional approaches to providing a synthetic inertial response typically rely on a measurement of the power systems rate of change of frequency. However, frequency is typically a noisy signal and the inertial response therefore has to be either filtered, introducing delay, triggered, removing linearity, or accepted as subject to noise, which reduces its benefit as a stabilising influence. Banham-Hall *et al.* [87] and section 4.3 therefore propose alternatives based on speed controlling the wind turbine, or generating a synthetic load angle, which offer the potential of a fast inertial response that is not as sensitive to noise on the power system's

frequency. These controllers are shown to be tuneable and potentially advantageous over the predominant controller that relies on a frequency derivative.

8.3 Vanadium Redox Flow Battery Energy Storage

The importance of frequency response from wind farms is growing as the wind industry grows and as National Grid increases the holding requirement to accommodate potential larger single generation losses. However, whilst the Grid Code has ensured that technical solutions are found so that wind farms can participate in frequency control, it does not address the economic case. Energy storage and battery manufacturers are increasingly looking to base business cases for energy storage on the ancillary service markets, including frequency response. As such, the increasing GB requirement for this service, along with high levels of wind power generation and an islanded system, may present an opportunity for energy storage on the GB system.

A review of the available energy storage technologies in chapter 5 has found that the high cycle life, relatively low energy capacity cost, and design flexibility of the Vanadium Redox Flow Battery makes it a favourable technology for integration with wind power and combined provision of frequency response. The freedom to independently optimise the flow battery's energy and power ratings, together with its higher round trip efficiency make it preferable to the nearest competitor of thermal energy storage.

A simplified power system representation of the VRFB has been developed and validated, with accurate representation of battery voltage, round trip efficiency and state of charge. Furthermore, this model has been integrated onto the DC link of a model of an IGBT SVC, as these are often already required to provide dynamic reactive power compensation for large AC connected offshore wind farms. As with the wind turbine, the power electronic interface offers fast response to grid transients. An adaptation to the wind turbine grid fault ride-through control is presented in Banham-Hall *et al.* [138] and section 6.5. This modification allows the battery to be used to support the IGBT SVC's DC link during a grid fault and thus ensure continued reactive power delivery to the grid even in the event of an extended duration severe voltage dip.

Banham-Hall *et al.* [138] and section 6.5 also explore the control of a VRFB, in conjunction with a wind farm, to offer frequency response capability to the power system. A novel fuzzy logic controller is developed which manages the battery's state of charge by modifying the planned future energy trades with the power system. Furthermore, the integrated controller can be scheduled to perform daily arbitrage and wind smoothing,

thereby aggregating multiple different revenue streams for the single storage facility. This controller is shown to successfully control the battery's state of charge even in the presence of significant unexpected wind turbulence. Furthermore, the scheduling of daily arbitrage is shown to increase the combined frequency response capability of the wind farm and energy store during the hours when the store is charging. The battery is also shown to be capable of extremely fast response, with a complete current reversal possible in a couple of mains cycles. In conjunction with the direct proportional response that the power converter can achieve with a droop controller, this successfully demonstrates that the VRFB potentially offers a technically excellent solution to the problem of securing the grid's frequency stability with rising levels of wind power.

8.4 Frequency Response from Wind and Energy Storage

Developing the technical potential of wind farms, with or without energy storage, to provide frequency response services is only one part of the solution. Ultimately the GB frequency response reserves are selected and optimised through an ancillary services market. This market based approach means that a particular provider will only be selected to hold and provide frequency response if they are an economically viable option. Assessment of the historic trends in frequency response prices, combined with the projected increase in holding volumes required, suggest that prices for frequency response are likely to rise in future.

GB technical requirements for provision of frequency response currently require regulation from a fixed output level. For an intermittent resource, such as wind, this means that the plant holds a variable reserve margin and excess wind energy is either spilt or diverted to the energy store. It is found that the round-trip energy losses of the VRFB are not adequately compensated for by the higher energy price that can be achieved through reduced imbalance when meeting this requirement. This contributes to the conclusion that a VRFB's business case would be damaged if it had to accommodate wind's variability.

Wind farms have excellent capability to offer high frequency response without continuous spilling of wind energy. It has been shown, in section 7.4.3, that an energy store combined with a wind farm can offer increased frequency response reserves whilst the battery charges (typically at low night time prices) with very little risk of the wind having to be spilt. Therefore, during periods of battery charging, greater frequency response revenues could be earned, whilst the stored energy can be released at times of higher price (typically day time peaks) to maximise revenues. This offers improved revenues over both

an isolated energy store and one fully incorporated with a wind farm. This method is the subject of a patent application.

Overall, discounted cash flow analysis has shown that a VRFB store can achieve positive net present value with modest price increases from today. This NPV is worst when the energy store has to compensate for the wind's variability, is improved by operating the energy store entirely independently but is best if the energy store can share high frequency response capability with the wind farm. Nevertheless, the payback periods associated with any of these energy store configurations are too long, even under best case projections, to offer an attractive return to investors. Hence, whilst energy storage looks like it is close to competitive for provision of frequency response, it is not sufficiently advantageous to break into the market.

Given that energy storage is unlikely to offer a commercially viable frequency response solution for the imminent future without targeted subsidy, it is likely that available conventional CCGT plant will be required to offer this service instead. However, operating CCGTs at part load has implications for their efficiency and therefore Carbon emissions. Analysis here suggests that energy storage would be justifiable receiving ROCs at a rate of at least 0.17ROCs/MWh for providing a frequency response service alone. This would save emissions and could well tip energy storage towards commercial viability for this application.

8.5 Future Work

This thesis has concentrated on active power control from large offshore wind farms that are AC connected to the GB transmission system and consist of full converter interfaced wind turbines. Whilst this represents a significant proportion of the UK's likely offshore wind development, it is not representative of the totality. Indeed whilst chapter 3 focussed on the development of models of full converter wind turbines, it ignored advances towards DC generation and distribution. In that context, system frequency has no meaning and hence frequency response would be entirely dependent on the control system of the wind farm. Furthermore, delivery of response could be complicated by multi-terminal connection to different power systems. This is an important area for research as wind farms are located in deeper water, further from shore.

This project has focussed on the UK's wind power development and the GB power system, which is appropriate given that the UK has an advanced de-regulated industry where ancillary services, such as frequency response, are technically and commercially

well defined. However, frequency response services and requirements differ globally and it would be of interest to understand whether there are global opportunities for wind or energy storage to provide ancillary services.

The novel control method of the chopper and brake resistor under grid faults, covered in section 4.2.5, considers the removal of the primary torsional resonant mode of the drive shaft. This method could be extended by investigation of other mechanical modes of the wind turbine system. Currently prototype PMG based wind turbines are on long term tests, but these do not have to meet the Grid Codes and this method will need to be proven by site tests as Grid Code testing is conducted. Furthermore, whilst this method offers a means to minimise the DBR under a single fault there is increasing interest in ensuring that turbines can ride-through multiple grid faults caused by auto-reclosure of faulted transmission lines. This would lead to thermal stress to the chopper switch and DBR which is worthy of further investigation as Grid Code requirements develop.

The development of methods to provide inertial response from wind turbines focussed on finding control methods that did not require taking the derivative of system frequency. However, there are two parallel questions worthy of consideration, first, efforts to provide synthetic inertia have largely focussed on emulating synchronous generators' behaviour. However, is this the best method from a power system perspective? Second, it is understood that with wind speed below rated, inertial response to a low frequency event would lead to over-production from the turbine and slowing of the rotor. It is known that this leads onto a period of underproduction as the turbine recovers. This under recovery has been the subject of a National Grid consultation with industry and it is largely through an industry consensus that the true value of wind's inertial contribution can be understood. However, there is further work to be done here and it is also worth considering the inertial capability from a wind farm where many turbines are operating under different conditions and therefore offering different inertial recovery periods.

Chapter 5 compared many different energy storage technologies and concluded that the VRFB had significant potential across many different time-scales, including for frequency response applications. However, there is significant investment and innovation in energy storage suggesting that it is worth tracking developments in the field. Of particular interest are advancements in high temperature batteries, thermal energy storage and any advances in the VRFB's round trip efficiency, any of which could have a significant impact on the commercial viability of energy storage.

Whilst it has been highlighted that provision of frequency response from wind power would involve spilling wind energy and therefore incur a cost. Chapter 7 referenced work considering wind curtailment as a proportion of demand, but still there is no comprehensive study on the likely practical requirement for wind farms to provide frequency response services as wind power grows.

The commercial analysis of energy storage and wind focussed on the economics under the current market structures. It is anticipated that, when finally formulated, the capacity mechanism introduced by the electricity market reform will significantly alter the financial landscape. Such a scheme could well create a favourable environment for storage projects and thereby accelerate commercial deployment.

A brief analysis in chapter 7 showed that energy storage for frequency response could offer potential Carbon savings over the use of gas plants. However, energy storage could potentially offer Carbon benefits in a greater range of applications through ensuring that the power system operates with the least Carbon intensive plants. Such a study ought to form the basis of a critical appraisal of the level of specific subsidy support that would be appropriate in order to incentivise the energy storage industry.

Chapter 4 onwards has highlighted that operation of wind to provide frequency response from a fixed output power has a significant hidden cost. National Grid take a significantly different perspective on the technical requirements of frequency response to many other system operators, who prefer the delta control requirement. There is significant scope for quantifying whether National Grid's approach would truly lead to more reliable reserve or whether it will just shut wind power out of offering this service.

Finally, this thesis has to a large extent focussed on the situation in Britain, however, some other small islanded networks, with extensive wind deployment, may reach commercial viability for storage earlier. Ireland is one such example. Further work addressing such systems may well prove fruitful.

9 Appendices

9.1 Wind Modelling

9.1.1 Ziggurat Algorithm

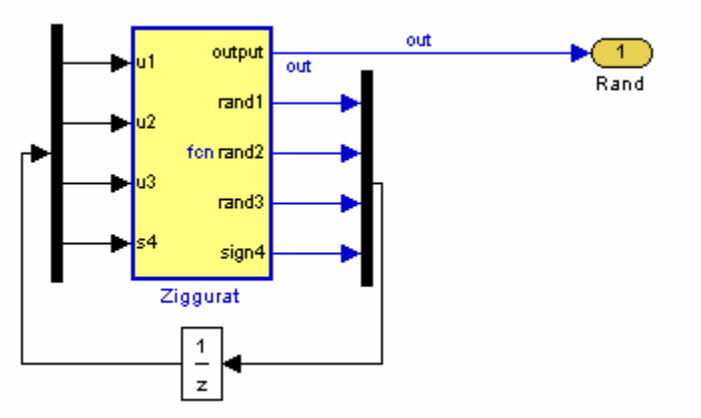

Figure 9.1: Ziggurat Algorithm Implementation

```
function [output,rand1,rand2,rand3,sign4] = fcn(u1,u2,u3,s4,ki,wi,r)
% This block calculates the output according to a linear congruential
generator
% The constants for the generator are from the Numerical Methods
generator
m = 2^32;
a = 1664525;
c = 1013904223;
% Initialise dummy variables
temp = u1;
temp2 = u2;
temp3 = u3;
temp4 = 10;
temp5 = 1;
temp6 = s4;
gen = 0;
% Initialise variables according to previous values to ensure they are
set on all executions
rand_out = u1;
rand1 = temp;
rand2 = temp2;
rand3 = temp3;
% Determine output's sign
s_int = a*temp6+c;
temp6 = mod(s_int,m);
s_rand = uint32(temp6);
s_bit = bitget(s_rand,17);
if s_bit ==1
    sign = 1;
else
    sign = -1;
end
sign4 = temp6;
while gen == 0
    int = a*temp+c;
    temp = mod(int,m);
    rand1 = temp;
    rand_temp = temp;               % Use the top 32 bits of Java's LCG
    index_int = bitand(uint32(rand_temp),uint32(255));
```

```
    index = double(index_int)+1;            % Use the eight MSBs as the
index
    if rand_temp < ki(index)
        rand_out = rand_temp*wi(index); % Set x output inside Ziggurat
rectangle
        gen = 1;
    elseif index == 1
        x = 2;
        while temp5 < temp4
            int2 = a*temp2+c;
            int3 = a*temp3+c;
            temp2 = mod(int2,m);
            temp3 = mod(int3,m);
            x = (-log(temp2/2^32))/r;
            y = -log(temp3/2^32);
            temp4 = x^2;
            temp5 = 2*y;
        end
        rand_out = x;
        gen = 1;
    end
    rand2 = temp2;
    rand3 = temp3;
end
output = 5*sign*rand_out;                   % Set the output on a unitary
scale
```

9.2 Full Energy Storage Comparison

9.2.1 Pumped Hydro

Source	CIGRE	Deane	Ibrahim	Kazempour	EU	ESA	Chen	Averages
Energy Cost ($/kWh Low)						40	5	22.5
Energy Cost ($/kWh High)						200	100	150
Power Cost ($/kW Low)	500	627		667	187	600	600	530.2
Power Cost ($/kW High)		2896		800	907	3000	2000	1920.6
O & M Cost (% of initial capital)				6.0%				6.00%
Cycle Life						20000		20000
Maximum Age (years)				50			50	50
Specific Energy (kWh/kg)							0.001	0.001
Specific Power (kW/kg)								
Round Trip Efficiency (%)	77.5%		72.5%	67.0%	77.5%	76.0%		74.10%
Self Discharge (%/month)							0	0.00%
Response Time (ms)								

Table 9.1: Pumped Hydroelectric Characteristics

9.2.2 Compressed Air Energy Storage

Source	Ibrahim	EPRI	DTI	EU	ESA	Chen	Averages
Energy Cost ($/kWh Low)		0.1			30	2	10.7
Energy Cost ($/kWh High)		30		534	100	50	178.5
Power Cost ($/kW Low)		350	500	224	500	400	394.8
Power Cost ($/kW High)			660		1000	800	820.0

O & M Cost (% of initial capital)								
Cycle Life			7000		15000			11000.0
Maximum Age (years)		30	25			30		28.3
Specific Energy (kWh/kg)						0.045		0.045
Specific Power (kW/kg)								
Round Trip Efficiency (%)	70.0%	75.0%			74.0%			73%
Self Discharge (%/month)						0		0.0%
Response Time (ms)		2000						2000.0

Table 9.2: Compressed Air Energy Storage Characteristics

9.2.3 Lead Acid

Source	Divya	Ibrahim	Dufo-Lopez	CIGRE	DTI	EU	ESA	Chen	Averages
Energy Cost ($/kWh Low)	66.7		160	150		305	200	200	180.3
Energy Cost ($/kWh High)	200		334	200		707	1100	400	490.2
Power Cost ($/kW Low)							350	300	325.0
Power Cost ($/kW High)							800	600	700.0
O & M Cost (% of initial capital)			2.5%						2.5%
Cycle Life	1500		1055		1000		500	750	961.0
Maximum Age (years)								10	10.0
Specific Energy (kWh/kg)	0.025	0.022			0.043	0.035	0.025	0.045	0.033
Specific Power (kW/kg)		0.5			0.19			0.19	0.293
Round Trip Efficiency (%)	75.0%		90.0%	72.5%	80.0%	78.0%	74.0%		78.3%
Self Discharge (%/month)	3.5%		2.5%		2.5%	3.5%		6.0%	3.6%
Response Time (ms)					3				3.0

Table 9.3: Lead Acid Battery Characteristics

9.2.4 Nickel Cadmium

Source	Divya	Ibrahim	Dufo-Lopez	CIGRE	DTI	EU	ESA	Chen	Averages
Energy Cost ($/kWh Low)	267		934	600		267	700	800	594.7
Energy Cost ($/kWh High)	800					1001	2000	1500	1325.3
Power Cost ($/kW Low)							600	500	550.0
Power Cost ($/kW High)							2000	1500	1750.0
O & M Cost (% of initial capital)			0.0%						0.0%
Cycle Life	3000		1850		2500	1500	1500	2250	2100.0
Maximum Age (years)								15	15.0
Specific Energy (kWh/kg)	0.063	0.05			0.075	0.07	0.05	0.063	0.1
Specific Power (kW/kg)		0.1			0.225			0.225	0.2
Round Trip Efficiency (%)	75.0%		75.0%		70.0%	70.0%	63.0%		70.6%

Self Discharge (%/month)	12.5%			12.5%				12.00%	12.3%
Response Time (ms)									

Table 9.4: Nickel Cadmium Battery Characteristics

9.2.5 Sodium Sulphur

Source	Divya	Dufo-Lopez	Kazempour	CIGRE	EPRI	DTI	EU	ESA	Chen	Averages
Energy Cost ($/kWh Low)		133		250	192		227	200	300	217.0
Energy Cost ($/kWh High)		400		350	585			1000	500	567.0
Power Cost ($/kW Low)			1535	300	250			1000	1000	817.0
Power Cost ($/kW High)			3003		300			2500	3000	2200.8
O & M Cost (% of initial capital)		3.0%	2.6%		6.0%					3.9%
Cycle Life	2500	5700			2500	2500	3500	3000	2500	3171.4
Maximum Age (years)			20		15		15		12.5	15.6
Specific Energy (kWh/kg)	0.1		0.4			0.195	0.195	0.125	0.195	0.202
Specific Power (kW/kg)						0.16			0.19	0.175
Round Trip Efficiency (%)	89.0%	80.0%	90.0%	89.0%	84.0%	90.0%	75.0%	87.0%		85.5%
Self Discharge (%/month)									600.00%	600.0%
Response Time (ms)					4					4.0

Table 9.5: Sodium Sulphur Battery Characteristics

9.2.6 Sodium Metal Halide (Zebra)

Source	Ibrahim	CIGRE	DTI	Chen	Averages
Energy Cost ($/kWh Low)		150		100	125.0
Energy Cost ($/kWh High)		800		200	500.0
Power Cost ($/kW Low)				150	150.0
Power Cost ($/kW High)				300	300.0
O & M Cost (% of initial capital)					
Cycle Life			2500	2500	2500.0
Maximum Age (years)				12	12.0
Specific Energy (kWh/kg)	0.11		0.125	0.11	0.115
Specific Power (kW/kg)	0.02		0.145	0.175	0.113
Round Trip Efficiency (%)			90.0%		90.0%
Self Discharge (%/month)				450.00%	450.0%
Response Time (ms)					

Table 9.6: Sodium Nickel Chloride (Zebra) Battery Characteristics

9.2.7 Lithium Ion

Source	Divya	Ibrahim	CIGRE	DTI	EU	ESA	Chen	Averages
Energy Cost ($/kWh Low)	934		780		200	700	600	642.8
Energy Cost ($/kWh High)	1335		1333		334	3000	2500	1700.4
Power Cost ($/kW Low)						1500	1200	1350.0
Power Cost ($/kW High)						3500	4000	3750.0
O & M Cost (% of initial capital)								
Cycle Life	3000			5000		4000	5500	4375.0
Maximum Age (years)							10	10.0
Specific Energy (kWh/kg)	0.14	0.15		0.175	0.125	0.125	0.14	0.143
Specific Power (kW/kg)		0.1		0.26			0.23	0.197
Round Trip Efficiency (%)	100.0%		100.0%	95.0%	95.0%	96.0%		97.2%
Self Discharge (%/month)	1.0%			1.0%			6.0%	2.7%
Response Time (ms)								

Table 9.7: Lithium Ion Battery Characteristics

9.2.8 Metal Air

Source	Divya	CIGRE	EU	ESA	Chen	Averages
Energy Cost ($/kWh Low)	67			20	10	32.3
Energy Cost ($/kWh High)	268			60	60	129.3
Power Cost ($/kW Low)				950	100	525.0
Power Cost ($/kW High)				2000	250	1125.0
O & M Cost (% of initial capital)						
Cycle Life	125	200		125	200	162.5
Maximum Age (years)						
Specific Energy (kWh/kg)	0.55		0.265	0.3	1.6	0.679
Specific Power (kW/kg)						
Round Trip Efficiency (%)		50.0%	50.0%	47.0%		49.0%
Self Discharge (%/month)					0.00%	0.0%
Response Time (ms)						

Table 9.8: Metal Air Battery Characteristics

9.2.9 Vanadium Redox

Source	Divya	Dufo-Lopez	Ponce de León	CIGRE	EPRI	DTI	EU	EPRI 2	ESA	Chen	Averages
Energy Cost ($/kWh Low)	480	267		500	100			210		150	284.5
Energy Cost ($/kWh High)	1335			1800	410			300		1000	969.0
Power Cost ($/kW Low)					425			1250	600	600	718.8
Power Cost ($/kW High)					700		1708	2300	2500	1500	1741.6
O & M Cost (% of initial capital)		4.0%			0.5%						0.0
Cycle Life	10000	2700				12000	14000	15000	2500	12000	9742.9
Maximum Age (years)					15	10		15		10	12.5
Specific Energy (kWh/kg)	0.04					0.025		0.02	0.02	0.02	0.025
Specific Power (kW/kg)											
Round Trip Efficiency (%)	85.0%	70.0%	72.0%		70.0%	79.0%	85.0%	60.0%	79.0%		0.8
Self Discharge (%/month)	0.0%									0	0.0
Response Time (ms)					10						10.0

Table 9.9: Vanadium Redox Flow Battery Characteristics

9.2.10 Zinc Bromine

Source	Divya	Dufo-Lopez	DTI	EU	ESA	Chen	Averages
Energy Cost ($/kWh Low)	480	254				150	294.7
Energy Cost ($/kWh High)	1335	334		900		1000	892.3
Power Cost ($/kW Low)					600	700	650.0
Power Cost ($/kW High)					2500	2500	2500.0
O & M Cost (% of initial capital)		6.0%					6.0%
Cycle Life		1710	2000		2500	2000	2052.5
Maximum Age (years)			10			8	9.0
Specific Energy (kWh/kg)	0.07		0.06	0.037	0.02	0.04	0.045
Specific Power (kW/kg)							
Round Trip Efficiency (%)	75.0%	77.0%	70.0%	75.0%	79.0%		75.2%
Self Discharge (%/month)						0	0.0%
Response Time (ms)							

Table 9.10: Zinc Bromine Flow Battery Characteristics

9.2.11 Polysulphide Bromine

Source	Divya	Ponce de León	EPRI	DTI	ESA	Chen	Averages
Energy Cost ($/kWh Low)	480		65		150	150	211.3
Energy Cost ($/kWh High)	1335		120		1800	1000	1063.8
Power Cost ($/kW Low)			150		600	700	483.3
Power Cost ($/kW High)			300		2500	2500	1766.7
O & M Cost (% of initial capital)			2.2%				2.2%
Cycle Life					400		400.0
Maximum Age (years)			15	15		12	14.0
Specific Energy (kWh/kg)					0.02		0.0
Specific Power (kW/kg)							
Round Trip Efficiency (%)	75.0%	67.0%	62.5 %	68.0 %			68.1%
Self Discharge (%/month)	0.0%					0	0.0%
Response Time (ms)			100				100.0

Table 9.11: Polysulphide Bromine Flow Battery Characteristics

9.2.12 Superconducting Magnetic Energy Store

Source	Ibrahim	CIGRE	EU	Chen	Averages
Energy Cost ($/kWh Low)				1000	1000.0
Energy Cost ($/kWh High)				10000	10000.0
Power Cost ($/kW Low)				200	200.0
Power Cost ($/kW High)			467	300	383.5
O & M Cost (% of initial capital)					
Cycle Life				100000	100000.0
Maximum Age (years)				20	20.0
Specific Energy (kWh/kg)				0.0025	0.003
Specific Power (kW/kg)				1.25	1.250
Round Trip Efficiency (%)	95.0%	95.0%	97.0%		95.7%
Self Discharge (%/month)				375.00%	375.0%
Response Time (ms)	100				100.0

Table 9.12: Superconducting Magnetic Energy Store Characteristics

9.2.13 Supercapacitors

Source	Ibrahim	CIGRE	EPRI	EU	ESA	Chen	Averages
Energy Cost ($/kWh Low)					6000	300	3150.0
Energy Cost ($/kWh High)					10000	2000	6000.0
Power Cost ($/kW Low)		350	210	267	100	100	205.4
Power Cost ($/kW High)			708	1335	800	300	785.8
O & M Cost (% of initial capital)			1.5%				1.5%
Cycle Life			100000	300000	30000	100000	132500.0
Maximum Age (years)	10					20	15.0
Specific Energy (kWh/kg)	0.01			0.06	0.015	0.008	0.023
Specific Power (kW/kg)	1.4					2.75	2.075
Round Trip Efficiency (%)	95.0%		93.0%	91.5%	98.0%		94.4%
Self Discharge (%/month)	150.0%					900.00%	525.0%
Response Time (ms)			5				5.0

Table 9.13: Supercapacitor Characteristics

9.2.14 Flywheels

Source	Ibrahim	EPRI	ESA	Walawalker	Chen	Averages
Energy Cost ($/kWh Low)		80	2000	2200	1000	1320.0
Energy Cost ($/kWh High)		231	4000	3000	5000	3057.8
Power Cost ($/kW Low)		189	200	550	250	297.3
Power Cost ($/kW High)		410	600	750	350	527.5
O & M Cost (% of initial capital)		7.5%		3.8%		5.7%
Cycle Life	100000	100000	25000	100000	20000	69000.0
Maximum Age (years)					15	15.0
Specific Energy (kWh/kg)			0.01	0.01	0.02	0.013
Specific Power (kW/kg)					0.95	0.950
Round Trip Efficiency (%)	85.0%	75.0%	94.0%			84.7%
Self Discharge (%/month)	1200.0%				3000.00%	2100.0%
Response Time (ms)		5				5.0

Table 9.14: Flywheel Characteristics

9.2.15 Thermal

Source	Chen Aquifers	Chen Cryogenic	Chen Molten Salt	Averages
Energy Cost ($/kWh Low)	20	3	30	17.7
Energy Cost ($/kWh High)	50	30	60	46.7
Power Cost ($/kW Low)		200		200.0
Power Cost ($/kW High)		300		300.0
O & M Cost (% of initial capital)				
Cycle Life				
Maximum Age (years)	15	30	10	18.3
Specific Energy (kWh/kg)	0.1	0.2	0.14	0.1
Specific Power (kW/kg)		0.02		0.0
Round Trip Efficiency (%)			40%	0.4
Self Discharge (%/month)	15.00%	15.00%		0.2
Response Time (ms)				

Table 9.15: Thermal Energy Store Characteristics

10 References

[1] UK Government. "Climate Change Act 2008." [Online] Available at: http://www.legislation.gov.uk/ukpga/2008/27/section/1 [Accessed 26 Jan. 2012].

[2] Department of Energy and Climate Change. "UK Renewable Energy Roadmap." [Online] Available at: http://www.decc.gov.uk/assets/decc/11/meeting-energy-demand/renewable-energy/2167-uk-renewable-energy-roadmap.pdf [Accessed 26 Jan 2012].

[3] National Grid. "'Operating the transmission networks in 2020 – Update June 2011." [Online] Available at: http://www.nationalgrid.com/NR/rdonlyres/DF928C19-9210-4629-AB78-BBAA7AD8B89D/47178/Operatingin2020_finalversion0806_final.pdf [Accessed 01 Feb. 2012].

[4] Energy Research Partnership. "The future role for energy storage in the UK main report." [Online] Available at: http://www.energyresearchpartnership.org.uk/tiki-index.php?page=page12 [Accessed 31 Oct. 2011].

[5] P. W. Carlin, A. S. Laxson, E. B. Muljadi. "The History and State of the Art of Variable-Speed Wind Turbine Technology." *Wind Energy*, vol. 6, no. 2, pp. 129-159, Apr. 2003.

[6] Global Wind Energy Council (GWEC). Apr. 2011. "Global Wind Report 2010" [Online] Available at: http://www.gwec.net/index.php?id=180 [Accessed Sept. 13 2011].

[7] Commission of the European Communities. Jan. 2008. "20 20 by 2020: Europe's Climate Change Opportunity", [Online] Available at: http://www.energy.eu/directives/com2008_0030en01.pdf [Accessed Sept. 22 2011].

[8] Department of Energy and Climate Change. 2011. "UK Energy Sector Indicators 2011", [Online] Available at: http://www.decc.gov.uk/assets/decc/11/stats/publications/indicators/3327-uk-energy-sector-indicators-2011.pdf [Accessed Oct. 31 2011]

[9] Department for Business, Enterprise and Regulatory Reform. Apr. 2008. “Atlas of UK Marine Renewable Energy Resources.” [Online] Available at: http://www.renewables-atlas.info/downloads/documents/Renewable_Atlas_Pages_A4_April08.pdf [Accessed Oct. 31 2011]

[10] D. Toke. “The UK offshore wind power programme: A sea-change in UK energy policy?”, *Energy Policy*, vol. 39, no. 2, pp526-534, Feb. 2011.

[11] Pöyry. Jul. 2009. “Impact of Intermittency: How wind variability could change the shape of the British and Irish electricity market.” [Online] Available at: http://www.poyry.com/linked/group/study [Accessed Mar. 4 2011]

[12] A. D. Hansen, L. Hansen. “Wind Turbine Concept Market Penetration over 10 years (1995-2004).” *Wind Energy*, vol. 10, no. 1, pp. 81-97, Jan. 2007.

[13] S. Soter, R. Wegener. "Development of Induction Machines in Wind Power Technology." *In IEEE Electric Machines & Drives Conf.,* Antalya, Turkey, 2007, vol.2, pp.1490-1495.

[14] E. Muljadi, N. Samaan, V. Gevorgian, L. Jun, S. Pasupulati. "Short circuit current contribution for different wind turbine generator types." *In IEEE Power and Energy Soc. General Meeting,* Minneapolis, MN, U.S.A., 2010, doi: 10.1109/PES.2010.5589677.

[15] A. D. Hansen, G. Michalke. “Fault ride-through capability of DFIG wind turbines.” *Renewable Energy*, vol. 32, no. 9, pp. 1594-1610, Jul. 2007.

[16] Z. Chen, J. M. Guerrero, F. Blaabjerg. “A Review of the State of the Art of Power Electronics for Wind Turbines.” *IEEE Trans. Power Electron*, vol. 24, no. 8, pp. 1859-1875, Aug. 2009.

[17] C. Jauch. “Transient and Dynamic Control of a Variable Speed Wind Turbine with Synchronous Generator.” *Wind Energy*, vol. 10, no. 3, pp247-269, May 2007.

[18] R. Peña, R. Cardenas, R. Blasco, G. Asher, J. Clare. "A cage induction generator using back to back PWM converters for variable speed grid connected wind energy system." *In Ind. Electron. Soc. Ann. Conf., IECON '01*, Denver, CO, U.S.A., 2001, vol.2, pp.1376-1381.

[19] M. Molinas, B. Naess, W. Gullvik, T. Undeland. “Cage induction generators for wind turbines with power electronics converters in the light of the new grid codes”, Presented at the European Conf. Power Electron. and Applicat., Dresden, Germany, 2005.

[20] V. Akhmatov. “Modelling and ride-through capability of variable speed wind turbines with permanent magnet generators.” *Wind Energy*, vol. 9, no. 4, pp.313–326, Jul. 2006.

[21] C. Lewis, J. Muller. "A Direct Drive Wind Turbine HTS Generator." *In IEEE Power and Energy Soc. General Meeting*, Tampa, FL, U.S.A., 2007, doi: 10.1109/PES.2007.386069.

[22] S. Loddick. "Active stator, a new generator topology for direct drive permanent magnet generators," Presented at the 9th IET Int. Conf. on AC and DC Power Transmission, ACDC, London, UK, 2010.

[23] P. Djapic, G. Strbac. “Grid Integration Options for Offshore Wind Farms.” Department for Trade and Industry (DTI). URN 06/2133. Dec. 2006.

[24] A. B. Morton, S. Cowdroy, J. R. A. Hill, M. Halliday, G. D. Nicholson. "AC or DC? economics of grid connection design for offshore wind farms." Presented at the 8th IEE Int. Conf. on AC and DC Power Transmission, ACDC, London, UK, 2006.

[25] C. Zhan, C. Smith, A. Crane, A. Bullock, D. Grieve. "DC transmission and distribution system for a large offshore wind farm," Presented at the 9th IET Int. Conf. on AC and DC Power Transmission, ACDC, London, UK, 2010.

[26] Offshore Grid. Oct. 2011. “Offshore Grid Direct Design Map.” [Online] Available at: http://www.offshoregrid.eu/ [Accessed Nov. 3 2011].

[27] J. Morren, J. Pierik, S. W. H. de Haan. “Inertial Response of Variable Speed Wind Turbines.” *Electric Power Syst. Research*, vol. 76, no.11, pp980-987, Jul. 2006.

[28] Renewable Energy Foundation. Jun. 2011. “Scottish Wind Power Constraint Payments Update.” [Online] Available at: http://www.ref.org.uk/publications/239-scottish-wind-power-constraint-payments-update [Accessed Oct. 31 2011].

[29] National Grid. 2009. “Report of the National Grid Investigation into the Frequency Deviation and Automatic Demand Disconnection that occurred on 27th May 2008”, [Online] Available at: http://www.nationalgrid.com/NR/rdonlyres/E19B4740-C056-4795-A567-91725ECF799B/32165/PublicFrequencyDeviationReport.pdf [Accessed Mar. 24 2010]

[30] National Grid. Jan. 2010. “Working Group Report: Small Embedded Generation Working Group Report.” [Online] Available at: http://www.nationalgrid.com/NR/rdonlyres/AAD8BBAB-82E3-4C02-9D35-D2575331609F/39699/pp10_01Workinggroupreportv1018Jan2010.pdf [Accessed Oct. 31 2011].

[31] National Grid. Aug. 2011. “Summary of Latest Simulation Results.” [Online] Available at: https://www.nationalgrid.com/NR/rdonlyres/D06C6209-24B4-4BA4-84F5-551FA87B2FA6/49693/SimResultsAugust2011.pdf [Accessed Oct. 31 2011]

[32] P. M. Ashton, G. A. Taylor, M. R. Irving, A. M. Carter, M. E. Bradley. “Prospective Wide Area Monitoring of the Great Britain Transmission System using Phasor Measurement Units.” Accepted for the IEEE Power and Energy Soc. General Meeting, San Diego, CA, U.S.A., July 2012.

[33] National Grid. “Future Balancing Services Requirements: Response.” [Online] Available at: http://www.nationalgrid.com/NR/rdonlyres/0F82BB0B-98E9-4B02-A514-3C87A85E60D8/42696/Future_Balancing_Services_Requirements_Response1.pdf [Accessed 17 Jun. 2010]

[34] R. Walawalkar, J. Apt, R. Mancini. “Economics of electric energy storage for energy arbitrage and regulation in New York.”, *Energy Policy*, vol. 35, no. 4, pp. 2558-2568, Apr. 2007.

[35] C. Vartanian, N. Bentley. "A123 systems' advanced battery energy storage for renewable integration." *In IEEE Power Syst. Conf. and Exposition (PSCE),* Phoenix, Az, U.S.A., 2011, doi: 10.1109/PSCE.2011.5772569.

[36] A. Oudalov, D. Chartouni, C. Ohler. "Optimizing a Battery Energy Storage System for Primary Frequency Control." *IEEE Trans. on Power Syst.*, vol.22, no.3, pp.1259-1266, Aug. 2007.

[37] T. Hals, R. Hampton. “Beacon Power bankrupt, had U.S. backing like Solyndra.” Oct. 31 2011, *Reuters*, [Online] Available at: http://www.reuters.com/article/2011/10/31/us-beaconpower-bankruptcy-idUSTRE79T39320111031 [Accessed 28 Nov. 2011]

[38] National Grid. “Initial Consultation: Operating the Electricity Transmission Networks in 2020.” [Online] Available at: http://www.nationalgrid.com/uk/Electricity/Operating+in+2020 [Accessed 19 Jun. 2009]

[39] J. Eyer, G. Corey. “Energy Storage for the Electricity Grid: Benefits and Market Potential Assessment Guide.” Sandia National Laboratories, SAND2010-0815, Feb. 2010.

[40] J. G. Slootweg, S. W. H. de Haan, H. Polinder, W. L. Kling. “General model for representing variable speed wind turbines in power system dynamics simulations.” *IEEE Trans. on Power Syst.*, vol.18, no.1, pp. 144-151, Feb. 2003.

[41] T. Burton, D. Sharpe, N. Jenkins, E. Bossanyi. *Wind Energy Handbook*. Chichester, UK: Wiley, 2001, pp. 45.

[42] P. Sørensen, N. A. Cutululis, A. Vigueras-Rodríguez, L. E. Jensen, J. Hjerrild, M. H. Donovan, H. Madsen. “Power Fluctuations From Large Wind Farms”, *IEEE Trans. on Power Syst.*, vol. 22, no. 3, pp. 958-965, Aug. 2007.

[43] P. Sorensen, A. D. Hansen, P. A. Carvalho Rosas. “Wind models for simulation of power fluctuations from wind farms.” *J. of Wind Eng. and Ind. Aerodynamics*, vol. 90, no. 12-15, pp. 1381-1402, Dec. 2002.

[44] *Wind Turbines: Design Requirements*, BS EN 61400-1, British Standards Institute, 2005.

[45] G. Marsaglia, W. W. Tsang. “The Ziggurat Method for Generating Random Variables”, [Online] Available at: http://www.jstatsoft.org/v05/i08/paper [Accessed Apr. 21 2010].

[46] A. D. Diop, E. Ceanga, J-L. Rétiveau, J-F. Méthot, A. Ilinca, A. “Real-time three dimensional wind simulation for windmill rig tests”, *Renewable Energy*, vol. 32, no. 13, pp2268-2290.

[47] S. Heier, *Grid Integration of Wind Energy Conversion Systems*. 2nd Ed, Chichester, UK: Wiley, 2006, pp. 44.

[48] G. Ramtharan, N. Jenkins, O. Anaya-Lara, E. Bossanyi. "Influence of rotor structural dynamics representations on the electrical transient performance of FSIG and DFIG wind turbines." *Wind Energy*, vol. 10, no. 4, pp. 293-301, Jul. 2007.

[49] S. M. Muyeen, Md. Hasan Ali, R. Takahashi, T. Murata, J. Tamura, Y. Tomaki, A. Sakahara, E. Sasano. "Comparative study on transient stability analysis of wind turbine generator system using different drive train models", *IET Renewable Power Generation*, vol. 1. no. 2, pp. 131-141, Jun. 2007.

[50] A. D. Hansen, G. Michalke. "Modelling and Control of Variable Speed Multi-pole Permanent Magnet Synchronous Generator Wind Turbine." *Wind Energy*, vol. 11, no. 5, pp. 537-554, Sept. 2008.

[51] V. Akhmatov. "Analysis of dynamic behavior of electric power systems with large amount of wind power". PhD Thesis, Ørsted DTU, Denmark, 2003, pp. 115.

[52] B. Adkins, R. G. Harley. *The General Theory of Alternating Current Machines.* London, UK: Chapman and Hall Ltd., 1975, pp61-65.

[53] B. K. Bose. *Modern Power Electronics and AC Drives*, Upper Saddle River, New Jersey, USA: Prentice Hall PTR, 2002, pp.357-380.

[54] A. Troedson, "PM Generator and Full Power Converter – The New Drive Train Standard." [Online] Available at: http://www.ngusummitapac.com/media/whitepapers/The_Switch_NGUAPAC.pdf [Accessed Oct. 04 2011].

[55] G. Michalke, A. D. Hansen, T. Hartkopf. "Control strategy of a variable speed wind turbine with multipole permanent magnet synchronous generator." *In European Wind Energy Conf., EWEC '07*, 2007. [Online] Available at: http://www.ewec2007proceedings.info/ [Accessed Mar. 17 2009].

[56] H. Li, Z. Chen. "Design optimization and site matching of direct-drive permanent magnet wind power generator systems." *Renewable Energy*, vol. 34, no. 4, pp. 1175-1184, Apr. 2009.

[57] Converteam. “MV3000 Full Power Wind Converters Low Voltage.”, [Online] Available at: www.converteam.com [Accessed Oct. 31 2011].

[58] R. C. Portillo, M. M. Prats, J. I. Leon, J. A. Sanchez, J. M. Carrasco, E. Galvan, L. G. Franquelo. “Modelling Strategy for Back-to-Back Three-Level Converters Applied to High-Power Wind Turbines.” *IEEE Trans. on Ind. Electron.*, vol.53, no.5, pp.1483-1491, Oct. 2006.

[59] A. D. Hansen, G. Michalke. "Multi-pole permanent magnet synchronous generator wind turbines' grid support capability in uninterrupted operation during grid faults." *IET Renewable Power Generation*, vol.3, no.3, pp.333-348, Sept. 2009

[60] J-K. Seok; J-K. Lee; D-C. Lee. "Sensorless speed control of nonsalient permanent-magnet synchronous motor using rotor-position-tracking PI controller." *IEEE Trans. on Ind. Electron.*, vol.53, no.2, pp. 399- 405, Apr. 2006.

[61] R. D. Richardson, W. L. Erdman. “Variable Speed Wind Turbine.” U.S. Patent 5,083,039, Jan. 21 1992.

[62] R. Jones, P. Brogan, E. Grøndahl, H. Stiesdal. “Power Converters.” G.B. Patent 2432267, Nov. 13 2006.

[63] H. Camblong, I. Martinez de Alegria, M. Rodriguez, G. Abad. “Experimental evaluation of wind turbines maximum power point tracking controllers.” *Energy Conversion and Manage.*, vol. 47, no. 18-19, pp. 2846-2858, Nov. 2006.

[64] W. E. Leithead, B. Connor. “Control of variable speed wind turbines: Design task.” *Int. J. of Control*, vol. 73, no. 13, pp. 1189-1212, Nov. 2000.

[65] T. Burton, D. Sharpe, N. Jenkins, E. Bossanyi. *Wind Energy Handbook*. Chichester, UK: Wiley, 2001, pp. 471-483.

[66] S. M. Muyeen, M. H. Ali, R. Takahashi, T. Murata, J. Tamura. “Damping of Blade-shaft torsional oscillations of wind turbine generator system.” *Electric Power Components and Syst.*, vol. 36, no. 2, pp195-211, 2008.

[67] E. Muljadi, C. P. Butterfield. "Pitch-controlled variable-speed wind turbine generation." *IEEE Trans. on Ind. Applica.*, vol. 37, no.1, pp.240-246, Jan/Feb 2001.

[68] E. A. Bossanyi. "Further load reductions with individual pitch control." *Wind Energy*, vol. 8, no. 4, pp.481–485, Oct. 2005.

[69] P. Christiansen. "A Sea of Turbines.", *Power Engineer*, vol. 17, pp.22-24, Feb. 2003.

[70] T. Gjengedal. "Large-scale wind power farms as power plants." *Wind Energy*, vol. 8, no. 3, pp. 361-373, Jul. 2005.

[71] D. D. Banham-Hall, C. A. Smith, G. A. Taylor, M. R. Irving. "Grid Connection Oriented Modelling of Wind Turbines with Full Converters." *In 44th Universities Power Eng. Conf.,* CD-ROM, 2009.

[72] F. Iov, A. D. Hansen, P. Sorensen, F. Blaabjerg. 2004. "Wind Turbine Blockset in Matlab/Simulink - General Overview and Description of the Models." [Online] Formerly Available at: http://www.iet.aau.dk/Research/research_prog/wind_turbine/ Projects/SimPlatformPrj/ [Accessed 8 July 2008].

[73] A. D. Hansen, C. Jauch, P. Sorensen, F. Iov, F. Blaabjerg. Dec. 2003. "Dynamic Wind Turbine Models in Power System Simulation Tool DIgSILENT." [Online] Available at: http://www.digsilent.es/Software/Application_Examples/ris-r-1400.pdf [Accessed 12 Jun 2009].

[74] F. Martin, I. Purellku, T. Gehlhaar. "Modelling of and Simulation with Grid Code validated Wind Turbine Models." *In 8th Int. Workshop on Large Scale Integration of Wind Power into Power Syst.,* Bremen, Germany, 2009, USB.

[75] J. N. Nielsen, V. Akhmatov, J. Thisted, E. Grondahl, P. Egedal, M. N. Frydensbjerg, K. H. Jensen. "Modelling and Fault-Ride-Trough Tests of Siemens Wind Power 3.6 MW Variable-speed Wind Turbines." *Wind Eng.*, vol. 31, no. 6, pp. 441-452, December 2007.

[76] H. Urdal, J. Horne. "2GW of wind and rising fast – Grid Code compliance of large wind farms in the Great Britain transmission system." Presented at the Nordic Wind Power Conf., NWPC'2007, Roskilde, Denmark, 2007.

[77] J. C. Ausin, D. N. Gevers, B. Andresen. "Fault Ride-through Capability Test Unit for Wind Turbines." *Wind Energy*, vol. 11, no. 1, pp3-12, January 2008.

[78] National Grid. Sept. 2008. "Guidance Notes for Power Park Developers." No. 2, [Online] Available at: http://www.nationalgrid.com/uk/Electricity/Codes/gridcode/associateddocs/ [Accessed 10 October 2008]

[79] Eon Netz. 2006. "Grid Code – High and Extra-high Voltage." pp. 18-19 [Online] Available at: http://www.pvupscale.org/IMG/pdf/D4_2_DE_annex_A-3_EON_HV_grid__connection_requirements_ENENARHS2006de.pdf [Accessed 10 October 2008]

[80] D. D. Banham-Hall, C. A. Smith, G. A. Taylor, M. R. Irving. "Meeting Modern Grid Codes with Large Direct-Drive Permanent Magnet Generators: Low Voltage Ride-through." *Wind Energy*, in press.

[81] D. D. Banham-Hall, C. A. Smith, G. A. Taylor. "Generator torque control methods." European Patent Application no. EP10006961.1 filed 6 Jul. 2010.

[82] L. M. Fernandez, C. A. Garcia, F. Jurado. "Operating capability as a PQ/PV node of a direct-drive wind turbine based on a permanent magnet synchronous generator." *Renewable Energy*, vol. 35, no. 5, pp.1308-1318, Jun. 2010.

[83] D. D. Banham-Hall, C. A. Smith, G. A. Taylor, M. R. Irving. "Towards Large-scale Direct Drive Wind Turbines with Permanent Magnet Generators and Full Converters.", *In IEEE Power and Energy Soc. General Meeting,* Minneaspolis, MN, U.S.A., 2010, doi: 10.1109/PES.2010.5589780.

[84] J. Conroy, R. Watson. "Low voltage ride-through of a full converter wind turbine with permanent magnet generator." *IET Renewable Power Generation*, vol. 1, no. 3, pp. 182-189, Sept. 2007.

[85] G. Michalke, A. D. Hansen. "Modelling and control of variable speed wind turbines for power system studies." *Wind Energy*, vol. 13, no. 4, pp.307-322, May 2010.

[86] J. Conroy, R. Watson. "Aggregate modelling of wind farms containing full-converter wind turbine generators with permanent magnet synchronous

machines: transient stability studies.", *IET Renewable Power Generation*, vol.3, no.1, pp.39-52, Mar. 2009.

[87] D. D. Banham-Hall, C. A. Smith, G. A. Taylor, M. R. Irving. "Meeting Modern Grid Codes with Large Direct-Drive Permanent Magnet Generators: Frequency Response and Inertia." *Wind Energy*, awaiting revisions.

[88] C. Bjerge, J. R. Kristoffersen. "How to run an offshore wind farm like a conventional power plant." *Modern Power Syst.*, vol. 27, no. 1, pp31-33, Jan. 2007.

[89] E. Malnick, R. Mendick. "Wind farm paid £1.2 million to produce no electricity." *The Telegraph* (Sept. 17 2011), Earth Section.

[90] J. Horne. "Wind Farms can provide Frequency Response – Experience of the Great Britain Transmission System Operator.", *In 7th Int. Workshop on Large Scale Integration of Wind Power into Power Syst*., Madrid, Spain, 2008, USB.

[91] L. Holdsworth, J. B. Ekanayake, N. Jenkins. "Power System Frequency Response from Fixed Speed and Doubly Fed Induction Generator based Wind Turbines." *Wind Energy*, vol. 7, no. 1, pp. 21-35, Jan. 2004.

[92] J. B. Ekanayake, N. Jenkins, G. Strbac. "Frequency Response from Wind Turbines." *Wind Eng.*, vol. 32, no. 6, pp573-586, Dec. 2008.

[93] R. W. Delmerico, N. W. Miller. "System and Method for Utility and Wind Turbine Control." U. S. Patent 7,345,373, Mar. 18 2008.

[94] J. Conroy, R. Watson. "Frequency Response Capability of Full Converter Wind Turbine Generators in Comparison to Conventional Generation", *IEEE Trans. on Power Syst.*, vol. 23, no. 2, pp649-656, May 2008.

[95] G. C. Tarnowski, P. C. Kjaer, P. E. Sorensen, J. Ostergaard. "Variable speed wind turbines capability for temporary over-production." *In IEEE Power and Energy Soc. General Meeting*, Calgary, AB, Canada, 2009, doi: 10.1109/PES.2009.5275387.

[96] D. D. Banham-Hall, C. A. Smith, G. A. Taylor, M. R. Irving. "Grid Connection Oriented Modelling of Wind Farms to Support Power Grid Stability", *In 21st Int. Conf. on Syst. Eng.,* Coventry, U.K., 2010, CD-ROM.

[97] A. Teninge, C. Jecu, D. Roye, S. Bacha, J. Duval, R. Belhomme. "Contribution to frequency control through wind turbine inertial energy storage." *IET Renewable Power Generation*, vol.3, no.3, pp.358-370, Sept. 2009.

[98] H. Urdal, Private Communication, Dec. 17 2010.

[99] Hydro-Quebec. "Transmission Provider Technical Requirements for the Connection of Power Plants to the Hydro-Quebec Transmission System." Feb. 2006.

[100] National Grid. Dec. 20 2010. "Frequency Response Working Group Minutes." [Online] Available at: http://www.nationalgrid.com/NR/rdonlyres/E71D0100-4FD7-4056-896C-0A72FB480D94/49130/Meeting15Minutes.pdf [Accessed 4 Jan. 2011].

[101] European Network of Transmission System Operators for Electricity [ENTSO-E], Mar. 22 2011, "ENTSO-E Draft Requirements for Grid Connection Applicable to all Generators." [Online] Available at: https://www.entsoe.eu/fileadmin/user_upload/_library/news/110322_Pilot_Network_Code_Connections.pdf [Accessed 12 June 2011]

[102] J. Morren, S. W. H. de Haan, W. L. Kling, J. A. Ferreira. "Wind Turbines Emulating Inertia and Supporting Primary Frequency Control." *IEEE Trans. on Power Syst.*, vol. 21, no. 1, pp. 433-434, Feb. 2006.

[103] J. Morren, J. Pierik, S. W. H. de Haan "Inertial response of variable speed wind turbines." *Electric Power Syst. Research*, vol. 76, no. 11, pp. 980-987, Jul. 2006.

[104] E. V. Larsen, R. W. Delmerico. "Battery Energy Storage Power Conditioning System." U. S. Patent 5,798,633, Aug. 25 1998.

[105] S. Wachtel, A. Beekmann. "Contribution of Wind Energy Converters with Inertial Emulation to Frequency Control and Frequency Stability in Power Systems." *In 8th Int. Workshop on Large Scale Integration of Wind Power into Power Syst.,* Bremen, Germany, 2009, USB.

[106] G. C. Tarnowski, P. Carne Kjær, P. E. Sørenson, J. Østergaard. "Study on Variable Speed Wind Turbines Capability for Frequency Response." *In Proc. of the European Wind Energy Conf., EWEC 2009.* [Online] Available at:

http://www.ewec2009proceedings.info/allfiles2/636_EWEC2009presentation.pdf [Accessed 23 Nov. 2009]

[107] H. Chen, T. N. Cong, W. Yang, C. Tan, Y. Li, Y. Ding. "Progress in electrical energy storage system: A critical review." *Progress in Natural Sci.*, vol. 19, no. 3, pp. 291-312, Mar. 2009.

[108] H. Ibrahim, A. Ilinca, J. Perron. "Energy Storage Systems – Characteristics and comparisons." *Renewable and Sustainable Energy Reviews*, vol. 12, no. 5, pp. 1221-1250, Jun. 2008.

[109] Department of Trade and Industry. "Review of electrical energy storage technologies and systems and of their potential for the UK." DG/DTI/00055/00/00, Jul. 2004.

[110] Electric Power Research Institute. "Comparison of Storage Technologies for Distributed Resource Applications." 1007301, Feb. 2003.

[111] International Council on Large Electric Systems. "Electric Energy Storage Systems." Working Group C6.15, Apr. 2011.

[112] European Parliament's committee on Industry, Research and Energy. "Outlook of Energy Storage Technologies." IP/A/ITRE/FWC/2006-087/Lot 4/C1/SC2, Feb. 2008.

[113] Electricity Storage Association. 2008. [Online] Available at: http://www.electricitystorage.org/about/welcome [Accessed 01 Dec. 2011].

[114] J. P. Deane, B. P. Ó Gallachóir, E. J. McKeogh. "Techno-economic review of existing and new pumped hydro energy storage plant." *Renewable and Sustainable Energy Reviews*, vol. 14, no. 4, pp. 1293-1302, May 2010.

[115] S. J. Kazempour, M. P. Moghaddam, M. R. Haghifam, G. R. Yousefi. "Electric energy storage systems in a market-based economy: Comparison of emerging and traditional technologies." *Renewable Energy*, vol. 34, no. 12, pp. 2630-2639, Dec. 2009.

[116] K. C. Divya, J. Østergaard. "Battery energy storage technology for power systems – An overview." *Electric Power Syst. Research*, vol. 79, no. 4, Apr. 2009.

[117] R. Dufo-López, J. L. Bernal-Agustín, J. A. Domínguez-Navarro. "Generation management using batteries in wind farms: Economical and technical analysis for Spain." *Energy Policy*, vol. 37, no. 1, pp. 126-139, Jan. 2009.

[118] J. Himelic, F. Novachek. "Sodium Sulphur Battery Energy Storage And Its Potential To Enable Further Integration of Wind." Xcel Energy Contract # RD3-12, Jul. 2010.

[119] P. Lang, N. Wade, P. Taylor, P. Jones, T. Larsson. "Early Findings of an energy storage practical demonstration", Presented at the 21st Int. Conf. on Electricity Distribution, Frankfurt, Germany, 2011.

[120] C. Ponce de León, A. Frías-Ferrer, J. González-García, D. A. Szánto, F. C. Walsh. "Redox flow cells for energy conversion." *J. of Power Sources*, vol. 160, no. 1, pp. 716-732, Sep. 2006.

[121] Department of Trade and Industry. "Regenesys Utility Scale Energy Storage." URN 04/1048, 2004.

[122] Isentropic. "The advantages of our system." [Online] Available at: http://www.isentropic.co.uk/ [Accessed 01 Dec. 2011]

[123] M. L. Lazarewicz, T. M. Ryan. "Integration of Flywheel-Based Energy Storage for Frequency Regulation in Deregulated Markets." *In IEEE Power and Energy Society General Meeting,* Minneapolis, MN, U.S.A., 2010, doi: 10.1109/PES.2010.5589748.

[124] S. M. Muyeen, R. Takahashi, T. Murata, J. Tamura. "A New Control Method of Energy Capacitor System in DC-Based Wind Farm." *In IEEE Energy Conversion Congr. and Exposition (ECCE*), San Jose, CA, U.S.A., pp. 1619-1625.

[125] Parsons Brinckerhoff, 2006, "Powering the Nation: A review of the costs of generating electricity", [Online] Available at: http://www.pbworld.co.uk/index.php?doc=528 [Accessed 30 June 2008]

[126] Parsons Brinckerhoff, 2010, "Powering the Nation Update 2010", [Online] Available at: http://www.pbworld.com/pdfs/regional/uk_europe/pb_ptn_update2010.pdf [Accessed 30 November 2010]

[127] M. Skyllas-Kazacos, M. Rychcik, R. G. Robins, A. G. Fane, M. A. Green. "New All-Vanadium Redox Flow Cell." *J. of the Electrochemical Soc.*, vol. 133, no. 5, pp.1057-1058, May 1986.

[128] G. Kear, A. A. Shah, F. C. Walsh. "Development of the all-vanadium redox flow battery for energy storage: a review of technological, financial and policy aspects." *Int. J. of Energy Research*, In press.

[129] Tapbury Management Ltd. "VRB ESS_{TM} Energy Storage & the development of dispatchable wind turbine output." [Online] Available at: http://www.seai.ie/Publications/Renewables_Publications/VRB-ESS-Energy-Storage-Rpt-Final.pdf [Accessed 06 Dec. 2011].

[130] S. Gray, H. Sharman. "Report on the commissioning of Prudent Energy's 500 kW, 2000 kWh battery and recent projects." Presented at the Int. Flow Battery Forum, Edinburgh, Scotland, 2011.

[131] M. Skyllas-Kazacos, G. Kazacos, G. Poon, H. Verseema. "Recent advances with UNSW vanadium-based redox flow batteries." *Int. J. of Energy Research*, vol. 34, no.2, pp.182–189, Feb. 2010.

[132] A. A. Shah, M. J. Watt-Smith, F. C. Walsh. "A dynamic performance model for redox-flow batteries involving soluable species." *Electrochemica Acta*, vol. 53, no. 27, pp. 8087-8100, Nov. 2008.

[133] D. You, H. Zhang, J. Chen. "A simple model for the vanadium redox battery." *Electrochemica Acta*, vol. 54, no. 27, pp. 6827-6836, Nov. 2009.

[134] C. Blanc. "Modelling of a Vanadium Redox Flow Battery Electricity Storage System", PhD Thesis, École Polytechnique Fédérale do Lausanne, Switzerland, 2009.

[135] A. Arulampalam, M. Barnes, N. Jenkins, J. B. Ekanayake. "Power quality and stability improvement of a wind farm using STATCOM supported with hybrid battery energy storage.", *In IEE Generation, Transmission and Distribution*, vol. 153, no. 6, pp.701-710, Nov. 2006.

[136] C. A. Smith, N. Hayward, E. A. Lewis. "Use of Statcom for offshore wind farm stability and grid compliance." Presented at the European Offshore Wind Conf., Stockholm, Sweden, 2009.

[137] H. Bindner, C. Ekman, O. Gehrke, F. Isleifsson. “Characterisation of Vanadium Flow Battery.” Risø-R-Report 1753, [Online] Available at: http://130.226.56.153/rispubl/reports/ris-r-1753.pdf [Accessed 05 Jan. 2011].

[138] D. D. Banham-Hall, C. A. Smith, G. A. Taylor, M. R. Irving. “Flow Batteries for Enhancing Wind Power Integration.” *Accepted for publication in IEEE Trans. on Power Syst.*

[139] W. Wang, B. Ge, D. Bi, D. Sun. “Grid-Connected Wind Farm Power Control using VRB-based Energy Storage System.” *In IEEE Energy Conversion Congr. and Exposition (ECCE),* Atlanta, GA, U.S.A., 2010, pp. 3772-3777.

[140] D. Newbery. “Contracting for Wind Generation.” University of Cambridge Electricity Policy Research Group Working Paper, [Online] Available at: http://www.econ.cam.ac.uk/dae/repec/cam/pdf/cwpe1143.pdf [Accessed 06 Jan 2012].

[141] H. Bludszuweit, J. A. Dominguez-Navarro, A.Llombart. "Statistical Analysis of Wind Power Forecast Error." *IEEE Trans. On Power Syst.*, vol.23, no.3, pp.983-991, Aug. 2008.

[142] K. Yoshimoto, T. Nanahara, G. Koshimizu. "New Control Method for Regulating State-of- Charge of a Battery in Hybrid Wind Power/Battery Energy Storage System." *In IEEE PES Power Syst. Conf. and Exposition, PSCE*, Atlanta, GA, U.S.A., 2006, pp.1244-1251.

[143] T. K. A. Brekken, A. Yokochi, A. von Jouanne, Z. Z. Yen, H. M. Hapke, D. A. Halamay. “Optimal Energy Storage Sizing and Control for Wind Power Applications.” *IEEE Trans. on Sustainable Energy*, vol. 2, no. 1, pp. 69-77, Jan. 2011.

[144] National Grid, 2006, “British Electricity Trading and Transmission Arrangements – 2006 7 year statement”, [Online] Available at: http://www.nationalgrid.com/uk/sys_06/default.asp?action=mnch10_2.htm&sNode=1&Exp=N [Accessed 12 Feb. 2011].

[145] G. L. Susteras, G. Hathaway, J. Caplin, G. Taylor. “Experiences of the Electricity System Operator Incentives Scheme in Great Britain”, *In Int. Congr. on Electricity Distribution, CIDEL*, Buenos Aires, Argentina, 2010.

[146] H. Bludszuweit, J. A. Dominguez-Navarro. "A Probabilistic Method for Energy Storage Sizing Based on Wind Power Forecast Uncertainty." *IEEE Trans. on Power Syst.*, vol.26, no.3, pp.1651-1658, Aug. 2011.

[147] M. Korpaas, A. T. Holen, R. Hildrum. "Operation and sizing of energy storage for wind power plants in a market system." *Int. J. of Elect. Power & Energy Syst.*, vol. 25, no. 8, pp. 599-606, Oct. 2003.

[148] J. Aston. "Financial Management." Brunel University, Uxbridge, Nov. 2011, Lecture.

[149] J. Cox (Pöyry Consulting). "Impact of Intermittency: How wind variability could change the shape of the British and Irish electricity markets." Jul. 2009.

[150] DECC. "Electricity Market Reform – Capacity Mechanism." [Online] Available at: http://www.decc.gov.uk/assets/decc/11/consultation/cap-mech/3883-capacity-mechanism-consultation-impact-assessment.pdf [Accessed 16 Jan. 2012].

[151] J. Collins, J. Parkes, A. Tindal. "Forecasting for utility-scale wind farms – The power model challenge." *In 2009 CIGRE/IEEE PES Joint Symp. on Integration of Wide-Scale Renewable Resources Into the Power Delivery Syst.*, Calgary, AB, Canada, CD-ROM.

[152] OFGEM, 2009, "Project Discovery; Energy Market Scenarios", pp7-8.

[153] G. N. Bathurst, G. Strbac. "Value of combining energy storage and wind in short-term energy and balancing markets." *Electric Power Syst. Research*, vol. 67, no. 1, pp. 1-8, Oct. 2003.

[154] National Grid. "Firm Frequency Response Market Information." [Online] Available at: www.nationalgrid.com/uk/Electricity/Balancing/services/frequencyresponse/ffr/ [Accessed 30 Apr. 2011].

[155] National Grid. "Mandatory Frequency Response: Frequency Response Reports." [Online] Available at: http://www.nationalgrid.com/uk/Electricity/Balancing/services/frequencyresponse/mandatoryfreqresp/ [Accessed 20 Apr. 2011].

[156] E. A. Lewis, H. Sharman. “Implementation of high capacity energy storage systems using high power inverters and advanced flow cells.” Presented at Energy Storage Solutions, London, UK, 2009.

[157] G. Kear, A. A. Shah, F. C. Walsh. “Development of the all-vanadium redox flow battery for energy storage: a review of technological, financial and policy aspects.” *Int. J. of Energy Research*, In press.

[158] Oak Ridge National Laboratory. “Economic Analysis of Deploying Used Batteries in Power Systems.” [Online] Available at: http://www.ms.ornl.gov/Physical/pdf/Publication%2030540.pdf [Accessed 16 Jan. 2012].

[159] Oxera. “Discount rates for low carbon and renewable generation technologies.” [Online] Available at: http://hmccc.s3.amazonaws.com/Renewables%20Review/Oxera%20low%20carbon%20discount%20rates%20180411.pdf [Accessed 16 Jan 2012]

[160] Ricardo, National Grid. “Bucks for Balancing: Can plug-in vehicles of the future extract cash – and carbon – from the power grid?” [Online] Available at: www.ricardo.com/Documents/Downloads/White%20Paper/Plug%20In%20Vehicle%20of%20Future/Bucks%20for%20balancing%20-%20can%20plug-in%20vehicles%20of%20the%20future%20extract%20cash%20%E2%80%93%20and%20carbon%20%E2%80%93%20from%20the%20power%20grid.pdf [Accessed 23 Aug 2011].

[161] J. Short. “Dynamic Demand Control: What is its financial value?” [Online] Available at: http://www.dynamicdemand.co.uk/pdf_economic_case.pdf [Accessed 8 Mar 2011].

[162] D. D. Banham-Hall, C. A. Smith, G. A. Taylor. Frequency reserves from an Energy store and a generator. European Patent Application no. EP10007692.4 filed 26/09/2011.

[163] G. Sinden. “Characteristics of the UK wind resource: Long-term patterns and relationship to electricity demand.” *Energy Policy*, vol. 35, pp.112-127, Jan. 2007.

[164] R. Pearmine. “Review of Primary Frequency Control Requirements on the GB Power System Against a Background of Increasing Renewable Generation.” PhD Thesis, Brunel University, UK, 2006, pp. 24.

[165] J. Tauschitz, M. Hochfellner. ‘State of the combined cycle power plants.’ *In Energy efficiency conf.*, Vienna, Austria, 2004.

[166] Department of Energy and Climate Change. “The UK Power Sector: Trends and Targets.” [Online] Available at: http://www.publications.parliament.uk/pa/cm201011/cmselect/cmenergy/523/52305.htm [Accessed 18 Jan. 2012].